



The University of
Nottingham

UNITED KINGDOM • CHINA • MALAYSIA

**INNOVATIVE HEATING, COOLING AND
VENTILATION TECHNOLOGIES FOR
LOW-CARBON BUILDINGS**

AYSE PINAR MERT CUCE
BSc (hons), MSc (hons)

Thesis submitted to the University of Nottingham
for the degree of Doctor of Philosophy
January 2016

ABSTRACT

Sectoral energy consumption analyses clearly indicate that building sector plays a key role in global energy consumption, which is almost 40% in developed countries. Among the building services; conventional heating, ventilation and air conditioning (HVAC) systems have the greatest percentage in total energy consumption of buildings. According to the latest research, HVAC is responsible for around 40% of total building energy consumption and 16% of total global energy consumption. In this respect, decisive measures need to be taken to mitigate the energy consumption due to HVAC. The research carried out within the scope of this thesis covers innovative heating, cooling and ventilation technologies for low-carbon buildings. The novel technologies developed are introduced and investigated both theoretically and experimentally. The results indicate that optimised HVAC systems with waste heat recovery have a significant potential to mitigate energy consumed in buildings, thus to halt carbon emissions. Especially plate-type roof waste heat recovery units are very attractive for the said hybrid applications with a thermal efficiency greater than 88%. The said systems are also promising in terms of overall coefficient of performance (COP). The average COP of plate-type roof waste heat recovery unit is determined to be about 4.5, which is incomparable with those of conventional ventilation systems. Preheating performance of fresh air in winter season is found to be remarkable. Comprehensive in-situ tests clearly reveal that the temperature rise in fresh air is found to be around 7 °C. Plate-type roof waste heat recovery units also provide thermal comfort conditions for occupants. Indoor CO₂ concentration is observed to be varying from 350 to 400 ppm which is very appropriate in term of air quality. In addition, average relative humidity is found to be 57%, which is in the desired range according to the latest building standards. Desiccant-based evaporative cooling systems are capable of providing

desired indoor environments for occupants as well as having considerably high COP ranges. An average of 5.3 °C reduction is achieved in supply air temperature by utilising those systems as well as having relative humidity distribution in thermal comfort range. The dehumidification effectiveness is found to be 63.7%, which is desirable and promising. The desiccant-based evaporative cooling system has a great potential to mitigate cooling demand of buildings not only in hot arid but also in temperate humid climates.

Keywords: Buildings, energy consumption, HVAC, waste heat recovery, efficiency.

ACKNOWLEDGEMENTS

I would like to start by thanking my supervisor, Professor Saffa Riffat, for his help, guidance and support throughout this work, for giving me the opportunity to join his research group. It was a great honour to be a member of his team as a researcher, and conduct my PhD under his supervision. I also would like to thank my second supervisor, Associate Professor Siddig Omer, for his kind enthusiasm and valuable assist. My special thanks must go to my internal assessor, Associate Professor Mohamed Gadi, and to my external assessor, Dr Liben Jiang, for taking time to read my work and for their constructive corrections and suggestions. Their invaluable comments support my work and encourage my patience during the period of my thesis. I am especially grateful to Technical Marketing Manager of Izocam AS, Dr Kemal Gani Bayraktar, for providing me with the opportunity to carry out my research under the financial support of HERB Project. I wish to thank Rick Richard to spend his valuable time and to give me opportunity to do my tests. I would like to thank my friends in Sustainable Research Building. In particular, special thanks go to Licheng Zhang for his kind wishes. My special greetings go to the technicians, Tony Lord and Johnathan Moss, in the Department of Architecture and Built Environment for their kind help and technical support.

My deep appreciations go to my Dad (Metin) and my Mum (Emine) for their everlasting love, support and patience. Without them, I would never complete my study. I always feel their endless prayer with me, and I cannot thank them in words. I will be grateful to them forever. My special thanks must go to my sisters, Cicek Fatma and Serpil, for their encouragement and kind help. I appreciate my newly joining niece, Azra, because of her fantastic surprise. I also would like to take this opportunity to acknowledge my Grandma (Sakine), Grandaunt (Fatma), Grandpa (Huseyin), and Aunt

(Fatma) for their support, best wishes and prayer. I also would like to thank my Father-in-law (Ali) and Mother-in-law (Henne) for their precious moral support and encouragement. I appreciate their all prayers and kind wishes.

Finally, my deepest thanks must go to my heart, Assistant Professor Erdem Cuce, who is not only a husband but also a friend, an intimate, comrade, guardian angel to me. Words cannot express how much you mean to me.

I gratefully acknowledge the financial support of EU Commission through the research project of Holistic energy-efficient retrofitting of residential buildings (HERB) under FP7-NMP with project code of 314283.

*“Look deep into nature,
and then you will understand everything better”*

Albert Einstein

CONTENTS	Page
ABSTRACT.....	II
ACKNOWLEDGEMENTS.....	IV
LIST OF FIGURES	XIV
LIST OF TABLES.....	XXVI
NOMENCLATURE	XXVIII
<i>CHAPTER 1 “An introduction to the research carried out within the scope of this thesis”</i>	
<hr/>	
CHAPTER 1	1
1.1. Introduction.....	2
1.2. Aim and Objectives	4
1.3. Research Methodology	5
1.4. Scope.....	6
1.4.1. Chapter 2.....	6
1.4.2. Chapter 3	7
1.4.3. Chapter 4.....	9
1.4.4. Chapter 5	10
1.4.5. Chapter 6.....	11
1.4.6. Chapter 7.....	12
1.4.7. Chapter 8.....	13
1.4.8. Chapter 9.....	14
1.4.9. Chapter 10.....	15
1.4.10. Chapter 11	16
1.4.11. Chapter 12.....	17

CHAPTER 2 *“A comprehensive review of heat recovery systems for building applications”*

CHAPTER 2	19
2.1. Introduction	20
2.2. Heat Recovery System.....	22
2.2.1. Working principle	24
2.2.2. System components	27
2.2.3. Operation and maintenance	27
2.3. Types of Heat Recovery System.....	28
2.3.1. Tubular heat exchangers	29
2.3.1.1. Double pipe	29
2.3.1.2. Shell and tube.....	30
2.3.1.3. Coiled (spiral) tube	31
2.3.2. Plate-type heat exchangers	32
2.3.2.1. Gasketed plate.....	32
2.3.2.2. Spiral plate	33
2.3.2.3. Plate coil	34
2.3.2.4. Lamella	34
2.3.3. Extended (finned) surface heat exchangers	35
2.3.3.1. Tube-fin	36
2.3.3.2. Plate-fin	36
2.3.3.3. Heat pipe	37
2.3.4. Regenerators	38
2.3.4.1. Fixed matrix	39
2.3.4.2. Rotary.....	39

<i>Contents</i>	IX
2.4. Applications of Heat Recovery Systems in Buildings	40
2.4.1. Practical applications from the University of Nottingham	48
2.5. Theoretical Studies on Heat Recovery Systems	53
2.6. Simulation Works on Heat Recovery Systems	54
2.7. Performance Assessment of Heat Recovery Systems	55
2.7.1. Energy analysis	60
2.7.2. Exergy analysis	61
2.8. Environmental Impacts of Heat Recovery Systems	61
2.8.1. Energy consumption	62
2.8.2. Greenhouse gasses	62
2.9. Future Potential of Heat Recovery Systems	63
2.10. Recommendations for Heat Recovery Systems	64
2.11. Conclusions	65
<i>CHAPTER 3 “Theoretical investigation and thermodynamic assessment of a solar powered heat recovery panel in buildings”</i>	

CHAPTER 3	67
3.1. Introduction	68
3.2. Methodology	74
3.3. Theoretical Investigation of a Solar Powered Heat Recovery System	75
3.4. Thermodynamic Assessment of Heat Recovery Systems.....	83
3.4.1. Exergy analysis of a solar powered heat recovery system.....	84
3.5. Results and Discussion	86
3.5.1. Results from theoretical investigation	86
3.5.2. Results from thermodynamic assessment	92

<i>Contents</i>	X
3.6. Conclusions.....	93
<i>CHAPTER 4 “An experimental investigation of a novel roof type heat recovery panel for low-carbon buildings”</i>	
<hr/>	
CHAPTER 4	95
4.1. Introduction.....	96
4.2. Description of the System.....	98
4.3. Experimental Investigation of the System	100
4.3.1. Experimental setup	100
4.4. Economic Analysis of the System	102
4.5. Results and Discussion	104
4.6. Conclusions.....	109
<i>CHAPTER 5 “Thermal performance monitoring of a novel heat recovery unit integrated to residential house”</i>	
<hr/>	
CHAPTER 5	112
5.1. Introduction.....	113
5.2. Pre-retrofitting Strategy	114
5.3. Retrofitting Plan.....	115
5.4. Monitoring Plan	116
5.5. Details of the Test House.....	118
5.6. Results and Discussion	120
5.7. Conclusions.....	123

CHAPTER 6 “Evaporative cooling systems for building applications: A review”

CHAPTER 6	125
6.1. Introduction.....	126
6.2. Evaporative Cooling System	128
6.2.1. Working principle of an evaporative cooling system	129
6.3. Building Applications.....	131
6.4. Thermal Performance Assessment.....	138
6.5. Thermodynamic Performance Analysis.....	142
6.6. Techno-Economic and Environmental Aspects.....	143
6.7. Conclusions.....	145

CHAPTER 7 “Theoretical investigation of a novel indirect-contact evaporative cooling system for building applications”

CHAPTER 7	147
7.1. Introduction.....	148
7.2. A Novel Evaporative Cooling System.....	153
7.3. Mathematical Model of the System	157
7.4. Results and Discussion	164
7.5. Conclusions.....	183

CHAPTER 8 “Comprehensive thermal performance investigation of a novel direct-contact evaporative cooling system”

CHAPTER 8	188
8.1. Introduction.....	189
8.2. Description of a Novel Evaporative Cooling System (ECS).....	191

<i>Contents</i>	XII
8.3. Experimental Setup and Analysis	192
8.4. Results and Discussion	194
8.5. Conclusions.....	200
 CHAPTER 9 <i>“A simplified model for liquid desiccant-based evaporative cooling system”</i>	
<hr/>	
CHAPTER 9	202
9.1. Introduction.....	203
9.2. Mathematical Model	206
9.3. Results and Discussion	212
9.4. Conclusions.....	214
 CHAPTER 10 <i>“Thermal performance assessment of a novel liquid desiccant-based evaporative cooling system: An experimental investigation”</i>	
<hr/>	
CHAPTER 10	216
10.1. Introduction	217
10.2. Description of Desiccant-Based Evaporative Cooling System (DECS)	219
10.3. Experimental Setup	221
10.4. Measurements.....	222
10.5. Results and Discussion.....	223
10.6. Conclusions	234
 CHAPTER 11 <i>“Theoretical investigation of a novel heating system for low-carbon buildings: Moist airflow system”</i>	
<hr/>	
CHAPTER 11	238

<i>Contents</i>	XIII
11.1. Introduction	239
11.2. Description of Moist Airflow System	240
11.3. Thermodynamic Model	241
11.4. Heat Transfer Analysis	246
11.5. Duct Diameter Analysis for Constant Energy Input	248
11.6. Results and Discussion	250
11.6.1. Results from thermodynamic optimisation.....	251
11.6.2. Results from heat transfer analysis	258
11.6.3. Results from duct diameter analysis	263
11.7. Conclusions.....	265
<i>CHAPTER 12 “Conclusions and future works”</i>	
<hr/>	
CHAPTER 12	268
12.1. Conclusions	269
12.2. Future Works	279
<i>BIBLIOGRAPHY</i>	
<hr/>	
BIBLIOGRAPHY	281
References.....	282
<i>APPENDICES</i>	
<hr/>	
Appendices.....	318
Publications.....	319
<hr/>	

LIST OF FIGURES**Page****CHAPTER 2**

Figure 2.1.	Sources of moisture loads in a medium size retail store	23
Figure 2.2.	Typical heat recovery system.....	25
Figure 2.3.	Classification of heat exchangers.....	29
Figure 2.4.	A double pipe heat exchanger.....	30
Figure 2.5.	Shell and tube type heat exchangers	31
Figure 2.6.	Titanium (left) and copper (right) coiled tube heat exchangers.....	32
Figure 2.7.	Gasketed plate heat exchangers	33
Figure 2.8.	Spiral plate heat exchangers.....	34
Figure 2.9.	Lamella heat exchangers	35
Figure 2.10.	Tube-fin (a) and plate-fin (b) heat exchangers.....	37
Figure 2.11.	Working principle of a heat pipe.....	38
Figure 2.12.	Fixed matrix (a) and rotary (b) regenerators.....	40
Figure 2.13.	A horizontal staggered heat pipe.....	41
Figure 2.14.	Heat transfer rate and thermal efficiency of plate type heat exchanger provided.....	43
Figure 2.15.	Heat recovery concept in the proposed system.....	44
Figure 2.16.	Monthly energy consumption of different air conditioners in Sydney ..	46
Figure 2.17.	Mechanical ventilation heat recovery heat pump system	47
Figure 2.18.	Detailed photos and the experimental results of the novel enthalpy recovery system.....	50
Figure 2.19.	An illustrative schematic, a test rig photo and experimental results from a novel heat recovery system	51

Figure 2.20.	A novel evaporative cooling system including polycarbonate heat exchanger	52
Figure 2.21.	Schematic for a typical heat recovery panel	56
Figure 2.22.	Optimum effectiveness and experimental effectiveness	60

CHAPTER 3

Figure 3.1.	Schematic of the solar powered heat recovery system.....	74
Figure 3.2.	Solar intensity dependencies of outlet fresh air and stale air temperatures for $T_{fa,0} = -5\text{ }^{\circ}\text{C}$	87
Figure 3.3.	Solar intensity dependencies of outlet fresh air and stale air temperatures for $T_{fa,0} = 0\text{ }^{\circ}\text{C}$	88
Figure 3.4.	Solar intensity dependencies of outlet fresh air and stale air temperatures for $T_{fa,0} = 5\text{ }^{\circ}\text{C}$	88
Figure 3.5.	Ambient temperature dependencies of outlet fresh air and stale air temperatures for $G = 100\text{ W/m}^2$	89
Figure 3.6.	Ambient temperature dependencies of outlet fresh air and stale air temperatures for $G = 300\text{ W/m}^2$	90
Figure 3.7.	Ambient temperature dependencies of outlet fresh air and stale air temperatures for $G = 500\text{ W/m}^2$	90
Figure 3.8.	Variation of electrical efficiency of the <i>SPHRS</i> by ambient temperature and solar intensity	91
Figure 3.9.	Exergy efficiency of the <i>SPHRS</i> with respect to the changes in ambient temperature and solar intensity	93

CHAPTER 4

Figure 4.1.	Schematic of the proposed heat recovery system	99
Figure 4.2.	Multi-channel ducts of the heat recovery system.....	99
Figure 4.3.	Installation of the polycarbonate heat exchanger to the test house.....	101
Figure 4.4.	A test house located in Southeastern UK.....	101
Figure 4.5.	Implementation of the thermocouples and humidity sensors to the different locations of the test house.	102
Figure 4.6.	Temperature variation of the inlet stale air	104
Figure 4.7.	Temperature variation of the outlet stale air	105
Figure 4.8.	Temperature variation of the inlet fresh air.....	105
Figure 4.9.	Temperature variation of the outlet fresh air.....	106
Figure 4.10.	Relative humidity variation of the inlet fresh air	107
Figure 4.11.	Relative humidity variation of the outlet fresh air	108
Figure 4.12.	Heat recovery efficiency of the system.....	110
Figure 4.13.	Coefficient of performance of the system.....	111

CHAPTER 5

Figure 5.1.	Dimensions of the plate type air to air heat exchanger	115
Figure 5.2.	100 mm glass wool insulation in the loft space of the residential house	117
Figure 5.3.	A 3D schematic for integration plan of the heat recovery system	117
Figure 5.4.	The test house which is integrated with a novel heat recovery system.....	118
Figure 5.5.	Detailed photos of the novel heat recovery system which is fixed beneath the roof (left), and flexible ducts (right).....	119

Figure 5.6.	Inlet and outlet ventilation ducts in the test house	119
Figure 5.7.	Data-logging system utilised in the test house	120
Figure 5.8.	Temperature variation of fresh air at the inlet and the outlet.....	122
Figure 5.9.	Temperature variation of stale air at the inlet and the outlet.....	122
Figure 5.10.	Indoor relative humidity variation at pre and post-retrofit cases	123
Figure 5.11.	CO_2 variation at pre-retrofit case.....	124
Figure 5.12.	CO_2 variation at post-retrofit case	124

CHAPTER 6

Figure 6.1.	Total primary energy supply by fuel in 2011	127
Figure 6.2.	Total final energy consumption by fuel (a) and by region (b), and CO_2 emissions by fuel (c) and by region (d) in 2011.....	127
Figure 6.3.	Total final energy consumption by sector (a) and CO_2 emissions by region (b) in 2035	129
Figure 6.4.	Direct evaporative cooling (a) and indirect evaporative cooling (b) ...	130
Figure 6.5.	Working principle of an M-cycle	131
Figure 6.6.	Wet and dry channels of a cross-flow heat exchanger in M-cycle.....	132
Figure 6.7.	Water spraying evaporative unit for passive cooling of buildings.....	133
Figure 6.8.	A test house covered with shade cloth and water flow arrangement ...	134
Figure 6.9.	Air temperature changes in the test room for ventilated and non-ventilated room case.....	135
Figure 6.10.	Thermal values of the air in psychrometric chart for a direct (a) and an indirect evaporative cooling.....	138

Figure 6.11.	Water consumption of direct and indirect/direct evaporative cooling system in different climatic conditions	139
Figure 6.12.	Semi-indirect contact evaporative cooling system.....	140
Figure 6.13.	Heat and mass exchange in ceramic pipes	140
Figure 6.14.	Monthly energy saving of indirect contact evaporative cooling unit for interior and coastal areas	144

CHAPTER 7

Figure 7.1.	Distribution of the total energy consumption of United Kingdom by sector (a) and by building type (b) in 2000	150
Figure 7.2.	A detailed schematic of a counter-flow indirect-contact evaporative cooling system.....	152
Figure 7.3.	A test house in Southeastern UK	154
Figure 7.4.	Square-sectioned ducts of the heat exchanger unit for hot and cold streams.....	155
Figure 7.5.	Polycarbonate sheets integrated to the test house	155
Figure 7.6.	Schematic of the proposed indirect-contact evaporative cooling system	156
Figure 7.7.	Combined effects of length of the spraying unit and hydraulic diameter on the amount of evaporated water vapour	165
Figure 7.8.	Combined effects of length of the spraying unit and velocity of working air on the amount of evaporated water vapour.....	165
Figure 7.9.	Combined effects of hydraulic diameter and velocity of working air on the amount of evaporated water vapour	166

- Figure 7.10. Dry-bulb temperature and relative humidity of working air at the outlet of the water spraying unit for $T_{wa,in} = 17$ °C, and as a function of the length of spraying unit 167
- Figure 7.11. Dry-bulb temperature and relative humidity of working air at the outlet of the water spraying unit for $T_{wa,in} = 20$ °C, and as a function of the length of spraying unit 168
- Figure 7.12. Dry-bulb temperature and relative humidity of working air at the outlet of the water spraying unit for $T_{wa,in} = 23$ °C, and as a function of the length of spraying unit 169
- Figure 7.13. Dry-bulb temperature and relative humidity of working air at the outlet of the water spraying unit for $T_{wa,in} = 26$ °C, and as a function of the length of spraying unit 170
- Figure 7.14. Dry-bulb temperature and relative humidity of working air at the outlet of the water spraying unit for $T_{wa,in} = 29$ °C, and as a function of the length of spraying unit 171
- Figure 7.15. Dry-bulb temperature and relative humidity of working air at the outlet of the water spraying unit for $T_{wa,in} = 17$ °C, and as a function of hydraulic diameter 173
- Figure 7.16. Dry-bulb temperature and relative humidity of working air at the outlet of the water spraying unit for $T_{wa,in} = 20$ °C, and as a function of hydraulic diameter 174
- Figure 7.17. Dry-bulb temperature and relative humidity of working air at the outlet of the water spraying unit for $T_{wa,in} = 23$ °C, and as a function of hydraulic diameter 175

- Figure 7.18. Dry-bulb temperature and relative humidity of working air at the outlet of the water spraying unit for $T_{wa,in} = 26$ °C, and as a function of hydraulic diameter 176
- Figure 7.19. Dry-bulb temperature and relative humidity of working air at the outlet of the water spraying unit for $T_{wa,in} = 29$ °C, and as a function of hydraulic diameter 177
- Figure 7.20. Dry-bulb temperature and relative humidity of working air at the outlet of the water spraying unit for $T_{wa,in} = 17$ °C, and as a function of velocity of working air 178
- Figure 7.21. Dry-bulb temperature and relative humidity of working air at the outlet of the water spraying unit for $T_{wa,in} = 20$ °C, and as a function of velocity of working air 179
- Figure 7.22. Dry-bulb temperature and relative humidity of working air at the outlet of the water spraying unit for $T_{wa,in} = 23$ °C, and as a function of velocity working air 180
- Figure 7.23. Dry-bulb temperature and relative humidity of working air at the outlet of the water spraying unit for $T_{wa,in} = 26$ °C, and as a function of velocity of working air 181
- Figure 7.24. Dry-bulb temperature and relative humidity of working air at the outlet of the water spraying unit for $T_{wa,in} = 29$ °C, and as a function of velocity of working air 182
- Figure 7.25. Indoor temperature of fresh air by outdoor temperature of fresh air and working air temperature at the inlet of polycarbonate heat exchanger . 183

Figure 7.26.	Indoor relative humidity of fresh air by outdoor temperature of fresh air and working air temperature at the inlet of polycarbonate heat exchanger for $\phi_{fa,outdoor} = 10\%$	185
Figure 7.27.	Indoor relative humidity of fresh air by outdoor temperature of fresh air and working air temperature at the inlet of polycarbonate heat exchanger for $\phi_{fa,outdoor} = 20\%$	186
Figure 7.28.	Indoor relative humidity of fresh air by outdoor temperature of fresh air and working air temperature at the inlet of polycarbonate heat exchanger for $\phi_{fa,outdoor} = 30\%$	186
Figure 7.29.	Indoor relative humidity of fresh air by outdoor temperature of fresh air and working air temperature at the inlet of polycarbonate heat exchanger for $\phi_{fa,outdoor} = 40\%$	187

CHAPTER 8

Figure 8.1.	Description of the proposed evaporative cooling system	192
Figure 8.2.	Detailed photos of a novel roof type evaporative cooling system	193
Figure 8.3.	Temperature measurement from the first test	195
Figure 8.4.	Relative humidity measurement from the first test.....	195
Figure 8.5.	Temperature measurement from the second test.....	196
Figure 8.6.	Relative humidity measurement from the second test	197
Figure 8.7.	Wet bulb effectiveness for the first and second tests	199
Figure 8.8.	Humidification effectiveness for the first and second tests	199
Figure 8.9.	Coefficient of performance values for the first and second tests	200

CHAPTER 9

Figure 9.1.	Schematic of a typical indirect-contact evaporative cooling system ...	205
Figure 9.2.	Schematic of a novel liquid desiccant-based evaporative cooling system.....	206
Figure 9.3.	Outlet desiccant temperature as a function of inlet desiccant temperature.....	213
Figure 9.4.	Humidity ratio of fresh air at the outlet of the dehumidifier as a function of inlet desiccant temperature	214
Figure 9.5.	Air temperature at the outlet of the dehumidifier as a function of inlet desiccant concentration	215

CHAPTER 10

Figure 10.1.	Detailed description of <i>DECS</i> : a) wooden structure of <i>DECS</i> , b) 12 <i>Watt</i> fan for circulating air, c) 15 <i>Watt</i> immersible pump, d) inlet duct to dehumidification, e) outlet duct after humidification, f) collecting ducts for drained water and desiccant, g) data logger, h) inlet fresh air to <i>DECS</i> from conditioned environmental chamber and i) digital and multi-functional environmental chamber.....	220
Figure 10.2.	Relative humidity and temperature measurement for the air velocity of 0.3 <i>m/s</i> at the inlet of the dehumidification unit.....	225
Figure 10.3.	Relative humidity and temperature measurement for the air velocity of 0.3 <i>m/s</i> at the outlet of the dehumidification unit.....	226
Figure 10.4.	Dehumidification effectiveness of the desiccant unit for the air velocity of 0.3 <i>m/s</i>	226

Figure 10.5.	Relative humidity and temperature measurement for the air velocity of 0.3 m/s at the inlet of the humidification unit	227
Figure 10.6.	Relative humidity and temperature measurement for the air velocity of 0.3 m/s at the outlet of the humidification unit	227
Figure 10.7.	Humidification effectiveness of the evaporative cooling unit for the air velocity of 0.3 m/s	228
Figure 10.8.	Relative humidity and temperature measurement for the air velocity of 0.5 m/s at the inlet of the dehumidification unit.....	229
Figure 10.9.	Relative humidity and temperature measurement for the air velocity of 0.5 m/s at the outlet of the dehumidification unit.....	229
Figure 10.10.	Dehumidification effectiveness of the desiccant unit for the air velocity of 0.5 m/s	230
Figure 10.11.	Relative humidity and temperature measurement for the air velocity of 0.5 m/s at the inlet of the humidification unit	230
Figure 10.12.	Relative humidity and temperature measurement for the air velocity of 0.5 m/s at the outlet of the humidification unit	231
Figure 10.13.	Humidification effectiveness of the evaporative cooling unit for the air velocity of 0.5 m/s	232
Figure 10.14.	Wet bulb effectiveness of the humidification unit for the air velocities of 0.3 and 0.5 m/s	233
Figure 10.15.	Time-dependant coefficient of performance values for the inlet air velocities of 0.3 m/s and 0.5 m/s.	236

CHAPTER 11

Figure 11.1.	Schematic of the proposed moist airflow system.....	242
--------------	---	-----

Figure 11.2.	Working principle of the moist airflow system.....	243
Figure 11.3.	Evaporation process and generation of moist-air in water tank	244
Figure 11.4.	Enthalpy exchange of working air in psychrometric chart	245
Figure 11.5.	Heat transfer surface area in a circular tube.....	248
Figure 11.6.	Thermal energy required for the water in the tank.....	252
Figure 11.7.	Final thermal energy required for the moist-air	252
Figure 11.8.	Coefficient of performance values for different working hours of MAS with a fan power of 25 W	254
Figure 11.9.	Coefficient of performance values for different working hours of MAS with a fan power of 50 W	255
Figure 11.10.	Coefficient of performance values for different working hours of MAS with a fan power of 75 W	255
Figure 11.11.	Coefficient of performance values for different working hours of MAS with a fan power of 100 W	256
Figure 11.12.	Coefficient of performance values for different working hours of MAS integrated with solar power with a fan power of 25 W	256
Figure 11.13.	Coefficient of performance values for different working hours of MAS integrated with solar power with a fan power of 50 W	257
Figure 11.14.	Coefficient of performance values for different working hours of MAS integrated with solar power with a fan power of 75 W	257
Figure 11.15.	Coefficient of performance values for different working hours of MAS integrated with solar power with a fan power of 100 W	258
Figure 11.16.	Variation of duct diameter with the operation time for the duct length of 40 metres.....	259

Figure 11.17. Variation of duct diameter with the operation time for the duct length of 50 metres..... 259

Figure 11.18. Variation of duct diameter with the operation time for the duct length of 60 metres..... 260

Figure 11.19. Variation of duct diameter with the operation time for the duct length of 70 metres..... 260

Figure 11.20. Variation of duct diameter with heat output and duct length of 40 to 70 metres for an operation time of 1 hour..... 261

Figure 11.21. Variation of duct diameter with heat output and duct length of 40 to 70 metres for an operation time of 1.5 hours 262

Figure 11.22. Variation of duct diameter with heat output and duct length of 40 to 70 metres for an operation time of 2 hours 262

Figure 11.23. Duct diameter ratio of water and air based heating system 263

Figure 11.24. Duct diameter ratio of water and moist-air based heating system 264

Figure 11.25. Duct diameter comparison for water, moist-air and air 265

LIST OF TABLES**Page****CHAPTER 2**

Table 2.1.	Fresh air requirements.....	26
Table 2.2.	A comparison of the types of heat recovery systems by their efficiency ranges and potential advantages.....	48

CHAPTER 4

Table 4.1.	Space heating requirements in multi-family building.....	97
Table 4.2.	Total economic savings after implementing a mechanical ventilation system with 90% heat recovery, air changer rate of $0.5 h^{-1}$ and an electricity consumption of $3 kWh/m^2/a$	98
Table 4.3.	Total investment cost of the proposed heat recovery system.....	103
Table 4.4.	Comparison of the proposed system with a commercial alternative....	109

CHAPTER 6

Table 6.1.	Pioneer works on building applications of evaporative cooling systems	136
Table 6.2.	Thermal performance assessment of evaporative cooling systems.....	141
Table 6.3.	Thermodynamic performance assessment of evaporative cooling systems	145
Table 6.4.	Annual energy consumptions (<i>MWh</i>) of three different types of air-conditioning systems.....	145

CHAPTER 7

Table 7.1.	Dimensions of the components in the test house	154
Table 7.2.	Dimensions of the proposed polycarbonate heat exchanger	156

CHAPTER 9

Table 9.1.	Verification of the present study through a previously published experimental work.....	209
------------	---	-----

CHAPTER 10

Table 10.1.	Inlet and outlet experimental parameters of the liquid desiccant based evaporative cooling system for the first test	233
Table 10.2.	Inlet and outlet experimental parameters of the liquid desiccant based evaporative cooling system for the second test.....	234

CHAPTER 11

Table 11.1.	Initial and final water temperatures considered for the MAS.....	251
Table 11.2.	Enthalpy exchange of air for different initial conditions	253

NOMENCLATURE

<i>A</i>	:	Area [m^2]
<i>AC</i>	:	Air conditioner
<i>BF</i>	:	Blowing factor
<i>c</i>	:	Specific heat capacity [J/kgK]
<i>C</i>	:	Concentration [%]
<i>CFD</i>	:	Computational fluid dynamics
<i>COP</i>	:	Coefficient of performance
<i>D</i>	:	Diameter [m]
<i>DECS</i>	:	Desiccant based evaporative cooling system
<i>Dh</i>	:	Hydraulic diameter [m]
<i>Dm</i>	:	Mass diffusivity [m^2/s]
<i>ECS</i>	:	Evaporative cooling system
<i>Ex</i>	:	Exergy [kJ]
<i>ERV</i>	:	Energy recovery ventilator
<i>EU</i>	:	European Union
<i>G</i>	:	Solar intensity [W/m^2]
<i>Gt</i>	:	Gigatonne
<i>GSM</i>	:	Global System for Mobile Communications
<i>h</i>	:	Heat transfer coefficient [W/m^2K]
\dot{h}	:	Specific enthalpy [kJ/kg]
<i>H</i>	:	Enthalpy [kJ]
<i>HCOOK</i>	:	Potassium formate
<i>HP</i>	:	Heat pump

<i>HRS</i>	:	Heat recovery system
<i>HVAC</i>	:	Heating, ventilation and air conditioning
<i>IEA</i>	:	International Energy Agency
<i>IEC</i>	:	Indirect evaporative cooler
<i>IEER</i>	:	Integrative energy efficiency ratio
<i>IPCC</i>	:	Intergovernmental Panel on Climate Change
<i>k</i>	:	Thermal conductivity [W/mK]
<i>K</i>	:	Mass transfer coefficient [m/s]
<i>L</i>	:	Length [m]
<i>LiBr</i>	:	Lithium bromide
<i>m</i>	:	Mass [kg]
\dot{m}	:	Mass flow rate [kg/s]
<i>mf</i>	:	Mass fraction
<i>MW</i>	:	Megawatt
<i>Mt</i>	:	Million tonne
<i>Mtoe</i>	:	Million tonnes of oil equivalent
<i>n</i>	:	Constant
<i>Nu</i>	:	The Nusselt number
<i>P</i>	:	Pressure [Pa]
<i>PCM</i>	:	Phase change material
<i>Pr</i>	:	The Prandtl number
<i>PV</i>	:	Photovoltaic
<i>PVC</i>	:	Polyvinyl chloride
<i>Pw</i>	:	Power [W]
<i>Q</i>	:	Heat transfer rate [W]

Re	:	The Reynolds number
s	:	Entropy [kJ/kgK]
Sc	:	The Schmidt number
Sh	:	The Sherwood number
$SPHRS$:	Solar powered heat recovery system
t	:	Time [s]
T	:	Temperature [$^{\circ}C$]
u	:	Thermal energy
U	:	Overall heat transfer coefficient [W/m^2K]
UK	:	United Kingdom
v	:	Velocity [m/s]
x	:	Constant

Subscripts

a	:	Air
amb	:	Ambient
bp	:	Blackened plate
con	:	Condensation
$cons$:	Consumption
cor	:	Corrected
db	:	Dry bulb
$dehum$:	Dehumidification
des	:	Destruction
eq	:	Equilibrium
ev	:	Evaporated

<i>ex</i>	:	Exergy
<i>fan</i>	:	Fan
<i>gc</i>	:	Glass cover
<i>gen</i>	:	Overall
<i>f</i>	:	Film
<i>fa</i>	:	Fresh air
<i>fs</i>	:	Final state
<i>h</i>	:	Hydraulic
<i>hc</i>	:	High operation temperature
<i>hex</i>	:	Heat exchanger
<i>hrs</i>	:	Heat recovery system
<i>hum</i>	:	Humidification
<i>i</i>	:	Internal
<i>im</i>	:	Insulation material
<i>in</i>	:	Inlet
<i>is</i>	:	Initial state
<i>j</i>	:	Stream
<i>L</i>	:	Length [<i>m</i>]
<i>lwf</i>	:	Liquid water film
<i>o</i>	:	External
<i>out</i>	:	Outlet
<i>p</i>	:	Penalty factor
<i>pc</i>	:	Photovoltaic cell
<i>s</i>	:	Solution
<i>sa</i>	:	Stale air

<i>sat</i>	:	Saturation
<i>tec</i>	:	Thermal energy content
<i>tot</i>	:	Total
<i>vap</i>	:	Vapour
<i>w</i>	:	Water
<i>wa</i>	:	Working air
<i>wb</i>	:	Wet bulb
<i>wf</i>	:	Working fluid
<i>wsu</i>	:	Water spraying unit

Greek Letters

α	:	Absorptivity coefficient
β	:	Packing factor
θ	:	Temperature coefficient
ε	:	Effectiveness
ξ	:	Thermal connection constant
η	:	Efficiency
μ	:	Dynamic viscosity [kg/m^2s]
σ	:	Constant
ρ	:	Perimeter [m]
λ	:	Energy saving coefficient
ψ	:	Thermal mass flow rate
Ω	:	Constant
ϕ	:	Relative humidity
θ	:	Constant

ρ	:	Density [kg/m^3]
\acute{u}	:	Kinematic viscosity [m^2/s]
ϑ	:	Width [m]
τ	:	Transmissivity coefficient
ϖ	:	Constant
ω	:	Thickness [m]
ω	:	Humidity ratio (Specific humidity) [$g_{water\ vapour}/kg_{dry\ air}$]
Υ	:	Total energy transferred [W]

CHAPTER 1

An introduction to the research
carried out within the scope of
this thesis

- 1.1. Introduction
- 1.2. Aim and Objectives
- 1.3. Research Methodology
- 1.4. Scope

CHAPTER 1

An introduction to the research carried out within the scope of this thesis

1.1. Introduction

Today, there is a growing concern about energy oriented problems as life is directly affected by energy and its consumption. Research to resolve problems related to energy is of vital importance due to rising trend of total world energy consumption as well as growing significance of environmental issues [1,2]. As a consequence of rapid technological developments and considerable population growth, energy demand of the world increases continually, hence decisive measures need to be taken in this respect [3,4]. Although there is a strong stimulation into clean energy generation technologies in recent years, the latest reports from International Energy Agency (*IEA*) clearly indicate that all the said attempts can meet only 14% of total world energy demand [5,6]. Therefore, there is a consensus among scientist that efficient utilisation and management of energy is as significant as its production. The expected exhaustion of energy sources in the near future forces both developed and developing countries to rechecked their energy policies regarding energy production and consumption [7,8]. Recent research of *IEA* reveals that building sector plays a significant role on global energy use, and hence environmental impacts [9]. It is reported by Perez-Lombard et al. [3] and Liu et al. [10] that buildings are responsible for about 20–40% of total energy consumption in the world. A similar output is given by Kolokotsa et al. [11] with 40%. In another work, Zhao and Magoules [12] note that 40% of total energy use in Europe is

attributed to building sector as well as 36% of total CO_2 emissions. Sadineni et al. [13] report almost the same situation for the United States. Therefore, building sector is considered as a key solution to be able to reduce primary energy consumption of the world [14]. Moreover, buildings have a long life span lasting for 50 years or more. Hence, minimisation of energy consumption levels of buildings has a notable potential to contribute in mitigating greenhouse gas concentrations for longer periods.

It is unequivocal in literature that the majority of energy consumed in buildings belongs to heating, ventilation and air conditioning (*HVAC*) systems [15]. According to Perez-Lombard et al. [16] *HVAC* systems are the most energy consuming devices, accounting for about 10–20% of final energy consumption in developed countries. Today, conventional *HVAC* systems still dominate the current market, and their dramatic role in total energy consumption is expected to remain high in the near future due to their insufficient efficiency range. Therefore, key solutions are definitely required to develop novel *HVAC* systems or at least to enhance their existing performance characteristics in a cost-effective, sustainable and environmentally friendly manner [17]. In addition, substantial improvements in overall performance of *HVAC* systems are needed to be able to meet the latest requirements of building energy codes invoked by developed and developing countries [16,18]. Finding novel ways to reduce energy consumption in buildings without compromising comfort and indoor air quality is important, and as discussed previously *HVAC* systems are of significant relevance. Energy efficient *HVAC* systems can be developed by re-configuring conventional systems in order to make more strategic use of existing system components [19]. Alternatively, novel material and design based solutions can be provided to improve practicality and reliability of existing *HVAC* systems. Furthermore, collaborative solutions such as enhancing heating and cooling efficiency of any *HVAC* unit via

constructional and operational optimisation can remarkably contribute in reducing both energy consumption levels and greenhouse gas emissions related to buildings [20].

Within the scope of this thesis, innovative heating, cooling and ventilation technologies are investigated both theoretically and experimentally. Unique solutions are provided not only in design, material selection and construction but also in optimisation of operational parameters. The accuracy of the theoretical attempts conducted is verified by the state-of-the-art data in the relevant scope. Moreover, the practicality and the reliability of the technologies developed are demonstrated through several case studies which are essentially based on comprehensive experimental research. Overall, it can be concluded from the results achieved that the technologies presented have a considerable potential to mitigate energy consumption of buildings as well as greenhouse gas emissions.

1.2. Aim and Objectives

HVAC accounts for one third of the total energy consumption in most of the developed and developing countries, and current predictions indicate that this trend will go on if required measures are not taken [21]. Current *HVAC* technologies are not cost-effective and energy efficient resulting to large amounts of energy consumption in buildings. In this respect, innovative heating, cooling and ventilation technologies need to be developed to be able to meet the latest requirements of low/zero carbon buildings. Therefore in this thesis, several unique solutions of *HVAC* systems are considered for both existing buildings and new-build applications. The research firstly aims at presenting the current status of the said technologies through a comprehensive literature review following the definition of novel research problems. Afterwards, novel designs of evaporative and desiccant-based heating, cooling and ventilation systems are

evaluated both theoretically and experimentally. In addition to these, cost-effective preheating/cooling units are devised, constructed, tested and integrated with the aforesaid novel *HVAC* systems for holistic and energy efficient retrofitting purposes of existing domestic buildings. Moreover, low-cost and easy to construct and operate heating systems are introduced aiming to be potential alternatives to the conventional heating systems.

1.3. Research Methodology

The research carried out within the scope of this thesis includes comprehensive theoretical, numerical and experimental analyses of novel *HVAC* systems for domestic buildings. For the theoretical and numerical assessment, a well-known commercial software *MATLAB* is utilised. Independent *MATLAB* codes are developed for a flexible theoretical research to be able to analyse the impact of each independent variable on the relevant output parameters. Relevant comparisons are made through the previously published works for accuracy verification. The experiments conducted cover both indoor and outdoor testing of various test units. Indoor testing of the units is mainly performed in a standardised environmental chamber located in the Marmont Laboratory of the Department of Architecture and Built Environment at the University of Nottingham, United Kingdom. In those tests, conditioned ambient air is utilised to characterise the different climatic conditions and their impact on performance parameters evaluated. The measurement systems and units are selected from those of having high sensitivity and very short response time. For temperature measurements, calibrated K/T types of thermocouples are utilised to get maximum accuracy. Humidity measurements are conducted through highly sensitive and calibrated Honeywell HIH4000-001 humidity sensors. In-situ testing of said technologies is conducted in

several test houses from different climatic regions in the UK. The test houses are selected from those of occupied by residents for a more realistic and scientific approach. The in-situ tests not only cover thermal performance assessment of the said technologies but also include comprehensive thermal comfort analyses in order to demonstrate the effectiveness of each unique solution in real time operating conditions. Life cycle cost analysis is also done for the feasibility assessment of the heat recovery technology considered. Within the scope of this techno-economic analysis, the information required for the calculations such as material and labour cost, lifetime, durability and efficiency are achieved from the current market. For the demonstration of the results achieved, another well-known commercial software *SIGMAPLOT* is used.

1.4. Scope

In the scope of this thesis, theoretical, experimental and numerical investigation of novel heating, cooling and ventilation technologies are presented. In this section, a brief summary of the research conducted in the following chapters is given as underlying the objective, methodology and key outputs.

1.4.1. Chapter 2

Heat recovery systems are very promising technologies since they provide considerable energy savings in various sectors especially in domestic and industrial buildings. As clean energy generation becomes important day by day, efficient utilisation of the energy appears much more significant due to the rising cost of energy production. Therefore, heat recovery systems draw attention throughout the world for their potential of saving energy and mitigating greenhouse gas concentrations in the atmosphere. In this chapter, a comprehensive review on building applications of heat

recovery systems is presented. The review is given as a clear and understandable summary of the previous works. The review covers detailed description of heat recovery systems with working principle and system components, current typical heat recovery technologies including the building applications, theoretical, experimental and simulation works carried out for different heat recovery technologies and findings from thermodynamic performance assessment. Moreover, environmental impacts of heat recovery systems are evaluated. Future scenarios for heat recovery technologies including some recommendations are also considered in the study. It is concluded from the results that the heat recovery systems are very promising to mitigate the fuel consumption amounts of buildings. Therefore, they can remarkably contribute in reducing greenhouse gas emissions in the atmosphere. Hybrid heat recovery technologies draw attention in recent years. Heat pump and/or photovoltaic/thermal collector integrated heat recovery panels become widespread for both space heating and ventilation purposes. Current cost of the heat recovery systems is still high, but future predictions indicate that the manufacturing costs of these systems will notably decrease as a consequence of the developments in material science and technology.

1.4.2. Chapter 3

Fossil fuels still have the largest share in global energy consumption although their hazardous effects on the environment are unequivocal. The carbon dioxide (CO_2) is directly released into the atmosphere when fossil fuels such as coal, gas or oil are used. Increasing concentrations of greenhouse gases (CO_2, CH_4, N_2O) cause crucial changes in global climate such as alterations in the biogeochemistry of the global nitrogen cycle and ongoing land use/cover change. Moreover, there is a consensus among scientists that the global warming is primarily caused by the greenhouse gas

emissions. In this respect, minimisation or even stabilisation of CO_2 concentration in the atmosphere is of vital importance for mitigating global environmental problems. Recent researches indicate that the buildings are responsible for more than 30% of greenhouse gas emissions in most of the developed countries. Energy consumption levels of buildings increase as a result of economic growth, expansion of building sectors and spread of heating, ventilation and air conditioning (*HVAC*) systems. Buildings have a long life span lasting for 50 years or more and thus, minimisation of energy consumption levels of buildings has a notable potential to contribute in mitigating greenhouse gas concentrations for longer periods. Most of the energy losses in buildings occur in heating, ventilation and air conditioning systems. Therefore, recovering the waste heat from *HVAC* systems may considerably contribute to efficient energy utilisation and hence, in degrading gas emissions. Heat recovery systems (*HRSs*) provide cost-effective energy as well as environmentally friendly. A significant amount of energy can be recovered via *HRSs* while exchanging the exhaust air with fresh air. In this chapter, a solar powered *HRS* is theoretically investigated for the climatic conditions of Nottingham, UK. Fresh air temperature at the outlet of the *HRS* is determined for different values of ambient temperature, solar intensity and mass flow rate of air. Effects of main environmental parameters on electrical and thermal outputs of the *HRS* are also evaluated in the study. In recent years, several attempts have been made to analyse heat recovery systems (*HRSs*) both theoretically and experimentally. However, a detailed thermodynamic analysis of *HRSs* has not been presented so far. Therefore in this chapter, second law analysis of *HRSs* is also presented. The data required for the analyses is obtained from the previous theoretical work. Unlike the energy analysis, exergy analysis enables to take into account the qualitative effects affecting the system performance. Exergy output and exergy efficiency of *HRSs* are

determined for different types of units. The results indicate that the proposed system is very efficient to preheat the cold fresh air from outdoor environment in winter, and hence to mitigate the heating demand of buildings especially in colder climates. The system can be utilised for both ventilation and heating purposes. Maximum exergy efficiency of the system has been found to be around 60% which is very promising. This efficiency value can be enhanced via optimization of the system parameters such as duct geometry, mass flow rates of the fluids, packing factor for the solar powered unit, etc.

1.4.3. Chapter 4

Energy saving and its efficient utilisation is of prime interest in today's world due to the limited energy resources and growing significance of environmental issues. Despite the intensive efforts to narrow the gap between conventional energy sources (wood, coal, gas, oil, etc.) and renewables, renewable energy resources currently supply only about 14% of total world energy demand. In this regard, energy management and optimization are considered compulsory as much as the clean energy generation. Recent works indicate that the buildings play a significant role on global energy consumption. They are responsible for about 40% of global energy demand. Among the different building types, domestic buildings have the largest share with 63% and most of energy is utilised for heating, ventilation and air conditioning (*HVAC*) systems in those buildings. Energy consumption levels of buildings can be notably reduced through waste heat recovery in *HVAC* systems. There are several attempts in literature addressing the possibility of decreasing energy consumption of buildings via waste heat recovery technologies. The heat recovery technologies are cost effective and user friendly applications. The use of heat recovery systems aims at mitigating the energy

consumption for *HVAC* applications as well as the greenhouse gas emissions, and hence decreasing the adverse effects of global warming on the Earth. It is well-documented in literature that the heat recovery systems are very promising for domestic applications. In this chapter, experimental results of a novel heat recovery system developed for low-carbon buildings are presented. The proposed heat recovery system consists of a plate-type heat exchanger, blower fans and ducts. The parallel-flow arrangement is used to run the system. The system is designed as under roof application. The aim of the system is to recover waste heat and to preheat fresh air using stale air. The experiments of the system are carried out in winter season in Kent, UK. The study aims to investigate the coefficient of performance (*COP*) of the system as well as the heat recovery efficiency. The results show that the heat recovery efficiency of the proposed system is around 89% while the *COP* is 4.5. The proposed system can be used in both winter and summer conditions without requiring additional work. Its labour cost is extremely low, so it is cost-effective and user friendly.

1.4.4. Chapter 5

Latest research indicates that the building sector is responsible for about 40% of the total energy consumption. Most of the energy consumption occurs due to heating, cooling and ventilation demand of the occupants. In addition to this figure, day by day, the energy demand in *HVAC* sector rises as a result of technological development and desire of better thermal comfort conditions. In this respect, researchers try to find alternative solutions to minimise energy consumption and to maximise energy gained from renewables or any other sources. A recent study reveals that energy demand of new office buildings for heating and cooling applications decreases with use of renewables. On the other hand, it is achieved to reduce heating or cooling demand of a

building as using heat recovery systems. Heat recovery technology is basically utilised to mitigate the heat loss, and hence energy consumption due to *HVAC*. Within the scope of this chapter, thermal comfort analyses of a test house integrated with a novel polycarbonate heat exchanger are conducted. At pre and post-retrofit case, temperature, relative humidity and CO_2 measurements are carried out for a test period of one week. The results indicate that the internal CO_2 concentration is not at desirable range due to lack of ventilation in the test house at the pre-retrofit case. However, following the integration of the novel ventilation system into the test house, CO_2 concentration is found to be varying notably from 350 to 400 *ppm* which corresponds to the actual comfort conditions for indoor environments. It is also concluded from the results that the average relative humidity inside the test house at the post-retrofit case is found to be 57%, which is in the desired range whereas it is considerably high before retrofitting.

1.4.5. Chapter 6

Building sector accounts for about 40% of total energy consumption in the world while the share of domestic buildings is about 20-40%. The energy consumed is mostly utilised for heating, cooling and ventilation purposes. It is noted that energy requirement for cooling reached 14.6% per annum between 1990 and 2000. The energy efficiency of buildings is of prime concern for an occupant who wants to make energy saving especially in *HVAC* sector. In this instance, it is essential to focus on energy efficient technologies and solutions not only in new buildings but also in existing buildings. One of the energy efficient technologies is evaporative cooling system which is very suitable especially for hot and dry climatic conditions. In this chapter, a thorough review of different types of energy-efficient evaporative cooling systems is given. Evaporative cooling is a novel technology that supplies cool air to the occupants as well as providing

a promising way to reduce carbon emissions and energy consumption. Evaporative cooling is a concept that is defined as making air cool via increasing its water vapour content. In other words, air becomes cooler while its humidity level increases. The results show that the evaporative cooling systems have a great potential to save energy in hot and arid climatic zones. It also seems that this novel solution is a very cost effective way compared to the alternative air-conditioning applications. This technology has a good efficiency/effectiveness value as well as a good *COP* range.

1.4.6. Chapter 7

Evaporative cooling is a cost-effective, environmentally friendly and sustainable method for air cooling in residential, industrial and agricultural sectors. Evaporative cooling systems are widely used especially in arid hot climates as an alternative to conventional air-conditioning technologies. Evaporative coolers are commonly classified as direct-contact and indirect-contact evaporative coolers. In a direct-contact evaporative cooler, air stream is in direct-contact with a water film and cooling is achieved by evaporation of water into the air stream which leads to a reduction in dry-bulb temperature. However, relative humidity of the supply air stream increases in a direct-contact evaporative cooler which is not desirable for indoor thermal comfort conditions. In an indirect-contact evaporative cooler, supply air is not in direct contact with the water film and the cooling is accomplished by a plate which separates the supply air and working air. Specific humidity of the supply air stream is not affected in indirect-contact evaporative cooling, and hence indirect type coolers are primarily preferred in building sector. Therefore in this chapter, theoretical investigation of a novel indirect-contact evaporative cooling system is presented. The system mainly consists of a plate type polycarbonate heat exchanger and a water spraying unit, and it is

placed on the roof of a test house in Southeastern UK. Within the concept of this study, operating and environmental parameters such as indoor and outdoor temperatures, mass flow rates and relative humidity values of supply and working air, duct geometry of the heat exchanger are analysed in detail and their effects on overall performance of the system are discussed.

1.4.7. Chapter 8

Buildings are responsible for about 40% of total energy consumption in the world. They are also one of the biggest contributors to greenhouse gas emissions as a consequence of the existing energy market dominated by fossil fuel based energy resources. Research to mitigate energy consumed in buildings is therefore vital of importance. Further investigations related to buildings reveal that almost 60% of total energy consumption in building sector is attributed to heating, ventilation and air conditioning (*HVAC*). From this point of view, *HVAC* is considered as a key solution for remarkable energy savings in buildings. Therefore in this chapter, a novel ventilation and air conditioning system is introduced. The system basically consists of a combination of dehumidification and humidification processes. First, humid air from outside is dehumidified as passing through a desiccant filled channel, then evaporative cooling is performed to dehumidified air, and it is cooled by humidification. The humidification process is performed in a direct contact via a secondary channel equipped with absorber fibre material. Within the concept of this research, performance evaluation of the evaporative cooling part of this novel system is presented. For different temperatures of inlet fresh air, outlet temperatures are measured time-dependently and the level of cooling achieved is determined. Proper temperature and relative humidity measurements are performed for a reliable performance assessment.

The results indicate that the efficiency of evaporative cooling is very promising. Even if extreme weather conditions are considered for air at the inlet, more than 10 °C temperature difference can be obtained with a remarkably high range of *COP*. In this respect, it can be easily concluded that the system provides very promising results for hot and arid climates.

1.4.8. Chapter 9

The demand for cooling increases day by day as a consequence of the growing demand for better thermal comfort conditions in buildings. Several researchers note that the evaporative cooling is a good alternative to mechanical vapour compression for air conditioning applications since it requires about four times less electric power than vapour-compression refrigeration. The challenging point of evaporative cooling systems is that they are not able to provide the desired conditions in hot and humid areas. Therefore, additional systems such as desiccant-based cooling are required. Liquid desiccant-based evaporative cooling system is a good alternative to conventional vapour compression cooling systems to be able to control both temperature and relative humidity, especially in hot and humid environmental conditions. In this chapter, a simple mathematical model for the preliminary design of a liquid desiccant-based evaporative cooling system is presented. The modeling work is split into two sections as dehumidification process and humidification process, and for each section, governing equations of the system are given in detail. For different operating parameters such as air temperature, desiccant temperature, mass flow rates of incoming air and desiccant, humidity ratio and desiccant concentration, humidity ratio and temperature of air at the outlet, cooling level and overall system performance are predicted. The model

predictions are compared with a previously published experimental work and an excellent agreement is observed between the results.

1.4.9. Chapter 10

Clean energy generation and its efficient use are significant due to growing significance of environmental issues especially over the last four decades. Sharp increases in energy consumption as a consequence of the population growth and economic development dominate the greenhouse gas concentrations in the atmosphere. Despite intensive efforts to narrow the gap between conventional energy sources and renewables, only about 14% of total world energy demand is supplied by renewable energy technologies at the moment. In this regard, there is a consensus among scientists that research on energy management and efficient minimisation of energy consumption is compulsory. It is well-documented in literature that evaporative cooling provides efficient cooling in a cost-effective way. However, it is expected to be inappropriate for using in humid climates since the air is already close to the state of adiabatic saturation. In this respect, it is required to dehumidify the outside air before humidification. In order to meet this requirement in a cost-effective way, a novel desiccant-based evaporative cooling system (*DECS*) is devised, constructed and tested. *DECS* is able to be utilised for both cooling and air conditioning purposes with a higher range of coefficient of performance compared to alternative systems. Within the scope of this research, experimental results of desiccant-based evaporative cooling system are introduced. In this chapter, dehumidification and humidification effectiveness of a novel desiccant-based evaporative cooling system is presented. For different values of inlet supply air temperature and relative humidity provided by a standard environmental chamber, temperature and relative humidity values are measured experimentally at the

inlet and outlet of dehumidification and humidification unit, respectively. Since the main purpose of the system developed is to provide cost-effective thermal comfort conditions especially in humid climates, dehumidification effectiveness is calculated for each case tested. The results indicate that the system provides attractive findings for temperate and humid climatic conditions, where stand-alone evaporative cooling systems are inconclusive. It is concluded from the results that the dehumidification efficiency of the system is highly dependent on the air velocity. For the air velocity of 0.3 m/s , the average outlet relative humidity and air temperature are determined to be 65.5% and $29.3 \text{ }^\circ\text{C}$, respectively where the average inlet relative humidity is 94.7% and the average inlet air temperature is $38.6 \text{ }^\circ\text{C}$. The decrease in air temperature is found to be $5.3 \text{ }^\circ\text{C}$ for the whole system whereas it is $6.7 \text{ }^\circ\text{C}$ for the evaporative cooling part. On the other hand, the dehumidification effectiveness drops from 63.7 to 56.1% when air velocity increases from 0.3 to 0.5 m/s . The humidification effectiveness of the system is calculated for two velocity ranges of air. The values are 37.3 and 30.2% for the air velocities of 0.3 and 0.5 m/s , respectively. In addition to these analyses, the time-dependant *COP* changes of the whole system are also specified with respect to the different air velocities given above. The average *COP* values of the system for the inlet air velocities of 0.3 and 0.5 m/s are determined to be 5.5 and 4.8, respectively.

1.4.10. Chapter 11

Buildings are responsible for a significant part of the total world energy consumption, and cost-effective solutions to mitigate their role in energy use are therefore important. Due to poor thermal insulation characteristics of the existing conventional building elements, heating demand of current building stock worldwide is remarkable. Intensive efforts are made to reduce heating demand of buildings through

low-cost and environmentally friendly applications. However, there is a consensus among scientists that further improvements are required to meet the latest low carbon targets released by the developed countries. Therefore in this chapter, a unique heating system called moist airflow system (*MAS*) is introduced. Thermal performance assessment of the *MAS* is given through a theoretical approach based on thermodynamic optimisation, heat transfer analysis and duct diameter analysis. The results show that thermal performance of the moist airflow system is highly affected by the moist-air temperature, fan power and the working time. Furthermore, duct diameter exponentially increases with final moist-air temperature. Within the scope of this research, the duct diameter analysis of a novel heating system is also presented for three different working fluids, which are mainly air, moist-air and water. The calculations are based on a constant power input (1 kW) to the reference system and conducted for a temperature difference in the range of 50-75 °C. It is concluded from the results that the duct diameter of water based system is considerably lower than that of air based system depending on the difference in the density values. A similar tendency is observed for the duct diameter ratio of water and moist-air based heating system. For the same temperature difference, the greatest duct diameter is required by air based heating system whereas the lowest one by the water based system as a consequence of the variations in density and specific heat capacity. The cost effectiveness of the *MAS* is incomparable with conventional heating systems as the system is powered by a fan only, and uses the moist air as the working fluid.

1.4.11. Chapter 12

In this chapter, bullet points from the works conducted and future prospects are presented. For each technology considered, overall system efficiency has been

determined for different constructional and operational conditions. In addition to these, in-situ performance assessment of the said technologies has been done through research conducted in different test houses. The works carried out so far have mainly been based on residential buildings, thus further works are expected to focus on different types of buildings such as commercial, industrial and public buildings. In this respect, more complicated monitoring analyses are planned to conduct at whole building scale. In order to improve the waste heat recovery efficiency in ventilation systems, novel cost-effective and highly thermally conductive materials will be developed and utilised. The units fabricated by these materials will be both theoretically and experimentally investigated prior to retrofit to target buildings. The accuracy of the results will be verified by *CFD* simulations performed via reliable commercial software such as *ANSYS FLUENT*. Further experimental attempts will be made for an accurate performance assessment of solar powered waste heat recovery systems. Different configurations of evaporative cooling systems such as direct-contact, indirect-contact or combination of both will be evaluated in terms of different techno-economic aspects. Different fibre materials such as membrane fibres and polymer fibres will be considered to use in desiccant-based evaporative cooling systems for better liquid absorption and greater mass transfer rates. Different desiccant solutions as well as potassium formate will be used for better dehumidification performance.

CHAPTER 2

A comprehensive review of heat recovery systems for building applications

- 2.1. Introduction
- 2.2. Heat Recovery System
- 2.3. Types of Heat Recovery System
- 2.4. Applications of HRSs in Buildings
- 2.5. Theoretical Studies on HRSs
- 2.6. Simulation Works on HRSs
- 2.7. Performance Assessment of HRSs
- 2.8. Environmental Impacts of HRSs
- 2.9. Future Potential of HRSs
- 2.10. Recommendations for HRSs
- 2.11. Conclusions

CHAPTER 2

A comprehensive review of heat recovery systems for building applications

2.1. Introduction

Carbon dioxide (CO_2) is naturally absorbed by trees and plants. However, the CO_2 is directly released into the atmosphere when fossil fuels such as coal, gas or oil are used. While that is happening quickly, the plants and trees have no enough time to soak up the CO_2 dioxide and remove it from the atmosphere. Therefore, the CO_2 emissions notably rise day by day. The continued increase of the CO_2 emissions into the atmosphere is predicted to lead to crucial changes in climate [1]. Three of the well-documented global changes can be ordered as increasing carbon dioxide concentrations in the atmosphere, alterations in the biogeochemistry of the global nitrogen cycle and ongoing land use/cover change [22]. A continuous increase of the CO_2 concentrations affects the Earth's ecosystems. For instance, approximately half of the existing emissions are being absorbed by the ocean and the land ecosystems [1,23]. On the other hand, certain gases in the atmosphere such as CO_2 , methane (CH_4) and nitrous oxide (N_2O) absorb some of the energy radiated from the Earth and trap that energy in the atmosphere. Those gases which are commonly called as greenhouse gasses make the surface of the Earth warmer because of behaving like a blanket. Since the early 20th century, the surface temperature of the Earth has risen by roughly 0.8 °C, with about two thirds of that aforementioned rise happening since 1980 [24]. It is a fact that deforestation for agricultural use, directly affects the greenhouse gas concentration in

the atmosphere so, it causes rising in the surface temperature of the Earth which is known as global warming. In this respect, stabilisation of gas concentrations in the atmosphere is considered as a first goal to achieve in developed and developing countries. Then, broad societal needs have focused attention on technologies that can reduce ozone depletion, greenhouse gas emissions and fossil fuel usage [25]. In other words, it is necessary to incline new alternative energy technologies in order to overcome or mitigate hazardous effects of global warming.

There is a growing concern about energy use and its impacts on the environment. The latest reports of the Intergovernmental Panel on Climate Change (*IPCC*) have enhanced the public awareness of energy use and its environmental impacts [26–28]. Furthermore, intensive efforts are made in recent years to expand the proportion of alternative energy resources in global energy production. However, fossil fuel based energy consumption still predominate with a lion's share and hence, renewable energy sources are not able to supply the global energy demand. From this point of view, minimisation of energy consumption levels in all sectors has become significant in the last decades. In the early 21st century, energy consumption levels were specified by sector and the results interestingly indicated that buildings play an important role on global energy consumption. Moreover, buildings are responsible for a 20–40% of the total annual energy consumption of the world [3,10]. It is also reported that buildings account for more than 30% greenhouse gas emissions in most of the developed countries. On the other hand, energy consumption levels of buildings increase as a result of economic growth, expansion of building sectors and spread of heating, ventilation and air conditioning (*HVAC*) systems. It is reported that electricity consumption of heating, ventilation and air conditioning (*HVAC*) typically accounts for around 40% of the total building energy consumption [29]. Buildings have a long life span lasting for

50 years or more and hence, minimisation of energy consumption levels of buildings has a notable potential to contribute in mitigating greenhouse gas concentrations for longer periods. Most of the energy losses in buildings occurs due to heating, cooling and ventilation. Therefore, recovering the waste heat from *HVAC* systems may considerably contribute to efficient energy utilisation and hence, in degrading gas emissions.

2.2. Heat Recovery System

Heat recovery system (*HRS*) provides cost-effective and environmentally friendly energy. Buildings consume energy mainly for cooling, heating and ventilation [30]. In this regard, the aim of heat recovery systems is to mitigate the energy consumption and cost of operating a building by transferring heat between two fluids [31]. Therefore, it saves significant amount of energy while exchanging the exhaust air with fresh air for domestic use. For Sweden and Germany, the first use of heat recovery from ventilation air in dwellings began in 1979 and 1976, respectively [32]. This was due to 1970s energy crisis and new building codes. The rapid rise in energy costs has followed that energy crisis. As a consequence, people develop new and more efficient appliances such as *HRSs* to reduce the energy consumption of buildings. The buildings are constructed as more tightly and well insulated to help saving energy [33]. The main aim of *HVAC* design in buildings is to supply comfortable indoor environment and good indoor air quality for occupants during different weather conditions [21,34]. Ventilation air is the major source of moisture load in air conditioning. For instance, ventilation air constitutes approximately 68% of the total moisture load in most commercial buildings as seen in Figure 2.1. For this reason, *HVAC* system is required to remove the moisture from the life space. It is a fact that in most of the countries, the energy consumption by

HVAC sectors account for one third of the total energy consumption of the whole society [21]. Therefore heating, cooling and ventilation of buildings using heat recovery become more significant in recent years since it contributes in decreasing energy demand for *HVAC*.

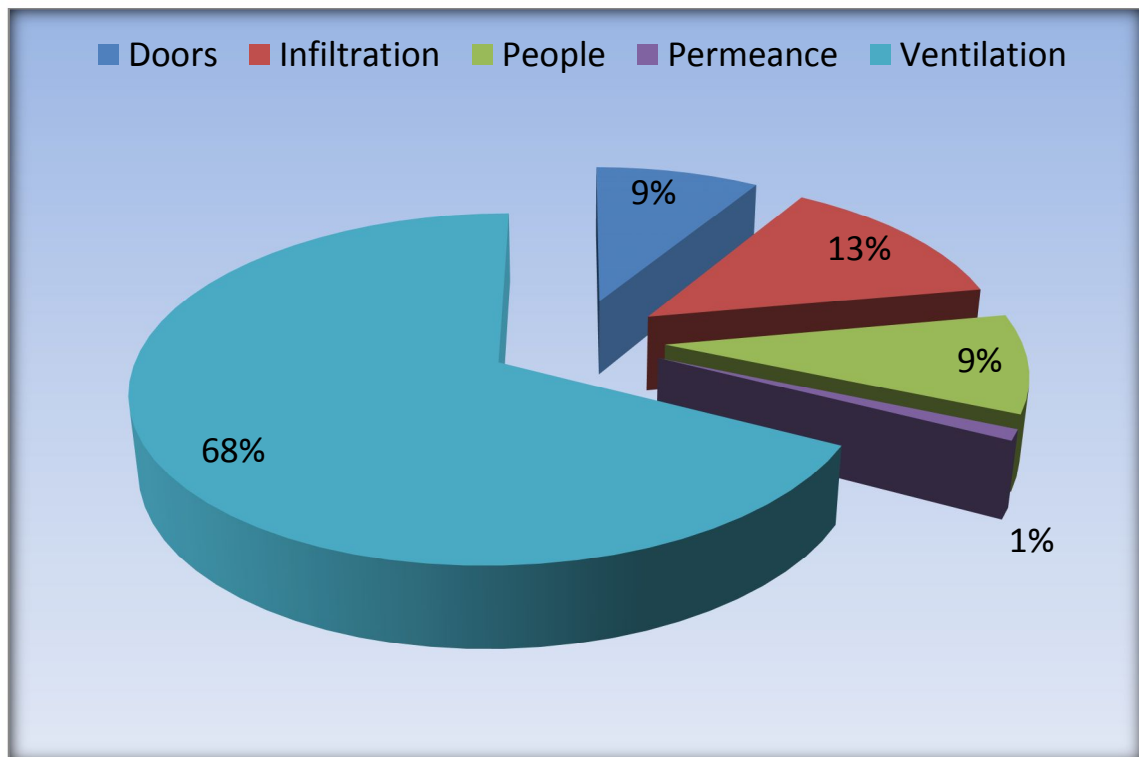


Figure 2.1. Sources of moisture loads in a medium size retail store [21].

Heat recovery term is commonly known as an air-to-air heat or energy recovery system which works between two sources at different temperatures. In other words, it is based on heating the incoming air via the recovered waste heat and hence, decreasing the heating loads. Heat recovery systems have many types to transfer waste energy from the exhaust air to the incoming air. However, all those heat recovery systems generally fall into two main categories namely sensible heat recovery systems and enthalpy heat recovery systems. A typical heat recovery system in buildings consists of channels for incoming fresh air and outgoing stale air, a heat exchanger core and blower fans. Roof

space is generally considered for the mounting of heat recovery systems. Current heat recovery systems are able to recover about 60–95% of the waste heat which is very promising. *HRSs* have a significant potential to reduce the heating demand of buildings in a cost-effective way. The need of effective ventilation for the places without window like bathrooms and toilets can also be maintained by heat recovery technologies [35].

2.2.1. Working principle

A heat recovery system is designed to supply conditioned air to the occupied space to continue the desired level of comfort [31]. *HRS* keeps the house fully ventilated by recovering the waste heat which is coming from inside environment [36] as seen in Figure 2.2. *HRS* basically works as transferring the thermal energy (enthalpy) from one fluid to another fluid, from one fluid to one solid or from a solid surface to a fluid, at different temperatures and in thermal contact. In addition, there is no direct interaction between fluid and fluid or fluid and solid in most of the *HRSs*. Some of *HRSs* allow fluid leakage from one fluid to the other due to pressure differences [37].

The building code requirement is roughly 0.57 cubic meter per minute of outside air for each individual, as it is shown in Table 2.1 for each structure. To calculate the total fresh air demand of building, that amount is multiplied by the number of occupant living in the aforementioned building. That figure can be increased depending on the entire fresh air demand of building. The calculation of air required is very crucial to provide a comfortable space for individuals. Moreover, if more air is supplied into a room than is extracted of a room, the room gets positively pressurised. If just the opposite of that case occurs, the room gets negatively pressurised. Therefore, there is a necessity to have an automatic control system for *HRS*. On the other hand, although *HRS* is designed to satisfy the maximum cooling and heating loads at design conditions,

the system is not adjusted to work at full capacity due to changes in outside temperature [31,34]. That's why temperature control plays an important role to operate the *HRS* in climate change. The temperature control in a space is commonly done by thermostat which helps to set to the requested temperature value or setpoint. The automatic control system is widely used for *HRS* to eliminate the need for constant human monitoring of a process, thus, it provides more consistent and better performance whereas decreasing the labour costs [38].

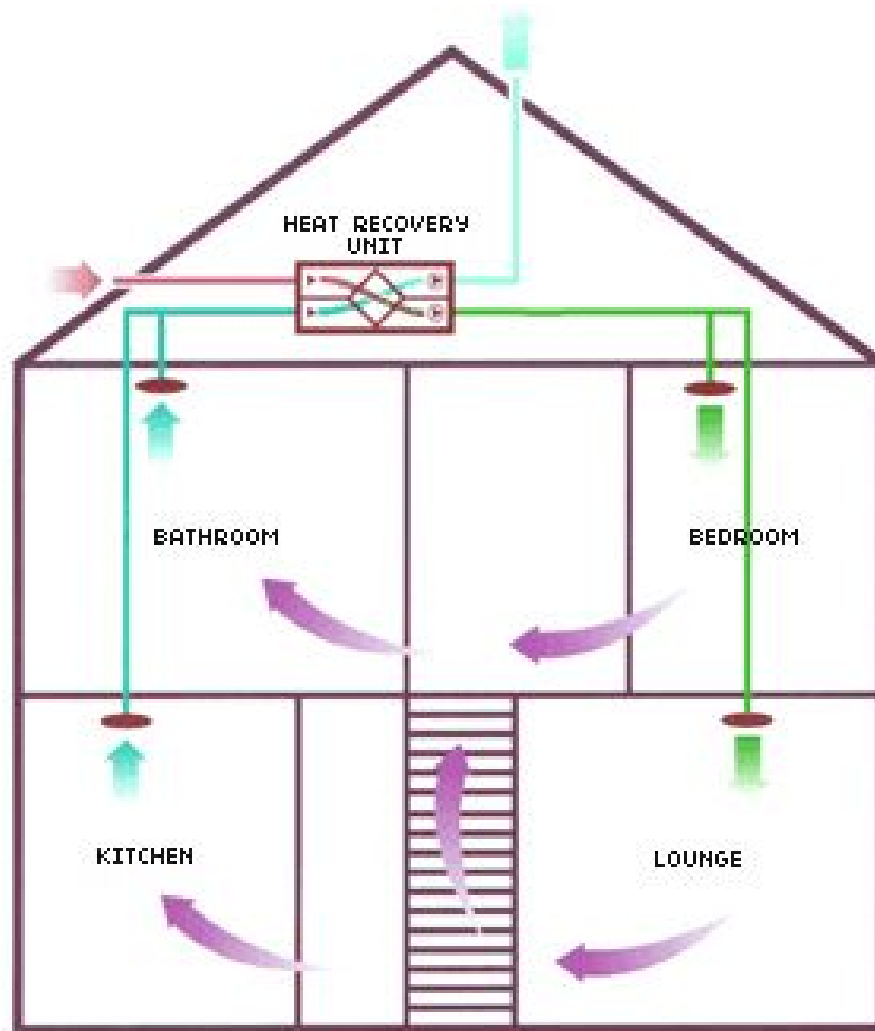


Figure 2.2. Typical heat recovery system [36].

Table 2.1. Fresh air requirements [33,39]

Type of building	Minimum air change per hour (minutes)	CMA * per minute per occupant
Attic spaces (for cooling)	12-15	
Auditoriums	8	0.57-0.85
Boiler rooms	15-20	
College classrooms		0.57-0.85
Dining rooms (hotel)	5	
Engine rooms	4-6	
Factory buildings (ordinary manufacturing)	2-4	
Factory buildings (extreme fumes or moisture)	10-15	
Foundries	15-20	
Galvanizing plants	20-30	
Garages (repair)	20-30	
Garages (storage)	4-6	
Homes (night cooling)	9-17	
Hospitals (general)		1.13-1.42
Hospitals (children's)		0.99-1.13
Hospitals (contagious diseases)		2.27-2.55
Kitchens (hotel)	10-20	
Kitchens (restaurant)	10-20	
Libraries (public)	4	
Laundries	10-15	
Mills (paper)	15-20	
Mills (textile-general buildings)	4	
Mills (textile-dyehouses)	15-20	
Offices (public)	3	
Offices (private)	4	
Pickling plants	10-15	
Pump rooms	5	
Restaurants	8-12	
Schools (grade)		0.42-0.71
Schools (high)		0.85-0.99
Shops (machine)	5	
Shops (paint)	15-20	
Shops (railroad)	5	
Shops (woodworking)	5	
Substations (electric)	5-10	
Theatres		0.28-0.42
Turbine rooms (electric)	5-10	
Warehouses	2	
Waiting rooms (public)	4	

* Cubic meter air

2.2.2. System components

A heat exchanger core ducts and fans are the main components of a typical heat recovery system. One of fans is utilised to take fresh air in whereas another one is used to exhaust the waste air. The heat exchanger core is the meeting point of the incoming fresh air from outside and the outgoing stale air from inside. Thus, depending on the season, the fresh air is preheated or precooled by the stale air. Although the system typically works in this way, it is possible to make some modification without making any changes related to the routine progression of the system. In this respect, the *PV* or *PV/T* panels may be easily added to the building roof in order to enhance the thermal efficiency of the *HRS*. Heat recovery system is usually installed in a roof or a building facade to recover heat from the internal air before it is discharged to the outside and, warm the incoming air [35].

2.2.3. Operation and maintenance

In most of the applications, *HRSs* provide reduced energy consumption and lower annual bills while including small or no additional cost to building operations or maintenance [31]. There are different kinds of energy saving opportunities and minimising the maintenance costs of *HRS* and its subsystems. Routine checking of time clock and other equipment is very significant for accurate operation and proper programming of on-off setpoint. Another important point is repairing or replacing of damaged interior shading devices. Because, closing the interior blinds and shades decreases the heat losses in winter and solar heat gain in summer. Moreover, it is necessary to clean the ducts and clean or replace ineffective filters regularly. Furthermore, fans have to be controlled whether or not they are in the right direction.

Cleaning coils and heat exchangers is indispensable for maintenance. These play an important role on working of the system properly.

2.3. Types of Heat Recovery System

Several types of heat recovery system are used in many industries, particularly metallurgy, chemistry, etc. Heat exchangers are an important part of the heat recovery systems. Heat exchanger is an energy utilisation device which has a wide use in power engineering, petroleum refineries, food industries etc. [40–42]. Heat exchangers are split into two categories as indirect and direct contact types [37,43]. In an indirect contact heat exchanger, there is a separating wall between hot and cold fluids throughout the duct. Therefore, there is no direct contact between two fluids with different initial temperatures. This type of heat exchanger is usually called as a surface heat exchanger. In indirect contact type of heat exchanger, the extent of the process is limited by the surface area and the heat transfer rate is possible through the surface. In a direct contact heat exchanger, heat is directly transferred between hot and cold fluids. In a direct contact heat exchanger both the hot and cold fluids flow into the same space without a partitioning wall [44,45]. Broad applications of direct contact heat exchanger contain mass transfer in addition to heat transfer. Compared to indirect-contact recuperators and regenerators, direct-contact heat exchangers have very high heat transfer rates. Heat exchangers are categorised as tubular, plate-type, extended (finned) surface and regenerators with regard to their construction properties [37,45,46] as it is clearly shown in [Figure 2.3](#).

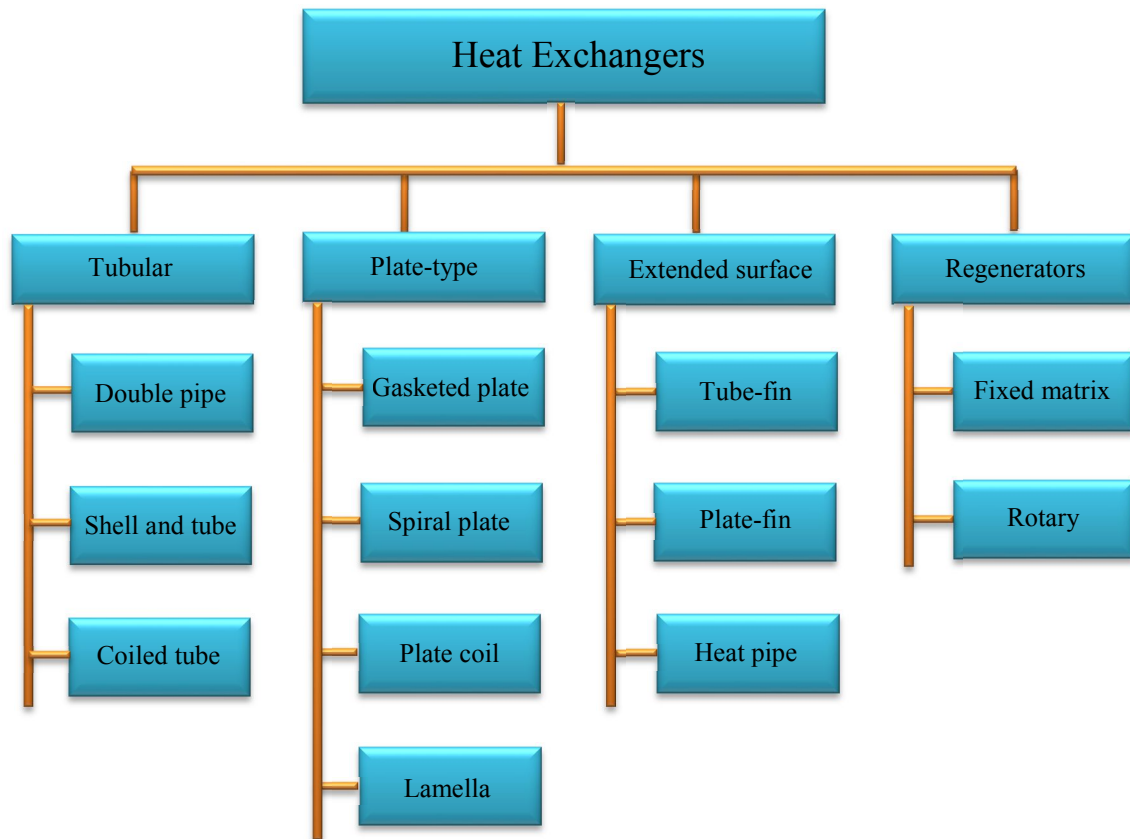


Figure 2.3. Classification of heat exchangers [37,46,47].

2.3.1. Tubular heat exchangers

Tubular heat exchangers are usually built of circular tubes despite the applications of rectangular, elliptical or round/flat twisted tubes [37,47]. One fluid flows inside the tubes while the other one flows on the outside of the tubes. It is also possible to make a change on their design. Tubular heat exchangers are classified as double pipe, shell and tube and coiled tube heat exchangers.

2.3.1.1. Double pipe

A double pipe heat exchanger basically comprises a tube or pipe fixed concentrically inside a larger pipe or tube as it is clearly illustrated in Figure 2.4. One fluid flows in the inner pipe while the other fluid flows in the annulus between pipes in

a counter-flow direction for the ideal highest performance for a given surface area [37]. A number of double pipe heat exchangers can be connected in various series and parallel arrangements to meet pressure drop and mean temperature difference requirements. Their regular applications are suitable for small works requiring, typically less than 30 m^2 because it is expensive on a cost per unit surface area basis [46–48].



Figure 2.4. A double pipe heat exchanger [49].

2.3.1.2. Shell and tube

Shell and tube type heat exchangers are usually constructed as a bundle of round tubes mounted in a cylindrical shell with the tube axis parallel to that of the shell as it is shown in Figure 2.5 [37,47]. One fluid runs through the tubes whereas other one flows over the tubes to transfer the heat between two fluids. In many process based industry, that type of heat exchangers are used by more than 90% due to their robustness and

capacity to handle high-pressure processes [46,50,51]. Moreover several different internal constructions are available for shell and tube type heat exchanger. In addition, there is actually no limit on the operating temperature and pressure. However, shell and tube construction is proposed for a small condensing unit. In medium size, for instance, that works more effectively [33].



Figure 2.5. Shell and tube type heat exchangers [52,53].

2.3.1.3. Coiled (spiral) tube

Coiled tube heat exchangers as it is seen in Figure 2.6 consist of one or more spirally wound coils fitted in a shell [37]. The heat transfer coefficient of a coiled tube heat exchanger is higher than that of a straight tube heat exchanger. This type of heat exchanger is also eligible for thermal expansion and clean fluids due to impossibility of cleaning process [47]. Aluminium alloys for cryogenics and stainless steels for high temperature applications are generally used as a material for coiled tube heat exchangers [46]. Therefore, they are expensive heat exchangers in terms of the material costs, high labour input in winding the tubes and the central mandrel.



Figure 2.6. Titanium (left) and copper (right) coiled tube heat exchangers [54,55].

2.3.2. Plate-type heat exchangers

Plate-type heat exchangers are constructed from thin plates which form flow channels. That type of heat exchanger is used for transferring the heat for any combination of gas, liquid and two-phase streams [47] and it uses metal plates to carry out the heat transfer. Plate-type heat exchangers are not suitable for very high pressures, temperatures or pressure and temperature differences [37]. These heat exchangers have a less wide use compared to the tubular heat exchangers. Plate-type heat exchangers are classified as gasketed plate, spiral plate, plate coil and lamella heat exchangers.

2.3.2.1. Gasketed plate

Gasketed plate heat exchanger consists of a few rectangular thin plates sealed around the edges by gaskets and held together in a frame as seen in Figure 2.7. Gasketed plate heat exchangers provide a relatively compact and lightweight heat transfer surface. However, there are temperature and pressure limitations for these types of heat exchangers due to the construction details and gasketing [47]. Opening, cleaning and sterilisation processes of these types of heat exchangers are so easy. Gasketed plate

heat exchangers are the most common type of heat recovery device [35] and there is a wide range of applications for gasketed plate heat exchangers in food processing industry.



Figure 2.7. Gasketed plate heat exchangers [56,57].

2.3.2.2. Spiral plate

Spiral plate heat exchangers comprise two long and parallel strips of sheet metal as it is shown in Figure 2.8. These heat exchangers are generated by rolling those parallel plates into a spiral using a mandrel and welding the edges of adjacent plates to form channels [47] and they have large diameter because of the spiral turns [37]. Typical construction material of spiral plate heat exchangers are carbon steel, stainless steels, nickel and nickel alloys, aluminium alloys, copper alloys and titanium. They are compact and easy to install. In addition they need less installation and servicing space compared to the conventional heat exchangers. For example, surface area requirement

of spiral plate heat exchanger is approximately 20% less than that of shell and tube heat exchanger. Mechanical cleaning is possible with removal of the end covers.



Figure 2.8. Spiral plate heat exchangers [58].

2.3.2.3. Plate coil

Plate coil heat exchangers are relatively cost-effective compared to the other types of heat exchangers. They can be made into any desired shapes and thickness for heat sinks and heat sources under various operating conditions. Thus, those types of heat exchangers are used in many industrial applications. Plate coil heat exchangers also provide the optimum method of heating and cooling process vessels in terms of control, efficiency and product quality [46].

2.3.2.4. Lamella

Lamella heat exchanger consists of a set of parallel, welded, thin plate channels placed longitudinally in a shell [47]. A kind of detailed illustrative schematic of shell and tube heat exchangers is seen in Figure 2.9. However its weight is considerable less than that of shell and tube heat exchanger while they have the same duty [37]. Lamella

heat exchangers can be manufactured from carbon steel, stainless steel and titanium [46]. Although they are inexpensive than plate heat exchangers and shell and tube heat exchangers, lamella heat exchangers are less capable of them for the same work. That type of heat exchanger is generally used for heat recovery in the pulp and paper industry, chemical process industry, etc.



Figure 2.9. Lamella heat exchangers [59].

2.3.3. Extended (finned) surface heat exchangers

Extended or finned surface heat exchangers are constructed by modifying the plate or tubular heat exchangers with additional fins and hence, the heat transfer area increases. It is fact that the heat transfer coefficient on the gas side is quite lower than on the liquid side [47]. That's why; extended surface heat exchangers are usually used on the gas side to enhance the heat transfer by increasing heat transfer surface area.

Additional fins can improve the surface area by 5 to 12 times depending on the design [37]. Extended surface heat exchangers are classified as tube-fin, plate-fin and heat pipe heat exchangers.

2.3.3.1. Tube-fin

Tube-fin heat exchangers (as seen in Figure 2.10a) are used in gas to liquid exchanges. There is a notable difference between heat transfer coefficient of gas and liquid. Therefore, tube-fin heat exchanger is utilised to increase the heat transfer surface area for gas and hence, thermal conductance is balanced on both sides. In that type of heat exchanger, although round and rectangular tubes are most common, elliptical tubes are also preferred [37]. There are some of inside applications of fins whereas they are normally fixed on the outside of the tubes. Extended surfaces on the insides of the tubes are commonly used in the condensers and evaporators of refrigeration system [47].

2.3.3.2. Plate-fin

Plate-fin heat exchangers consist of fins or spacers that are inserted between parallel plates as shown in Figure 2.10b. Triangular and rectangular shapes of fins are commonly used for those types of heat exchangers to increase the heat transfer surface area. Use of fins is available for both sides in gas to gas heat exchangers while it is generally useful for gas side in gas to liquid applications. Fins are also used for pressure containment and rigidity [37]. The thickness of plates and fins usually ranges from 0.5 to 1 mm and 0.15 to 0.75 mm, respectively. The mass velocity of plate-fin heat exchangers has to be arranged as an optimum range to prevent heavy pressure drops [47]. Those types of heat exchangers have a wide range of use in various industrial

applications because of their compactness. However they are not so cheaper due to the construction process and manufacturing cost.



Figure 2.10. Tube-fin (a) and plate-fin (b) heat exchangers [64,65].

2.3.3.3. Heat pipe

A heat pipe concept was first defined by Gaugler in 1942 [60,61]. A heat pipe is a simple device which allows heat transfer from one point to another point without needing an external power supply. The heat pipe (as it is illustrated in Figure 2.11) transfers large amounts of heat via small cross-sectional area with small temperature differences [45]. It consists of an individual closed tube at both ends that partially contains a working fluid [62]. That aforementioned fluid works as refrigerant in *HVAC* applications of heat pipe. The heat pipe heat exchanger is used for gas to gas heat recovery applications. The heat pipe promises higher capacity because of its higher thermal conductance than conventional heat exchangers [63]. The heat pipe unit comprises two parts which are evaporator and condenser [35]. Heat is transferred from the hot gas to the evaporation part of the heat pipe through convective heat transfer.

Then the thermal energy is carried away by the vapour to the condensation part of the heat pipe where it transfers heat to the cold gas via convection [37]. Today, heat pipes are used in several industrial applications [60]. Heat pipe heat exchangers require very little maintenance and have low pay back period.

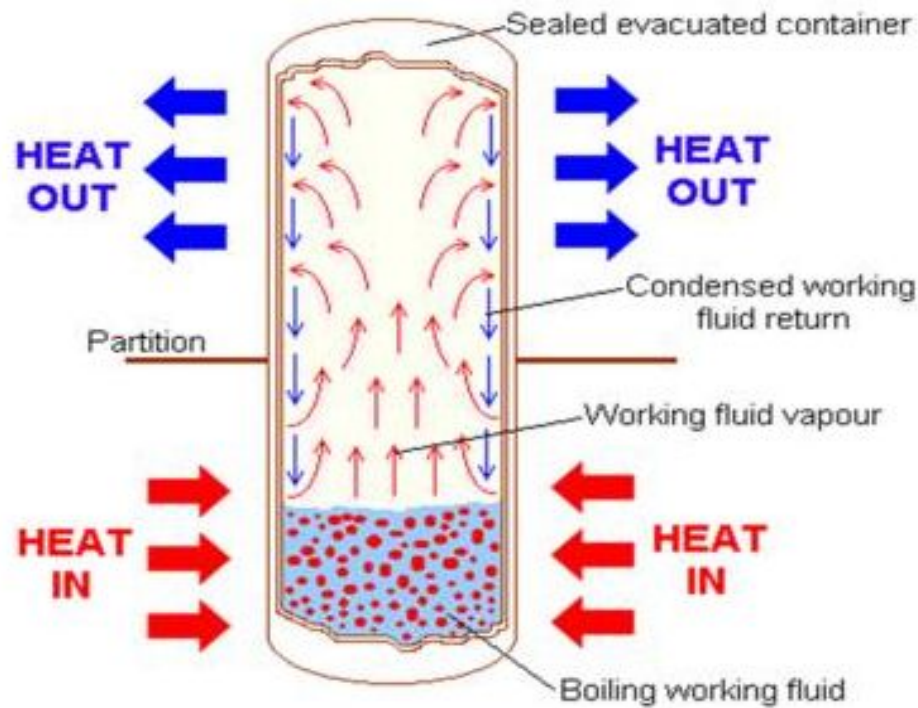


Figure 2.11. Working principle of a heat pipe [66].

2.3.4. Regenerators

The heat exchanger used to preheat combustion air is called a regenerator. The regenerator is a thermal energy storage device in which the heat storage and the heat retrieval processes are repeated periodically [60]. A regenerator comprises a matrix through which the hot stream and cold stream run periodically and alternatively [46]. In a regenerator the hot and cold streams alternately occupy the same space in the heat exchanger core [45]. Regenerators cover counter-flow, parallel-flow and cross-flow

patterns. Depending on the application, regenerators are produced from metals, plastics, nylon, ceramics and paper. Their compact surface area and the counter-flow arrangement make them fit for gas to gas applications demanding high exchanger effectiveness (at least 85% or more). Furthermore, regenerators are only used for gas to gas heat transfer for waste heat recovery applications. That means they are not used with liquid or phase-changing fluids [37]. Regenerators are split into two categories as fixed matrix and rotary.

2.3.4.1. Fixed matrix

Fixed matrix regenerator (as shown in [Figure 2.12a](#)) is referred as a periodic flow heat transfer device. It has a fixed matrix in a disk shape and streams of fluid are ducted through rotating hoods. It consists of at two or more parallel matrices. The form of matrix used varies with regard to type of the application. It has also two types of heat transfer elements called checker-work and pebble beds [37,46]. The fixed matrix heat exchangers generally utilise for too large applications up to 50 m height. Those regenerators have a wide use in the glassmaking, metallurgical and chemical processing industries [60]. They can be easily cleaned, removed or replaced. Fouling and contamination do not affect the capability of regenerator but resistance of flow.

2.3.4.2. Rotary

A rotary regenerator (as seen in [Figure 2.12b](#)) is a unit in which the storage material periodically runs from one fluid to another fluid [60]. Thus, a rotary regenerator comprises a rotating matrix driven by a motor through which the hot stream and cold stream continually flow. The performance of the rotor mainly depends on its single channels parameters and the type of flow material combinations [67]. A notable

advantage of rotary regenerators is their capability of transferring both sensible and latent heat. Both parallel-flow and counter-flow configurations can be used for this type of regenerators. Rotary regenerators are designed for high operating temperature up to 2000 °C and low pressure application 615 *kPa* or lower, depending on the construction material [46]. Gas turbine engines are typical application areas of such ultrahigh temperature rotary regenerators as reported by Shah and Sekulic [37]. They have an excessive use, especially in electrical power generating stations for air preheating [60], because of their considerable temperature efficiency mostly 80% [35]. A major disadvantage of rotary regenerator is the intermixing of two gas streams [68].

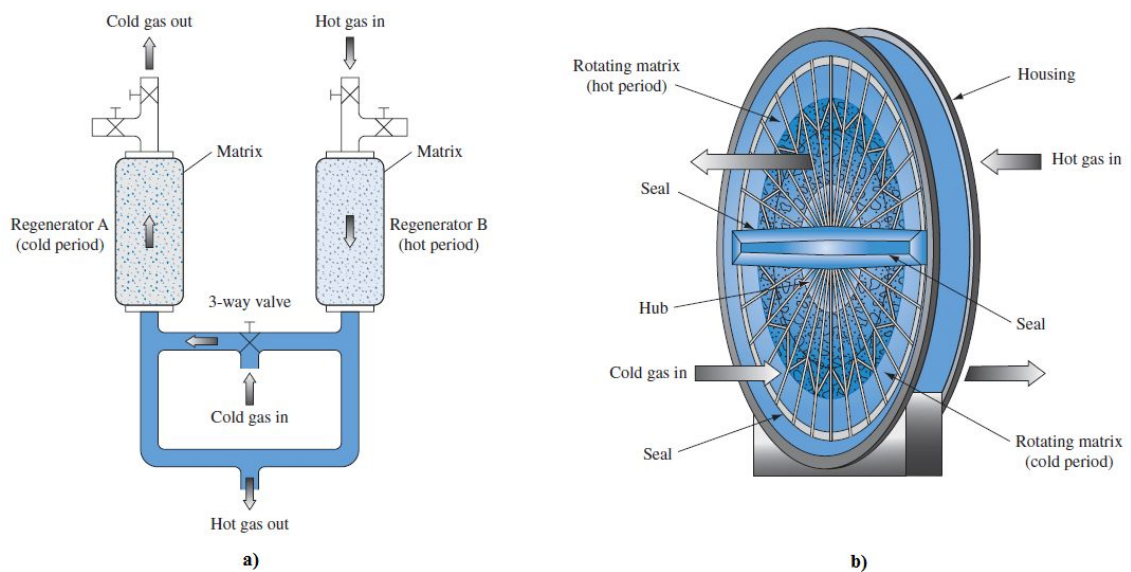


Figure 2.12. Fixed matrix (a) and rotary (b) regenerators [45].

2.4. Applications of Heat Recovery Systems in Buildings

Heating, ventilation and air conditioning (*HVAC*) systems are an indispensable necessity for comfortable and healthy indoor environment for residents of a building. However, energy saving in buildings becomes more significant due to the high energy

demand of buildings for *HVAC* systems. Recent efforts are made by researchers to reduce energy consumption used by *HRSs* and to improve the thermal efficiency of *HRSs*. Recently, Mardiana-Idayu and Riffat [69] develop an enthalpy recovery system and the performance of the system is analysed. The sensible energy efficiency is found to be roughly 66% whereas it is 59% for latent energy. Abd El-Baky and Mohamed [70] design a horizontal staggered heat pipe as it is seen in Figure 2.13. They use heat pipe heat exchanger to cool fresh air in air conditioning application. The aim of the study is to investigate the thermal performance and effectiveness of *HRS* by connecting the fresh air and stale air with heat pipe heat exchanger. The results indicate that the temperature changes of fresh and exhaust air increase with increasing fresh air temperature. The heat recovery also reaches about 85% with increasing fresh air temperature. In addition to those results, the thermal effectiveness rises with increasing fresh air temperature.

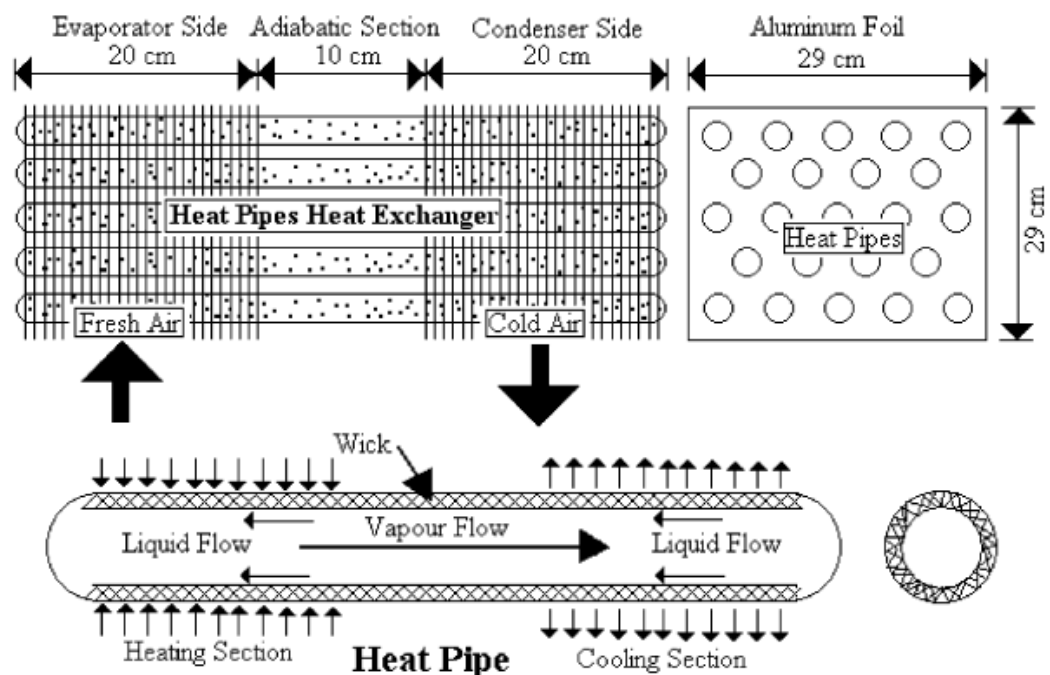


Figure 2.13. A horizontal staggered heat pipe [70].

A sensible polymer plate type heat exchanger arranged as parallel triangular ducts is used for balanced ventilation systems in residential buildings [71]. The results show that the relative humidity decreases from 95% to 34%. Under the steady-state operation, the thermal efficiency of the plate type heat exchanger and the heat transfer rate in the plate type heat exchanger (as it is illustrated in Figure 2.14) are calculated as 80% and 672 W, respectively. Buildings are getting less ventilated due to the insufficient natural ventilation and high ventilation demand of today's buildings. Lu et al. [72] develop a new type film heat recovery ventilator using a plastic film. The study aims to enhance the performance of heat recovery ventilator under cross-flow mode. The results underline that the effectiveness of the heat exchanger varies from 0.65 to 0.85 with airflow rate. The study also shows that the film vibration improves heat transfer. Pressure drop increases with air flow rate and decreases with film thickness. The quality of thermal insulation of a building and official energy saving requirements become more strict regulated [73]. However, higher indoor air quality demand of today's buildings causes increasing ventilation loss in buildings. In this regard, building designers work to construct buildings having low energy consumption and good indoor environment. Hviid and Svendsen [74] develop a heat recovery concept for innovative passive ventilation systems. The system is also devised to provide cooling for temperate climates. An illustrative schematic of the system is clearly seen in Figure 2.15. The pressure drop and heat transfer efficiency of heat recovery system are calculated as 0.37 Pa and 75.6% for a given airflow rate of 560 L/s, respectively. Persily [75] also works on air to air heat exchanger concept. The heat recovery efficiency is found to be 55 to 60%, depending on the fan speed. However, it is underlined that this efficiency range is for without considering losses in fan power and heat conduction through the metal case of the heat exchanger. Riffat and Gan [76] test the performance of three

types of heat pipe heat recovery unit. The results indicate that the effectiveness decreases with increasing air velocity. In addition to this, the effectiveness is affected by the shape of fins and pipe arrangement. Thus, poor thermal contact between fins and pipes substantially deteriorates the effectiveness of heat pipes. Air tightness of heat recovery system is so important since it directly affects system performance. Numerical calculations indicate that unintentional air flow (leakage) has an adverse effect on the performance of ventilation units since it decreases the efficiency of ventilation and heat recovery [77,78]. Another study is carried out by Hemzal [79] to identify the impacts of air leakage on thermal effectiveness of rotary heat exchangers. It is understood from the study that the heat recovery effectiveness of a rotary heat exchanger under higher pressure changes is lower than that of the well tight one. The results from one study on rotary heat exchanger show that the effectiveness increases when the time is constant and wheel speed increases [80,81].

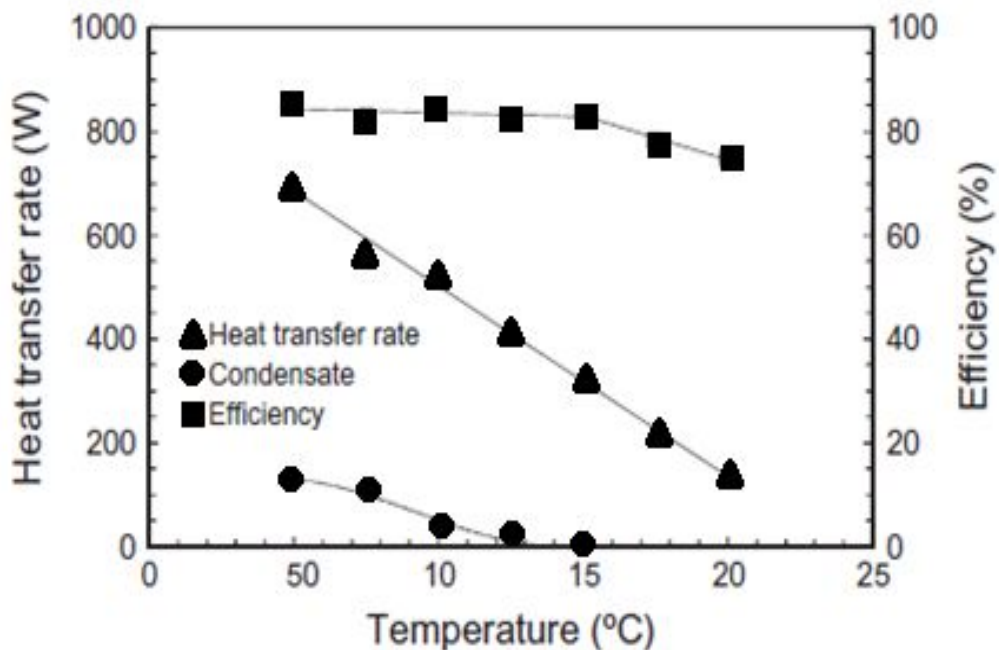


Figure 2.14. Heat transfer rate and thermal efficiency of plate type heat exchanger provided [71].

Energy consumption of buildings increases with a rapid rising in urbanisation. Therefore, it is a necessity to save this energy. It is possible to save considerable amounts of *HVAC* energy using heat recovery system. Zhong and Kang [82] carry out a study in order to estimate the applicability of energy recovery ventilators by selecting eight cities in four different climates in China. It is stressed in the study that the single heat exchanger cannot meet the energy demand in the aforementioned climate zones. Therefore, the double heat exchanger should be used in ventilation systems to adapt the requirement of energy recovering in ventilation systems. An air source heat pump system with none, single and double heat recovery capabilities is built and tested by Nguyen et al. [83]. The analyses indicate that a heat pump system with double heat recovery mechanism is the most efficient one in terms of energy saving performance compared to the other variations.

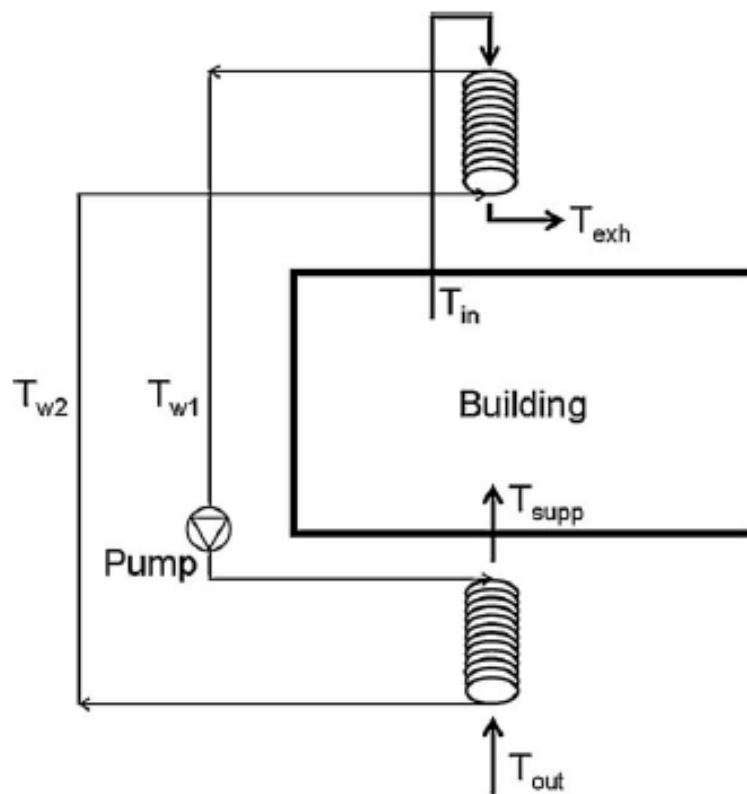


Figure 2.15. Heat recovery concept in the proposed system [74].

Martinez et al. [84] develop a mixed air recovery system including two heat pipes and indirect evaporative recuperators. Yau [85] investigates the performance characteristics of an eight-row thermosyphon-based heat pipe heat exchanger for building *HVAC* systems in Malaysia. It is recommended that, in tropical climates, *HVAC* systems should be integrated with heat pipe to enhance the dehumidification performance. Nasif et al. [86] study the thermal performance of a membrane heat exchanger in hot and humid climates. The analyses of the study indicate that an air conditioning system combined with a membrane heat exchanger consumes less energy than a conventional one as it is shown in Figure 2.16. Liang et al. [87] also present in their study that a membrane based total heat exchanger is more powerful than conventional air dehumidification systems. Zhang [88] perform a study proposing four systems in mechanical dehumidification like a heat pump, membrane enthalpy exchanger, sensible heat exchanger and desiccant wheel. According to results, the mechanical dehumidification with a membrane enthalpy exchanger spends the least energy while a sensible one consumes the most energy. A novel run-around membrane heat exchanger system is developed and tested by Mahmud et al. [89]. During the summer, the total effectiveness of a new system increases with the increasing desiccant flow rate while it decreases with growing air flow rate. The total effectiveness of the system is calculated between 50 to 55%.

A heat pipe heat exchanger is designed and tested for heat recovery in hospital and laboratories where the ventilation is crucially needed [90]. The tests are carried out using three working fluids which are acetone, methanol and water. The rotary heat pump is environmentally friendly as it uses water as the refrigerant and a gas engine to drive the system [91]. Riffat and Gillott [92] propose a novel mechanical ventilation heat recovery heat pump system for the domestic market as it is shown in Figure 2.17.

The system consists of environmentally friendly refrigerant with zero ozone depletion and low global warming potential. The system is also found to be compact and energy efficient since it saves £200 a year. Kragh et al. [93] develop a new counter-flow heat exchanger for extreme climatic conditions. That high effective mechanical ventilation system is successfully capable of defrosting itself at outside temperatures below the freezing point. The system efficiency is calculated to be about 85% and the temperature efficiency at freezing condition is 88%. In another study carried out by Manz et al. [94], the thermal efficiency is found as 78% at low electric energy input. Manz and Huber [95] achieve an experimental study for building ventilation using a duct/heat exchanger. It is observed that the concept presented in that study reaches temperature efficiency of 70%. An experimental study proposed by Nazaroff et al. [96] shows that the use of mechanical ventilation systems offers a practical, cost-effective and energy efficient indoor air quality.

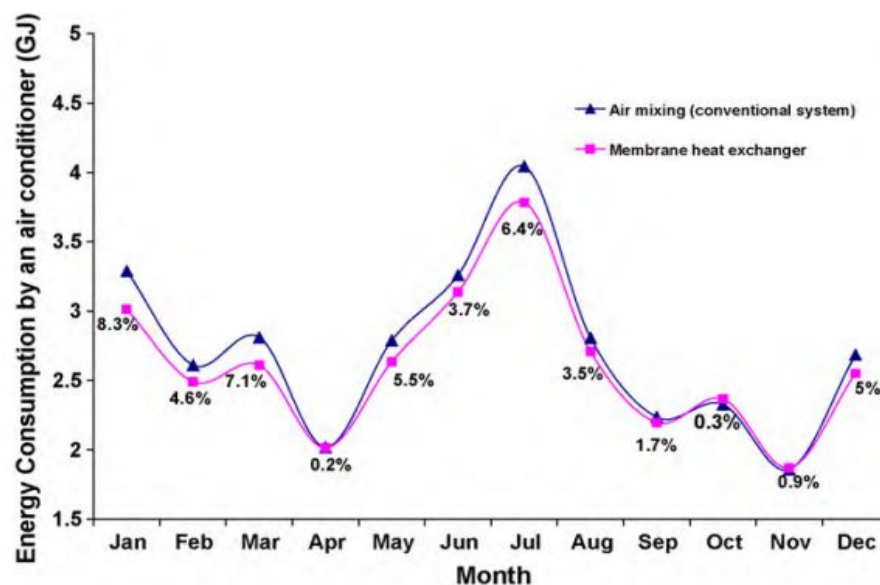


Figure 2.16. Monthly energy consumption of different air conditioners in Sydney [86].

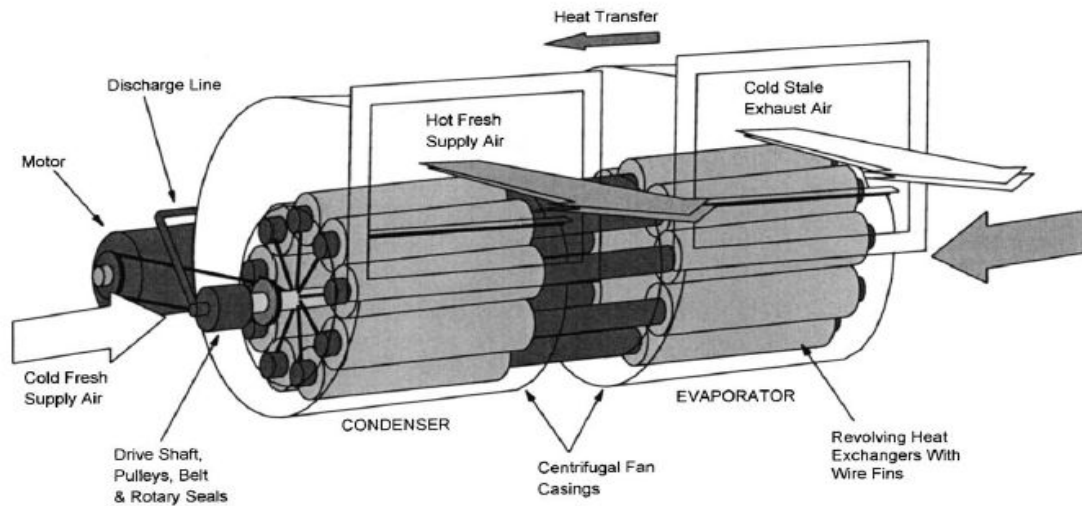


Figure 2.17. Mechanical ventilation heat recovery heat pump system [92].

In recent years, the air source air-conditioner/heat pump (*AC/HP*) system is one of the most common used heating and cooling equipment in buildings in China. The outdoor air is used as a heating or cooling thermal source by aforementioned system. A new heat recovery technique for the *AC/HP* system is urged by Gong et al. [97]. The technique uses a compound air cooling and water cooling condensing module to replace the sole air-cooling system in the conventional *AC/HP* system. The results of the experiments lasting four seasons represent that the new heat pump system works steadily and efficiently. Gu et al. [98] describe a heat recovery system using phase change materials (*PCMs*) to store the sensible and latent heat. It is observed from the analyses that the integrative energy efficiency ratio (*IEER*) of the system has an effective improvement when all exhaust heat is recovered. Besides its contribution to halt the carbon dioxide emission, *PV* systems are very promising in the upcoming future due to limited energy reserves and rapidly growing importance of environmental issues [99–108]. Sukamongkol et al. [109] carry out an experimental tests conducting

condenser heat recovery integrated with a *PV/T* air heating collector. The results show that energy saving of 18% is possible by using aforementioned system.

2.4.1. Practical applications from the University of Nottingham

Numerous works are done to date on innovative heat recovery technologies for low-carbon buildings by Sustainable Energy Technologies Research Group at the University of Nottingham. In this part of research, an overview of the previous experiences is given with the remarkable findings obtained and illustrative figures and plots. Mardiana-Idayu and Riffat [35] evaluate different opportunities of heat recovery systems for building applications. They provide a comparative analysis for system type, efficiency range and potential advantages as it is given in Table 2.2.

Table 2.2. A comparison of the types of heat recovery systems by their efficiency ranges and potential advantages [35]

System type	System efficiency	Advantages
Fixed-plate	50-80%	Compact, highly efficient due to high heat transfer coefficient, no cross contamination, can be coupled with counter-current flow which enabling to produce close end-temperature differences
Heat pipe	45-55%	No moving parts, no external power requirements, high reliability, no cross contamination, compact, suitable for naturally ventilated building, fully reversible, easy cleaning
Rotary-wheel	above 80%	High efficiency, capability of recovering sensible and latent heat
Run-around	45-65%	Does not require the supply and exhaust air ducts to be located side by side, supply and exhaust duct can be physically separated, no cross contamination

In another study, a novel enthalpy recovery system is developed by the same researchers. Throughout the research, the performance of sensible and latent energy is experimentally investigated. The photos of heat exchanger core and the test results are clearly shown in [Figure 2.18](#). Sensible energy efficiency and latent energy efficiency of the system are found to be 66% and 59%, respectively. Energy recovered is calculated to be 167 W at 3.0 m/s of air velocity with 4.3 °C temperature difference.

Liu [110] develops a novel heat recovery/desiccant cooling system as illustrated in [Figure 2.19](#) utilising plate type air-to-air heat exchanger. Several parameters are analysed in terms of their impacts on heat recovery efficiency. The results indicate that the heat recovery efficiency exponentially increases with heat exchanger length and the ratio of exchanger width to length. On the other hand, the efficiency remarkably decreases with the mass flow rate of fresh air. Cuce et al. [15,111] present a mathematical model for performance assessment of a novel indirect-contact evaporative cooling system installed under the roof of a test house. A unique polycarbonate heat exchanger is utilised and analysed in the study as shown in [Figure 2.20](#). It is understood from the results that the heat exchanger efficiency is dominantly affected by the system geometry such as the hydraulic diameter and module length, and also the operating parameters such as mass flow rates, relative humidity and temperatures of fresh and stale air.

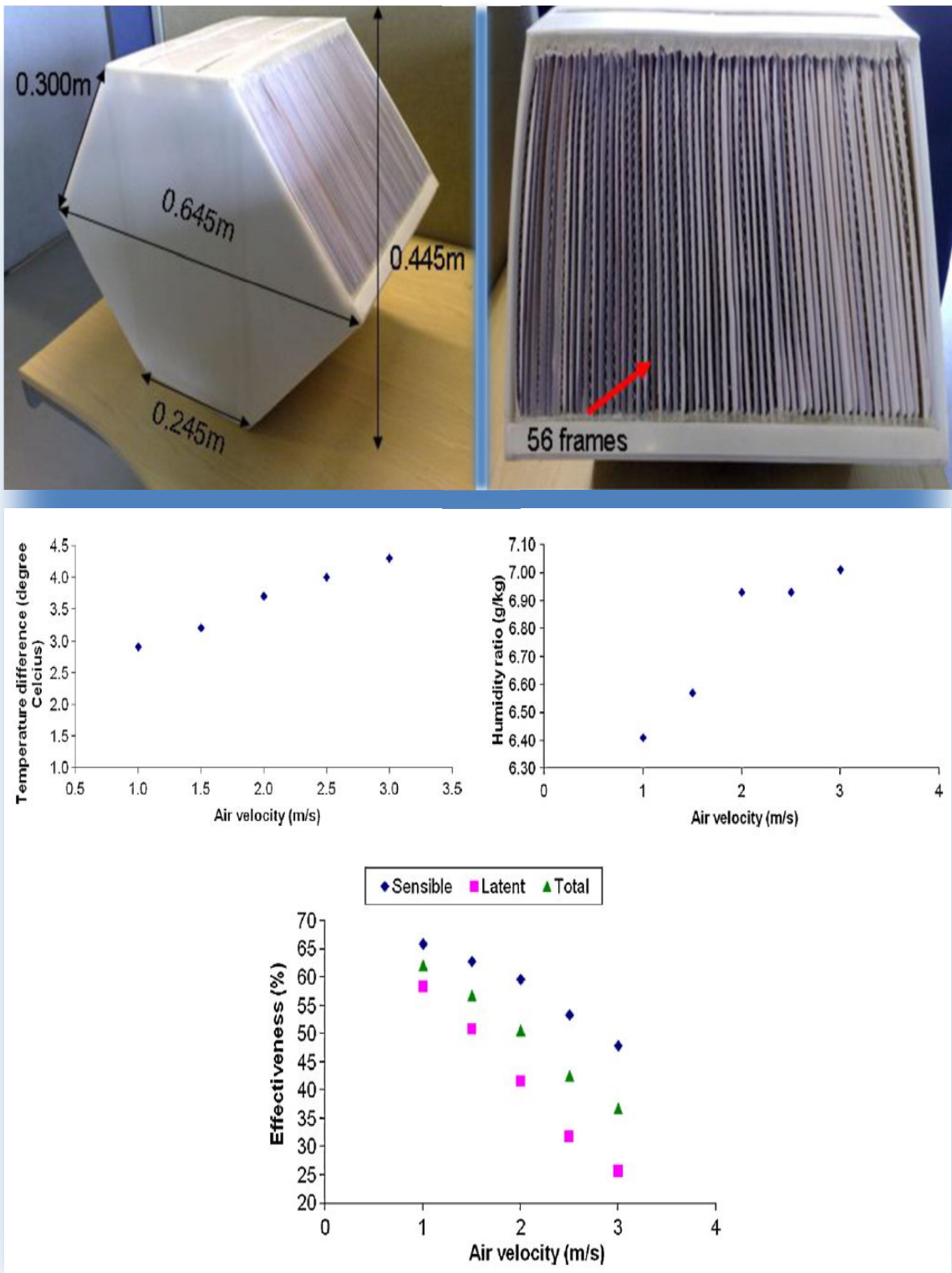


Figure 2.18. Detailed photos and the experimental results of the novel enthalpy recovery system [69].

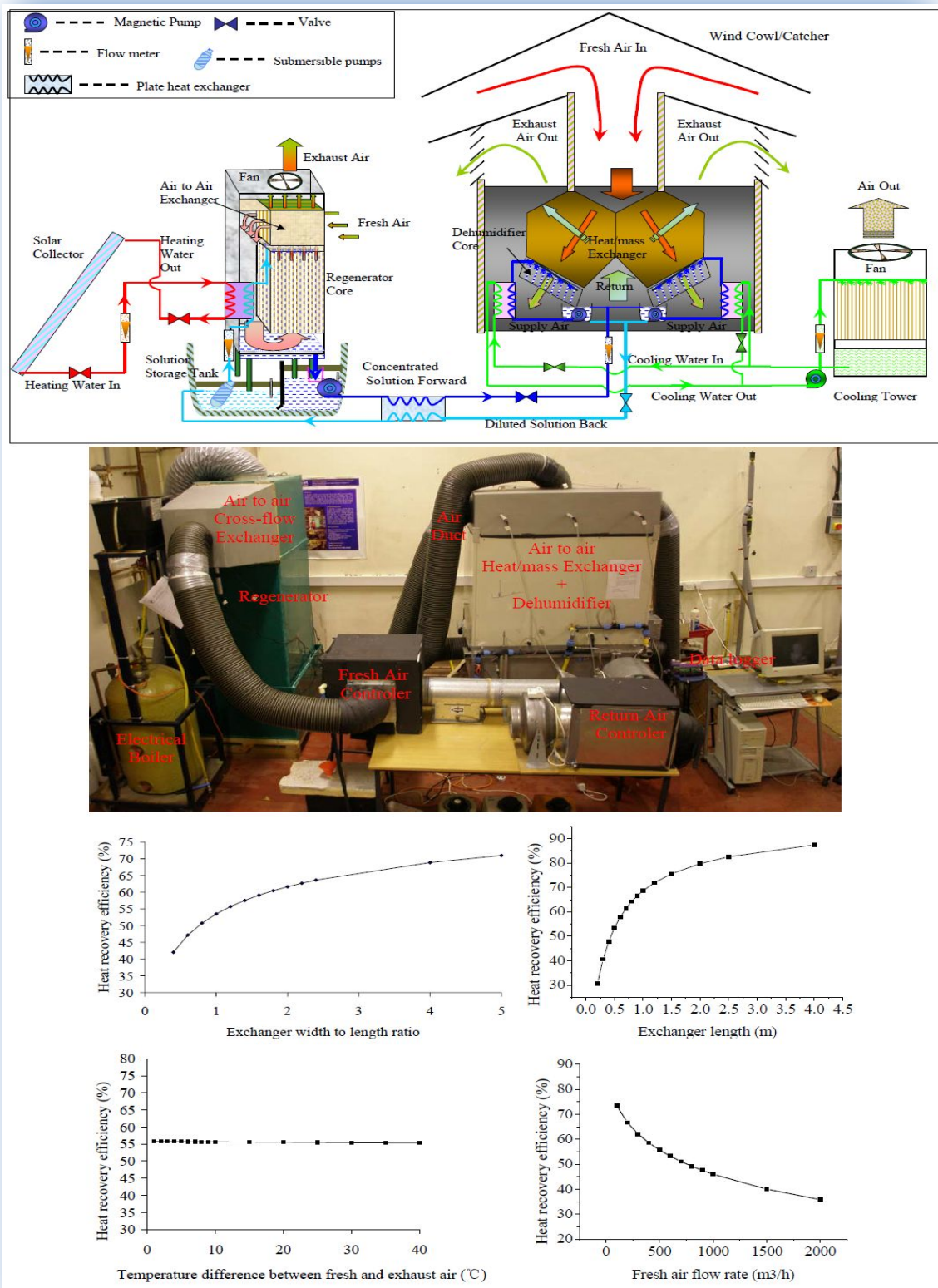


Figure 2.19. An illustrative schematic, a test rig photo and experimental results from a novel heat recovery system [110].

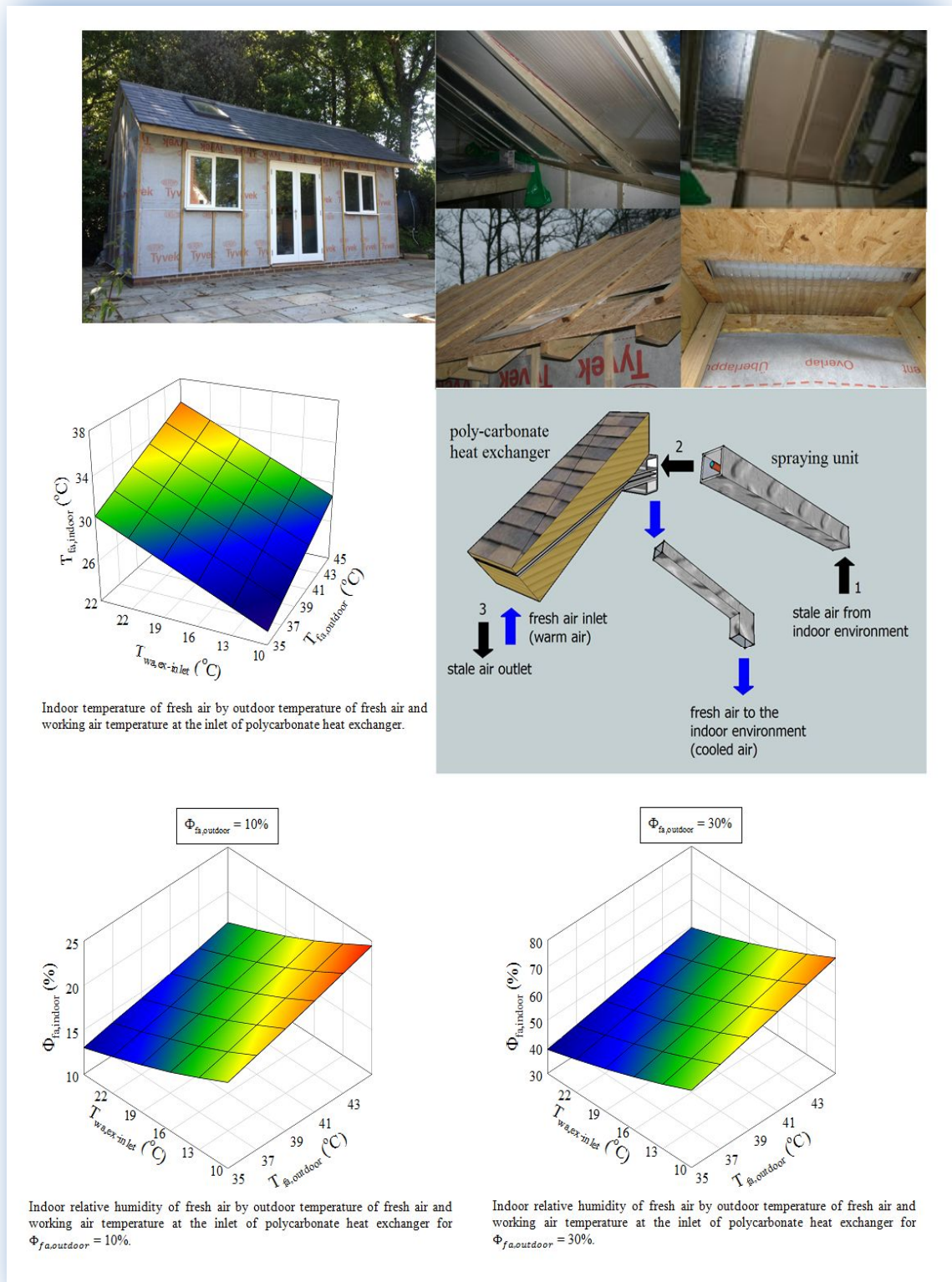


Figure 2.20. A novel evaporative cooling system including polycarbonate heat exchanger [15,111].

2.5. Theoretical Studies on Heat Recovery Systems

Several numerical studies are carried out by researchers to examine the performance, effectiveness and efficiency of the heat recovery systems. Golubovic et al. [112] present a theoretical study to evaluate the performance of rotary dehumidifier with and without heated purge. Dallaire et al. [113] numerically investigate the thermal performance of a rotary heat exchanger where its internal structure is modelled as a porous medium. Results illustrate that the performance of rotary heat exchanger severely develops by choosing proper thickness and the porosity of the internal thermal mass. In another study, the performance of desiccant wheels for air dehumidification and enthalpy recovery is compared each other [114]. Ghodsipour et al. [115] theoretically study the effect of the dimensionless parameters on the effectiveness of rotary heat exchangers, and the theoretical results are validated by comparing the experimental and theoretic results of the study. Simonson and Besant [116] improve the governing dimensionless groups for simultaneous heat and moisture transfer in energy wheels. Nobrega and Brum [117] develop a mathematical model to investigate the heat and mass transfer in rotary heat exchangers. The enthalpy wheels are found to be more efficient compared to the heat wheels. Liu et al. [118] perform an analytical study for the air and desiccant parameters inside parallel, counter and cross-flow dehumidifiers/regenerators.

Zhang et al. [119] thermodynamically model a novel air dehumidification system combined with a membrane-based heat exchanger. The study divulges that the proposed novel system saves 33% of energy. Similarly, heat and moisture transfer in membrane-based enthalpy exchangers are numerically studied by Niu and Zhang [120]. In that study, the performance of different membrane materials is compared each other. Another study is carried out by Liang et al. [121] to investigate the performance of air

dehumidification system integrated with a membrane-based heat exchanger. Min and Su [122] represent a mathematical model to analyse the performance of a membrane based energy recovery ventilator. Zhang and Jiang [123] define that the sensible, moisture and the enthalpy effectiveness find to be higher using a membrane-based energy recovery ventilator with counter-flow arrangement. A performance evaluation of building integrated photovoltaic heat recovery system is numerically performed by Bazillan and Prasad [124]. Similarly, Maffezzoni et al. [125] present a hybrid photovoltaic module combined with a heat recovery system. The energy payback period analysis of building integrated photovoltaic systems with heat recovery unit is carried out by Crawford et al. [126]. A numerical model is developed for a run-around heat and moisture exchanger system by Sayed-Ahmadi et al. [127]. Another numerical study for a run-around heat recovery system is carried out by Vali et al. [128] in order to define the effectiveness correlations of different flow arrangements. Xia et al. [43] present a modelling work for a heat exchanger under parallel-flow arrangement. Roulet et al. [78] theoretically study to predict global heat recovery efficiency using air handling unit.

2.6. Simulation Works on Heat Recovery Systems

Lin et al. [129] carry out a simulation work of dehumidification process with heat pipe heat exchangers. The results illustrate that the computational fluid dynamics (*CFD*) analyses provide rational results to predict the thermal performance of the system combined with a heat pipe. Another *CFD* study performed by Gan and Riffat [130] underlines that a heat pipe heat recovery system generates sufficient thermal comfort with minimum energy consumption in naturally ventilated buildings. Similarly, the thermal performance of heat pipe exchangers in naturally ventilated buildings is simulated by Yau [131]. On the other hand, Shao et al. [132] work on a low pressure

loss heat recovery device combined with heat pipes. The results show that the heat recovery efficiency and the pressure loss coefficient decrease with increasing air velocity.

Energy recovery ventilators (*ERVs*) transfer the energy between the stale and fresh air to mitigate the energy consumption. Recently, Rasouli et al. [133] study the effects of the *ERVs* on annual cooling and heating energy consumption. The *ERV* achieves 40% of energy saving for annual heating, depending on the climate and system effectiveness. On the other hand, the energy performance of *ERVs* is examined by Zhou et al. [134] for different climatic conditions of Shanghai and Beijing in China. The availability of *ERV* in Shanghai is found to be better than that of Beijing during the weather conditions in winter. Arias and Lundqvist [135] use a computer model to compare the potential of the heat recovery and floating condensing in supermarkets in Sweden. Results show that it is possible to save highest amount of energy using both heat recovery and floating condensing. Simonson and Besant [136] study the effectiveness correlations to predict the sensible, latent and total effectiveness of energy wheels. Sayed-Ahmadi et al. [137] similarly present the transient effectiveness of run-around membrane energy exchanger system. Jokisalo et al. [138] carry out a simulation study to investigate the performance of different mechanical ventilation systems for residential buildings in Finland. It is found that the energy efficiency of ventilation heat recovery system significantly increases in extreme climatic conditions.

2.7. Performance Assessment of Heat Recovery Systems

In literature, many attempts are made to date for performance assessment of heat recovery systems. Those works can be split into two categories as theoretical and experimental researches. In terms of theoretical approach, it can be easily said that a

heat recovery system is a particular application of the first law of thermodynamics. In this respect, governing equations characterising the energy transfer in a heat recovery system are given in this section in order to investigate the performance parameters in an analytical approach. In Figure 2.21, a schematic is illustrated for a typical heat recovery panel.

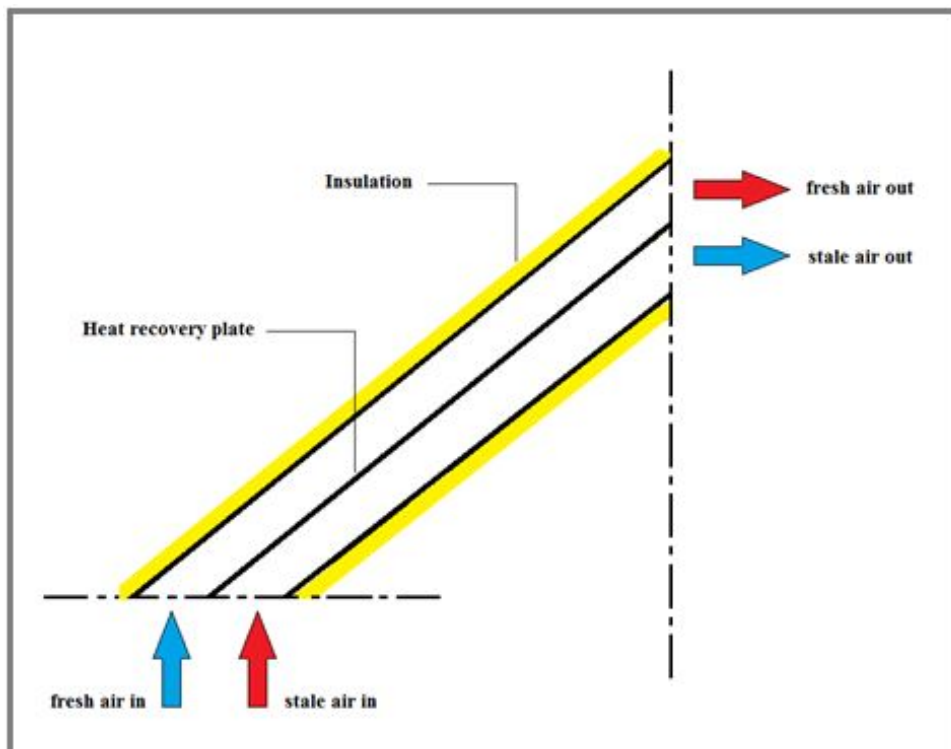


Figure 2.21. Schematic for a typical heat recovery panel [17].

The heat recovery panel can be thought of as two straight ducts with fluid flow, which are thermally connected. Let the ducts be of equal length L , carrying streams with heat capacity c_j and let mass flow rate of the streams \dot{m}_j , where the subscript j applies to stale air (sa) or fresh air (fa). The temperature profiles for the streams are $T_{sa}(x)$ and $T_{fa}(x)$ where x is the distance along the duct. The analyses are carried out for the steady-state conditions so that the temperature profiles are not functions of time. It is

also assumed that the only transfer of heat from a small volume of fluid in one duct is to the fluid element in the other duct at the same position. The amount of heat transfer along a duct due to temperature differences is neglected. Through the Newton's law of cooling, the rate of change in energy of a small volume of the stream is proportional to the difference in temperatures between it and the corresponding element in the other duct:

$$\frac{\partial u_{sa}}{\partial t} = \xi(T_{fa} - T_{sa}) \quad (2.1)$$

$$\frac{\partial u_{fa}}{\partial t} = \xi(T_{sa} - T_{fa}) \quad (2.2)$$

where $u_j(x)$ is the thermal energy per unit length and ξ is the thermal connection constant per unit length between the two ducts. This change in internal energy results in a change in the temperature of the stream element. The time rate of change for the stream element being carried along by the flow is:

$$\frac{\partial u_{sa}}{\partial t} = \psi_{sa} \frac{dT_{sa}}{dx} \quad (2.3)$$

$$\frac{\partial u_{fa}}{\partial t} = \psi_{fa} \frac{dT_{fa}}{dx} \quad (2.4)$$

where $\psi_j = c_j \dot{m}_j$ is the thermal mass flow rate. The differential equations governing the parallel-flow heat exchanger in the first part of the system can now be written as:

$$\psi_{sa} \frac{dT_{sa}}{dx} = \xi(T_{fa} - T_{sa}) \quad (2.5)$$

$$\psi_{fa} \frac{dT_{fa}}{dx} = \xi(T_{sa} - T_{fa}) \quad (2.6)$$

As it is seen from the equations that there are no partial derivatives of temperature with respect to time since the system is in a steady state. In addition, there are no second derivatives in x as is found in the heat equation since there is no heat transfer along the pipe. These two coupled first-order differential equations can be solved as follows:

$$T_{sa} = \Omega_1 - \Omega_2 \frac{\sigma_1}{\sigma} \exp(-\sigma x) \quad (2.7)$$

$$T_{fa} = \Omega_1 + \Omega_2 \frac{\sigma_2}{\sigma} \exp(-\sigma x) \quad (2.8)$$

where

$$\sigma_1 = \frac{\xi}{\psi_{sa}} \quad (2.9)$$

$$\sigma_2 = \frac{\xi}{\psi_{fa}} \quad (2.10)$$

$$\sigma = \sigma_1 + \sigma_2 \quad (2.11)$$

where Ω_1 and Ω_2 are the constants of integration. Let $T_{sa,0}$ and $T_{fa,0}$ be the temperatures at $x = 0$ and let $T_{sa,L}$ and $T_{fa,L}$ be the temperatures at the end of the duct at $x = L$. In this regard, the average temperatures in each duct can be given by:

$$\bar{T}_{sa} = \frac{1}{L} \int_0^L T_{sa} dx \quad (2.12)$$

$$\bar{T}_{fa} = \frac{1}{L} \int_0^L T_{fa} dx \quad (2.13)$$

The temperatures for the inlet and the outlet conditions are calculated as follows:

$$T_{sa,0} = \Omega_1 - \Omega_2 \frac{\sigma_1}{\sigma} \quad (2.14)$$

$$T_{fa,0} = \Omega_1 + \Omega_2 \frac{\sigma_2}{\sigma} \quad (2.15)$$

$$T_{sa,L} = \Omega_1 - \Omega_2 \frac{\sigma_1}{\sigma} \exp(-\sigma L) \quad (2.16)$$

$$T_{fa,L} = \Omega_1 + \Omega_2 \frac{\sigma_2}{\sigma} \exp(-\sigma L) \quad (2.17)$$

$$\bar{T}_{sa} = \Omega_1 - \Omega_2 \frac{\sigma_1}{\sigma^2 L} (1 - \exp(-\sigma L)) \quad (2.18)$$

$$\bar{T}_{fa} = \Omega_1 + \Omega_2 \frac{\sigma_2}{\sigma^2 L} (1 - \exp(-\sigma L)) \quad (2.19)$$

In equations, (2.14 – 2.19) choosing any two of the temperatures eliminates the constants of integration and enables to find the other four temperatures. Total energy transferred can be determined by integrating the expressions for the time rate of change of internal energy per unit length:

$$\frac{dY_{sa}}{dt} = \int_0^L \frac{du_{sa}}{dt} dx = \psi_{sa}(T_{sa,L} - T_{sa,0}) = \xi L(\bar{T}_{fa} - \bar{T}_{sa}) \quad (2.20)$$

$$\frac{dY_{fa}}{dt} = \int_0^L \frac{du_{fa}}{dt} dx = \psi_{fa}(T_{fa,L} - T_{fa,0}) = \xi L(\bar{T}_{sa} - \bar{T}_{fa}) \quad (2.21)$$

It can be clearly noted from the equations above that the sum of the energy changes is zero as a consequence of the conservation of energy. The quantity $\bar{T}_{fa} - \bar{T}_{sa}$ is known as the logarithmic mean temperature difference, and it is a measure of the effectiveness of the heat exchanger.

2.7.1. Energy analysis

El-Baky and Mohamed [70] carry out the energy analysis of heat pipe heat exchanger. The optimum effectiveness at low fresh air temperature is found to be close the experimental effectiveness as it is illustrated in Figure 2.22. The energy efficiency also reaches approximately 85% [70,93]. Similarly, it is calculated as about 80% by Fernandez-Seara et al. [71]. In another study, the efficiency is similarly found to be 75.6% [74]. A study shows that the performance could be reached 85% by modifying the heat exchanger components [113]. In contrast to these results, the efficiency is found to be between 55 and 60% depending on the fan speed [75]. A study presented by Lu et al. [72] shows that the heat exchanger effectiveness changes from 65 to 85% depending on the airflow rate. The effectiveness of heat exchangers is also studied by researchers [79–81]. In another study, the total effectiveness of system is studied. The results indicate that the total effectiveness varies from 50 to 55% [89].

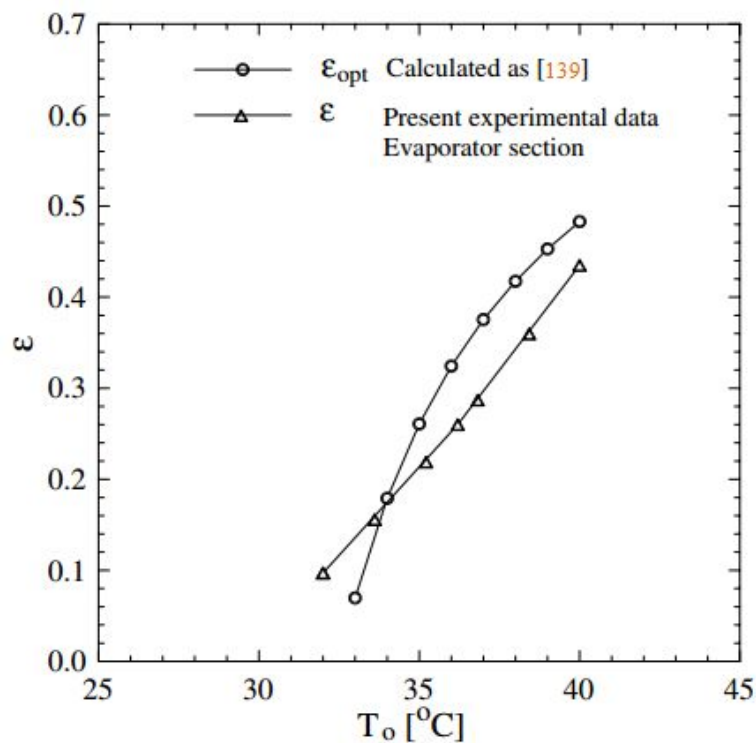


Figure 2.22. Optimum effectiveness and experimental effectiveness [70,139].

2.7.2. Exergy analysis

The second law performance of waste heat recovery based on power generation system is investigated by researchers [140,141]. It is understood from the analysis that the gas inlet temperature improves second law efficiency of the system. Exergy analysis of a ground coupled heat pump system combined with two horizontal heat exchangers is carried out by Esen et al. [142]. The results stress that the exergy efficiency mitigates with increasing outside temperature. Similarly, exergy analysis of transcritical CO_2 heat pump is achieved by Sarkar et al. [143]. Recently, exergy analysis of a cross-flow heat exchanger is performed by Kotcioglu et al. [144]. The heat exchanger efficiency decreases with the increasing air flow velocity. Yilmaz et al. [40] also present exergy based performance assessment for heat exchangers. On the other hand, the exergy transfer effectiveness for heat exchanger is described by Wu et al. [145]. Hepbasli and Akdemir [146] achieve the exergy analysis of a ground source heat pump system. Pulat et al. [147] conclude that the exergy efficiency of proposed system decreases with increasing waste fluid inlet temperature.

2.8. Environmental Impacts of Heat Recovery Systems

Energy saving is one of the key issues for both fossil fuel consumption and protection of global environment [115]. The rising cost of energy and the global warming address that development of the improved energy systems is necessary to increase the energy efficiency while reducing greenhouse gas emissions. The most effective way to reduce energy demand is to use energy more efficiently [40]. Therefore, waste heat recovery is becoming popular in recent years since it improves energy efficiency. About 26% of industrial energy is still wasted as hot gas or fluid in many countries [148]. However, during last two decades there is remarkable attention to

recover waste heat from various industries and to optimise the units which are used to absorb heat from waste gases [140,141]. Thus, these attempts enhance reducing of global warming as well as of energy demand.

2.8.1. Energy consumption

In most industrialised countries, *HVAC* is responsible for one third of the total energy consumption. Moreover, cooling and dehumidifying fresh ventilation air composes 20-40% of the total energy load for *HVAC* in hot and humid climatic regions. However, that percentage can be higher where 100% fresh air ventilation is required [21,149]. This means more energy is needed to meet the fresh air requirements of the occupants. The heat recovery is getting a necessity due to an increasing energy cost for treatment of fresh air. The main purpose of heat recovery systems is to mitigate the energy consumption of buildings for heating, cooling and ventilation by recovering the waste heat. In this regard, stand alone or combined heat recovery systems can be incorporated into the residential or commercial buildings for energy saving. Reduction in energy consumption levels can also notably contribute in reducing greenhouse gas emissions for a sustainable world.

2.8.2. Greenhouse gasses

CO_2 , N_2O and CH_4 are common greenhouse gasses and CO_2 is the most deleterious one in terms of environmental issues. Therefore the greenhouse gas emissions are frequently denoted as CO_2 equivalent emissions [150]. Total global greenhouse gas emissions increased 12.7% between 2000 and 2005 [151]. In 2005, around 8.3 Gt CO_2 was released by building sector. Moreover buildings are responsible for more than 30% of greenhouse gas emissions each year in most of developed

countries [152]. According to another study, buildings in European Union countries cause about 50% of the CO_2 emissions in the atmosphere [153,154]. It is possible to mitigate the greenhouse gas emissions by 70% compared to the levels expected to be seen in 2030 if the proper measures are taken [155–157]. The increase in greenhouse gas emissions due to high demand of energy use results to heavy environmental effects notably global warming [158]. In this regard, mitigating gas emissions in the atmosphere stands out as one of the most crucial problems of the world today that should be resolved. Heat recovery systems have a remarkable potential to contribute in decreasing greenhouse gas emissions. The Scotch Whisky Association carries out a project at Glenmorangie distillery to recover latent heat from new wash stills to heat other process waters. It is found that 175 tonnes a year of CO_2 will be saved with a payback period of under one year [159]. In another report, it is underlined that 10 MW of recovered heat can be utilised for saving €350,000 per year in emission costs [160]. UK Climate Change Act of 2008 is targeting a 34% reduction in greenhouse gas emissions by 2020 compared with 1990 levels and an 80% reduction by 2050. They emphasize the notable potential and importance of heat recovery technologies to achieve this goal [161].

2.9. Future Potential of Heat Recovery Systems

Heat recovery systems are very promising technologies since they provide considerable energy savings in various sectors especially in domestic and industrial buildings. As clean energy generation becomes important day by day, efficient utilisation of the energy appears much more significant due to the rising cost of energy production. Therefore, heat recovery systems draw attention throughout the world for their potential of saving energy and mitigating greenhouse gas concentrations in the

atmosphere. The current cost of the heat recovery systems completely depends on the technology that they have. The payback period of them varies from a couple of years to 15 years with respect to the heat recovery technology [35]. As reported by Crawford et al. [126] for a building integrated photovoltaic system with heat recovery unit, heat recovery systems have a dominant impact on reducing the payback period of the energy supplying system. Future predictions indicate that the heat recovery systems will play an important role in the energy sector as a consequence of the developments in material sciences and growing significance of environmental issues [162–165].

2.10. Recommendations for Heat Recovery Systems

As previously reported by Perez-Lombard et al. [3], heating, ventilation and air conditioning systems play a significant role in energy consumption levels of buildings. Therefore, efficient utilisation of these systems is compulsory for mitigating fuel consumption amounts, and thus the greenhouse gas emissions. Heat recovery technologies have a notable potential to reduce the energy demand of buildings especially for the colder climates such as Germany and Sweden [32,166]. Among the various heat recovery technologies, mechanical ventilation with heat recovery can be considered the most common type that enables a heat recovery efficiency of the outgoing ventilation air of about 75% [167]. However, it is well-documented in literature that the operational costs of the air-to-air heat recovery systems are quite high due to the electrical energy demand to run the fans in the system [168]. The notably high energy consumption by the fans is a consequence of the pressure drop occurring during the energy transfer from stale air to fresh air. In order to avoid this pressure drop, air treatment components, such as aftercoolers, moisture separators, dryers, and filters should be selected with the lowest possible pressure drop at specified maximum

operating conditions as recommended by McGuire [169]. Another problem for the air-to-air heat recovery systems is the disturbing noise due to the fans of the ventilation unit. Recent works indicate that heat recovery panels can be modified to work in natural or hybrid ventilation systems in order to eliminate the noise effect [74,170]. Heat recovery systems can be integrated with different systems such heat pumps, photovoltaic panels or photovoltaic/thermal collectors.

2.11. Conclusions

Heat recovery technologies are commercially available in different types, and utilised in building sector for different purposes. The previous attempts are essentially based on determining the overall performance of any heat recovery system as function of constructional and operational parameters. However, it can be easily noted that no research has been conducted so far for a thorough assessment of existing heat recovery technologies in a holistic and comparative way as mainly focusing on heat recovery efficiency, cost and application areas.

In this chapter, a detailed review on building applications of heat recovery technologies is presented. It is noted from the results that there are many different heat recovery systems in the market today. However, as previously reported by Mardiana-Idayu and Riffat [35], fixed plate, heat pipe, rotary wheel and run-around heat exchangers are the most common types, and rotary wheel heat recovery systems still have the highest efficiency levels as it is clearly illustrated in Table 2.2. The results from the literature analysis indicate that heat recovery systems have a remarkable potential to mitigate the energy demand of buildings, and thus the greenhouse gas emissions in the atmosphere. Hybrid heat recovery technologies draw attention in recent years. Heat pump and/or photovoltaic/thermal collector integrated heat recovery panels

become widespread for both space heating and ventilation purposes. Current cost of the heat recovery systems is still high, but future predictions indicate that the manufacturing costs of these systems will notably decrease as a consequence of the developments in material science and technology.

CHAPTER 3

Theoretical investigation and thermodynamic assessment of a solar powered heat recovery panel in buildings

- 3.1. Introduction
- 3.2. Methodology
- 3.3. Theoretical Investigation of an SPHRS
- 3.4. Thermodynamic Assessment of HRSs
- 3.5. Results and Discussion
- 3.6. Conclusions

CHAPTER 3

Theoretical investigation and thermodynamic assessment of a solar powered heat recovery panel in buildings

3.1. Introduction

Energy is simply defined as the ability or the capacity to do work. It is of vital importance for our relations with the environment [99,101,162]. Efforts to sort out the problems related to energy are therefore important [2]. Current scenarios indicate that the energy-based problems continue to threaten the world. Especially global warming and its dramatic environmental impacts are unequivocal. As presented in a recent report [24], Earth's average surface temperature has increased by about 0.8 °C and approximately two thirds of this increment has occurred over just the past three decades. The predictions for global warming clearly show that the urgent global measures need to be taken to stabilise greenhouse gas concentrations in the atmosphere and thus to minimise the adverse environmental effects associated with the gas emissions such as acid precipitation and stratospheric ozone depletion [171]. On the other hand, greenhouse gases are dominated by human activities like fossil fuel consumption and deforestation [27,28,172]. As a consequence of the global population growth and economic development, world energy consumption per capita dramatically increases as contributing to the pollution, environmental deterioration and global greenhouse gas emissions [173].

In recent years, intensive works have been done in order to create public awareness on some key concepts such as the trend of greenhouse gas concentrations in the atmosphere [174] and its influences on global climate [1,175]. Developed countries have offered sharp measures to achieve a notable mitigation in fossil fuel consumption levels. In addition, a strong stimulation of research into renewable energy technologies has been commenced throughout the world especially in the last decade [99,104] in order to narrow the gap between conventional and renewable energy resources due to the growing significance of environmental issues [163,176,177]. Currently, renewable energy resources supply about 14% of total world energy demand and their future potential is notable [5,6]. However, this notable progress is not still sufficient for the urgent stabilisation of greenhouse gas concentration in the atmosphere. Therefore, research on energy management as well as efficient minimisation of energy consumption has become vital more than ever in recent years.

As reported by Riffat and Cuce [106], buildings are responsible for more than 30% of greenhouse gas emissions in most of the developed countries. Buildings have a long life span lasting for 50 years or more and thus, minimisation of energy consumption levels of buildings has a notable potential to contribute in mitigating greenhouse gas concentrations for longer periods. Most of the energy losses in buildings are associated with heating, ventilation and air conditioning (*HVAC*) systems. Therefore, recovering the waste heat for *HVAC* purpose may considerably contribute to the efficient energy utilisation and hence, in degrading greenhouse gas emissions. Heat recovery systems (*HRSs*) are very promising devices in order to reduce energy consumption in buildings and thus, to mitigate the greenhouse gas emissions. The aim of *HRSs* is to mitigate the energy consumption and cost of operating a building by transferring heat between two fluids [31]. A significant amount of energy can be recovered in *HRSs* while exchanging

the exhaust air with fresh air for domestic use. Therefore heating, cooling and ventilation of buildings using heat recovery have become more significant in recent years since it has notable potential to contribute in decreasing energy demand for *HVAC*.

Heat recovery term basically corresponds to an air-to-air heat or energy recovery system which works between two streams at different temperatures. In other words, it is defined as heating the incoming air via the recovered waste heat and hence, decreasing the heating loads. Heat recovery systems include many different types to transfer waste energy from the exhaust air to the incoming air. However, all those heat recovery systems generally fall into two main categories namely sensible heat recovery systems and enthalpy heat recovery systems. A typical heat recovery system in buildings consists of channels for incoming fresh air and outgoing stale air, a heat exchanger core and blower fans. The heat recovery devices are often installed in a roof space or within the building interior. Current heat recovery systems are able to recover about 60-95% of the waste heat [35]. *HRSs* have significant potential to reduce the heating demand of buildings in a cost-effective way. The need of effective ventilation for the places without window like bathrooms and toilets can also be maintained by heat recovery technologies.

Efficient ventilation is an indispensable necessity for residents in buildings for a comfortable and healthy indoor environment. In recent years, many attempts have been made to use *HRSs* in buildings for ventilation purposes. In this respect, several experimental studies have been conducted to investigate performance assessment of *HRSs* primarily designed for ventilation. Abd El-Baky and Mohamed [70] design a horizontal staggered heat pipe to cool fresh air in air conditioning application. The aim of the study is to investigate the thermal performance and effectiveness of *HRS* by connecting the fresh air and stale air with heat pipe heat exchanger. The results indicate that the temperature changes of fresh and exhaust air increase with increasing fresh air

temperature. The heat recovery also reaches about 85% with increasing fresh air temperature. In addition to those results, the thermal effectiveness rises with increasing fresh air temperature. A sensible polymer plate type heat exchanger arranged as parallel triangular ducts is used for balanced ventilation systems in residential buildings by Fernandez-Seara et al. [71]. The results show that the relative humidity decreases from 95% to 34%. Under the steady-state condition, the thermal efficiency of plate type heat exchanger and the heat transfer rate in the plate type heat exchanger are calculated as 80% and 672 W, respectively. Lu et al. [72] develop a new type film heat recovery ventilator using a plastic film to enhance the performance under cross-flow mode. The results reveal that the effectiveness of the heat exchanger varies from 0.65 to 0.85 with airflow rate. The study also shows that the film vibration improves heat transfer. Pressure drop increases with air flow rate and decreases with film thickness. Hviid and Svendsen [74] develop a heat recovery concept for innovative passive ventilation systems with heat recovery. The system is also devised to provide cooling for temperate climates. The pressure drop and heat transfer efficiency of heat recovery system are calculated as 0.37 Pa and 75.6% for a given airflow rate of 560 L/s, respectively. Persily [75] similarly conducts a performance analysis of an air to air heat exchanger. The heat recovery efficiency is found to be 55 to 60%, depending on the fan speed. However, it is underlined that this efficiency range is for without considering losses in fan power and heat conduction through the metal case of the heat exchanger. Riffat and Gan [76] test the performance of three types of heat pipe heat recovery unit. They observe that the effectiveness decreases with increasing air velocity. In addition, the shape of fins and pipe arrangement affect the effectiveness. Thus, poor thermal contact between fins and pipes substantially deteriorates the effectiveness of heat pipes. Air tightness of heat recovery system is so important since it directly affects system performance. Numerical

calculations indicate that unintentional air flow (leakage) adversely affects the performance of ventilation units [77]. Zhong and Kang [82] carry out a study in order to estimate the applicability of energy recovery ventilators by selecting eight cities in four different climates in China. It is found that the single heat exchanger cannot meet the energy demand in the aforementioned climate zones. Therefore, it is recommended that the double heat exchanger should be used to meet the requirement of energy recovering in ventilation systems. An air source heat pump system with none, single and double heat recovery capabilities is built and tested by Nguyen et al. [83]. The analyses indicate that a heat pump system with double heat recovery mechanism is found to be the most efficient one in terms of energy saving performance compared to the other variations.

Besides the above-mentioned experimental works, some theoretical studies are conducted for analysis of *HRSs* based on ventilation purposes. Zhang et al. [119] present a thermodynamic model for a novel air dehumidification system. The system devised incorporates a membrane-based total heat exchanger into a mechanical air dehumidification system, where the fresh air flows through the enthalpy exchanger, the evaporator and the condenser subsequently. The theoretical results indicate that the system provides 33% energy saving. Zhang and Jiang [123] investigate the heat and mass transfer in a membrane-based energy recovery ventilator. Through the finite difference simulations, the temperature, and humidity fields in the unit are measured. The results show that heat and humidity would be recovered from the exhaust stream (sweep) in winter and excess heat and moisture would be transferred to the sweep in order to cool and dehumidify the incoming air (feed) in the summer. Xia et al. [43] present a mathematical model to analyse a parallel flow heat exchanger. Vali et al. [128] develop a two-dimensional steady-state numerical model to analyse the heat transfer in a run-around heat recovery system with two exchangers each with a combination of

counter and cross flow between parallel plates or membranes. It is observed that the highest overall sensible effectiveness is achieved with exchangers that have a small exchanger aspect ratio and relatively small solution flow inlet and outlet lengths. A mathematical model for the adiabatic adsorption within a hygroscopic material (silica-gel) is developed and solved by Nobrega and Brum [117]. It is revealed that even for a small mass transfer potential between exhaust and ventilation air streams, enthalpy wheels can be significantly more efficient than heat wheels, as an energy saving technique. A mathematical model is developed by Min and Su [122] to predict the thermal–hydraulic performance of a membrane-based energy recovery ventilator. The results indicate that for a fixed fan power, as the channel height increases, the total heat transfer rate initially increases, after reaching a maximum at a certain channel height, turns to decrease. Lin et al. [129] numerically investigate a heat pipe application in heat recovery systems.

Comprehensive literature review indicates that no attempt has been made to date to incorporate solar photovoltaic systems into *HRSs* for ventilation purposes in order to increase thermal energy content of the fresh air while keeping the temperature of photovoltaic cells as low as possible for better electrical output. Therefore in this study, a novel solar powered heat recovery system (*SPHRS*) is theoretically investigated for the climatic conditions of Nottingham, UK. As illustrated in Figure 3.1, the *SPHRS* consists of two parts namely heat recovery unit and solar powered unit. In the heat recovery duct, incoming fresh air is preheated via stale air coming from the indoor environment. In the solar powered duct, the preheated air is utilised to cool the photovoltaic cells while its thermal energy increases. The system presented in this chapter is offered for the winter season in order to decrease the *HVAC* cost of the buildings and increase the electrical power output of photovoltaic systems.

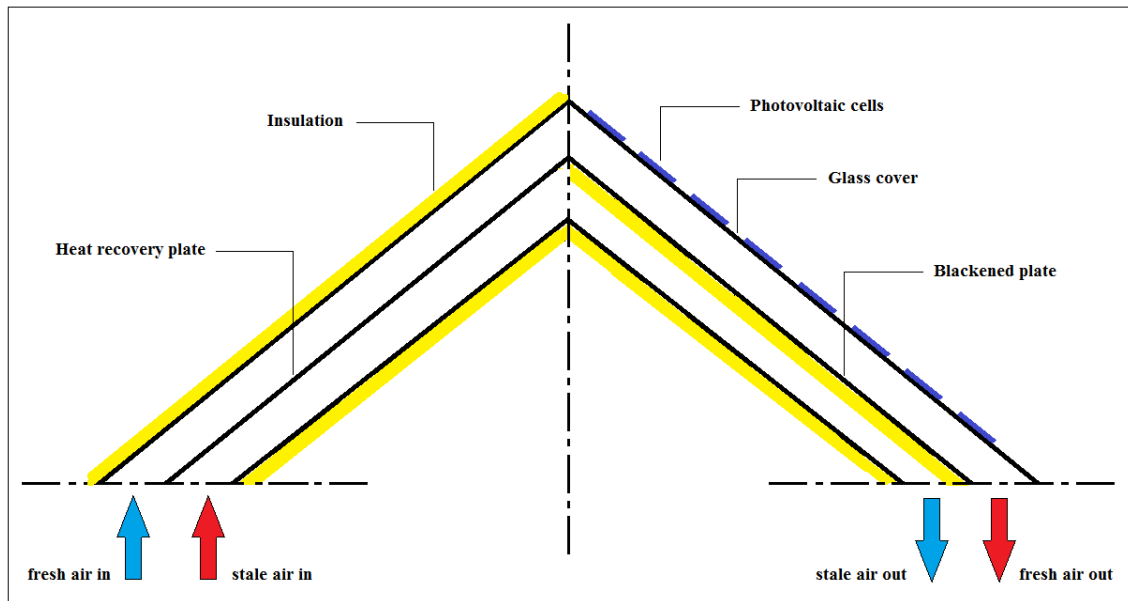


Figure 3.1. Schematic of the solar powered heat recovery system [15,111].

3.2. Methodology

The methodology adopted in this chapter is a theoretical investigation of a solar powered heat recovery system. Through the conservation principle of energy, energy equilibrium is written for air flowing through a duct which is integrated with solar panels. As it is a well-known design of air type hybrid photovoltaic thermal collectors, it is very easy to prove the reliability of the methodology. In this respect, a recent research on the said field is utilised for accuracy justification. Outlet temperature of fresh air is theoretically determined by demonstrating the waste heat recovery effectiveness from back side of PV panels to incoming fresh air. At this time of the research, the methodology is entirely based on theoretical approach.

Although the objective of this chapter is to determine the practicality and applicability of the proposed solar powered heat recovery system to be utilised in buildings, the independent variables of the research are painstakingly selected to cover various climatic conditions. For instance, inlet fresh air temperature is varied from

–5 to 5 °C to have an understanding about the feasibility of the technology developed under both severe and temperate environmental parameters. Hence, it can be easily asserted that the data collection in the research methodology is satisfactory in terms of a realistic approach.

3.3. Theoretical Investigation of a Solar Powered Heat Recovery System

A heat exchanger is a device that is used to change the thermal energy contents of two streams when they are in direct or indirect contact. A heat exchanger can be classified into two types in terms of flow directions of the streams, namely, parallel flow and counter flow. The *SPHRS* presented in this chapter is a parallel flow heat exchanger as it is understood from the flow directions in [Figure 3.1](#). Rectangular duct shape is considered in the theoretical research. Either parallel or counter flow can be preferred in the research depending on the operational requirements. The theoretical analysis of the system can be split into two categories: heat recovery from stale air and heat recovery from photovoltaic cells. In the first part, fresh air from outside is preheated via the stale air from indoor environment. Afterwards, the preheated air is used to recover the waste heat from photovoltaic cells. The proposed system aims at keeping photovoltaic cell temperature as low as possible for better electrical efficiency as well as providing heated fresh air to the indoor environment for various uses.

The first part of the *SPHRS* might be thought of as two straight ducts with fluid flow, which are thermally connected. Let the ducts be of equal length L , carrying streams with heat capacity c_j and let mass flow rate of the streams \dot{m}_j , where the subscript j applies to stale air (*sa*) or fresh air (*fa*). The temperature profiles for the streams are $T_{sa}(x)$ and $T_{fa}(x)$ where x is the distance along the duct. The analyses are carried out for the steady-state conditions so that the temperature profiles are not functions of time.

It is also assumed that the only transfer of heat from a small volume of fluid in one duct is to the fluid element in the other duct at the same position. The amount of heat transfer along a duct due to temperature differences is neglected. Through the Newton's law of cooling, the rate of change in energy of a small volume of the stream is proportional to the difference in temperatures between it and the corresponding element in the other duct:

$$\frac{\partial u_{sa}}{\partial t} = \xi(T_{fa} - T_{sa}) \quad (3.1)$$

$$\frac{\partial u_{fa}}{\partial t} = \xi(T_{sa} - T_{fa}) \quad (3.2)$$

where $u_j(x)$ is the thermal energy per unit length and ξ is the thermal connection constant per unit length between the two ducts. This change in internal energy results in a change in the temperature of the stream element. The time rate of change for the stream element being carried along by the flow is:

$$\frac{\partial u_{sa}}{\partial t} = \psi_{sa} \frac{dT_{sa}}{dx} \quad (3.3)$$

$$\frac{\partial u_{fa}}{\partial t} = \psi_{fa} \frac{dT_{fa}}{dx} \quad (3.4)$$

where $\psi_j = c_j \dot{m}_j$ is the thermal mass flow rate. The differential equations governing the parallel flow heat exchanger in the first part of the system can now be written as:

$$\psi_{sa} \frac{dT_{sa}}{dx} = \xi(T_{fa} - T_{sa}) \quad (3.5)$$

$$\psi_{fa} \frac{dT_{fa}}{dx} = \xi(T_{sa} - T_{fa}) \quad (3.6)$$

As it is seen from the equations that there are no partial derivatives of temperature with respect to time since the system is in a steady state. In addition, there are no second derivatives in x as is found in the heat equation since there is no heat transfer along the pipe. These two coupled first-order differential equations can be solved as follows:

$$T_{sa} = \Omega_1 - \Omega_2 \frac{\sigma_1}{\sigma} \exp(-\sigma x) \quad (3.7)$$

$$T_{fa} = \Omega_1 + \Omega_2 \frac{\sigma_2}{\sigma} \exp(-\sigma x) \quad (3.8)$$

where

$$\sigma_1 = \frac{\xi}{\Psi_{sa}} \quad (3.9)$$

$$\sigma_2 = \frac{\xi}{\Psi_{fa}} \quad (3.10)$$

$$\sigma = \sigma_1 + \sigma_2 \quad (3.11)$$

where σ_1 and σ_2 are the constants of integration. Let $T_{sa,0}$ and $T_{fa,0}$ be the temperatures at $x = 0$ and let $T_{sa,L}$ and $T_{fa,L}$ be the temperatures at the end of the duct at $x = L$. In this regard, the average temperatures in each duct can be given by:

$$\bar{T}_{sa} = \frac{1}{L} \int_0^L T_{sa} dx \quad (3.12)$$

$$\bar{T}_{fa} = \frac{1}{L} \int_0^L T_{fa} dx \quad (3.13)$$

The temperatures for the inlet and the outlet conditions are calculated as follows:

$$T_{sa,0} = \Omega_1 - \Omega_2 \frac{\sigma_1}{\sigma} \quad (3.14)$$

$$T_{fa,0} = \Omega_1 + \Omega_2 \frac{\sigma_2}{\sigma} \quad (3.15)$$

$$T_{sa,L} = \Omega_1 - \Omega_2 \frac{\sigma_1}{\sigma} \exp(-\sigma L) \quad (3.16)$$

$$T_{fa,L} = \Omega_1 + \Omega_2 \frac{\sigma_2}{\sigma} \exp(-\sigma L) \quad (3.17)$$

$$\bar{T}_{sa} = \Omega_1 - \Omega_2 \frac{\sigma_1}{\sigma^2 L} (1 - \exp(-\sigma L)) \quad (3.18)$$

$$\bar{T}_{fa} = \Omega_1 + \Omega_2 \frac{\sigma_2}{\sigma^2 L} (1 - \exp(-\sigma L)) \quad (3.19)$$

In equations, (3.14 – 3.19) choosing any two of the temperatures eliminates the constants of integration and enables to find the other four temperatures. Total energy transferred can be determined by integrating the expressions for the time rate of change of internal energy per unit length:

$$\frac{dY_{sa}}{dt} = \int_0^L \frac{du_{sa}}{dt} dx = \psi_{sa}(T_{sa,L} - T_{sa,0}) = \xi L(\bar{T}_{fa} - \bar{T}_{sa}) \quad (3.20)$$

$$\frac{dY_{fa}}{dt} = \int_0^L \frac{du_{fa}}{dt} dx = \psi_{fa}(T_{fa,L} - T_{fa,0}) = \xi L(\bar{T}_{sa} - \bar{T}_{fa}) \quad (3.21)$$

It can be clearly noted from the equations above that the sum of the energy changes is zero as a consequence of the conservation of energy. The quantity $\bar{T}_{fa} - \bar{T}_{sa}$

is known as the logarithmic mean temperature difference, and it is a measure of the effectiveness of the heat exchanger.

The second part of the system is simply an air type hybrid photovoltaic/thermal (PV/T) collector. In recent years, numerous attempts have been made to investigate the performance characteristics of both air and water type PV/T collectors [178–189]. In theoretical studies, several assumptions have been incorporated into the governing equations which significantly affect the results. In this chapter, a thermodynamic model is introduced to minimise the aforementioned errors arising from the assumptions. The model analyses one dimensional heat transfer which is usually considered as a good approximation for this study as previously reported by Dubey et al. [188]. The results are for the steady-state conditions. The ohmic losses in the photovoltaic cells are negligible and the glass cover has a uniform temperature.

The theoretical analysis of the second part is required to write the energy balance equations for each system component. First of all, the governing equation for photovoltaic cells is given by:

$$\alpha_{pc}\tau_{gc}\beta_{pc}G\vartheta dx = [U_{pc,amb}(T_{pc} - T_{amb}) + U_{pc,fa^*}(T_{pc} - T_{fa^*})]\vartheta dx + \eta\alpha_{pc}\tau_{gc}\beta_{pc}G\vartheta dx \quad (3.22)$$

where α_{pc} , β_{pc} and T_{pc} are the absorptivity coefficient, the packing factor and the temperature of photovoltaic cells, respectively, τ_{gc} is the transmissivity coefficient of the glass cover, G is the solar intensity, ϑ is the width of solar powered duct, T_{amb} is the ambient temperature, T_{fa^*} is the preheated fresh air temperature and η is the electrical efficiency of the photovoltaic cells. $U_{pc,amb}$ and U_{pc,fa^*} are the overall heat transfer coefficients from photovoltaic cells to ambient, and from photovoltaic cells to preheated fresh air, respectively and they are expressed as follows:

$$U_{pc,amb} = \left[\frac{\omega_{gc}}{k_{gc}} + \frac{1}{h_o} \right]^{-1} \quad (3.23)$$

$$U_{pc,fa^*} = \left[\frac{\omega_{gc}}{k_{gc}} + \frac{1}{h_i} \right]^{-1} \quad (3.24)$$

where ω_{gc} , k_{gc} , h_o and h_i are the thickness of glass cover, thermal conductivity of glass cover, external heat transfer coefficient and internal heat transfer coefficient, respectively. Photovoltaic cell temperature can be obtained through equation (3.22) as follows:

$$T_{pc} = \frac{(1 - \eta)\alpha_{pc}\tau_{gc}\beta_{pc}G + U_{pc,amb}T_{amb} + U_{pc,fa^*}T_{fa^*}}{U_{pc,amb} + U_{pc,fa^*}} \quad (3.25)$$

Evans [190], and Skoplaki and Palyvos [191] develop an expression for temperature dependent electrical efficiency of photovoltaic cells which is given by the following equation:

$$\eta = \eta_0 \left[1 - \beta_0(T_{pc} - T_0) \frac{G}{G_{ref}} \right] \quad (3.26)$$

where β_0 is the temperature coefficient, T_0 is the cell temperature at standard conditions and G_{ref} is the solar intensity at standard test conditions.

$$\beta_0 = \frac{1}{T_{hc} - T_0} \quad (3.27)$$

In equation (3.27), where T_{hc} is the (high) temperature at which the photovoltaic cells' electrical efficiency drops to zero. For crystalline silicon solar cells, this

temperature is 270 °C. The next energy balance equation should be written for the blackened plate as follows:

$$[\alpha_{pc}(1 - \beta_{pc})\tau_{gc}^2 G]\vartheta dx = [h_{bp,fa^*}(T_{bp} - T_{fa^*}) + U_{bp,amb}(T_{bp} - T_{amb})]\vartheta dx \quad (3.28)$$

where h_{bp,fa^*} is the heat transfer coefficient from blackened plate to the preheated fresh air, T_{bp} is the blackened plate temperature and $U_{bp,amb}$ is the heat loss coefficient between blackened plate and the ambient. T_{bp} can be obtained via equation (3.28) as follows:

$$T_{bp} = \frac{\alpha_{pc}(1 - \beta_{pc})\tau_{gc}^2 G + h_{bp,fa^*}T_{fa^*} + U_{bp,amb}T_{amb}}{h_{bp,fa^*} + U_{bp,amb}} \quad (3.29)$$

where

$$h_{bp,fa^*} = h_i = 2.8 + 3v, \quad v = 2m/s \quad (3.30)$$

$$U_{bp,amb} = \left[\frac{\omega_{im}}{k_{im}} + \frac{1}{h_i} \right]^{-1} \quad (3.31)$$

In equation (3.31), ω_{im} and k_{im} are the thickness and the thermal conductivity of the insulation material, respectively. Final energy balance equation is written for the preheated fresh air flowing through the second duct:

$$\dot{m}_{fa^*}c_{fa^*} \frac{dT_{fa^*}}{dx} dx = [h_{bp,fa^*}(T_{bp} - T_{fa^*}) + U_{pc,fa^*}(T_{pc} - T_{fa^*})]\vartheta dx \quad (3.32)$$

where \dot{m}_{fa^*} and c_{fa^*} are the mass flow rate and specific heat capacity of the preheated fresh air, respectively. By involving equations (3.25) and (3.29) into (3.32) under the initial conditions namely:

$$T_{fa^*}|_{x=0} = T_{fa^*,in} \quad (3.33)$$

$$T_{fa^*}|_{x=L} = T_{fa^*,out} \quad (3.34)$$

one gets:

$$T_{fa^*,out} = \frac{(\alpha\tau)G}{U_*} \left(1 - \exp\left(-\frac{U_*}{\dot{m}_{fa^*}c_{fa^*}}\vartheta L\right) \right) + T_{fa^*,in} \exp\left(-\frac{U_*}{\dot{m}_{fa^*}c_{fa^*}}\vartheta L\right) - T_{amb} \exp\left(-\frac{U_*}{\dot{m}_{fa^*}c_{fa^*}}\vartheta L\right) + T_{amb} \quad (3.35)$$

where $(\alpha\tau)$ is the product of effective absorptivity and transmissivity and U_* is the overall heat transfer coefficient for the second part of the system. $(\alpha\tau)$ and U_* are given by the following equations:

$$(\alpha\tau) = h_{p1}(\alpha\tau)_1 + h_{p2}(\alpha\tau)_2 \quad (3.36)$$

where

$$h_{p1} = \frac{U_{pc,fa^*}}{U_{pc,amb} + U_{pc,fa^*}} \quad (3.37)$$

$$h_{p2} = \frac{h_{bp,fa^*}}{U_{bp,amb} + h_{bp,fa^*}} \quad (3.38)$$

$$(\alpha\tau)_1 = (1 - \eta)\alpha_{pc}\tau_{gc}\beta_{pc} \quad (3.39)$$

$$(\alpha\tau)_2 = \alpha_{pc}(1 - \beta_{pc})\tau_{gc}^2 \quad (3.40)$$

$$U_* = \frac{U_{pc,amb}U_{pc,fa^*}}{U_{pc,amb} + U_{pc,fa^*}} + \frac{U_{bp,amb}h_{bp,fa^*}}{U_{bp,amb} + h_{bp,fa^*}} \quad (3.41)$$

The average preheated air temperature over the length of the second duct can be determined via the following equation:

$$\bar{T}_{fa^*} = \frac{1}{L} \int_0^L T_{fa^*} dx \quad (3.42)$$

$$\bar{T}_{fa^*} = \left[\frac{(\alpha\tau)G}{U_*} + T_{amb} \right] \left[1 - \frac{1 - \exp(-\Theta)}{\Theta} \right] + T_{fa^*,i} \frac{1 - \exp(-\Theta)}{\Theta} \quad (3.43)$$

where

$$\Theta = \frac{U_*}{\dot{m}_{fa^*} c_{fa^*}} \vartheta L \quad (3.44)$$

For the solution of combined system in terms of both thermal and electrical performance, $T_{fa^*,in}$ is set equal to $T_{fa,L}$ and the average preheated air temperature is numerically determined. For the temperature dependent electrical efficiency of the system, the expression of Dubey et al. [188] can be utilised.

3.4. Thermodynamic Assessment of Heat Recovery Systems

In the last decades, increasing demand of air conditioning has resulted in growing trend on energy consumption and demand. Around 80% of energy consumed is based on non-renewable energy resources such as fossil fuels [192]. Energy consumed due to HVAC is responsible for more than 20% of total energy consumption in the world. Therefore, it is important to find proper solutions to diminish the utilisation of non-renewables as to be primary energy sources. Several attempts are made by researchers to mitigate the energy consumption and thus carbon emissions during HVAC. Besides the minimisation of energy consumption, effective use of available energy plays a significant role in increasing the system performance. Moreover, effective evaluation of

heating, cooling and ventilation performance of heat recovery system is of vital importance to improve the utilisation of the energy and desired thermal comfort conditions of indoor environment [193]. In order to identify the energy performance of residential *HVAC* systems, first law of thermodynamics is applied to the system which overcomes the quantity of energy [194]. Sometimes energy analysis is not enough alone to define the effective use of energy in a process. In other words, exergy analysis helps to find location of inefficiencies accurately. Moreover, second law analysis can be used for performance optimisation of *HVAC* systems. In literature, exergy efficiency is studied by almost few researchers to make the analyses of building services in buildings such as space heating system, thermal energy storage, solar assisted domestic hot water systems etc [195]. In this study, second law analysis of thermodynamics is applied to a novel solar powered heat recovery system, and the results are analysed and discussed thermodynamically.

3.4.1. Exergy analysis of a solar powered heat recovery system

As reported by McGovern and Smyth [196], exergy analysis of a heat exchanger is straightforward if a fluid enters and leaves a heat exchanger at known states (with negligible values of specific kinetic and potential energy) and the temperature of the environment is also known. Net exergy interaction in a heat exchanger can be defined as the difference between the flow exergy function at inlet and at the outlet. In this respect, exergy efficiency of a *HRS* is determined as the ratio of the net exergy output to the net exergy input. Previously developed solar-powered heat recovery system (*SPHRS*) will be investigated within the concept of this study, and the data required for the analyses will be obtained from the mathematical model developed for the aforementioned

system. The schematic of the proposed *SPHRS* is illustrated in [Figure 3.1](#). Through the explanations above, exergy efficiency of the *SPHRS* can be written as follows:

$$\eta_{ex} = \frac{\dot{m}_{fa,in}[(\dot{h}_{fa,out} - \dot{h}_{fa,in}) - T_{amb}(s_{fa,out} - s_{fa,in})]}{\dot{m}_{sa,in}[(\dot{h}_{sa,in} - \dot{h}_{sa,out}) - T_{amb}(s_{sa,in} - s_{sa,out})]} \quad (3.45)$$

where $\dot{m}_{fa,in}$ is the mass flow rate of the fresh air, $\dot{m}_{sa,in}$ is the mass flow rate of the stale air, $\dot{h}_{fa,in}$ is the enthalpy of fresh air at the inlet, $\dot{h}_{fa,out}$ is the enthalpy of fresh air at the outlet, $\dot{h}_{sa,in}$ is the enthalpy of stale air at the inlet, $\dot{h}_{sa,out}$ is the enthalpy of stale air at the outlet, $s_{fa,in}$ is the entropy of fresh air at the inlet, $s_{fa,out}$ is the entropy of fresh air at the outlet, $s_{sa,in}$ is the entropy of stale air at the inlet, $s_{sa,out}$ is the entropy of stale air at the outlet, and T_{amb} is the ambient temperature.

The overall rate of entropy creation (\dot{S}_{gen}) is expressed as the ratio of total exergy destruction rate (Ex_{des}) to the T_{amb} as given below:

$$\dot{S}_{gen} = \frac{Ex_{des}}{T_{amb}} \quad (3.46)$$

The ratio of total exergy destruction rate can be expressed as the difference between the net rates of exergy input and output as follows:

$$Ex_{des} = \dot{m}_{sa,in}[(\dot{h}_{sa,in} - \dot{h}_{sa,out}) - T_{amb}(s_{sa,in} - s_{sa,out})] - \dot{m}_{fa,in}[(\dot{h}_{fa,out} - \dot{h}_{fa,in}) - T_{amb}(s_{fa,out} - s_{fa,in})] \quad (3.47)$$

If equation (3.46) is substituted into equation (3.47), one gets:

$$\dot{S}_{gen} = \dot{m}_{fa,in}(s_{fa,out} - s_{fa,in}) + \dot{m}_{sa,in}(s_{sa,out} - s_{sa,in}) \quad (3.48)$$

As a consequence of the energy conservation requires:

$$\dot{m}_{sa,in}(\dot{h}_{sa,in} - \dot{h}_{sa,out}) = \dot{m}_{fa,in}(\dot{h}_{fa,out} - \dot{h}_{fa,in}) \quad (3.49)$$

Total exergy destruction rate ($Ex_{des,tot}$) is calculated by:

$$Ex_{des,tot} = T_{amb}[\dot{m}_{fa,in}(s_{fa,out} - s_{fa,in}) + \dot{m}_{sa,in}(s_{sa,out} - s_{sa,in})] \quad (3.50)$$

3.5. Results and Discussion

In this part of the research, key results of theoretical investigation and thermodynamic assessment of solar powered heat recovery panels is given.

3.5.1. Results from theoretical investigation

The *SPHRS* is devised to preheat the fresh air from outdoor environment in order to reduce the heating load of the buildings in winter conditions. Also, the system aims at keeping the surface temperature of photovoltaic modules as low as possible to improve the electrical output of the system. The theoretical analyses are carried out by considering the environmental conditions of Nottingham, UK. In this respect, the temperature of stale from indoor environment is taken to be 25 °C due to the thermal comfort conditions. The results are obtained for six solar intensity levels in the range of 0-500 W/m^2 , and for three fresh air temperature values from outdoor environment from -5 to 5 °C. For different temperature values of the incoming fresh air, outlet temperatures of fresh air and stale air are illustrated in [Figure 3.2](#), [Figure 3.3](#) and [Figure 3.4](#). The length of the *SPHRS* is selected to be 2 m; 1 m for the heat recovery unit and 1 m for the solar powered unit. It is found from the results that the fresh air temperature increases exponentially along the heat recovery unit while the stale air

temperature decreases. In the solar powered unit, stale air temperature remains constant as a consequence of the perfect insulation. On the other hand, fresh air temperature increases linearly along the solar powered unit. It is also observed from the results that the solar intensity has a linear impact on the outlet fresh air temperature of the solar powered unit. $T_{fa^*,o}$ is found to be 8.18, 12.18, 16.21, 20.26, 24.32 and 28.40 °C for the solar intensity of 0, 100, 200, 300, 400 and 500 W/m^2 , respectively for $T_{fa,0} = -5$ °C. Maximum values of $T_{fa^*,o}$ have been found to be 31.21 and 34.01 °C for $T_{fa,0} = 0$ and 5 °C, respectively.

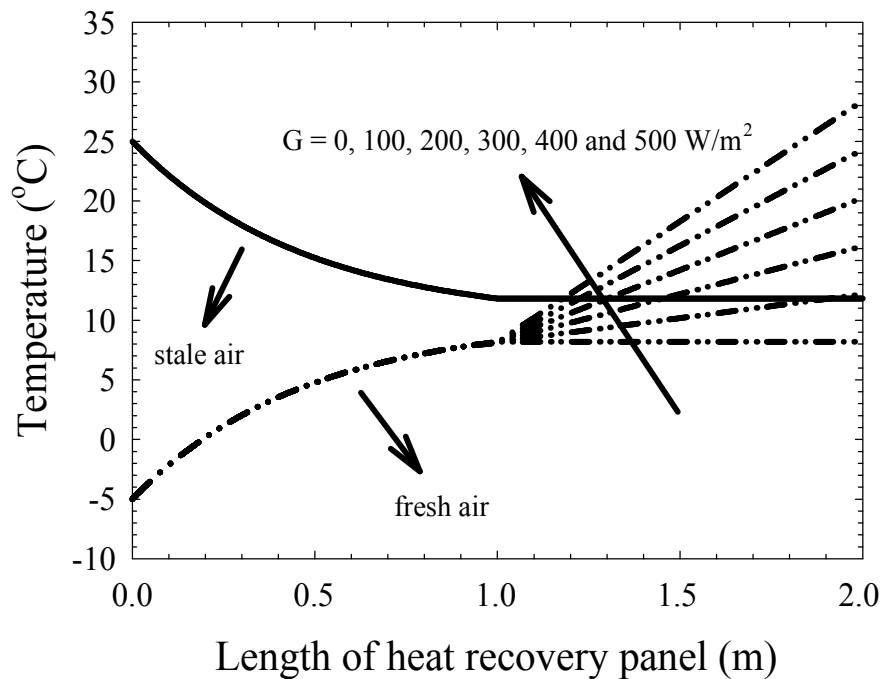


Figure 3.2. Solar intensity dependencies of outlet fresh air and stale air temperatures for

$$T_{fa,0} = -5 \text{ } ^\circ\text{C}.$$

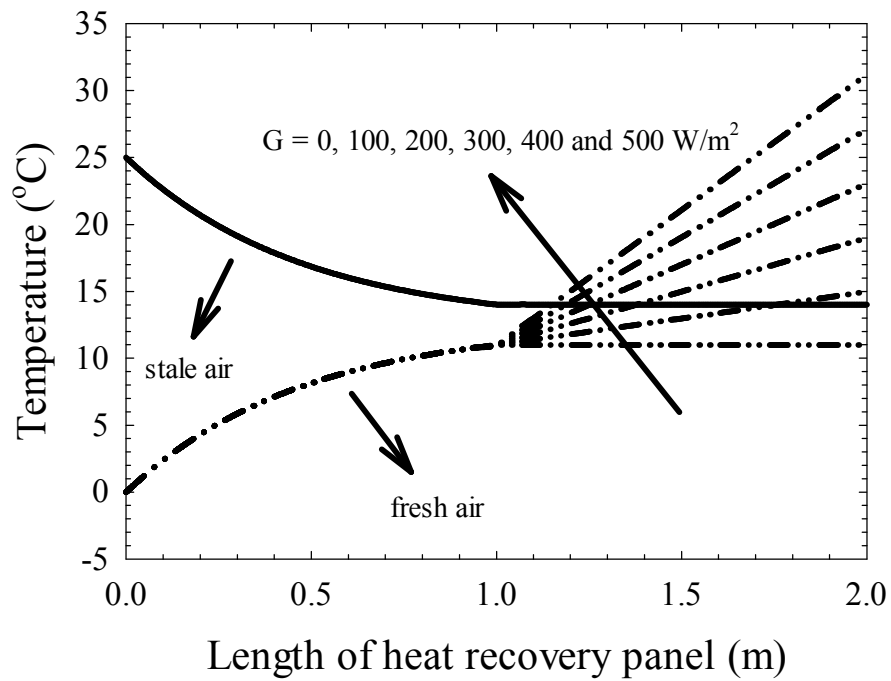


Figure 3.3. Solar intensity dependencies of outlet fresh air and stale air temperatures for $T_{fa,0} = 0$ °C.

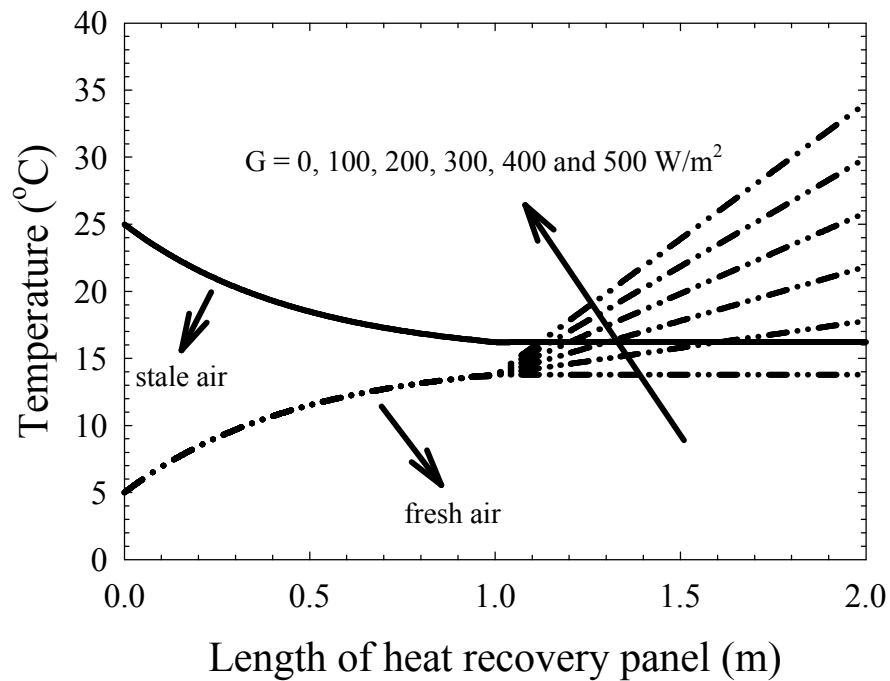


Figure 3.4. Solar intensity dependencies of outlet fresh air and stale air temperatures for $T_{fa,0} = 5$ °C.

In the second part of analyses, outlet fresh air and stale air temperatures are determined for different values of ambient temperature as shown in Figure 3.5, Figure 3.6 and Figure 3.7. A different demonstration of the previous results is given in terms of changes in ambient temperature. The results indicate that it is possible to preheat the fresh air temperature from $-5\text{ }^{\circ}\text{C}$ to 12.18 , 20.26 and $28.40\text{ }^{\circ}\text{C}$ for the solar intensity of 100 , 300 and 500 W/m^2 , respectively. It can be noted from the results that the *SPHRS* is quite appropriate for both heating and ventilation purposes in colder climates. Heating load of the buildings can be considerably reduced in winter by utilising the *SPHRS*.

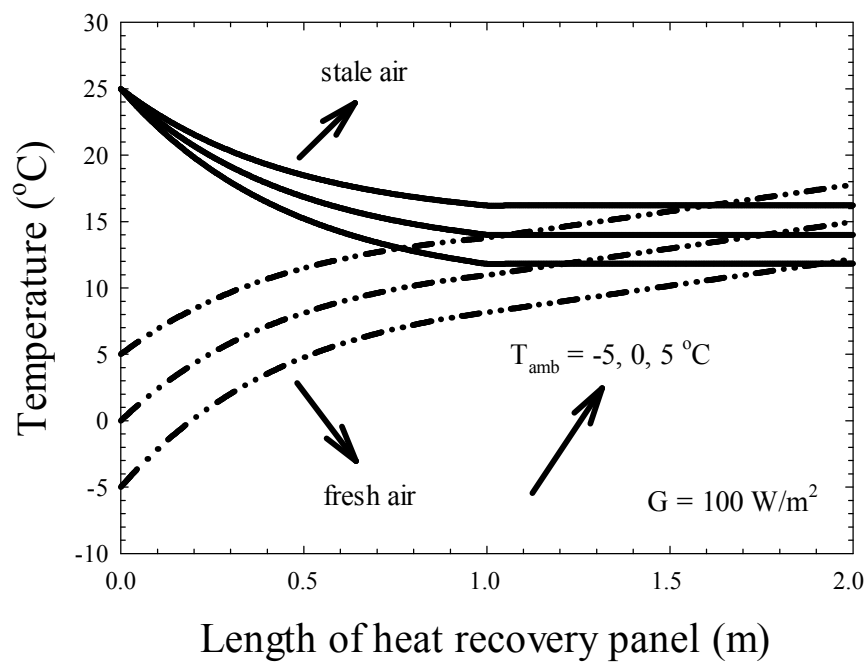


Figure 3.5. Ambient temperature dependencies of outlet fresh air and stale air temperatures for $G = 100\text{ W/m}^2$.

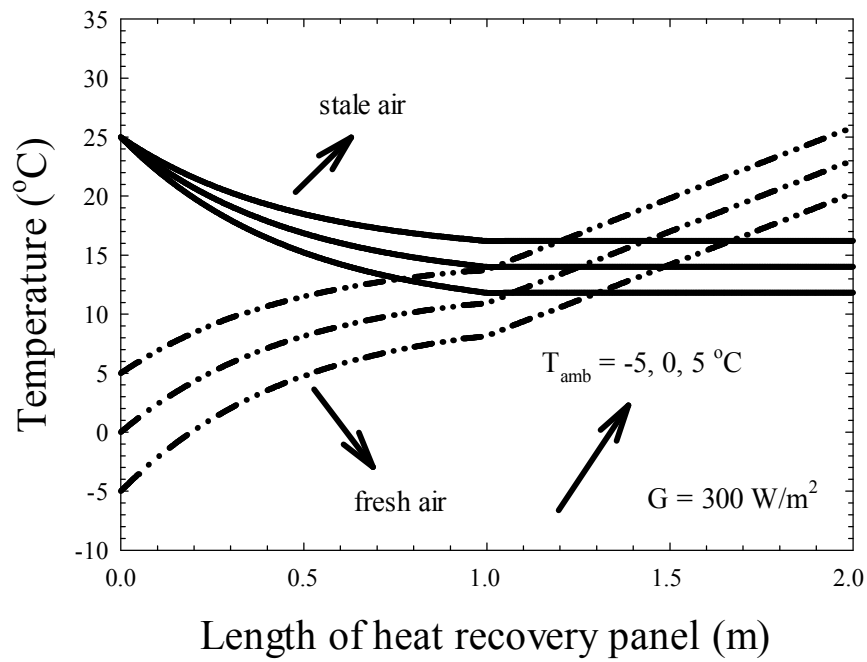


Figure 3.6. Ambient temperature dependencies of outlet fresh air and stale air temperatures for $G = 300 \text{ W/m}^2$.

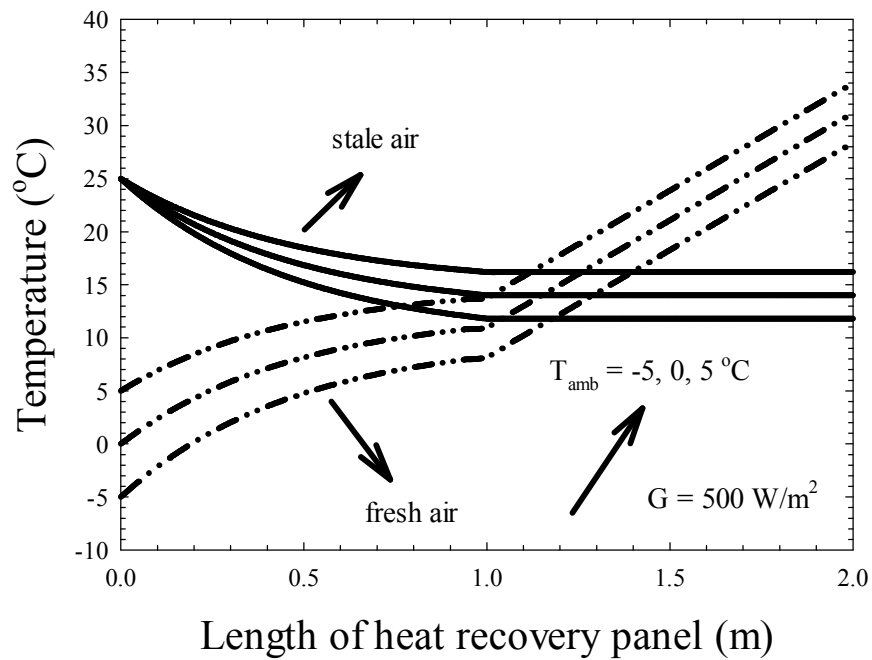


Figure 3.7. Ambient temperature dependencies of outlet fresh air and stale air temperatures for $G = 500 \text{ W/m}^2$.

Finally, ambient temperature and solar intensity dependencies of the electrical efficiency of the *SPHRS* are evaluated as illustrated in Figure 3.8. It is understood from the results that the electrical efficiency increases linearly with increasing solar intensity level for constant ambient temperature. On the other hand, the electrical efficiency decreases with increasing values of ambient temperature. It can be concluded that the surface temperature of photovoltaic modules increases with increasing ambient temperature and solar intensity level. As a consequence of that, electrical efficiency of the solar powered unit decreases. In this regard, passive or active cooling techniques can be performed to enhance the electrical output of the *SPHRS*.

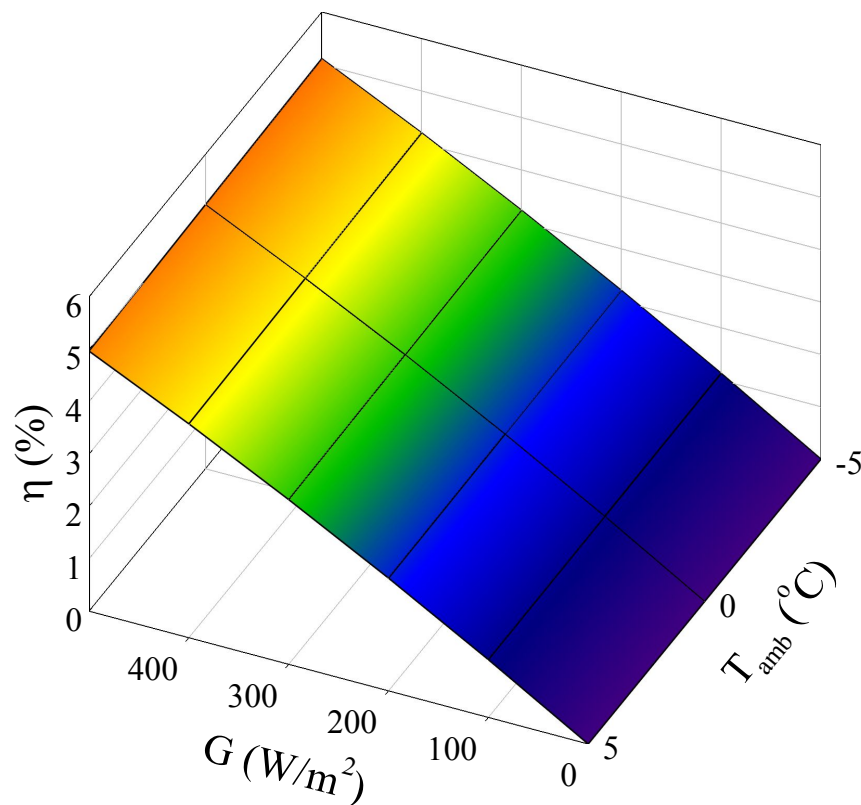


Figure 3.8. Variation of electrical efficiency of the *SPHRS* by ambient temperature and solar intensity.

3.5.2. Results from thermodynamic assessment

In previous work, a novel heat recovery system for heating and ventilation purposes (*SPHRS*) is developed. The *SPHRS* is devised to preheat the fresh air from outdoor environment in order to reduce the heating load of the buildings in winter conditions. Also, the system aims at keeping the surface temperature of photovoltaic modules as low as possible to improve the electrical output of the system. The theoretical analyses are carried out by considering the environmental conditions of Nottingham, UK. In this respect, the temperature of stale from indoor environment is taken to be 25 °C due to the thermal comfort conditions. The results are obtained for six solar intensity levels in the range of 0-500 W/m^2 , and for three fresh air temperature values from outdoor environment from -5 to 5 °C. For different temperature values of the incoming fresh air, outlet temperatures of fresh air and stale air are obtained as given in [Figure 3.2](#), [Figure 3.3](#) and [Figure 3.4](#), and this data is used in the second law analysis of the aforementioned system. The length of the *SPHRS* is selected to be 2 m; 1 m for the heat recovery unit and 1 m for the solar powered unit. The ratio of mass flow rates ($\dot{m}_{fa}/\dot{m}_{sa}$) is selected to be 0.1 for a realistic approach. The reason of selecting such a figure can be attributed to maximising the time of fresh air as it is passing through the heat recovery channel. Finally, exergy efficiency of the *SPHRS* is determined as shown in [Figure 3.9](#). The results indicate that both ambient temperature and solar intensity have a positive effect on exergy efficiency. For higher values of ambient temperature and solar intensity, second law efficiency of the *SPHRS* shows a remarkable increase as it is unequivocal from the results. For the best case of the analyses ($T_{amb} = 5$ °C and $G = 500$ W/m^2), η_{ex} is found to be 60.7%, whereas it is 4.3% for the worst case. It can be easily concluded from the results that the *SPHRS* is a very promising technology, and

it can be utilised especially in colder climates to reduce the energy consumption levels of buildings.

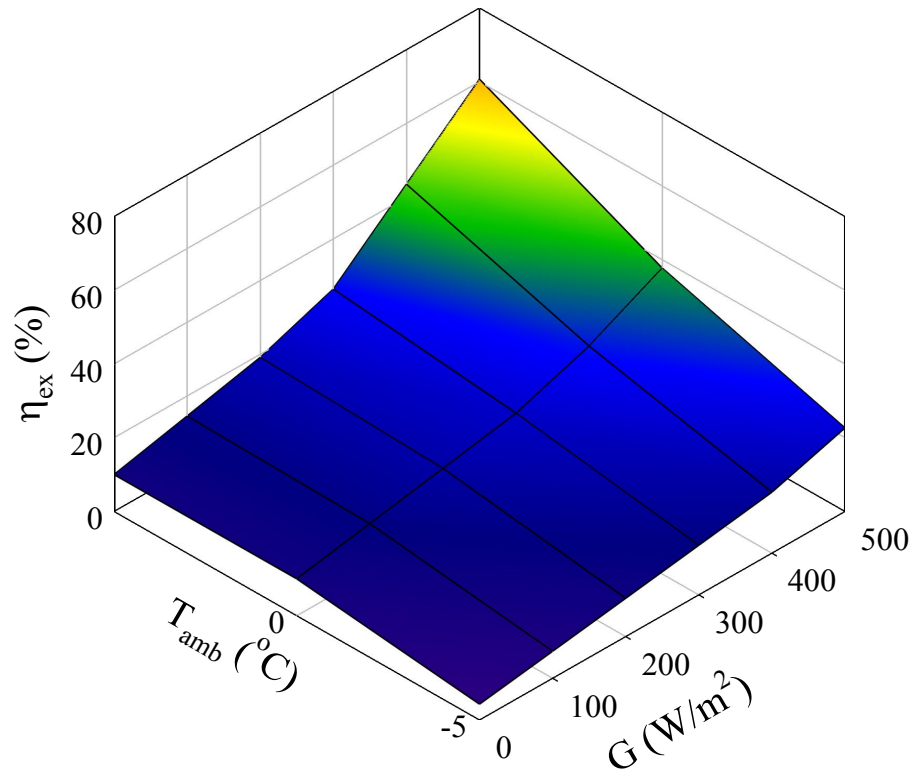


Figure 3.9. Exergy efficiency of the *SPHRS* with respect to the changes in ambient temperature and solar intensity.

3.6. Conclusions

In this chapter, theoretical investigation of a novel heat recovery system is presented. The results indicate that the proposed system is very efficient to preheat the cold fresh air from outdoor environment in winter, and hence to mitigate the heating demand of buildings especially in colder climates. The system can be utilised for both ventilation and heating purposes. In the second part of this research, the aforementioned system will be investigated experimentally. Second law analysis of a novel heat recovery

system is also presented in this research. The results indicate that the proposed system is very efficient to preheat the cold fresh air from outdoor environment in winter, and hence to mitigate the heating demand of buildings especially in colder climates. The system can be utilised for both ventilation and heating purposes. Maximum exergy efficiency of the system is found to be around 60% which is very promising. This efficiency value can be enhanced via optimisation of the system parameters such as duct geometry, mass flow rates of the fluids, packing factor for the solar powered unit, etc. In the second part of this research, the aforementioned system will be investigated experimentally.

CHAPTER 4

An experimental investigation of a novel roof type heat recovery panel for low-carbon buildings

- 4.1. Introduction
- 4.2. Description of the System
- 4.3. Experimental Investigation of the System
- 4.4. Economic Analysis of the System
- 4.5. Results and Discussion
- 4.6. Conclusions

CHAPTER 4

An experimental investigation of a novel roof type heat recovery panel for low-carbon buildings

4.1. Introduction

Ventilation constitutes a significant part of total energy consumed in buildings as a consequence of rising thermal comfort levels of occupants. In this point, good insulation of building envelope is crucial to reduce heating and cooling loads. It is reported in literature that even well insulated and tight buildings consume about 60% of total annual energy demand for *HVAC* [32,166,197]. However, roughly 20-40% of the overall energy consumption of *HVAC* system is utilised for the ventilation air conditioning purposes in most of the commercial building sector [128]. That's why the building sector is responsible for the major energy depletion worldwide and this issue is rising continually [10]. It is clearly underlined in literature that it is possible to make a significant contribution to mitigate the energy consumption of buildings by using heat recovery technologies along with the insulation. Heat recovery technologies are in fact user friendly and cost effective for buildings with insignificant maintenance issues. Besides, the heat recovery technologies are up-and-coming for further developments. Energy is used to cover the heat losses due to the ventilation air and to move the ventilation air for mechanical ventilation [198]. It is reported that the ventilation heat losses can reach 35-40 kWh/m^2 a year in residential buildings, and 80-90% of this can be recovered [199]. Mechanical ventilation systems can meet the energy

requirement for ventilation via recovering waste heat to mitigate heat losses and energy use [198,200]. Space heating requirement before and after renovation is illustrated in Table 4.1.

Heat recovery systems are widely studied by numerous researchers both theoretically and experimentally. For instance, Hviid and Svendsen [74] investigate the heat recovery efficiency of a liquid coupled heat exchanger. Their results indicate that, the heat exchanger efficiency changes between 64.5-75.4%. Another empiric study reveals that it is possible to achieve 8% of energy saving when membrane based heat recovery system is used rather than conventional *HVAC* in humid climatic conditions [86]. In another study, Zhang et al. [119] use an air dehumidification system combined with membrane based enthalpy heat exchanger and the simulation results demonstrated that 33% of primary energy saving is achieved. Table 4.2 shows the total economic savings after implementation of a mechanical ventilation system. Gong et al. [97] experimentally investigate a new heat recovery technique and the test results indicate that the system has relatively large coefficient of performance (*COP*) around 6.

Use of passive and low energy systems in residential buildings provides to maintain the thermal comfort of the dwelling with the cheapest way [202]. In this paper, an experimental study of a novel heat recovery unit is presented in detail. The efficiency, practicality, reliability and sustainability of the system are discussed.

Table 4.1. Space heating requirements in multi-family building [201]

Case	Heating requirement* (kWh/m ²)
Before renovation	80
After renovation	46
After renovation, assuming 90% heat recovery	19

*20 °C indoor set-point temperature, internal gains of 5 W/m² normal Danish climate conditions are assumed.

Table 4.2. Total economic savings after implementing a mechanical ventilation system with 90% heat recovery, air changer rate of 0.5 h^{-1} and an electricity consumption of $3 \text{ kWh/m}^2/\text{a}$ [201]

Reference system	Construction expenses (€/m ²)	Predicted savings over 30 years (€/m ²)			
		I1*	I2*	B1*	B2*
Energy price (€/kWh)		0.08	0.16	0.08	0.16
Real interest rate (%/a)		2.5	2.5	0	0
Natural (single-family house)	40	-26	19	3	67
Natural (residential block)	18	13	57	35	98
Exhaust only (residential block)	7	40	91	63	137

* Scenario.

4.2. Description of the System

The system that is presented here aims at cooling or heating the stale air from indoor environment to be able to reduce or increase the temperature of intake fresh air in the counter-flow heat exchanger as it is seen in [Figure 4.1](#). Moreover, polycarbonate shows good chemical resistance to mineral acids, organic acids, greases and oils [203]. Its service temperature is the range of -4 to $135 \text{ }^{\circ}\text{C}$ which is suitable for *HVAC* applications. In the proposed heat recovery system, polycarbonate sheet has been used to generate an air to air heat exchanger because of its lightweightness and cost effectiveness [204]. A multi-channel heat recovery plate internally places under the roof of the test house as seen in [Figure 4.2](#). The system is well insulated both internally and externally to prevent the unwanted heat loss. The test house externally has 7 m length, 3 m width and 4.3 m height. It has two windows plus a velux window on the roof and a double door all double glazed. The walls, the roof and the floor have 150 mm mineral wool insulation.

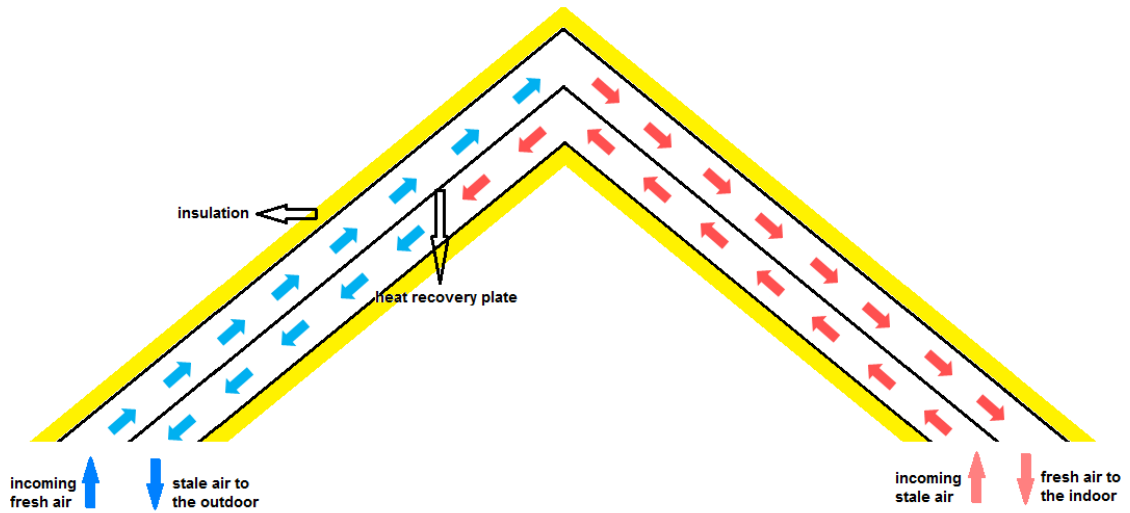


Figure 4.1. Schematic of the proposed heat recovery system [204].



Figure 4.2. Multi-channel ducts of the heat recovery system.

Four polycarbonate heat exchanger sheets have been constructed. Two of them have been placed at the front of the building while the rest two at the back as shown in Figure 4.3. The end of each polycarbonate sheet within the building is followed by an

extract duct connected to the upper channels and an inlet duct connected to the lower channels. The extract and the inlet ducts are square with internal dimensions of $60\text{ mm} \times 60\text{ mm}$. Both the extract and inlet ducts are then integrated into rectangular ducts with internal dimensions of $105\text{ mm} \times 50\text{ mm}$. Finally, the rectangular ducts are connected to fans which can be operated at different velocities of air.

4.3. Experimental Investigation of the System

The proposed system is experimentally investigated in terms of the heat recovery efficiency and coefficient of performance (*COP*). The test of the system is carried out in winter season to measure the pre-heating performance of the unit. Similar results are expected for the cooling performance of the system because of the independency of the heat recovery efficiency from the season. Inlet fresh air temperature, inlet fresh air relative humidity, inlet stale air temperature, inlet stale air relative humidity, mass flow rate, and fan speed are measured as input data. Through the data obtained, the heat recovery efficiency, *COP* value, outlet fresh air temperature, outlet fresh air relative humidity, outlet stale air temperature and outlet stale air relative humidity are calculated.

4.3.1. Experimental setup

The polycarbonate heat recovery system is integrated to a small test house, as it is shown in [Figure 4.4](#), which is located in Southeastern UK. The test house consists of a small living space, a bathroom and an under roof resting place. A temperature-controlled convective heater is used to keep the room temperature constant. Following providing steady-state conditions in the test house, thermocouples are placed at particular locations. 12 points are determined for this purpose as illustrated in

Figure 4.5. Standardized co-heating methodology is conducted for performance evaluation of the polycarbonate heat recovery system. Time-dependent electricity consumption through fans is measured for a timeframe of 24 hours as well as relative humidity and temperature measurements of fresh and stale air. Through the data obtained, heat recovery efficiency and coefficient of performance of the system are calculated.



Figure 4.3. Installation of the polycarbonate heat exchanger to the test house.



Figure 4.4. A test house located in Southeastern UK.



Figure 4.5. Implementation of the thermocouples and humidity sensors to the different locations of the test house.

4.4. Economic Analysis of the System

The economic analysis of such a heat recovery system requires some particular assumptions as the cost structure can be different from one user to another user. Therefore, it is difficult to generalise the results [166]. The costs related to the materials for manufacturing of the heat recovery panel are given in European Union Economic Area joint currency of Euro (€) to make the financial figures easy to understand, even if the original calculation is made in Great Britain Pound (£). The exchange rate is obtained to be actual rate at the time of the research. At that time, £1 equals around €1.36. In this research, an economic analysis of the proposed innovation is also carried out. The results are compared with those of commercial alternative of the system in terms of costing. The related investment and running costs are shown in Table 4.3. The total annual HVAC cost of a typical UK building is taken to be around €10.7255/m² [204], and total external surface area of a typical UK building is considered to be

80 m². In this respect, to be able to calculate the payback period of the innovation, the energy saving coefficient is needed to be figured out with respect to the *COP* of the proposed system.

Table 4.3. Total investment cost of the proposed heat recovery system

System element	Unit	Unit cost (€)	Total cost (€)
Polycarbonate sheet	4	27.28	109.11
Centrifugal fan	2	75.58	151.16
Labour cost	5	136.11	680.55
Other	1	204.16	204.16
Total			1144.98

The energy saving coefficient of the proposed heat recovery system is calculated by using the following equation:

$$\lambda_{hrs} = 1 - \frac{1}{COP_{hrs}} \quad (4.1)$$

where λ_{hrs} is the energy saving coefficient and COP_{hrs} is the coefficient of the performance of the heat recovery system. After the calculation of the energy saving coefficient of the system, it is multiplied by the annual *HVAC* cost of the total external surface area of 80 m². Finally, the total investment cost of the heat recovery system is divided by the result of the calculation above to find out the payback period of proposed innovation. In next step, the aforementioned system is compared with the commercial alternative to make it understandable in terms of reliability and affordability.

4.5. Results and Discussion

In this study, a novel heat recovery system implemented to a test house in Kent is experimentally investigated. Relative humidity and temperature values of the air are measured for both inlet and outlet lines of the test house. The variation of the relative humidity and temperature values for stale air and fresh air are shown in Figure 4.6–4.9. It is easy to understand from the results that the outlet stale air temperature decreases from 16.17 °C to 4.75 °C whereas outlet fresh air temperature increases from 4.26 °C to 14.81 °C.

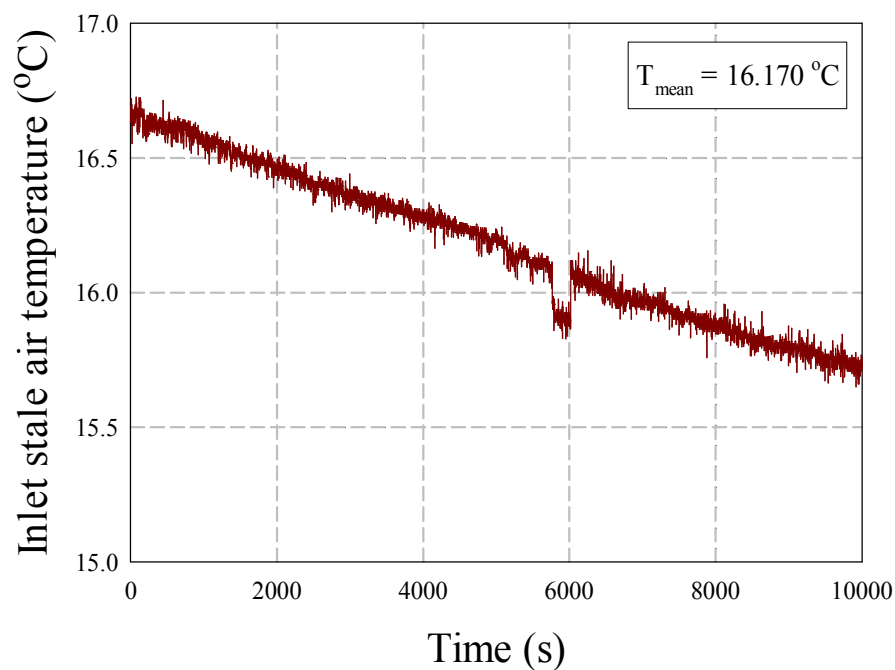


Figure 4.6. Temperature variation of the inlet stale air.

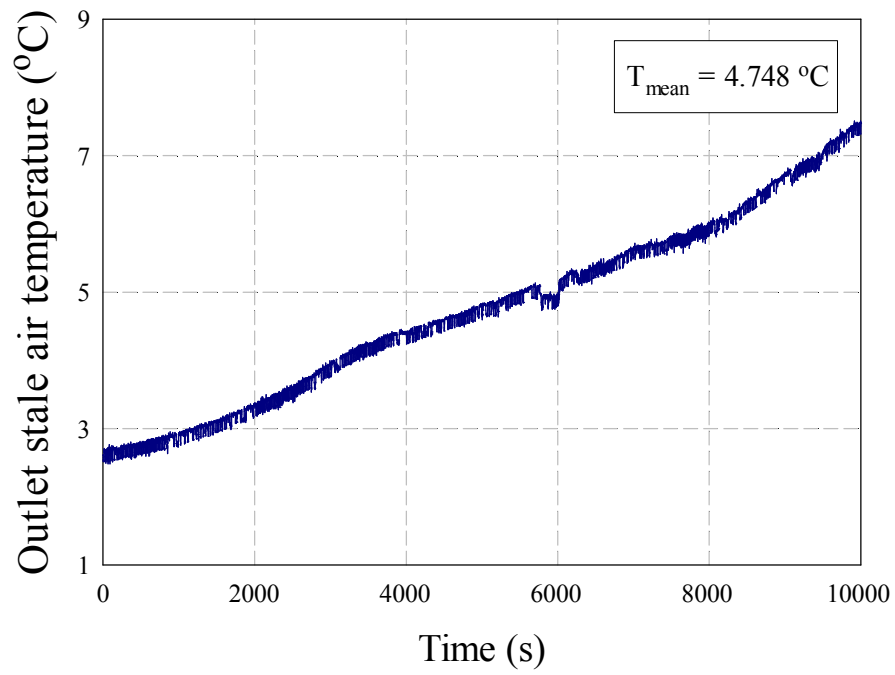


Figure 4.7. Temperature variation of the outlet stale air.

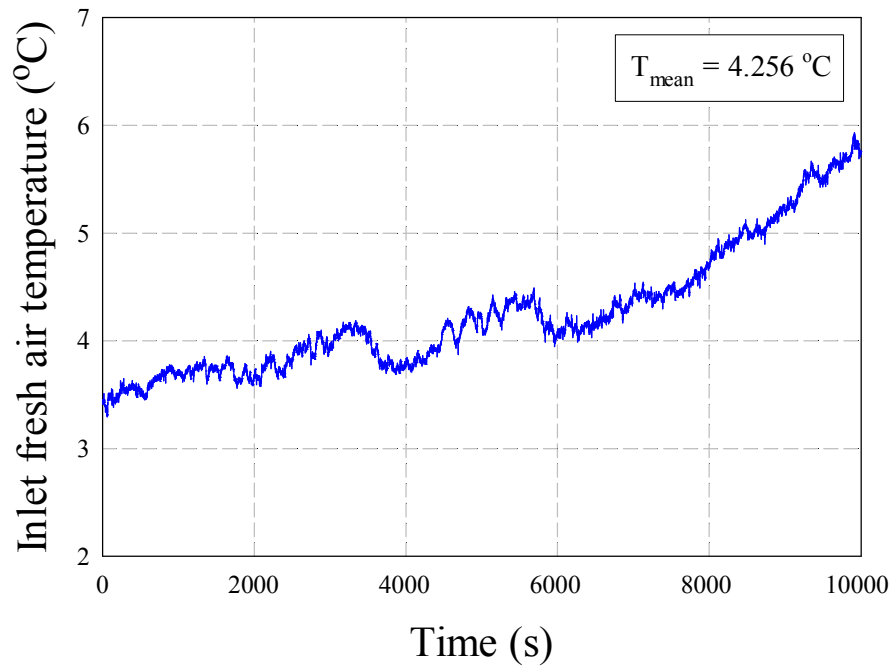


Figure 4.8. Temperature variation of the inlet fresh air.

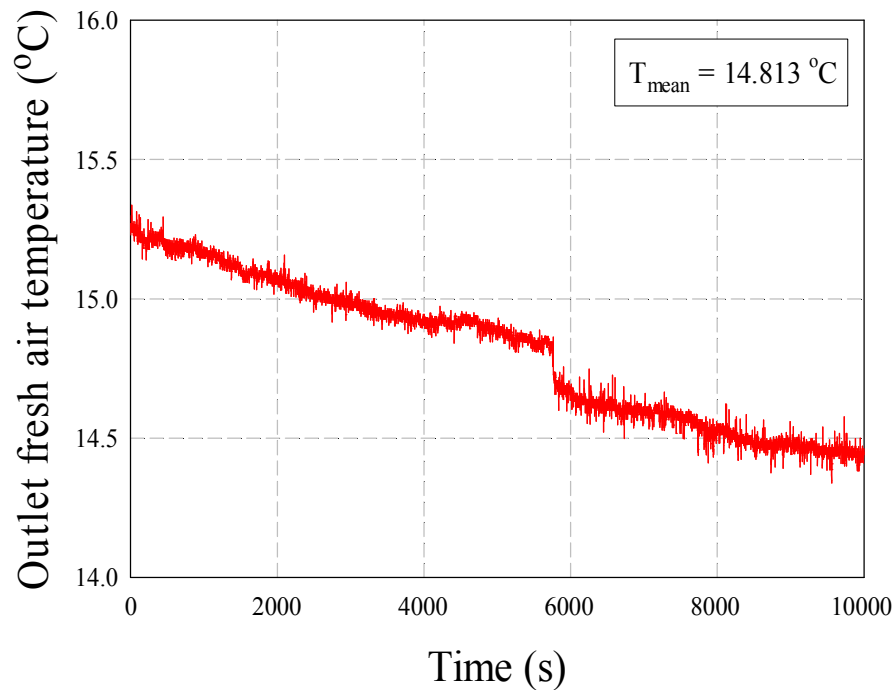


Figure 4.9. Temperature variation of the outlet fresh air.

In the proposed system, the fresh air from outdoor is preheated by the waste air from indoor environment. Here, the stale air is collected from bathroom of the test house by using a small fan, and it is directed to the plate type heat exchanger. Then, the fresh air and the stale air are welcomed in a multi-channel heat exchanger unit. In this system, the fresh air outlet temperature increases as its relative humidity decreases at a level which is good for desired comfort conditions as it is seen in Figure 4.10 and Figure 4.11. The average relative humidity of inlet fresh air is calculated roughly 76% which is not so suitable for healthy indoor environment. After the heat exchange process in the heat exchanger unit, the relative humidity is measured as 54% approximately which is good for the occupants. In this experimental study, the thermal efficiency of the heat exchanger is measured depending on the temperature change during the test.

The heat exchanger efficiency is calculated by using the following equation:

$$\eta_{hex} = \frac{T_{fa,out} - T_{fa,in}}{T_{sa,in} - T_{fa,in}} \quad (4.2)$$

where η_{hex} is heat exchanger efficiency, $T_{fa,in}$ is inlet fresh air temperature, $T_{fa,out}$ is outlet fresh air temperature and $T_{sa,in}$ is inlet stale air temperature.

The following equation is used to figure out the coefficient of performance of the proposed system:

$$COP = \frac{\dot{m}_a c \Delta T}{P_{wfan}} \quad (4.3)$$

where COP is the coefficient of performance, \dot{m}_a is mass flow rate, c is specific heat capacity, ΔT is temperature difference and P_{wfan} is power output of the fan.

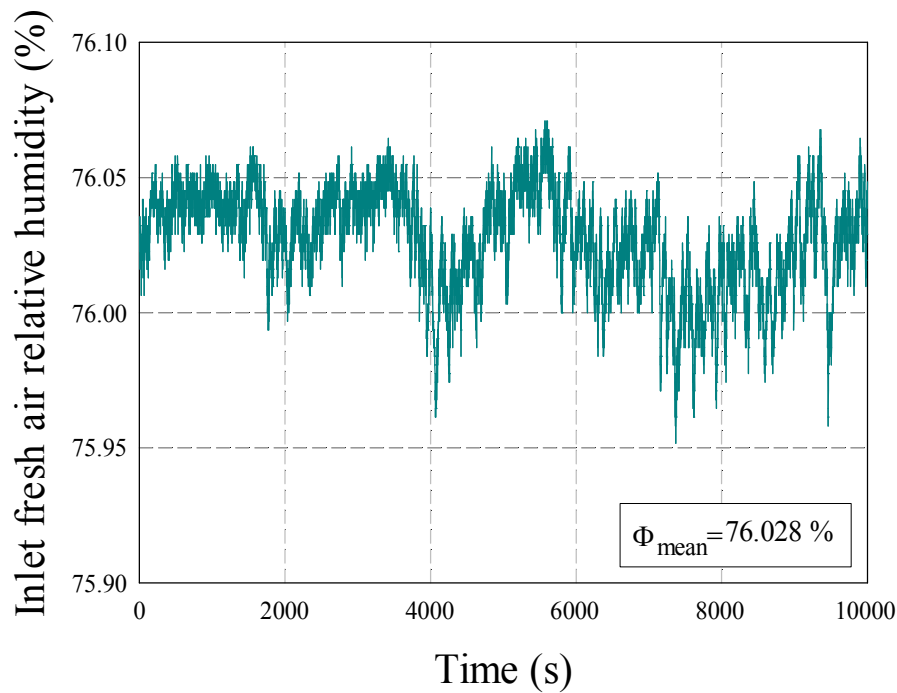


Figure 4.10. Relative humidity variation of the inlet fresh air.

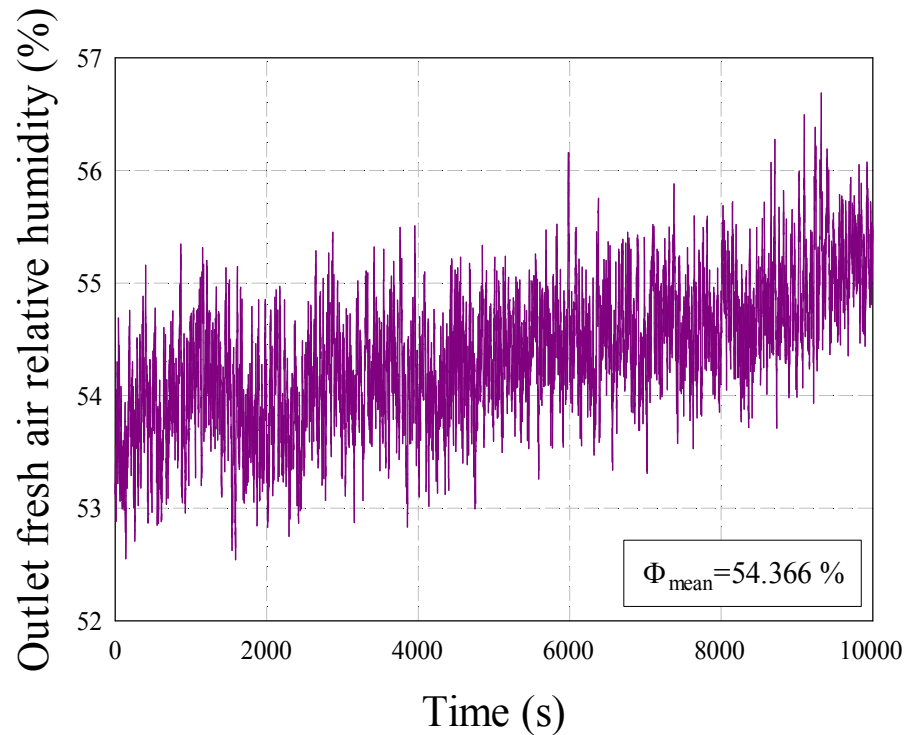


Figure 4.11. Relative humidity variation of the outlet fresh air.

Within the scope of this research, an economic analysis of the system is also carried out, and the details of the capital cost of the system are given in Table 4.3. For the analysis, the total annual *HVAC* cost of a typical UK building is assumed to be €858.04 [204] as considering a total external surface area of 80 m^2 . Through the *COP* calculation, energy saving coefficient of the system is found to be 0.77 which yields a payback period of around 1.7 years. Comparison of the roof type heat recovery system with commercial alternative is made, and related metric costs are shown in Table 4.4.

Table 4.4. Comparison of the proposed system with a commercial alternative

Component	Related Cost/m ²	Commercial Alternative	Related Cost/m ²	Justification for choice
Polycarbonate sheet based roof type heat recovery panel	€14.31/m ²	Conventional air conditioner	€11.65/m ²	Although the cost of polycarbonate sheet based roof type heat recovery panel is higher than its commercial alternative (Split Air Conditioning Systems), it has some characteristic features. First of all, the payback period of polycarbonate sheet based roof type heat recovery panel is very short as the system is only powered by centrifugal fans. Secondly, the system is easy to fabricate and environmentally friendly. Moreover, the system does not require any periodic maintenance.

4.6. Conclusions

In this research, a novel heat recovery system is installed to a small test house which is located in Southeastern UK. The system is designed as under roof application. The aim of the system is to recover waste heat and to preheat fresh air using stale air. It can be noted that the proposed system aims at mitigating the heating or cooling load depending on the season while providing ventilation as well. Thermal performance characteristics of the system are experimentally investigated. Heat recovery efficiency is affected by many parameters. One of those parameters is fan speed. In this study, the fan speed is determined to be 0.4 m/s which is reasonable for the thermal comfort conditions. It is concluded from the results that the system efficiency is high enough as well as good *COP* range. Considering the experimental results, the heat recovery

efficiency of the system is found to be around 89% as seen in Figure 4.12. On the other hand, the coefficient of performance of the system is calculated to be around 4.5 as it is shown in Figure 4.13. The system is found to be reasonable in terms of investment and payback time. The payback period of the proposed innovation is calculated to be around 1.7 years. The proposed system can be used in both winter and summer conditions without requiring additional work. Its labour cost is extremely low, so it is cost-effective and user friendly.

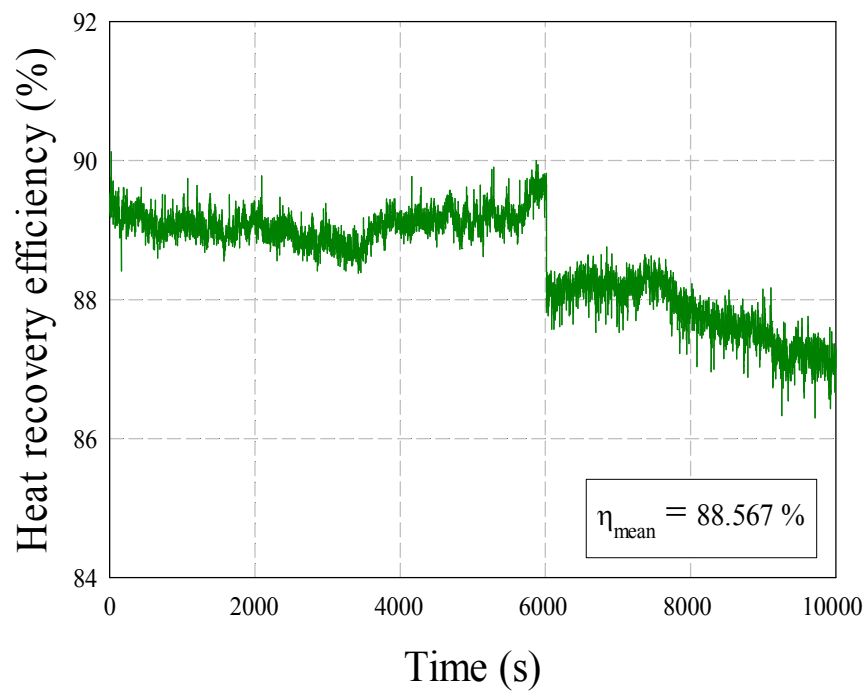


Figure 4.12. Heat recovery efficiency of the system.

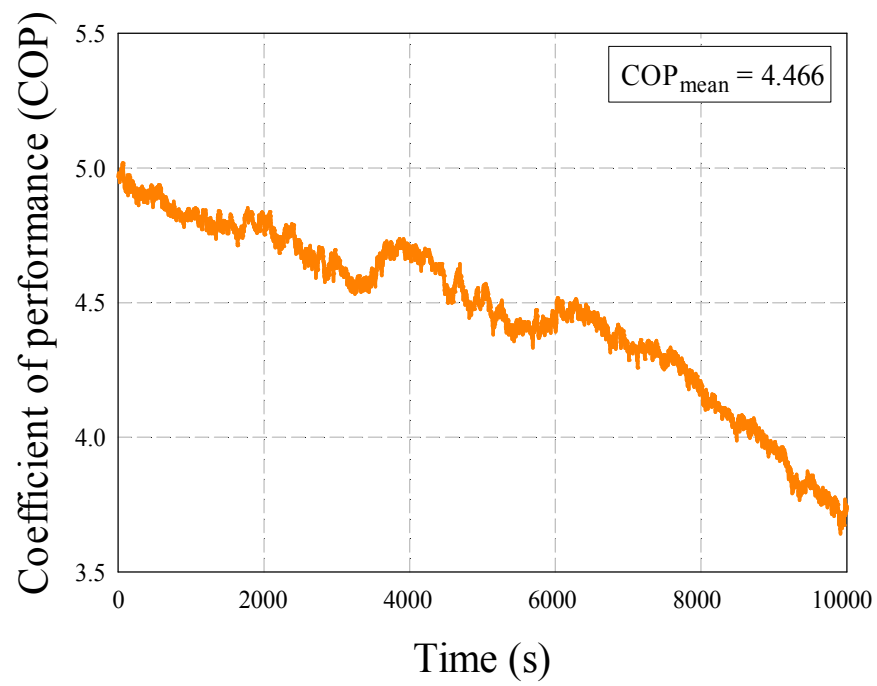


Figure 4.13. Coefficient of performance of the system.

CHAPTER 5

Thermal performance monitoring of a novel heat recovery unit integrated to a residential house

- 5.1. Introduction
- 5.2. Pre-retrofitting Strategy
- 5.3. Retrofitting Plan
- 5.4. Monitoring Plan
- 5.5. Details of the Test House
- 5.6. Results and Discussion
- 5.7. Conclusions

CHAPTER 5

Thermal performance monitoring of a novel heat recovery unit integrated to a residential house

5.1. Introduction

Total energy consumption of the world, and hence energy demand increases due to rapid growth of the world. Current predictions and data gathered by International Energy Agency (*IEA*) show that the growing trend will continue [3]. Latest research indicates that the building sector is responsible for 20-40% of the total energy consumption. Most of the energy consumption occurs due to heating, cooling and ventilation demand of the occupants. In addition to this figure, day by day, the energy demand in *HVAC* sector rises as a result of technological development and desire of better thermal comfort conditions. In this respect, researchers try to find alternative solutions to minimise energy consumption and to maximise energy gained from renewables or any other sources. A recent study reveals that energy demand of new office buildings for heating and cooling applications decreases with use of renewables [205]. On the other hand, it is achieved to reduce heating or cooling demand of a building as using heat recovery systems. Heat recovery technology is basically utilised to mitigate the heat loss, and hence energy consumption due to *HVAC*. A basic heat recovery system is simply defined as heat exchange between two streams at different temperatures. It provides an effective pre-heating or pre-cooling of inlet fresh air depending on the season. The system slightly decreases the space heating cost in winter

as supplying pre-heated fresh air. Main advantages of such a system are its high pre-heating and pre-cooling potential, its simplicity and cost-effectiveness. Additionally it requires almost no maintenance and low operational cost. Moreover, the system presented here contributes in reducing CO_2 emissions. Despite having remarkable efficiency, effectiveness and COP values, these performance figures depend on the sort of stream, material type, target area of the application etc. Previous test results which are performed within the concept of the HERB (Holistic Energy-Efficient Retrofitting of Residential Buildings) Project indicate that it is possible to get around 90% of thermal efficiency via a proper heat recovery system [17]. In this study, pre and after-retrofitting details of a novel heat recovery system integrated to a residential house in United Kingdom is presented in detail. Standardized thermal comfort analyses [206] are conducted before and after the integration of novel ventilation system and the enhancements achieved are evaluated.

5.2. Pre-retrofitting Strategy

In this section, the fabrication details of the product and installation plan are presented. A multi-channel polycarbonate sheet is used to produce a plate type air to air heat exchanger. The dimensions of the heat exchanger are $1000\text{ mm} \times 2000\text{ mm} \times 50\text{ mm}$. The system consists of two separate sections. One is for inlet or outlet fresh air while the other one belongs to outlet or inlet stale air. 40 ducts are used for each section, and thus the system consists of 80 ducts in total as seen in Figure 5.1. Each channel is a square and has a 625 mm^2 of total area. The heat recovery system is powered by two centrifuge fans with 35 W power output each. Stale air from indoor environment and fresh air from outdoor environment are welcomed in the heat exchanger interface of the unit via the said centrifuge fans. Air velocities in each

channel are determined complying with the thermal comfort conditions for indoor environment which is in the range of 0.3-0.5 m/s.

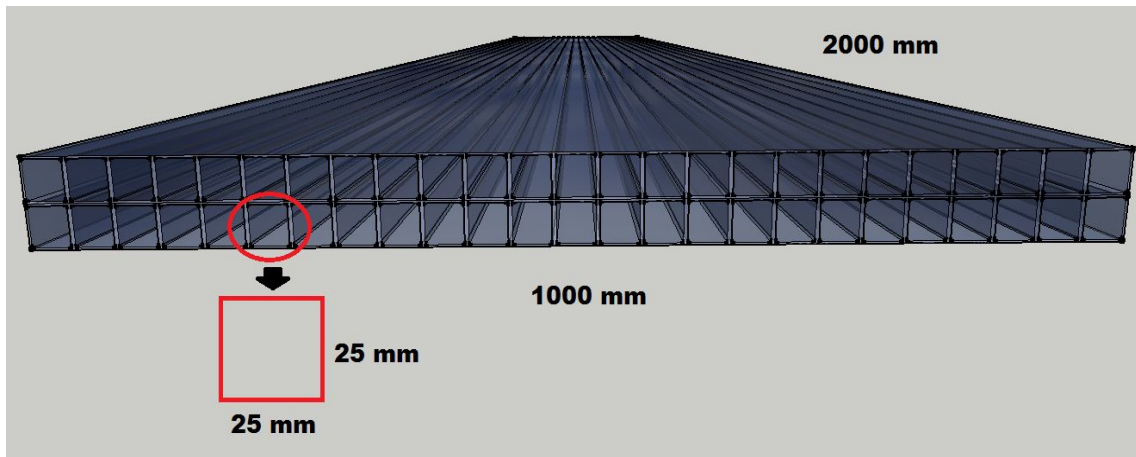


Figure 5.1. Dimensions of the plate type air to air heat exchanger.

Effective constructional parameters on thermal performance of the heat recovery unit can be summarised as thickness of the polycarbonate sheet, thermal conductivity of the material and dimensions of the system. There are also some operational parameters such as mass flow rate of fresh and stale air, thermophysical properties of the streams etc. which can affect the overall thermal efficiency of the system. Agrawal et al. [207] present an experimental work on polycarbonate based heat exchanger covering various effective independent parameters on the heat recovery efficiency. The same constructional and operational parameters are addressed for thermal performance evaluation of polycarbonate heat exchangers.

5.3. Retrofitting Plan

The aforesaid polycarbonate waste heat recovery system is retrofitted to a semi-detached residential building in UK. The most convenient place for retrofitting is considered to be the loft space due to the existence of glass wool insulation as shown in

Figure 5.2. The unit is fixed beneath the 10 mm glass wool insulation in the loft space for proper thermal insulation. Upper surface of the heat recovery unit is insulated by additional thermally resistive materials. For the reference test bedroom in the ground floor, two vents are provided at two different corners for the air streams. Stale from indoor environment is collected via a 100 mm diameter flexible duct powered by 35 W centrifuged fan, whereas the fresh air from outside environment is taken into the unit through a secondary flexible duct. The centrifuged fans utilised in the system have two different speed rates. Regular operational power of fans is 25 W while it is 35 W for the cases of instant ventilation. The heat recovery unit is fixed under the glass wool insulation horizontally. Due to the highly thermally conductive interface between air streams, 100 mm mineral wool insulation is assumed to provide sufficient thermal resistance to prevent undesired heat loss.

5.4. Monitoring Plan

The polycarbonate heat exchanger unit is monitored time dependently. The monitoring stage is based on triggering relevant operational parameters over a timeframe. These parameters can be expressed as temperature of air streams at the inlet and outlet, relative humidity of air streams at the inlet and outlet, air velocities and power consumption of centrifuged fans. Each operational parameter is tracked by a data logging system and monitored at the same time. A GSM monitoring system is used for data collection. Temperature and humidity measurements are performed via highly sensitive sensors at the inlet and outlet of each channel. A 3D schematic of the monitoring system is given in [Figure 5.3](#).



Figure 5.2. 100 mm glass wool insulation in the loft space of the residential house.

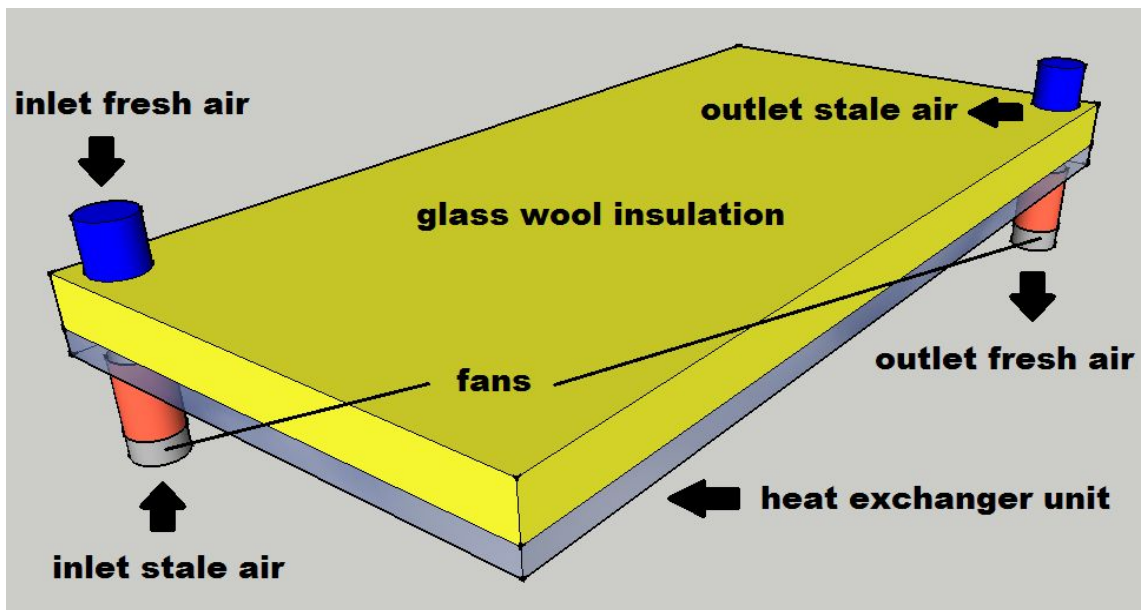


Figure 5.3. A 3D schematic for integration plan of the heat recovery system.

5.5. Details of the Test House

For the thermal comfort analyses of the test house which is integrated with the novel polycarbonate based heat exchanger, a particular summer time is considered and the monitoring takes a whole week for a reliable and realistic assessment. The external view of the test house is shown in [Figure 5.4](#). The test house is constructed by the *PVC* based materials on the facade and wooden structures on the roof, and represents conventional farm houses in the rural areas of the UK. The heat recovery system is fixed just beneath the roof for an easy and effective retrofitting. The ducts and control units are placed in the loft space as shown in [Figure 5.5](#). The separate fans are utilised to circulate the fresh and stale air in the system simultaneously. The separate ducts are also illustrated in [Figure 5.5](#). Flexible duct materials are utilised in the retrofitting for easier connection.



[Figure 5.4](#). The test house which is integrated with a novel heat recovery system.

The stale air from indoor and the fresh air from outdoor are welcomed in the polycarbonate based novel heat recovery system and their thermal energy content is

exchanged as a consequence of the temperature difference. The ducts where the stale air collected and where the fresh air supplied to the system are depicted in Figure 5.6. Relevant temperature, relative humidity and CO_2 measurements are conducted in the test house for the thermal comfort analyses. The test rig set in the test house is shown in Figure 5.7.



Figure 5.5. Detailed photos of the novel heat recovery system which is fixed beneath the roof (left), and flexible ducts (right).



Figure 5.6. Inlet and outlet ventilation ducts in the test house.

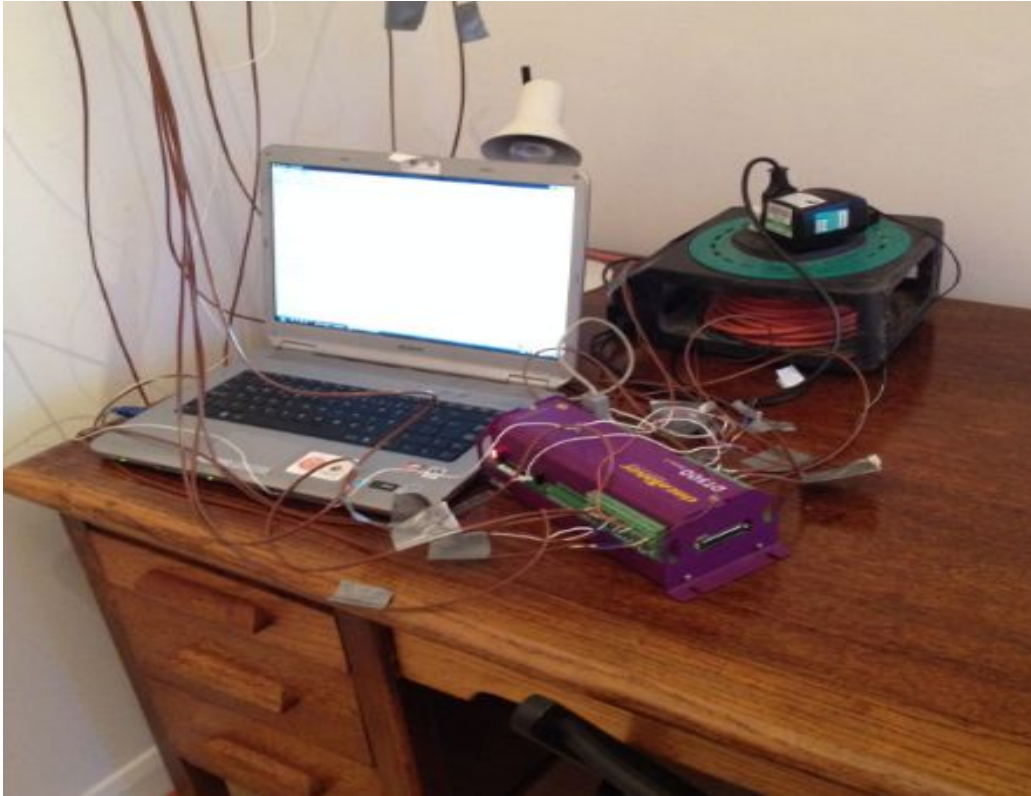


Figure 5.7. Data-logging system utilised in the test house.

5.6. Results and Discussion

Thermal comfort analysis of the test house has been carried out for typical summer days in Kent, UK. Within the scope of the research, three main parameters in the thermal comfort analysis, which are basically CO_2 concentration, relative humidity and internal air temperature are monitored and the results are analysed time-dependently. The most significant parameter for internal comfort conditions can be considered to be CO_2 concentration as it directly affects the human health. The results from the pre-retrofitting case indicate that the CO_2 concentration level inside the test house varies from 1600 to 1720 *ppm* which corresponds to a level where complaints regarding air quality and headaches start. The tests are repeated at the post-retrofit case and it is observed that the CO_2 concentration drops to a level ranging from 350 to 480 *ppm* which addresses the thermal comfort range for occupants. The second

important parameter is of course the relative humidity which totally affects the comfort level of the occupants in internal environments. Relative humidity measurements are carried out at both pre and post-retrofit case. The results are shown that although the relative humidity is notably high before the retrofitting of the ventilation system, thermal comfort range for relative humidity is achieved at the post-retrofit.

The temperatures of fresh air and stale at the inlet and outlet are illustrated in [Figure 5.8](#) and [Figure 5.9](#), respectively whereas the relative humidity variation of indoor environment at pre and post-retrofit is shown in [Figure 5.10](#). In terms of numerical assessment, the relative humidity is in a range of 61 to 72% before retrofitting, whereas it is 53 to 62% after retrofitting. Variation of fresh and stale air temperatures with time are also analysed through the data obtained from the thermal comfort tests. It is understood from the results that the ventilation system notably affects the thermal energy exchange between fresh and stale air. Throughout the test time, a sensible increment is observed in the temperature of fresh air. Maximum temperature rise in fresh air temperature is noted to be about 7 °C. Similarly, a considerable change is observed in the temperature of stale air at inlet and outlet. An average 4 °C temperature decrease of stale air is achieved within the test period. It is clearly understood from the results that the good thermal energy exchange between fresh and stale air results to a cost-effective ventilation system for a typical residential building as well as efficient thermal comfort levels for the occupants.

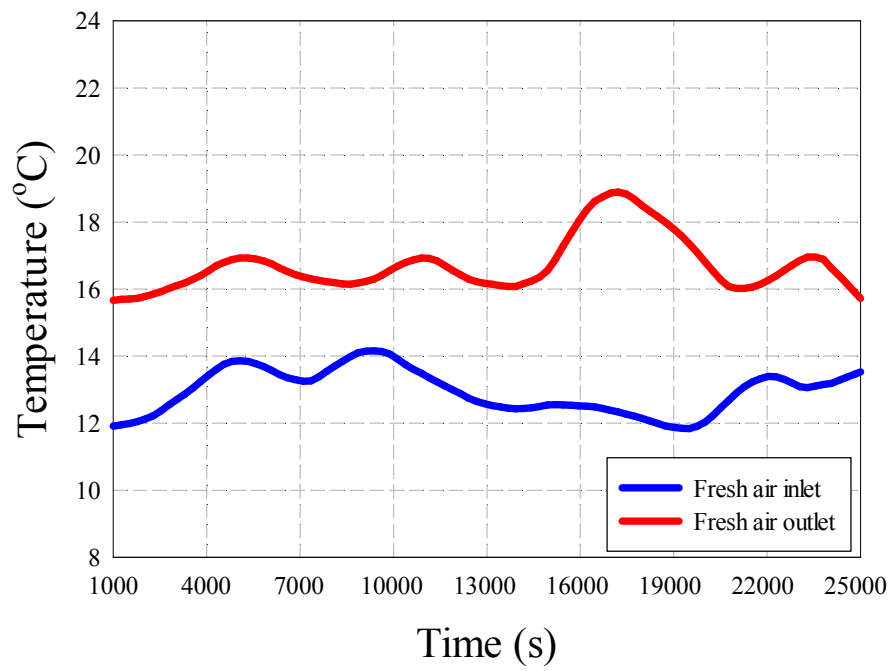


Figure 5.8. Temperature variation of fresh air at the inlet and the outlet.

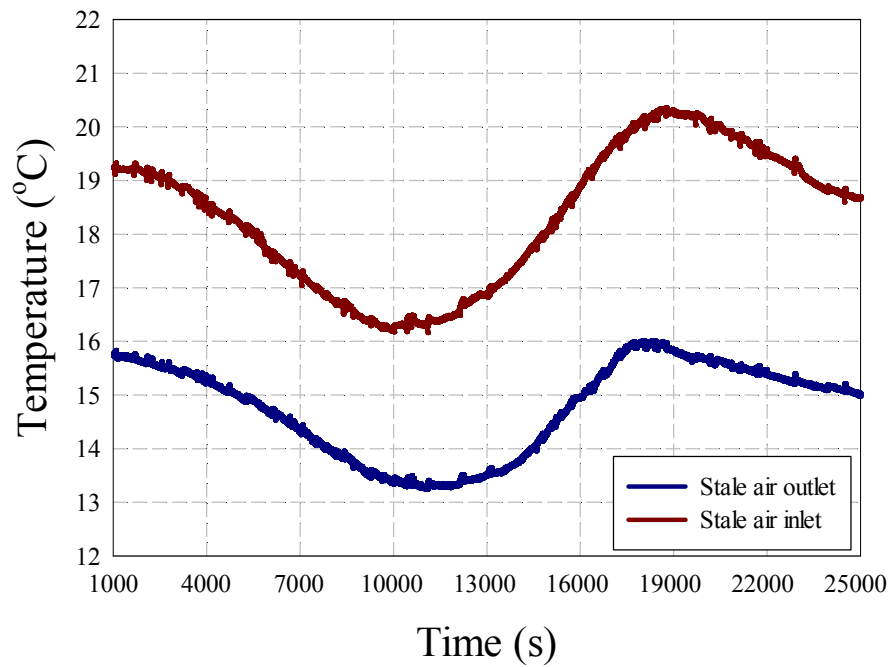


Figure 5.9. Temperature variation of stale air at the inlet and the outlet.

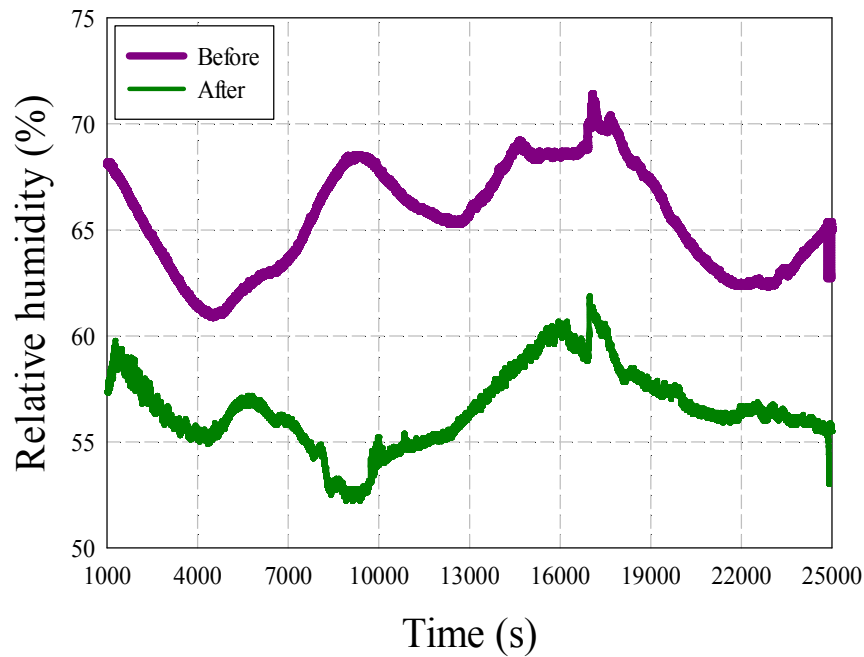


Figure 5.10. Indoor relative humidity variation at pre and post-retrofit cases.

5.7. Conclusions

Within the scope of this experimental research, thermal comfort analyses of a residential house integrated with a novel roof type polycarbonate heat exchanger are conducted. At pre and post-retrofit case, temperature, relative humidity and CO_2 measurements are carried out for a test period of one week. The results indicate that the internal CO_2 concentration is not at desirable range due to lack of ventilation in the test house at the pre-retrofit case as shown in Figure 5.11. However, following the integration of the novel ventilation system into the test house, CO_2 concentration is found to be varying notably from 350 to 400 *ppm* as illustrated in Figure 5.12, which corresponds to the actual comfort conditions for indoor environments. It is also concluded from the results that the average relative humidity inside the test house at the post-retrofit case is found to be 57%, which is in the desired range whereas it is considerably high before retrofitting.

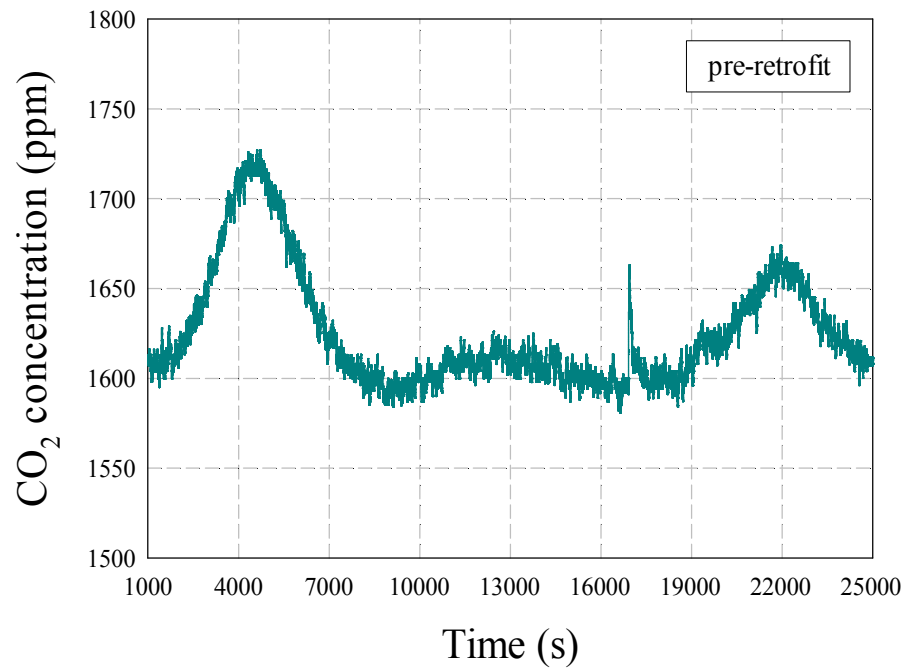


Figure 5.11. CO₂ variation at pre-retrofit case.

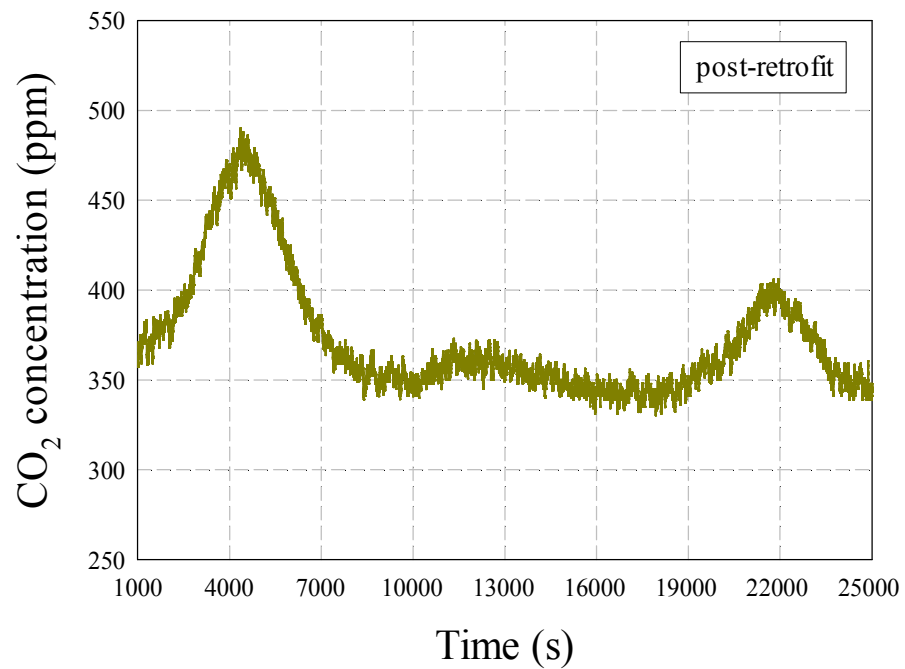


Figure 5.12. CO₂ variation at post-retrofit case.

CHAPTER 6

Evaporative cooling systems for building applications: A review

- 6.1. Introduction
- 6.2. Evaporative Cooling System
- 6.3. Building Applications
- 6.4. Thermal Performance Assessment
- 6.5. Thermodynamic Performance Analysis
- 6.6. Techno-Economic and Environmental Aspects
- 6.7. Conclusions

CHAPTER 6

Evaporative cooling systems for building applications: A review

6.1. Introduction

The rapidly growing world and rising technological advances increase the energy consumption, and hence the energy demand of the world. The rapid growth of energy use worldwide has increased attentions over the difficulties of energy providing, insufficient primary energy resources and adverse effects such as global warming, climate change, ozone depletion, etc [3,4]. According to data of International Energy Agency (IEA), the primary energy consumption showed an upward trend during the last two decades (1984-2004). The average energy use growth 10% per person while world population continued to increase of 27%. Thus the primary energy consumption and CO_2 emissions risen by 49% and 43%, respectively, with an average annual increase of 2% and 1.8%, respectively [3,208]. According to data of International Energy Agency, the total primary energy supply was calculated 13,113 *Mtoe* (as seen in Figure 6.1) while the total energy consumption and CO_2 emissions were 8,918 *Mtoe* and 31,342 *Mt*, respectively, for the year of 2011 as it is illustrated in Figure 6.2. In current scenario for 2035, it is predicted by the experts that the total final consumption will reach to 11,750 *Mtoe* and CO_2 emissions will be 37,037 *Mt* as it is clearly shown in Figure 6.3a and Figure 6.3b, respectively. Recent statistics also reveal that there was an increment of 2.78% in total final energy consumption from 2010 to 2011, and hence a 3.35% rise in CO_2 emissions [209,210].

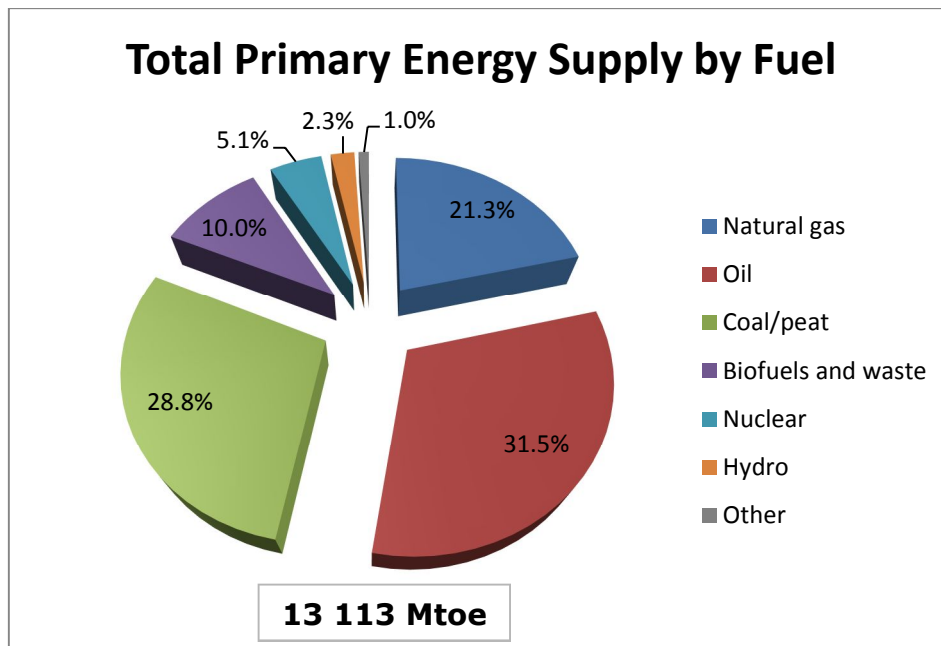


Figure 6.1. Total primary energy supply by fuel in 2011 [209].

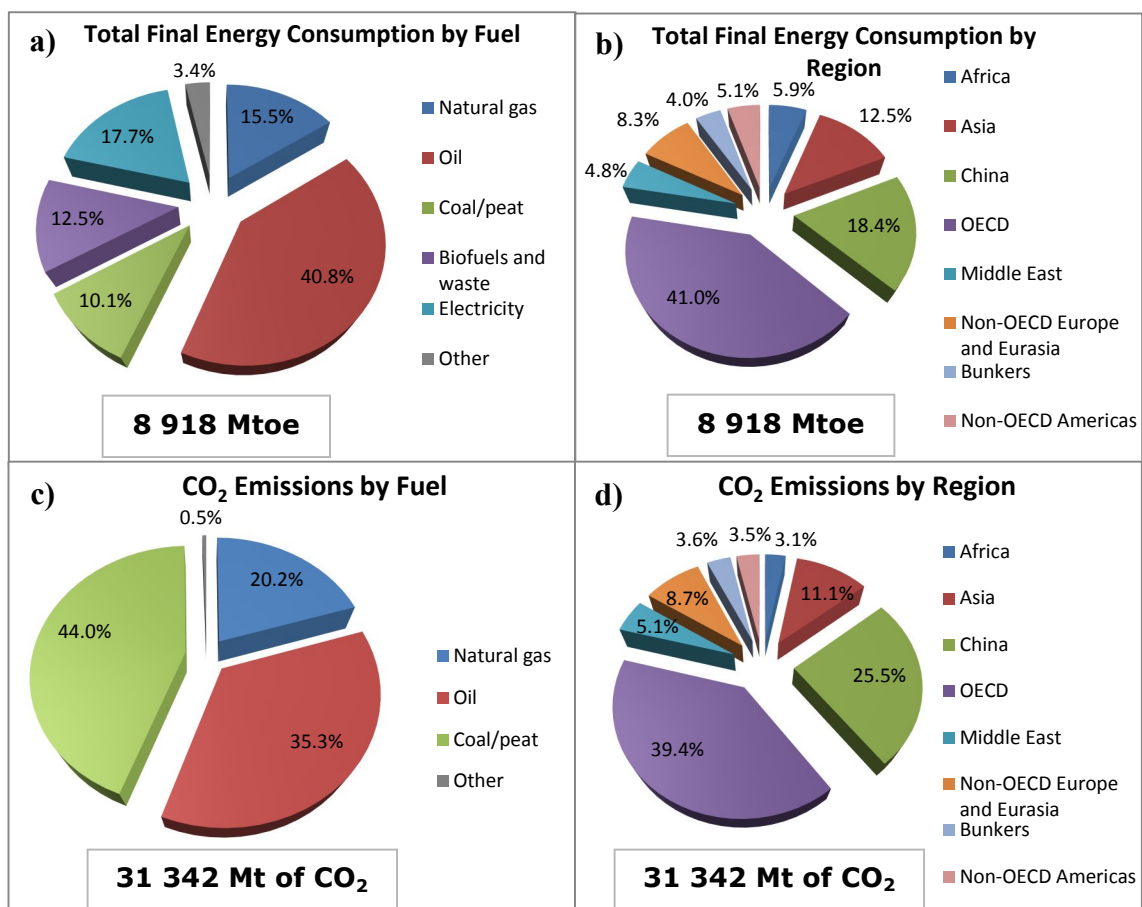


Figure 6.2. Total final energy consumption by fuel (a) and by region (b), and CO₂ emissions by fuel (c) and by region (d) in 2011 [209].

Building sector accounts for more than 60% of total energy consumption in the world while the share of domestic buildings is 20-40%. Most of the energy consumed is essentially utilised for heating and cooling applications in domestic buildings. It is noted that energy requirement for cooling reached 14.6% per annum between 1990 and 2000 [211]. In *EU* residential building sector is responsible for about 57% of the total energy consumption for space heating, 25% for domestic hot water and 11% for electricity.

Energy demand of buildings will continue to rise in near future owing to long-term use of buildings, increasing comfort demand of occupants and growth in population. In literature, energy saving for *HVAC* is achieved using alternative technologies instead of traditional one. The energy efficiency of buildings is of prime concern for an occupant who wants to make energy saving especially in *HVAC* sector [199,212]. In this instance, it is essential to focus on energy efficient technologies and solutions not only in new buildings but also in existing buildings. There are many technologies to mitigate the energy consumption used for cooling in hot climatic conditions. One of these technologies is evaporative cooling system which is a very effective technology for hot and dry climates. In this paper, a thorough review of evaporative cooling technologies and their building applications is presented.

6.2. Evaporative Cooling System

There are many types of cooling systems that provide cool fresh air for domestic or commercial use. The choice of any system directly affects the amount of energy consumed along with the amount of the carbon dioxide emission released to the atmosphere. Evaporative cooling is a novel technology that supplies cool air to the occupants as well as providing a promising way to reduce carbon emissions and energy consumption. Evaporative cooling is a concept that is defined as making air cool via

increasing its water vapour content. In other words, air becomes cooler while its humidity level increases. An evaporative cooling system is mainly attractive in hot and arid climatic conditions in terms of thermal performance owing to the notable potential of humidity increment of air which results in significant reductions of temperature. On the contrary, humid climates are not appropriate for the said system since the air is almost saturated, hence the cooling capacity of the system is limited. In terms of thermal comfort, stand-alone evaporative cooling systems can address the needs of occupants in hot and arid conditions as the final relative humidity stays in the range of 60–70%. However, it is very difficult to get the same results for humid climates since almost saturated conditions are required for the desired temperature drop. In such circumstances, hybrid systems such as desiccant based evaporative cooling are preferred.

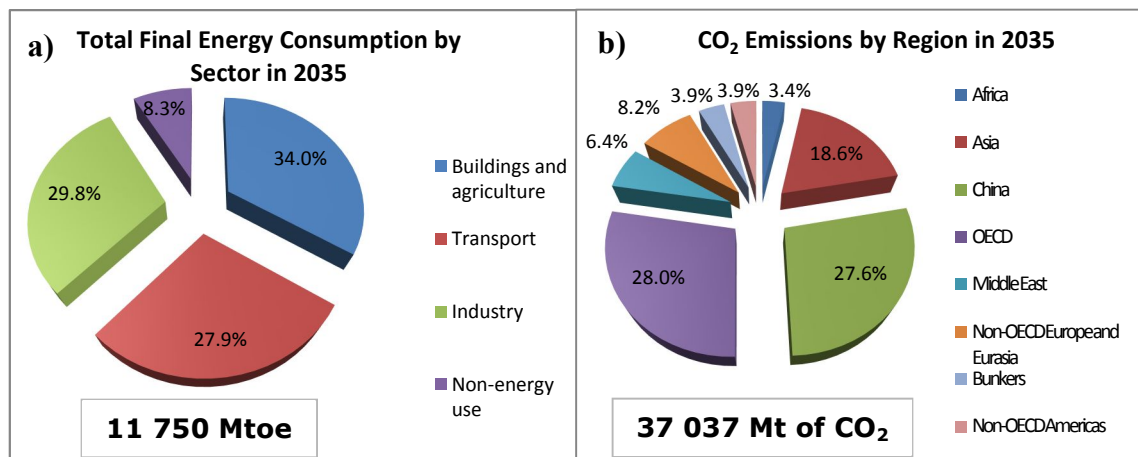


Figure 6.3. Total final energy consumption by sector (a) and CO_2 emissions by region (b) in 2035 [209].

6.2.1. Working principle of an evaporative cooling system

An evaporative cooling system simply works as increasing the moisture contents of the air with use of water. When a hot and dry air welcomes water, the water starts to

evaporate with help of energy taken from the air. Thus the air becomes cooler whereas its relative humidity ratio goes up. The evaporative cooling system can be categorised as direct contact or indirect contact with respect to interaction between the streams as illustrated in Figure 6.4.

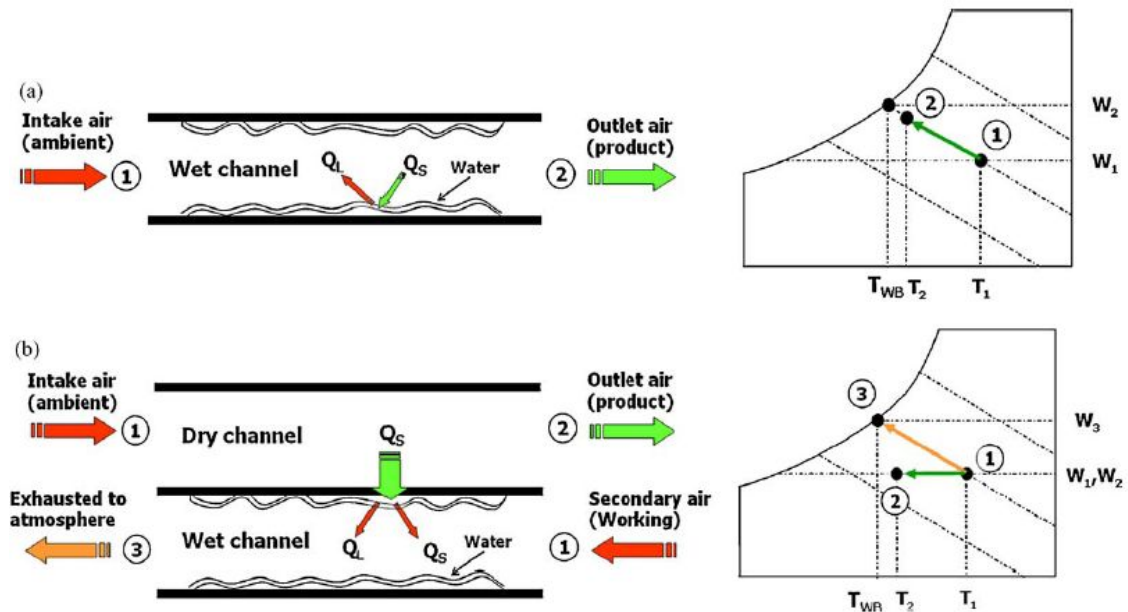


Figure 6.4. Direct evaporative cooling (a) and indirect evaporative cooling (b) [213].

The direct contact evaporative cooling systems are utilised to cool the intake air in hot and dry climatic conditions. It is possible to get adequate cooling by use of this system, but the increasing level of the air humidity might make the occupants uncomfortable. On contrary to direct contact system, an indirect contact evaporative cooling system can deal with undesired living conditions for the occupants owing to its characteristic configuration. In an indirect contact evaporative cooling system, however, the cooling performance is well below compared to the direct contact one. In this respect, a new system called M-cycle has been introduced to get a better cooling performance as well as reasonable relative humidity ratio. A simple working principle

of the M-cycle is shown in Figure 6.5. A typical M-cycle uses a cross-flow heat exchanger (as seen in Figure 6.6) and indirect evaporative coolers. This cycle allows any liquid or vapour to be cooled below the wet bulb temperature and towards the dew point temperature to increase the cooling performance of the system, hence achieving the maximum cooling of incoming air [214].

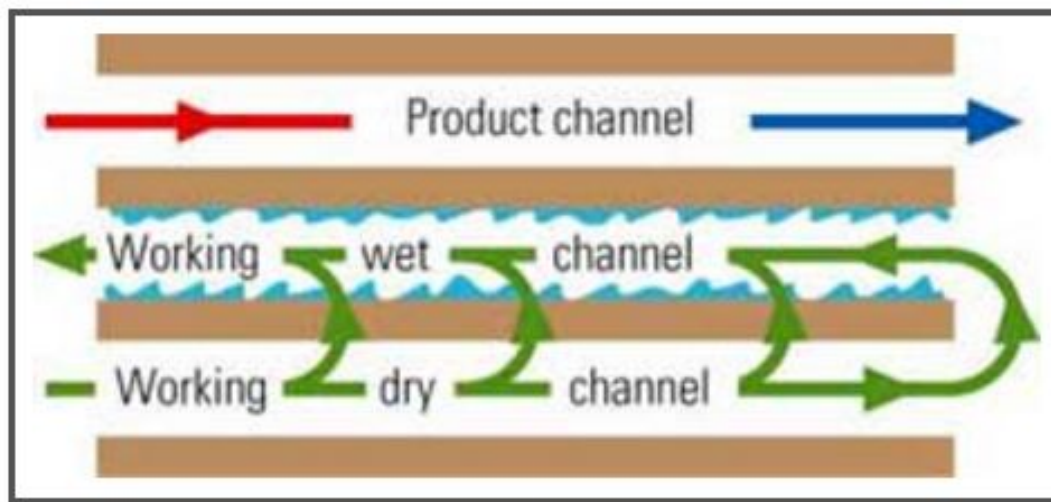


Figure 6.5. Working principle of an M-cycle [214].

6.3. Building Applications

Evaporative cooling systems are widely used in building sector nowadays as an alternative to conventional air conditioners. Energy consumed in *HVAC* systems accounts for about 20% of the total world energy consumption [193], and hence novel solution to mitigate this figure is of vital importance due to growing significance of environmental issues [101]. Evaporative cooling technology offers a wide range of opportunities for buildings to fulfil this purpose owing to low retrofit costs, high efficiency ranges, insignificant maintenance and attractive payback periods [215]. In this respect, numerous attempts are made worldwide especially in recent years for energy-efficient retrofitting of building sector. Belarbi et al. [216] develop a novel water

spraying evaporation system for passive cooling of buildings. A test building illustrated in Figure 6.7a is constructed in Catania, Italy, and integrated with a shower tower within the scope of a European project PDEC/JOULE. For different orientations of nozzles, evaporative cooling performance is determined as shown in Figure 6.7b. The results indicate that the system developed provides thermal comfort conditions with a minimal water use. For the outside temperature of 33 °C, the temperature in the tower does not exceed 27 °C with a water consumption of 10 L/h. Ghosal et al. [217] theoretically and experimentally investigate the thermal performance of a novel evaporative cooling unit with moving water film as shown in Figure 6.8. Parametric analyses including the effects of flow rate of water, length of roof, relative humidity of ambient air and absorptivity of shading material on the cooling performance of greenhouse room air temperature are carried out. The results reveal that the air temperature of the test house is reduced by 6 and 2 °C in shaded with water flow and shaded conditions, respectively compared to without shading conditions.

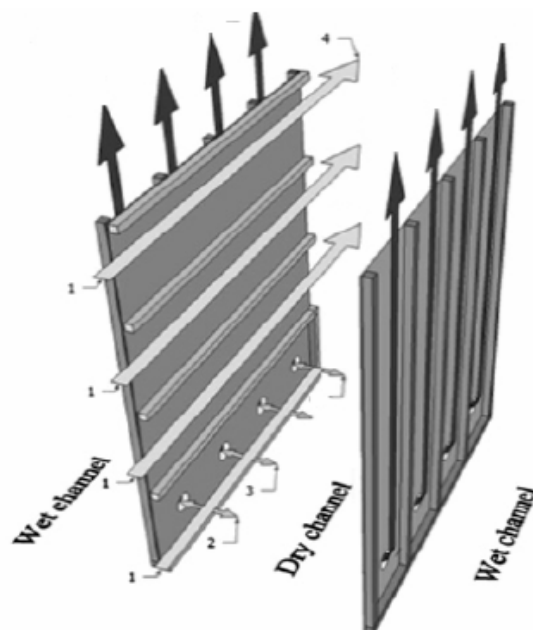


Figure 6.6. Wet and dry channels of a cross-flow heat exchanger in M-cycle [214].

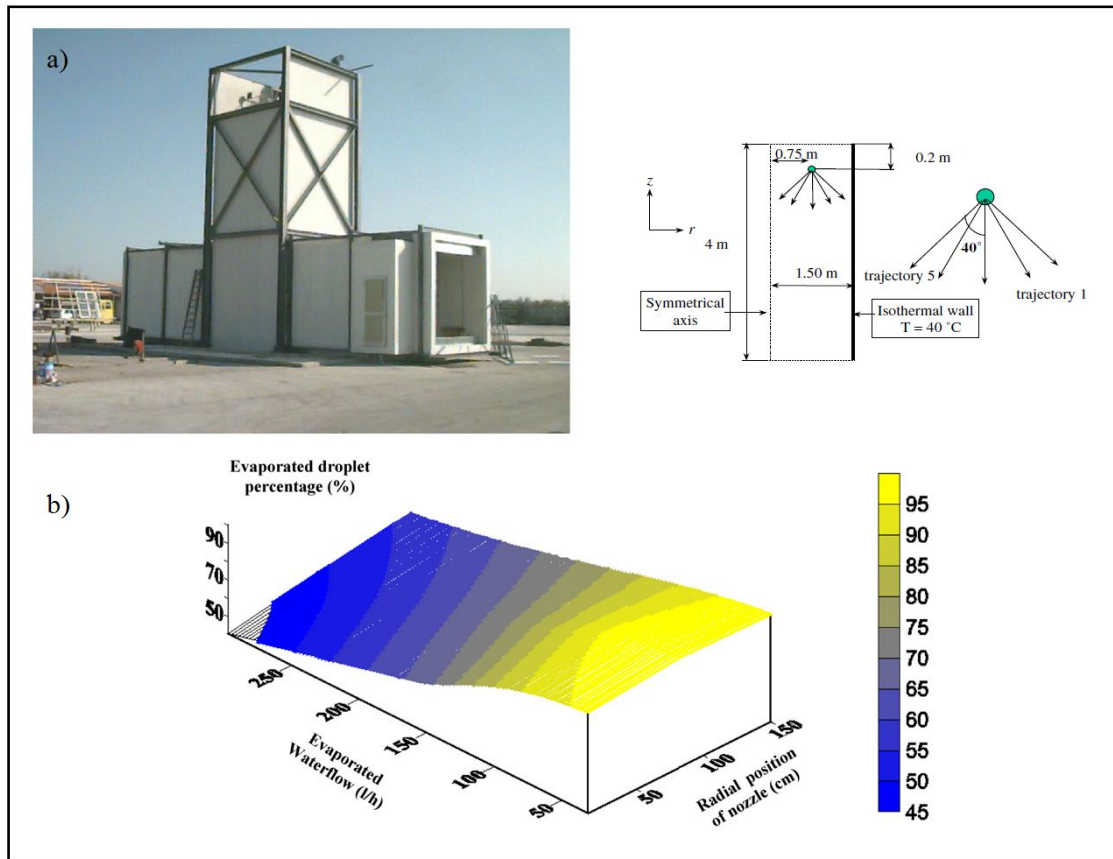


Figure 6.7. Water spraying evaporative unit for passive cooling of buildings [216].

Wanphen and Nagano [218] investigate the impact of several porous materials on the performance of evaporative cooling system. The measurement results indicate that the porous materials can satisfactorily reduce surface temperature of the roof. Among the tested samples, siliceous shale of both small and large particle diameter is found to decrease the daily average surface temperature by up to 6.8 and 8.6 °C, respectively. Cheikh and Bouchair [219] develop an evapo-reflective roof for hot dry climates as shown in Figure 6.9a. The roof sample is composed of a concrete ceiling and a flat aluminium plate separated by an air space partially filled with high thermal capacity rocks placed in a small amount of water. The system is adequately closed to prevent water vapour escaping outside. The results indicate that the most significant factors affecting the cooling power of the passive cooling roof are the rocks, water volume,

aluminium roof thickness and roof air space width. Air temperature changes in the test room for ventilated and non-ventilated room case are illustrated in Figure 6.9b.

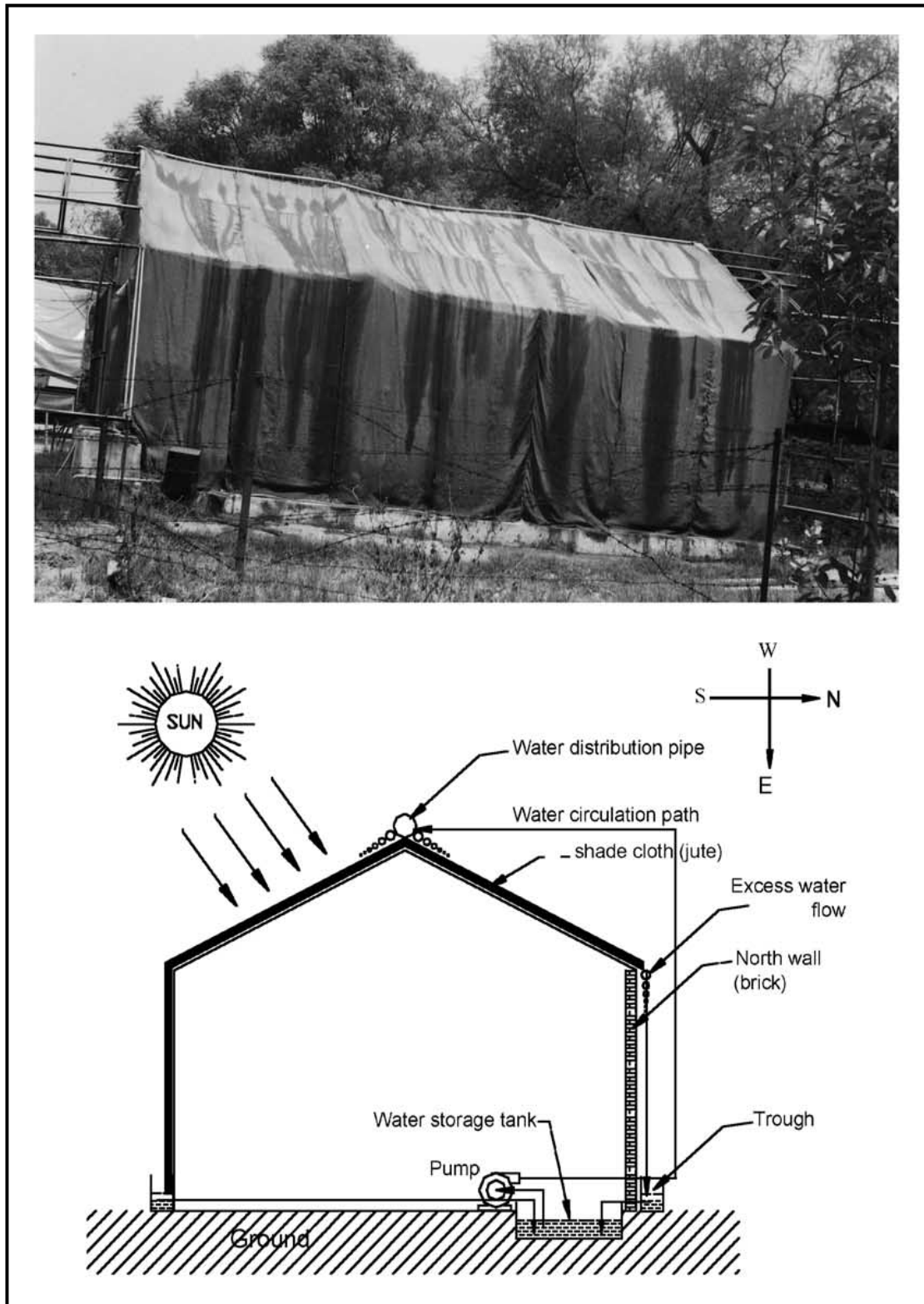


Figure 6.8. A test house covered with shade cloth and water flow arrangement [217].

He and Hoyano [220] develop a novel passive evaporative cooling wall including porous ceramics with high water soaking-up ability. The passive cooling strategy aims at controlling the increased surface temperatures and creating cooler environments especially during summer. The ceramic pipes enable the pipe's vertical surface to be wet to a level higher than 1 m in an outdoor location exposed to the sunlight when the lower end of the pipe is placed in water. Wet surface conditions can be maintained throughout a period of sunny days in summer. Surface temperatures can also be kept below outside temperature. As a consequence of several successful applications of evaporative cooling systems in buildings, novel designs of evaporative cooling technology are constructed, retrofitted to different types of buildings and tested for various climatic conditions. Table 6.1 provides a comprehensive overview of pioneer works on the scope. It can be easily concluded from the previous works that evaporative cooling systems can successfully be an alternative to traditional air conditioners and provide large amounts of energy saving with attractive payback periods.

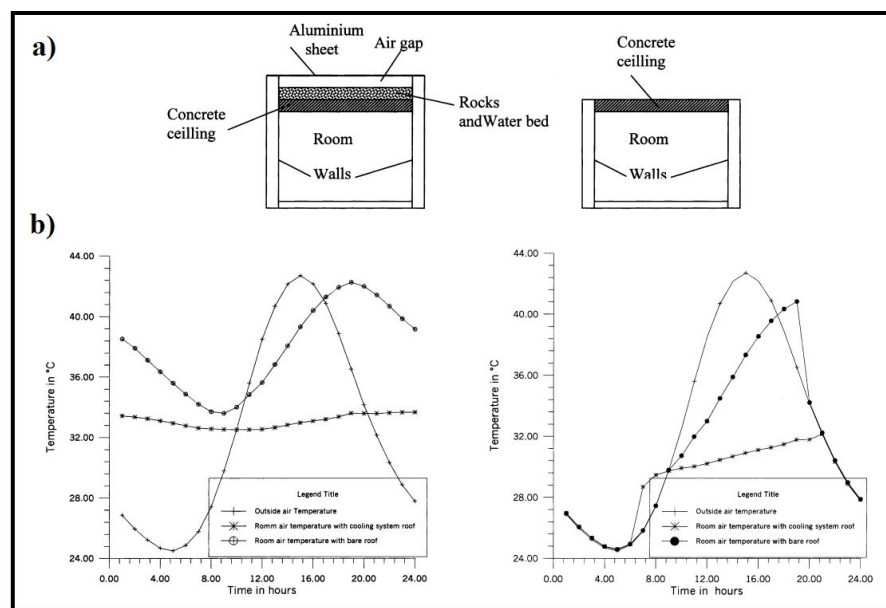


Figure 6.9. Air temperature changes in the test room for ventilated and non-ventilated room case [219].

Table 6.1. Pioneer works on building applications of evaporative cooling systems

Authors	System type	Building type	Region	Climate	Key findings
Bowman et al. [221]	Passive draught evaporative cooling system	Non-domestic buildings	Southern Europe	Hot dry	A new CFD code is presented to simulate the injection of cold water
Costelloe and Finn [222]	Indirect contact evaporative cooling system	Office buildings	Dublin and Milan	Temperate	As a consequence of 16 °C cooling water from October to May, the office buildings in Dublin can be cooled throughout the year without use of conventional cooling. In Milan, a similar performance can be achieved from November to March.
Heidarimejad et al. [223]	Two-stage indirect-direct evaporative cooling system	Public buildings	Tehran	Multi	Two-stage indirect/direct evaporative cooling system can be preferred to mechanical vapour compression systems in regions with higher wet bulb temperatures to minimise energy consumption. However, water consumption of the two stage system is 55% greater than that of traditional direct evaporative cooling systems.
Ibrahim et al. [224]	Direct evaporative cooling system equipped with porous ceramic evaporators	Residential buildings	Nottingham	Multi	Direct evaporative cooling system supported with porous ceramic evaporators can provide 6-8 °C in dry bulb temperature with a 30% rise in relative humidity. Maximum cooling achieved of the system is 224 W/m ² .

Hajidavalloo [225]	Indirect contact evaporative cooling system	Residential buildings	Khoozestan	Very hot	Through the indirect contact evaporative cooling system, power consumption can be decreased by about 16% in very hot climates, and the COP can be enhanced by 55% compared to conventional air conditioners.
Maheshwari et al. [226]	Indirect contact evaporative cooling system	Residential buildings	Kuwait	Extreme	Indirect evaporative cooling system are found to be much more appropriate compared to conventional air conditioners in terms of energy consumption. It is underlined that they are able to provide 40% reduction in peak power demand.
Riangvilaikul and Kumar [227]	Dew point evaporative cooling system	Various buildings	Thailand	Multi	Dew point effectiveness varies notable from 65 to 86% when the inlet air humidity ratio changes from 6.9 to 26.4 g/kg at constant inlet temperature. However, wet bulb effectiveness is less sensitive varying from 106 to 109% for the same inlet condition.
Bruno [228]	Dew point evaporative cooling system	Commercial buildings	Australia	Temperate	Dew point effectiveness varies from 57 to 74% whereas the wet bulb effectiveness ranges from 93 to 106%. The annual energy saving related to ventilation is between 52 to 56%.
Zhao et al. [229]	Indirect contact evaporative cooling system	Residential buildings	Nottingham	Temperate	Fibre material is cost-effective in air-conditioning systems. Wick-equipped aluminium sheets are more adequate for evaporative cooling applications in buildings.

6.4. Thermal Performance Assessment

An evaporative cooling system is an environmentally friendly, energy efficient and cost effective application for hot and arid climates. The type of the evaporative cooling system affects its thermal performance characteristics. In a direct contact cooling system, for instance, the cooling efficiency of such a system is expected to be higher compared to the indirect contact one as seen in Figure 6.10. This is one of the parameters that influence the thermal performance of the system. In literature, many attempts have been made by researchers to investigate the thermal performance of different types of the evaporative cooling systems. Heidarinejad et al. [223] experimentally investigate the cooling performance of two-stage indirect/direct evaporative cooling system for various climatic conditions. The effectiveness of indirect and indirect/direct system is calculated to be in the range of 55-61% and 108-111%, respectively. It is obtained from the results that the water consumption of hybrid system somewhat higher than direct cooling system as illustrated in Figure 6.11.

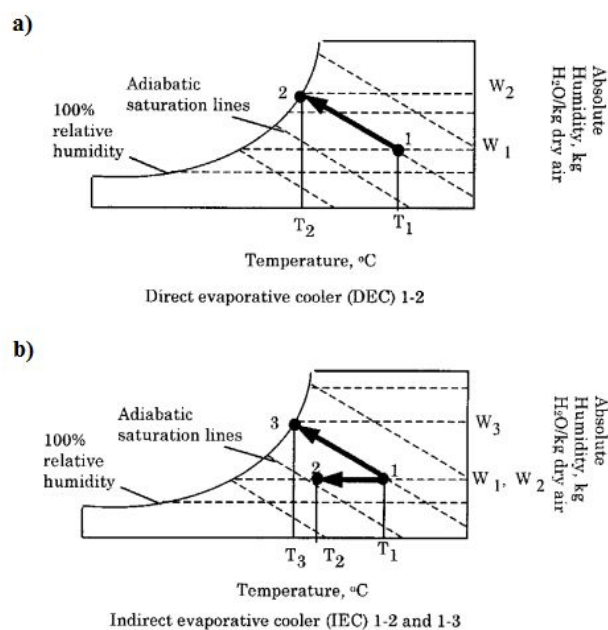


Figure 6.10. Thermal values of the air in psychrometric chart for a direct (a) and an indirect (b) evaporative cooling [230].

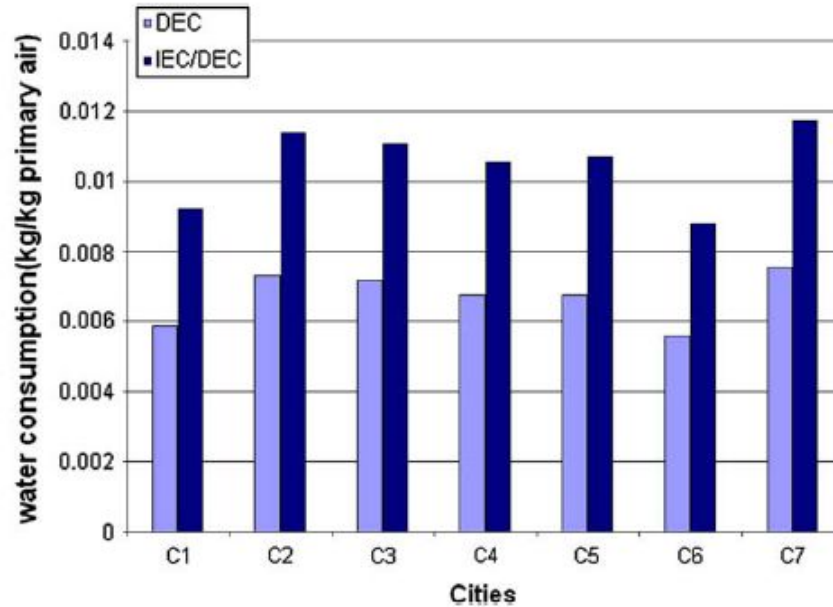


Figure 6.11. Water consumption of direct and indirect/direct evaporative cooling system in different climatic conditions [223].

An experimental analysis of semi-indirect contact evaporative cooling system is carried out by Velasco Gomez et al. [231]. The system designed consists of two independent air flows separated by ceramic material. In this system, the partial pressure of the water vapour in the outdoor air is the controlling factor in mass transport process. When the relative humidity of the outdoor air is low, evaporation is achieved towards the air flow from the external pores of the pipes. Depending on the permeability of the wall of the porous solid separating the two air flows, greater or lower water diffusion is observed. If outdoor humidity is high, with a dew point temperature higher than the surface temperature, outdoor air can be dehumidified. As illustrated in Figure 6.12, a return air is in direct contact with water in a cooling tower to make the supply air cool. Figure 6.13 shows the heat and mass exchange in ceramic pipes. Maximum *COP* value of the system is found to be 9.64, and the efficiency of the system is 70%. Thermal performance assessment of recent papers related to evaporative cooling system is given

in Table 6.2. In this table, effects of various climatic conditions from different regions on thermal performance of evaporative cooling systems are investigated by researchers. In most of the applications, efficiency/effectiveness of the system is calculated to be above 60%.

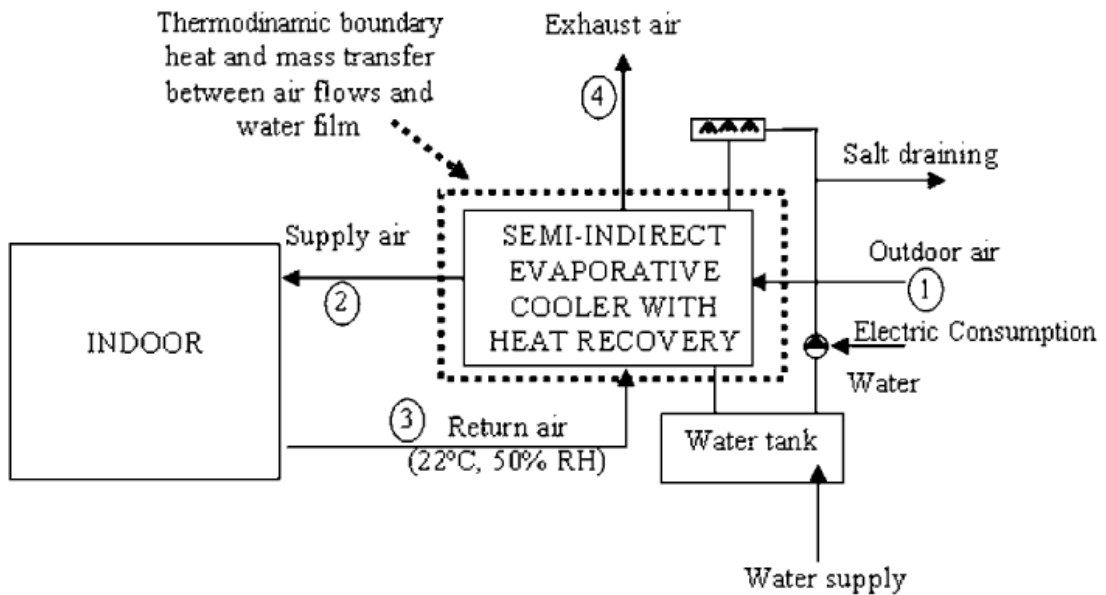


Figure 6.12. Semi-indirect contact evaporative cooling system [231].

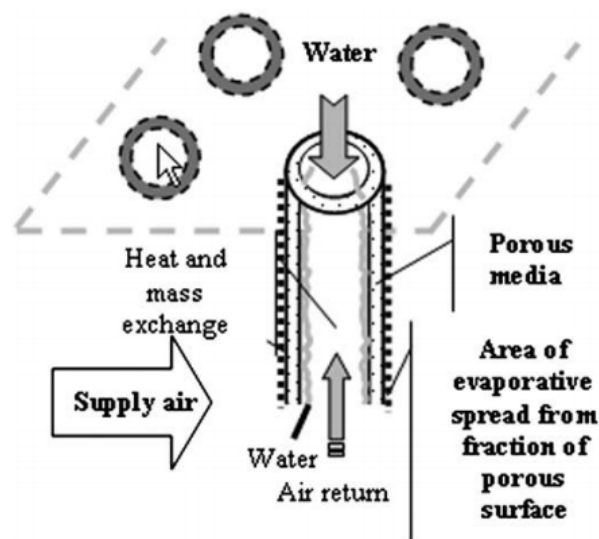


Figure 6.13. Heat and mass exchange in ceramic pipes [231].

Table 6.2. Thermal performance assessment of evaporative cooling systems

Authors	System type	Application	Region	COP	Efficiency/effectiveness
Heidarinejad et al. [223]	Two-stage indirect/direct evaporative cooling system	Domestic and non-domestic buildings	Iran	-----	The effectiveness for indirect evaporative cooling unit is found to be 55-61% whereas it is 108-111% for indirect/direct cooler.
Riangvilaikul and Kumar [227]	Dew point evaporative cooling system	Multi	Thailand	-----	The dew point and wet bulb effectiveness are in the range of 65-86% and 106-109%, respectively.
Velasco Gomez et al. [231]	Semi-indirect evaporative cooling system	Domestic building	Spain	0.74-9.64	The efficiency of evaporative cooler is calculated to be 70%.
Chen et al. [232]	Indirect contact evaporative cooling system	Domestic and non-domestic buildings	USA and China	-----	The effectiveness of the systems tested varies from 40 to 80% depending on primary air flow rate.
El-Dessouky et al. [233]	Both indirect and direct contact evaporative cooling system	-----	Kuwait	-----	The efficiency of indirect contact evaporative cooler changes between 20-40% while that of direct contact cooling unit is 63-93%.
Zhang et al. [234]	Direct evaporative cooling system	Multi	China	2.88	The direct evaporative cooling effectiveness changes from 67-86%, depending on the air velocity and sprinkling density.
Kruger et al. [235]	Indirect evaporative cooling system	Multi	Venezuela and Israel	0.29-0.47	-----

6.5. Thermodynamic Performance Analysis

Thermal performance investigation of evaporative cooling systems is commonly referred to efficiency or effectiveness assessment with a *COP* calculation. However, as emphasised by Kanoglu et al. [236], exergy analysis also needs to be considered for a thorough thermodynamic performance analysis of evaporative cooling systems. Exergy analysis is a significant tool in the design, optimisation, and performance evaluation of energy systems including evaporative coolers. Basically, exergy analysis aims at determining the maximum performance of the system as well as identifying exergy destruction.

Wet bulb effectiveness, which is the ratio of temperature depression of the device to the potential wet bulb depression [237], is commonly utilised in literature for the energy efficiency assessment of evaporative cooling systems. It is defined as follows:

$$\varepsilon_{wb} = \frac{T_{in} - T_{out}}{T_{in} - T_{wb,in}} \quad (6.1)$$

where ε_{wb} is the wet bulb effectiveness, T_{in} is the inlet temperature of supply air, T_{out} is the outlet temperature of supply air and $T_{wb,in}$ is the wet bulb temperature of inlet air. The wet bulb effectiveness simply indicates the ability to cool the inlet air below wet bulb temperature with minimal moisture addition. The techno-economic performance assessment of evaporative cooling systems is mostly explained by *COP* analysis. The *COP* calculation is basically performed as determining the cost of cooling achieved from the evaporative cooling systems as follows [238]:

$$COP = \frac{\dot{m}_{in}c_{in}(T_{in} - T_{out})}{P_{W_{cons}}} \quad (6.2)$$

where \dot{m}_{in} is the mass flow rate of inlet air, c_{in} is the specific heat capacity of inlet air and $P_{w_{cons}}$ total power consumption of the system through fans or water pumps. Exergy analysis provides an exergy destruction term for a more reliable performance assessment as follows:

$$\eta_{ex} = \frac{\dot{h}_{in} - \dot{h}_{out} - T_{in}(s_{in} - s_{out})}{\dot{h}_{in} - \dot{h}_{wb,in} - T_{in}(s_{in} - s_{wb,in})} \quad (6.3)$$

where η_{ex} is the exergy efficiency of the system, \dot{h}_{in} is enthalpy of inlet air, \dot{h}_{out} is the enthalpy of outlet air, s_{in} is the entropy of inlet air, s_{out} is the entropy of outlet air, $\dot{h}_{wb,in}$ is the wet bulb enthalpy of inlet air and $s_{wb,in}$ is the wet bulb entropy of inlet air.

Thermodynamic performance assessment of evaporative cooling systems has been taken into consideration by several researchers as illustrated in [Table 6.3](#). It is understood from the pioneer works that the overall energy efficiency of evaporative cooling systems is greater than 90%, whereas the exergy efficiency varies from 19.1 to 38.0% depending on the system type. The *COP* range of the said systems ranges from 0.190 to 0.345.

6.6. Techno-Economic and Environmental Aspects

Building sector has a high impact on world's total energy consumption. Especially in hot and arid climates, significant part of this energy is consumed due to air-conditioning to make the occupants more comfortable. In India, for instance, air-conditioning is responsible from about 32% of electricity consumption in a typical building [240]. Water-cooled air-conditioning systems are energy efficient technologies compared to the conventional one [241]. A recent study shows that 12.05% saving in annual power consumption of a building is achieved with use of a simple evaporative

cooling system [242]. The energy saving potential is found to be relatively higher when a regenerative evaporative cooling system is used as seen in Table 6.4. In another study, energy saving potential of indirect evaporative cooler (IEC) is tested [226]. It is reported that 12,418 and 6,320 kWh seasonal energy savings are achieved for interior and coastal areas, respectively. Figure 6.14 shows monthly energy saving of indirect evaporative cooler for two locations in Kuwait. A passive downdraught evaporative cooling is studied by Ford et al. [243] in Indian climatic conditions. A 10-15 °C decrease in supply air temperature is succeeded as well as providing good air movement. In addition to these, 64% of substantial energy saving is obtained as supplying good thermal comfort conditions for the occupants. An energy efficient evaporative cooling system contributes to reach global targets in energy saving, and hence carbon reduction measures [244]. A desiccant based indirect evaporative cooling is studied by Goldsworthy and White [245]. Similarly, the results show that the evaporative cooling system has a high potential to save energy and to reduce greenhouse gas emissions associated with cooling of buildings.

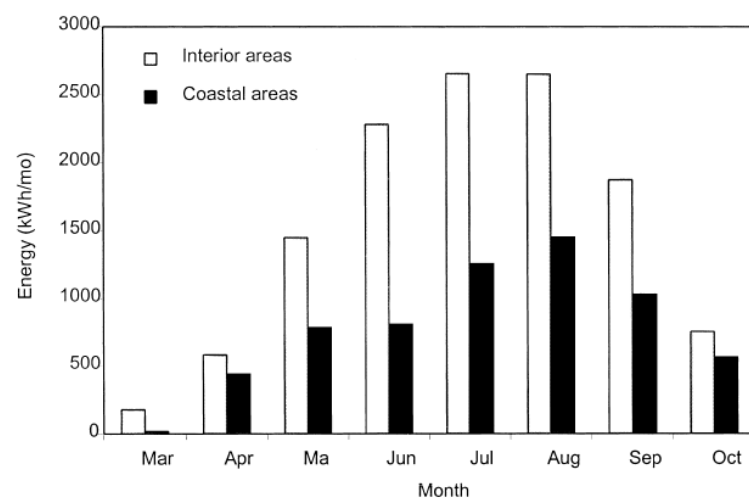


Figure 6.14. Monthly energy saving of indirect contact evaporative cooling unit for interior and coastal areas [226].

Table 6.3. Thermodynamic performance assessment of evaporative cooling systems

Authors	System type	Energy efficiency (%)	Exergy efficiency (%)	COP
Kanoglu et al. [236]	Open cycle desiccant-based evaporative cooling system	93.6	36.5	0.345
Caliskan et al. [237]	Dew point evaporative cooling system	90.0	19.1	0.190
Taufiq et al. [239]	Direct contact evaporative cooling system	-----	38.0	-----

Table 6.4. Annual energy consumptions (*MWh*) of three different types of air-conditioning systems [242]

	Existing chiller	Coupled evaporative cooling	Coupled regenerative evaporative cooling
Chiller energy	320.06	140.28	85.90
Heating energy	125.13	131.62	127.35
Fan energy	340.71	340.71	340.71
Pump energy	182.52	182.52	182.52
Additional energy	---	9.44	18.70
Total air-conditioning energy	968.42	804.57	755.18
Light and equipment	390.80	390.80	390.80
Total energy	1359.21	1195.36	1145.97
Percentage of air-conditioning energy	71.25	67.31	65.90
Air conditioning energy saving (%)	---	16.92	22.02
Total energy saving (%)	---	12.05	15.69

6.7. Conclusions

An intelligent building is defined as maximising the efficiency of the service with a minimum cost [246]. Energy consumption of the building sector increases day by day due to good thermal comfort demand of the occupants. That's why, use of energy-

efficient technologies in buildings is of prime concern for anyone wishing to save both energy and money [212]. In this study, a thorough review of different types of energy-efficient evaporative cooling systems is given. The results show that the evaporative cooling systems have a great potential to save energy in hot and arid climatic zones. It also seems that this novel solution is a very cost effective way compared to the alternative air-conditioning applications. This technology has a good efficiency/effectiveness value as well as a good *COP* range. In future works, evaporative cooling systems might be integrated with liquid or solid desiccant units to cover the requirements of different climatic regions. Thus, not only the desired temperature range but also the expected thermal comfort conditions of occupants can be provided for any type of climatic zone.

CHAPTER 7

Theoretical investigation of a novel indirect-contact evaporative cooling system for building applications

- 7.1. Introduction
- 7.2. A Novel Evaporative Cooling System
- 7.3. Mathematical Model of the System
- 7.4. Results and Discussion
- 7.5. Conclusions

CHAPTER 7

Theoretical investigation of a novel indirect-contact evaporative cooling system for building applications

7.1. Introduction

Clean energy generation and its effective utilisation is of vital importance worldwide due to growing significance of environmental issues depending on global warming [99–104]. Fast increases in energy consumption as a result of the population growth and economic development dominate the greenhouse gas concentrations in the atmosphere. Despite intensive efforts to narrow the gap between conventional energy sources and renewables, only about 14% of total world energy demand is supplied by renewable energy technologies at the moment [5,6]. In this regard, there is a consensus among scientists that research on energy management and efficient minimisation of energy consumption is compulsory. Several measures are taken throughout the world for the urgent stabilisation of greenhouse gas concentrations in the atmosphere by reducing the energy demand in all sectors. Previous works indicate that buildings account for a significant part of the world's energy consumption. As an instance, a research carried out in 1999 indicates that the total energy consumption in Europe is 1780 million tons of oil equivalent, and 35% of this amount is consumed by residential and commercial sector [106]. In another report, total energy consumption of the United Kingdom by sector and by building type is specified [247]. As illustrated in Figure 7.1, building sector and domestic buildings are responsible for 46% and 63% of the total

energy consumption, respectively. Baetens et al. [152] also report that buildings emitted 8.3 Gt CO₂ in 2005 accounting for more than 30% of the greenhouse gas emissions in many developed countries. Therefore, dominant impacts of buildings on both the energy consumption levels and the environment are unequivocal.

Cooling energy has an important part in buildings' energy consumption levels. As reported by Hasan [248] in a recent work, the demand for cooling increases day by day as a consequence of the growing demand for better thermal comfort conditions in buildings. Evaporative cooling has a high potential to meet cooling demands at low energy costs [249]. Riangvilaikul and Kumar [213] note that the evaporative cooling is a good alternative to mechanical vapour compression for air conditioning applications since it requires about four times less electric power than vapour-compression refrigeration [250].

Current available evaporative cooling systems can be classified as direct-contact and indirect-contact evaporative coolers. In a direct evaporative cooling system, working air to be cooled is in a direct contact with a liquid water film. Cooling is accomplished by the adiabatic heat exchange between the working air and the liquid water film [251]. Direct-contact evaporative cooling systems are appropriate for use only in dry, hot environmental conditions, or in rooms needing both cooling and humidification [252]. On the other hand, in an indirect-contact evaporative cooler, the inlet air is cooled by so-called working (secondary) air which is cooled through evaporation [253]. Thermodynamically, the wet passage absorbs heat from the dry passage by evaporating water, and thus cools the dry passage, while the latent heat of vaporizing water is dissipated into the working air. Figure 7.2 shows the schematic of an indirect-contact evaporative cooler. The metallic sheet between product and working air is usually an air-to-air heat exchanger, which can be plate type [254,255], tube type

[254,256] and heat pipe type [254,257]. Indirect-contact evaporative cooling systems have the advantage of being able to cool the product air without changing its specific humidity [229]. Therefore, these systems are widely utilised in domestic buildings as air-conditioning units since more than a century [253].

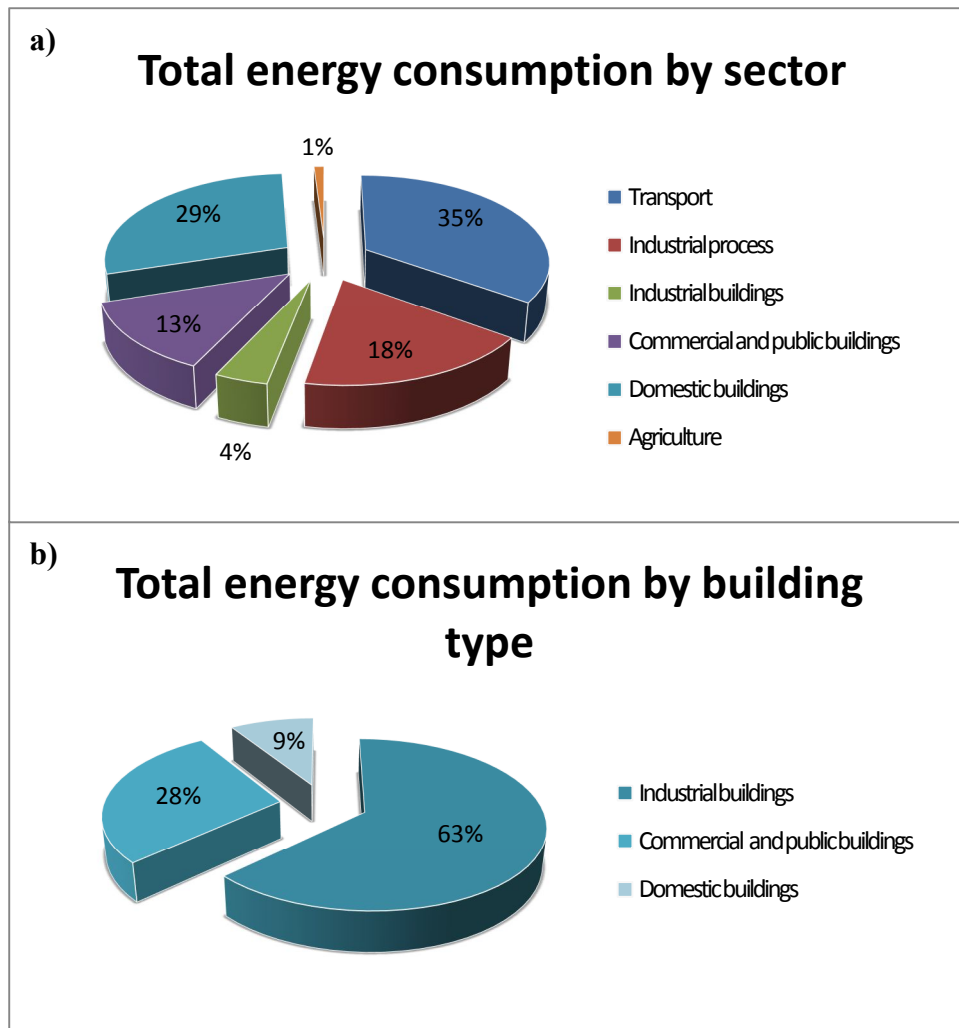


Figure 7.1. Distribution of the total energy consumption of United Kingdom by sector (a) and by building type (b) in 2000 [247].

Theoretical investigation of indirect-contact evaporative cooling systems is somewhat complicated since the cooling of air involves simultaneous heat and mass transfer at the water film-air interface. Several attempts have been made for an accurate

understanding of thermal behaviour of these systems. Earlier theoretical works were carried out by using one-dimensional mathematical models [258–262]. Erens and Dreyer [263] evaluate three analytical models and their results indicate that the optimum shape of the cooling system results in a primary to secondary air velocity ratio of about 1.4, assuming the mass flow rates are the same. Tsay [264] numerically investigates a counter-flow wet surface heat exchanger. It is observed that most of the energy transportation across the water film is absorbed by the film vaporization process. Guo and Zhao [251] present a parametric study for an indirect-contact evaporative cooler. The effects of various parameters such as the velocities of the primary and secondary air streams, the channel width, the inlet relative humidity and the wettability of the plate on the thermal performance are investigated. They state that lower inlet relative humidity of secondary air, a higher wettability of the plate, a higher velocity ratio of the secondary air to primary air provide a higher effectiveness for the cooling system. San Jose Alonso et al. [249] develop a heat and mass transfer model for indirect-contact evaporative coolers. The model is based on basic principles which are already presented in previous works, however it enables to analyse different indirect evaporative cooler designs and conditions. Halasz [265] presents a general mathematical model of evaporative cooling systems. The model is developed by writing a system of four partial differential equations specifying a process of non-adiabatic evaporation with arbitrary flow direction of water, cooled fluid and air. Riffat and Zhu [266] present a heat and mass transfer mathematical model for their novel design of indirect evaporative cooler using porous ceramic and heat pipe. Their results indicate that it is possible to achieve a high cooling capacity under dry and windy conditions. They also note that the indoor air velocity should be set properly (0.6 m/s) for higher efficiency. Zhan et al. [267] compare the performance of counter-flow and cross-flow

heat exchangers for indirect evaporative air coolers. Belarbi et al. [216] theoretically investigate the water spray evaporation for passive cooling of buildings. Similar modelling works are carried out by other researchers [268,269]. Maheshwari et al. [226] evaluate the energy saving potential of indirect-contact evaporative coolers. They observe that interior areas provide notably higher energy saving compared to the coastal areas. An indirect evaporative cooler operating in the interior areas is found to be 30% more cost-effective than a conventional air-conditioning system.

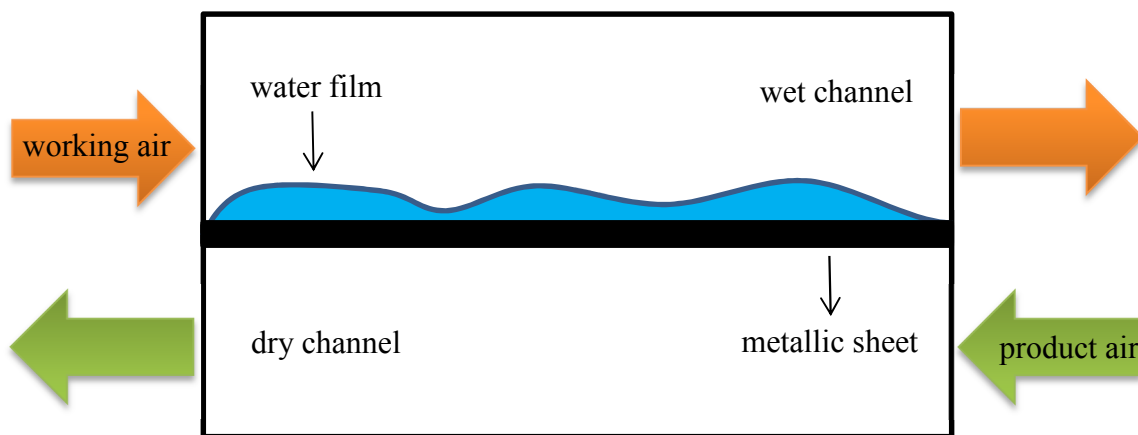


Figure 7.2. A detailed schematic of a counter-flow indirect-contact evaporative cooling system.

A detailed literature review clearly shows that many efforts have been made so far for theoretical investigation of indirect-contact evaporative cooling systems. However, it can be concluded from the previous works that a good agreement between experimental and theoretical results could not be achieved since the process is complicated and the assumptions are not totally accurate. Moreover, the studies focusing on novel indirect-contact evaporative cooling systems for domestic buildings are very limited, and hence a thorough analysis including theoretical investigation and experimental verification is required for a better understanding of the techno-economic

assessment of these systems. Therefore in this study, a mathematical model is presented for a novel design of indirect-contact evaporative cooling system which has already been installed under the roof of a test house in Southeastern UK. This chapter as the first part of the work only includes the description of the novel cooling system, the model and the preliminary results. In the second part of the work, experimental results of the system will be presented in detail.

7.2. A Novel Evaporative Cooling System

This research is the first part of a research on a novel design of indirect-contact evaporative cooling system. The goal of this part is to figure out the operating characteristics of the system through a theoretical work. In this regard, it covers the effects of operating and environmental parameters such as indoor and outdoor temperatures, mass flow rates and relative humidity values of supply and working air, and the duct geometry of the heat exchanger on overall performance of the system. The system has been devised and constructed to ventilate and cool the residential buildings. In this respect, a test house has been built in Southeastern UK as shown in [Figure 7.3](#) and the system has been installed beneath the roof. The test house externally has 7 m length, 3 m width and 4.3 m height. It has two windows plus a velux window in the roof and a double door all double glazed. The dimensions of the test house's components are given in [Table 7.1](#). The walls and the roof have 150 mm mineral wool insulation, whereas the floor has 150 mm.

The proposed indirect-contact evaporative cooling system can be split into two main parts as water spraying unit and heat exchanger unit. The system aims at cooling the stale air coming from indoor environment via humidification in the water spraying unit, then directing it to the polycarbonate heat exchanger unit when the adiabatic

saturation condition is achieved, and thus being able to reduce the temperature of intake fresh air in the counter-flow heat exchanger. Four polycarbonate heat exchanger sheets have been constructed as combining 0.2 mm thick polycarbonate sheets together with a highly thermally conductive adhesive yielding a 10 mm² cross sectional area. Figure 7.4 illustrates the square-sectioned ducts of polycarbonate heat exchanger for incoming and outgoing air. Two of the polycarbonate sheets have been placed at the front of the building while the rest two at the back as it is shown in Figure 7.5.



Figure 7.3. A test house in Southeastern UK.

Table 7.1. Dimensions of the components in the test house

	Test house		Components		
	External	Internal	Windows	Velux window	Door
Length [mm]	7000	6700	1200	750	1500
Width [mm]	3000	2700	100	100	100
Height [mm]	4300	2450 – 3300	1000	900	2050

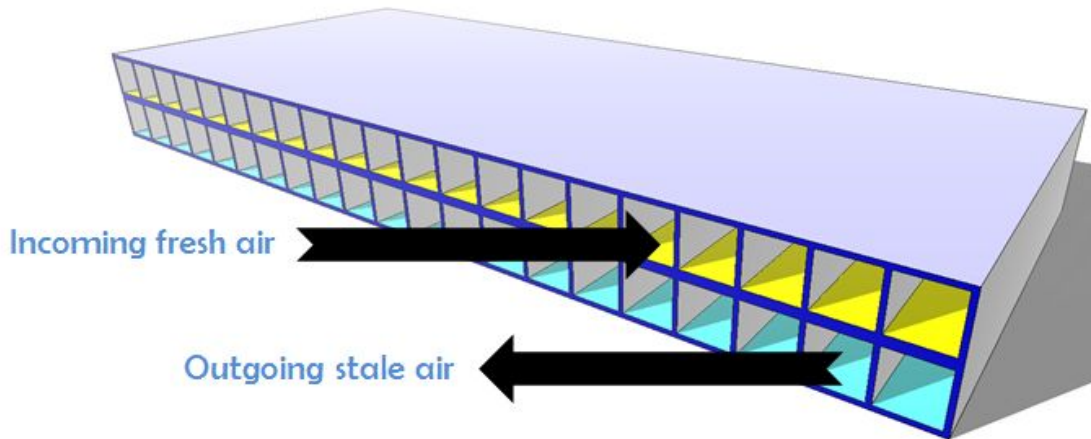


Figure 7.4. Square-sectioned ducts of the heat exchanger unit for hot and cold streams.



Figure 7.5. A polycarbonate sheets integrated to the test house.

The dimensions and the wall thicknesses of polycarbonate heat exchanger are given in [Table 7.2](#). The end of each polycarbonate sheet within the building is followed by an extract duct connected to the upper channels and an inlet duct connected to the lower channels. The extract and the inlet ducts are square with internal dimensions of

60 mm × 60 mm. Both the extract and inlet ducts are then integrated into rectangular ducts with internal dimensions of 105 mm × 50 mm. Finally, the rectangular ducts are connected to fans which can be operated at different velocities of air. The external ends of the polycarbonate heat exchanger terminate beneath the roof slates to let the condensed water run to the gutters. On the other hand, the fresh air is driven from beneath the eaves through air filters. The spraying unit is operated by a valve which adjusts the mass flow rate of the spraying water. The spraying is performed by tap water flowing inside a copper pipe with internal dimensions of 8 mm diameter and 1 m length which is placed at the centre of the extract duct just before the heat exchanger unit. A simplified schematic of the whole system is illustrated in Figure 7.6.

Table 7.2. Dimensions of the proposed polycarbonate heat exchanger

Heat exchanger sheet			Wall thickness [mm]		
Length [mm]	Width [mm]	Depth [mm]	Top	Middle	Bottom
1700	425	10	0.8	0.2	0.8

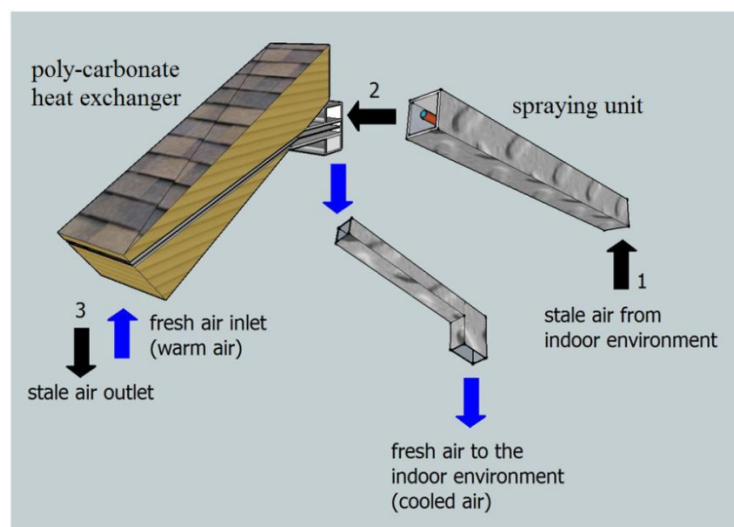


Figure 7.6. Schematic of the proposed indirect-contact evaporative cooling system.

7.3. Mathematical Model of the System

In this section, an accurate mathematical model of the novel indirect-contact evaporative cooling system is presented. The model consists of two parts: theoretical investigation of the water spraying unit and numerical analysis of the polycarbonate heat exchanger unit. First of all, the evaporation rate from the water film to the working air (exhaust air from indoor environment) is determined for different operating conditions, and the thermophysical properties of the working air are determined at the outlet of the water spraying unit. A heat transfer analogy for flow in ducts is employed to estimate the evaporation rate. The evaporation rate is a function of the mass transfer coefficient which is characterised by Sherwood number. The Sherwood number represents the ratio of convective to diffusive mass transport, and it is calculated by correlations of Reynolds and Schmidt numbers. To determine the aforementioned dimensionless numbers, thermophysical properties of air at the film temperature are utilised. The film temperature (T_f) is given as follows:

$$T_f = \frac{T_{lwf} + T_{wa,in}}{2} \quad (7.1)$$

where T_{lwf} and $T_{wa,in}$ are the liquid water film temperature and working air temperature at the inlet, respectively. The characteristic of the flow is then determined by Reynolds number. Reynolds number is a dimensionless number that gives a measure of the ratio of inertial forces to viscous forces and thus, quantifies the relative importance of these two types of forces for given flow conditions [270]. For flow through noncircular tubes, Reynolds number is based on the hydraulic diameter (D_h) and given as follows:

$$Re = \frac{v\rho D_h}{\mu} \quad (7.2)$$

where Re is the Reynolds number, D_h is the hydraulic diameter, v is the velocity, ρ is the density and μ is the dynamic viscosity.

$$D_h = \frac{4A}{p} \quad (7.3)$$

In equation (7.3), A is the cross sectional area of the duct and p is the wetted perimeter. As a second step, Schmidt number is determined by the following equation:

$$Sc = \frac{\nu}{Dm} \quad (7.4)$$

where Sc is the Schmidt number, ν is the kinematic viscosity and Dm is the mass diffusivity. Schmidt number is a dimensionless number which is defined as the ratio of momentum diffusivity and mass diffusivity, and is utilised to characterise fluid flows in which there are simultaneous momentum and mass diffusion convection processes [271]. After determining Re and Sc numbers, Sherwood number (Sh) is calculated as follows:

$$Sh = \frac{KD_h}{Dm} \quad (7.5)$$

where K is the mass transfer coefficient. Sherwood number is a dimensionless number which represents the ratio of convective to diffusive mass transport. The average mass transfer coefficient is computed by the average Sherwood number as follows:

$$\bar{K} = \frac{\bar{Sh}Dm}{D_h} \quad (7.6)$$

where \bar{K} is the average mass transfer coefficient and \bar{Sh} is the average Sherwood number.

To determine the Sherwood number, the following semi-theoretical equation developed by Frossling [272] can be used:

$$Sh = 2 + 0.552Re^{\frac{1}{2}}Sc^{\frac{1}{3}} \quad (7.7)$$

For the mass diffusion coefficient of water vapour, the regression curve fit obtained from the data of Bolz and Tuve [273] can be utilised:

$$Dm = -2.775 \times 10^{-6} + 4.479 \times 10^{-8}T + 1.656 \times 10^{-10}T^2 \quad (7.8)$$

The mass transfer rate is driven by the difference between the concentration of water vapour at the water spraying unit and in the working air. The partial pressure of the water vapour at the water spraying is the saturation pressure of water at T_{lwf} . The concentration of water vapour (C_w) at the water spraying unit is the density of water vapour evaluated at the partial pressure and temperature. The mass fraction of water vapour (mf_w) at the water spraying unit is given by:

$$mf_w = \frac{C_w}{\rho} \quad (7.9)$$

The partial pressure of water in the working air ($P_{w,wa}$) is the product of the relative humidity (ϕ) and the saturation pressure of water vapour ($P_{sat,w}$) at T_{lwf} as given below:

$$P_{w,wa} = \phi P_{sat,w} \quad (7.10)$$

The concentration of water vapour in the working air ($C_{w,wa}$) is the density of water vapour evaluated at the partial pressure and temperature. The mass fraction of water vapour in the working air ($mf_{w,wa}$) is determined by:

$$mf_{w,wa} = \frac{C_{w,wa}}{\rho} \quad (7.11)$$

Blowing factor (BF) is defined as follows to calculate the corrected mass transfer coefficient (\bar{K}_{cor}):

$$BF = \ln \frac{1 + \varpi}{\varpi} \quad (7.12)$$

where

$$\varpi = \frac{mf_w - mf_{w,wa}}{mf_{w,wa} - 1} \quad (7.13)$$

The corrected mass transfer coefficient is given as follows:

$$\bar{K}_{cor} = \bar{K}BF \quad (7.14)$$

Finally, the mass flow rate of water due to evaporation is calculated by the following equation:

$$\dot{m}_w = \bar{K}_{cor} A_{tot,wsu} (C_w - C_{w,wa}) \quad (7.15)$$

where $A_{tot,wsu}$ is the total heat transfer surface area of the water spraying unit. Determining the mass flow rate of water due to evaporation enables to specify the temperature and the relative humidity of the working air at the outlet of the spraying unit. The working air leaving the spraying duct as being cooled and humidified is directed to the polycarbonate counter-flow heat exchanger to cool the incoming warm fresh air. In this regard, the second part of the modelling work aims at investigating the heat transfer in the novel plate type polycarbonate heat exchanger.

The polycarbonate heat exchanger might be thought of as two straight ducts with fluid flow, which are thermally connected. Let the ducts be of equal length L , carrying streams with heat capacity c_j and let mass flow rate of the streams \dot{m}_j , where the subscript j applies to stale air (sa) or fresh air (fa). The temperature profiles for the streams are $T_{sa}(x)$ and $T_{fa}(x)$ where x is the distance along the duct. The analyses are carried out for the steady-state conditions so that the temperature profiles are not functions of time. It is also assumed that the only transfer of heat from a small volume of fluid in one duct is to the fluid element in the other duct at the same position. The amount of heat transfer along a duct due to temperature differences is neglected. Through the Newton's law of cooling, the rate of change in energy of a small volume of the stream is proportional to the difference in temperatures between it and the corresponding element in the other duct:

$$\frac{\partial u_{sa}}{\partial t} = \xi(T_{fa} - T_{sa}) \quad (7.16)$$

$$\frac{\partial u_{fa}}{\partial t} = \xi(T_{sa} - T_{fa}) \quad (7.17)$$

where $u_j(x)$ is the thermal energy per unit length and ξ is the thermal connection constant per unit length between the two ducts. This change in internal energy results in a change in the temperature of the stream element. The time rate of change for the stream element being carried along by the flow is:

$$\frac{\partial u_{sa}}{\partial t} = \psi_{sa} \frac{dT_{sa}}{dx} \quad (7.18)$$

$$\frac{\partial u_{fa}}{\partial t} = \psi_{fa} \frac{dT_{fa}}{dx} \quad (7.19)$$

where $\psi_j = c_j \dot{m}_j$ is the thermal mass flow rate. The differential equations governing the parallel flow heat exchanger in the first part of the system can now be written as:

$$\psi_{sa} \frac{dT_{sa}}{dx} = \xi (T_{fa} - T_{sa}) \quad (7.20)$$

$$\psi_{fa} \frac{dT_{fa}}{dx} = \xi (T_{sa} - T_{fa}) \quad (7.21)$$

As it is seen from the equations that there are no partial derivatives of temperature with respect to time since the system is in a steady state. In addition, there are no second derivatives in x as is found in the heat equation since there is no heat transfer along the pipe. These two coupled first-order differential equations can be solved as follows:

$$T_{sa} = \Omega_1 - \Omega_2 \frac{\sigma_1}{\sigma} \exp(-\sigma x) \quad (7.22)$$

$$T_{fa} = \Omega_1 + \Omega_2 \frac{\sigma_2}{\sigma} \exp(-\sigma x) \quad (7.23)$$

where

$$\sigma_1 = \frac{\xi}{\psi_{sa}} \quad (7.24)$$

$$\sigma_2 = \frac{\xi}{\psi_{fa}} \quad (7.25)$$

$$\sigma = \sigma_1 + \sigma_2 \quad (7.26)$$

where Ω_1 and Ω_2 are the constants of integration. Let $T_{sa,0}$ and $T_{fa,0}$ be the temperatures at $x = 0$ and let $T_{sa,L}$ and $T_{fa,L}$ be the temperatures at the end of the duct at $x = L$. In this regard, the average temperatures in each duct can be given by:

$$\bar{T}_{sa} = \frac{1}{L} \int_0^L T_{sa} dx \quad (7.27)$$

$$\bar{T}_{fa} = \frac{1}{L} \int_0^L T_{fa} dx \quad (7.28)$$

The temperatures for the inlet and the outlet conditions are calculated as follows:

$$T_{sa,0} = \Omega_1 - \Omega_2 \frac{\sigma_1}{\sigma} \quad (7.29)$$

$$T_{fa,0} = \Omega_1 + \Omega_2 \frac{\sigma_2}{\sigma} \quad (7.30)$$

$$T_{sa,L} = \Omega_1 - \Omega_2 \frac{\sigma_1}{\sigma} \exp(-\sigma L) \quad (7.31)$$

$$T_{fa,L} = \Omega_1 + \Omega_2 \frac{\sigma_2}{\sigma} \exp(-\sigma L) \quad (7.32)$$

$$\bar{T}_{sa} = \Omega_1 - \Omega_2 \frac{\sigma_1}{\sigma^2 L} (1 - \exp(-\sigma L)) \quad (7.33)$$

$$\bar{T}_{fa} = \Omega_1 + \Omega_2 \frac{\sigma_2}{\sigma^2 L} (1 - \exp(-\sigma L)) \quad (7.34)$$

In equations (7.30–7.34), choosing any two of the temperatures eliminates the constants of integration and enables to find the other four temperatures. Total energy transferred can be determined by integrating the expressions for the time rate of change of internal energy per unit length:

$$\frac{dY_{sa}}{dt} = \int_0^L \frac{du_{sa}}{dt} dx = \psi_{sa}(T_{sa,L} - T_{sa,0}) = \xi L (\bar{T}_{fa} - \bar{T}_{sa}) \quad (7.35)$$

$$\frac{dY_{fa}}{dt} = \int_0^L \frac{du_{fa}}{dt} dx = \psi_{fa}(T_{fa,L} - T_{fa,0}) = \xi L(\bar{T}_{sa} - \bar{T}_{fa}) \quad (7.36)$$

where Y_{sa} is the total energy transferred for stale air, Y_{fa} is the total energy transferred for fresh air, u_{sa} is the internal energy of stale air and u_{fa} is the internal energy of fresh air. It can be clearly noted from the equations above that the sum of the energy changes is zero as a consequence of the conservation of energy. The quantity $\bar{T}_{fa} - \bar{T}_{sa}$ is known as the logarithmic mean temperature difference, and it is a measure of the effectiveness of the heat exchanger.

7.4. Results and Discussion

In the first part of the analyses, combined effects of the length of spraying unit, velocity of working air and hydraulic diameter on the amount of evaporated water vapour are evaluated theoretically as shown in [Figure 7.7](#), [7.8](#) and [7.9](#). The final water vapour content of air is of vital importance as it remarkably affects the evaporative cooling performance. It is understood from the results that the hydraulic diameter and the length of spraying unit have positive impact on the evaporation as expected and the amount of water evaporated is found to be increasing with the said independent variables. On the contrary, the amount of evaporated water vapour reduces with increasing velocity of working air as the air is not able to find the sufficient time inside the system to increase its moisture content.

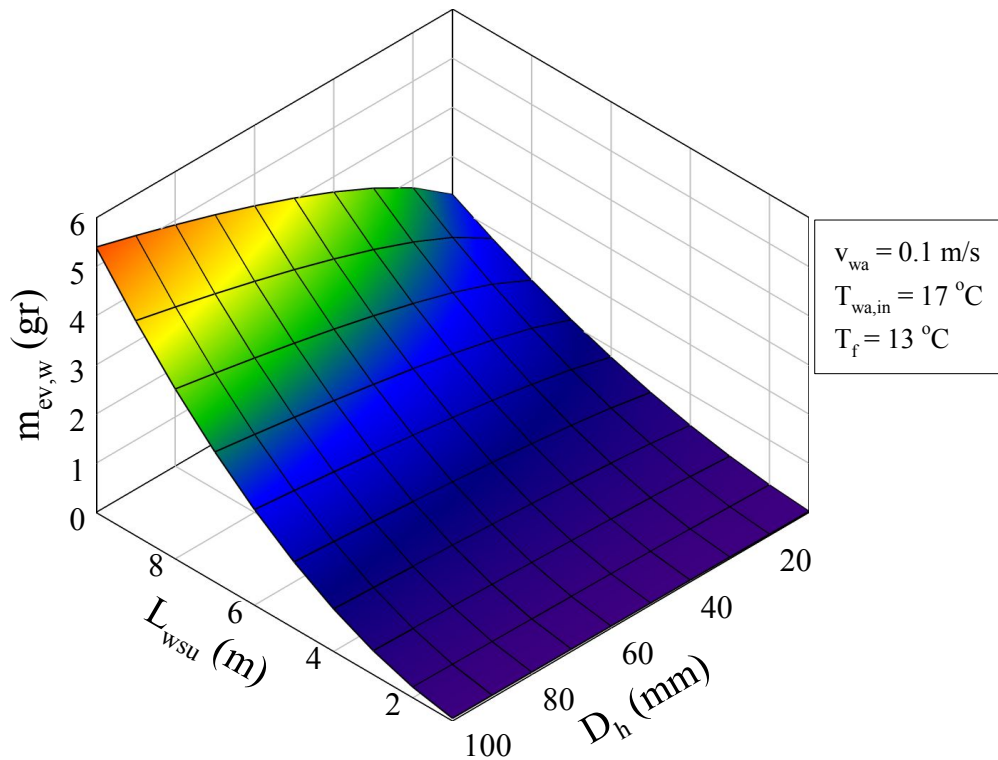


Figure 7.7. Combined effects of length of the spraying unit and hydraulic diameter on the amount of evaporated water vapour.

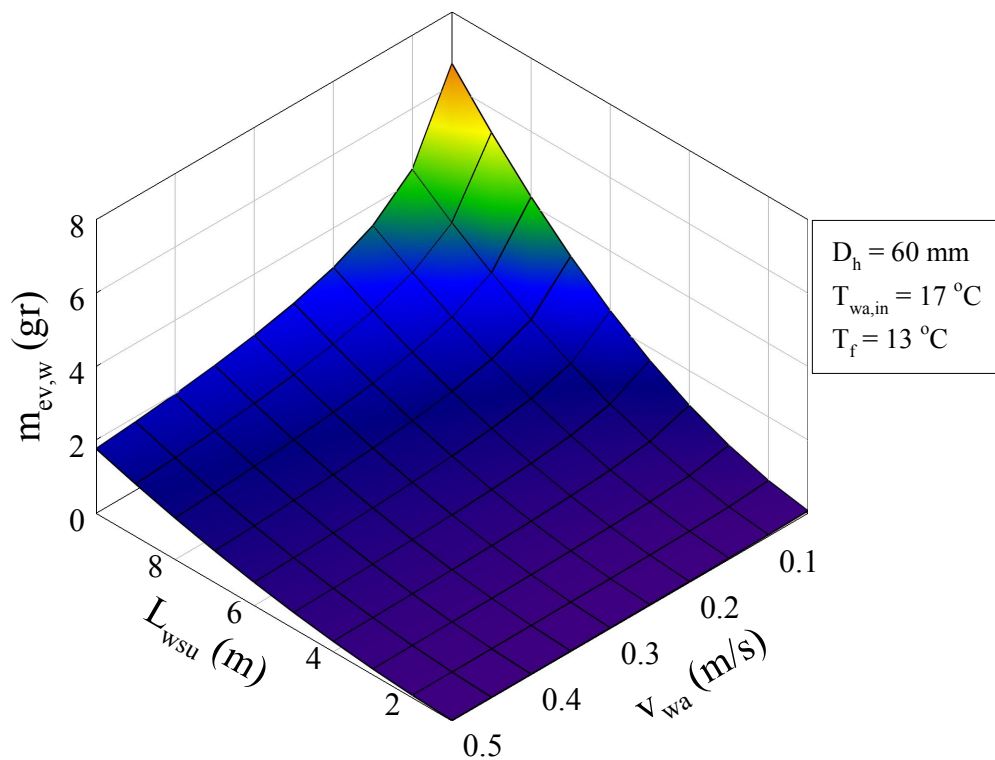


Figure 7.8. Combined effects of length of the spraying unit and velocity of working air on the amount of evaporated water vapour.

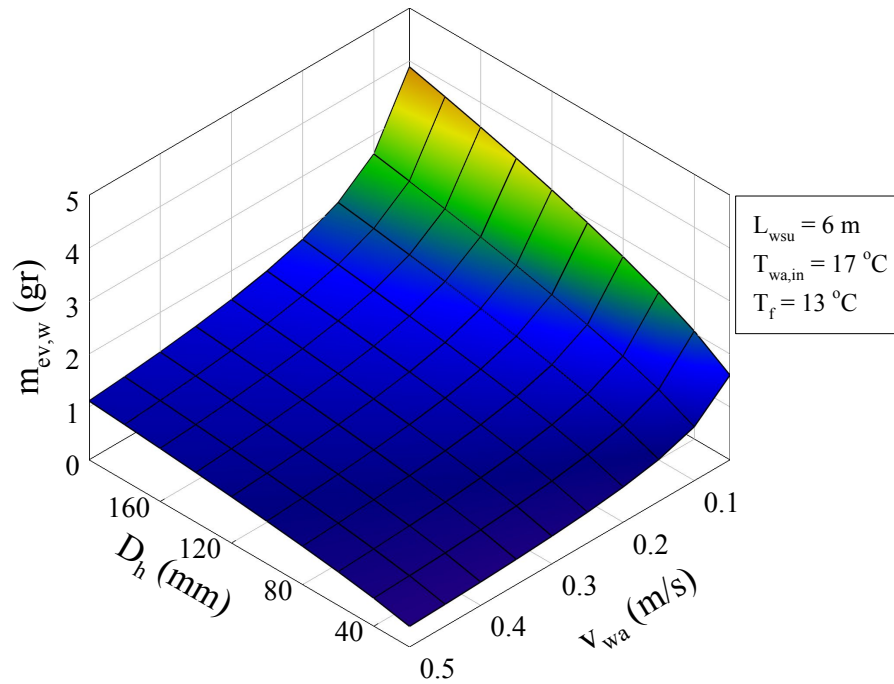


Figure 7.9. Combined effects of hydraulic diameter and velocity of working air on the amount of evaporated water vapour.

In the second part of the analyses, dry-bulb temperature and relative humidity of working air at the outlet of the water spraying unit are determined theoretically for different values of inlet working air temperature and as a function of the length of spraying unit as shown in Figure 7.10-14. For this part of the research, the hydraulic diameter and the air velocity are assumed to be 60 mm and 0.1 m/s , respectively whereas the temperature of working air is varied from 17 to $29\text{ }^{\circ}\text{C}$. It is well-documented in literature that temperature and relative humidity of working air are significant for the cooling capacity of evaporative cooling system. The first output of the results is the decreasing trend of outlet temperature of working air with spraying unit length. On the other hand, relative humidity of working air reaches adiabatic saturation condition after a particular value of spraying unit length which corresponds to maximum cooling condition for any case. Through the further optimisation works, it is concluded that the spraying unit length needs to be at least 8 m to be able to reach the

adiabatic saturation condition which represents the maximum cooling point that can be achieved. The results also indicate that both temperature and relative humidity of working air at the outlet rises with increasing inlet relative humidity of working air.

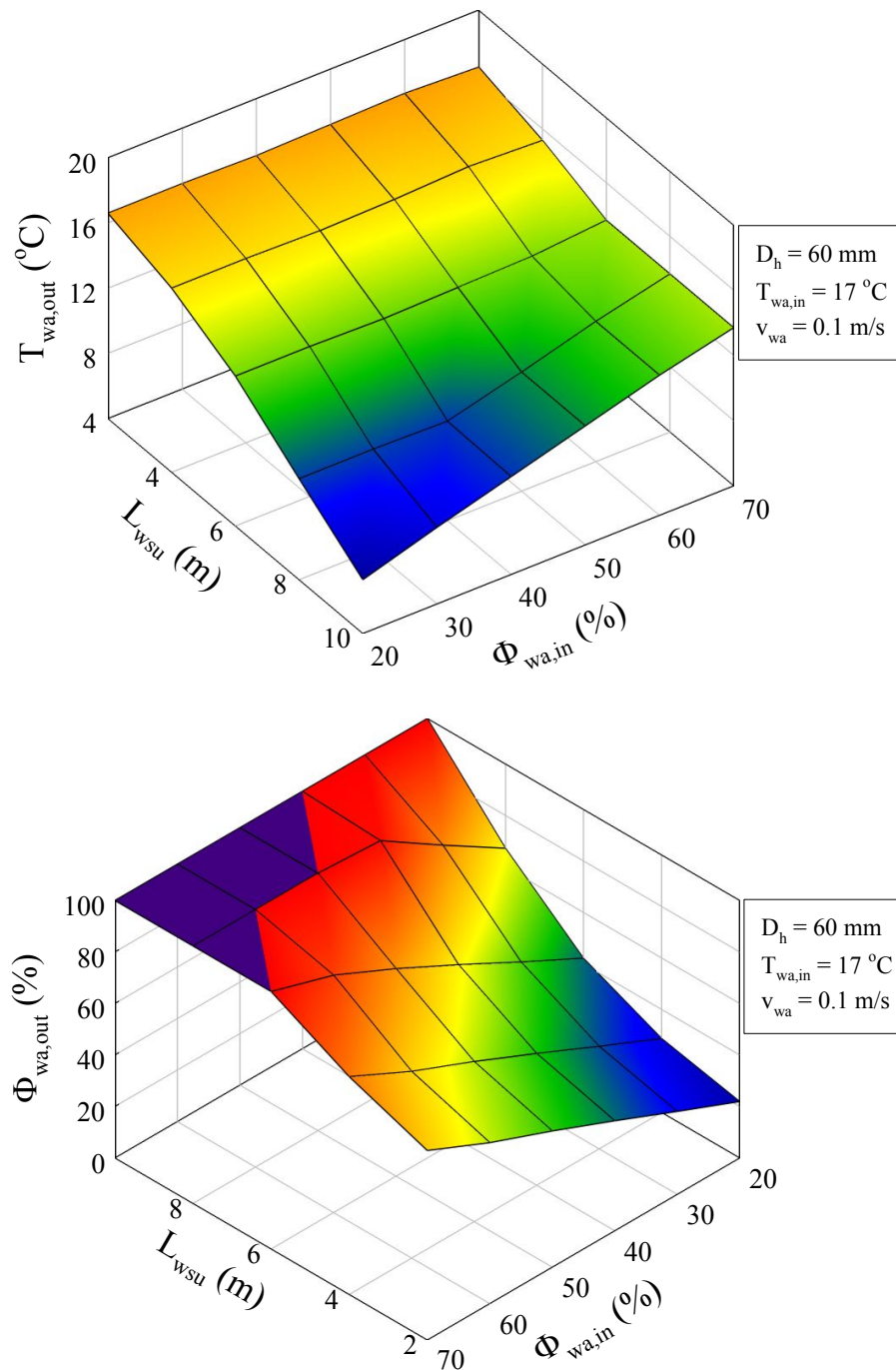


Figure 7.10. Dry-bulb temperature and relative humidity of working air at the outlet of the water spraying unit for $T_{wa,in} = 17$ °C, and as a function of the length of spraying unit.

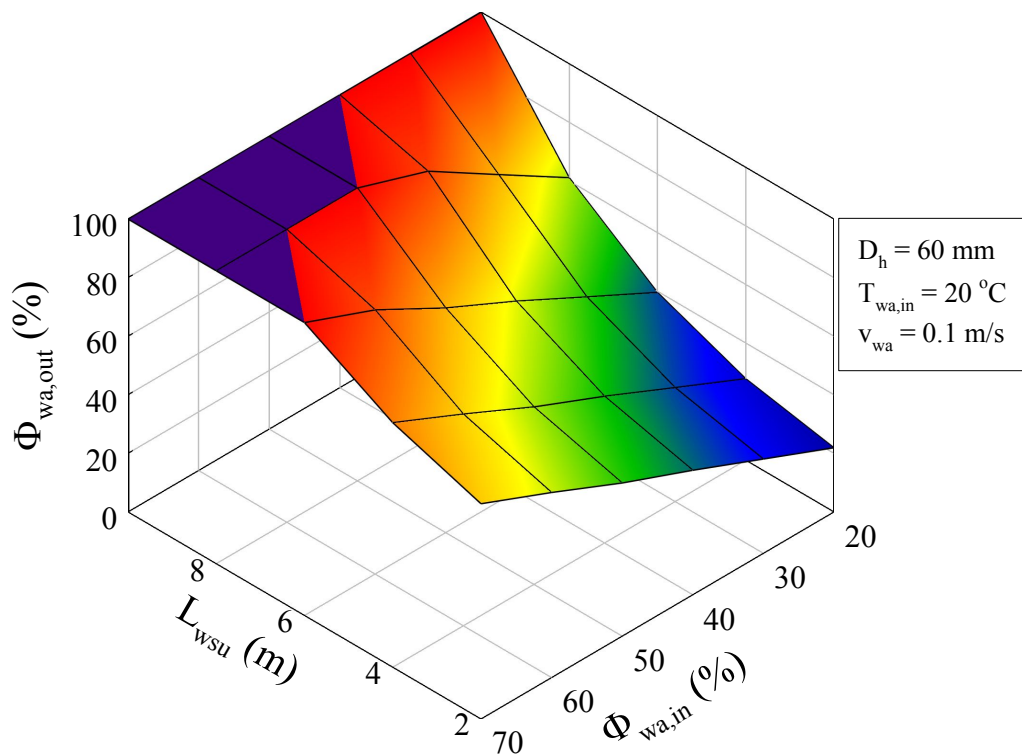
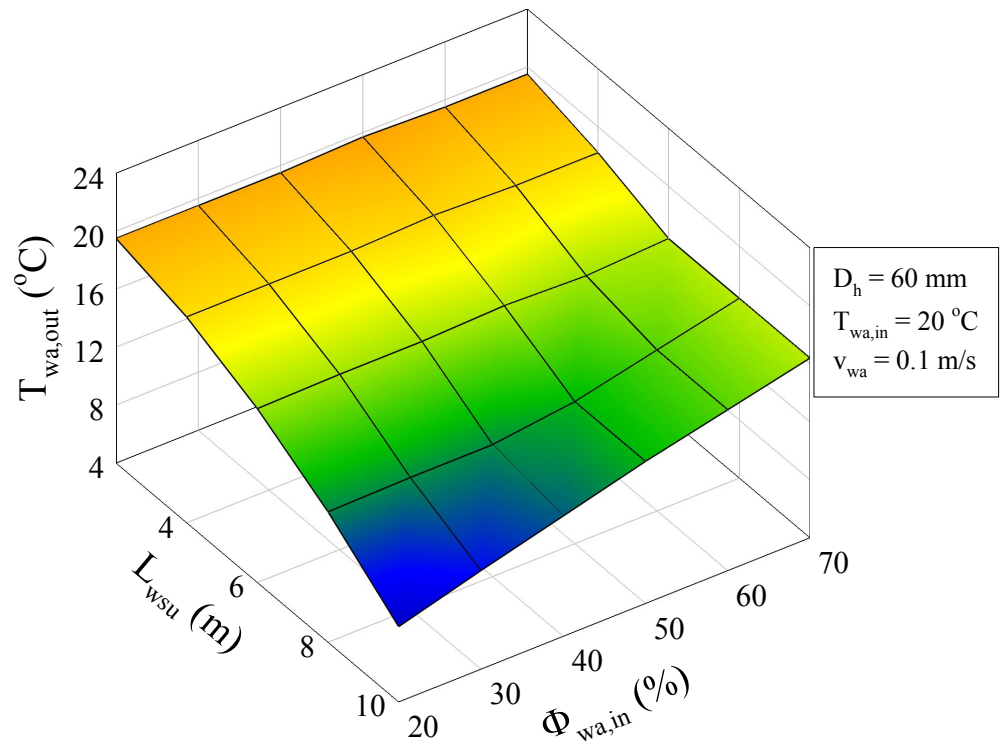


Figure 7.11. Dry-bulb temperature and relative humidity of working air at the outlet of the water spraying unit for $T_{wa,in} = 20$ °C, and as a function of the length of spraying unit.

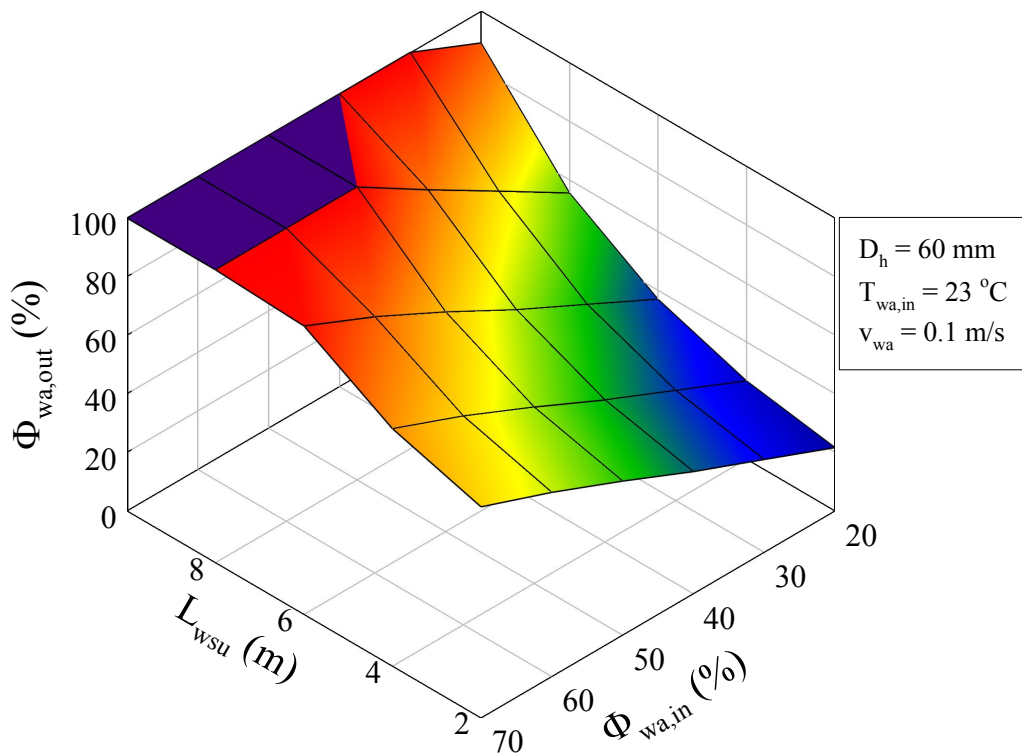
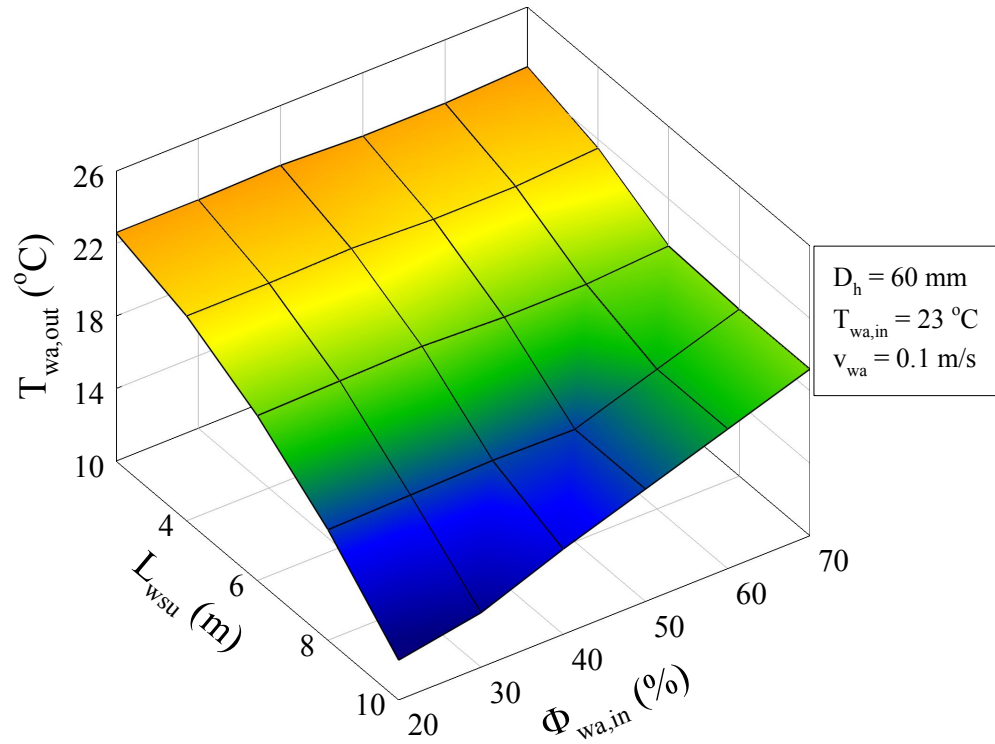


Figure 7.12. Dry-bulb temperature and relative humidity of working air at the outlet of the water spraying unit for $T_{wa,in} = 23$ °C, and as a function of the length of spraying unit.

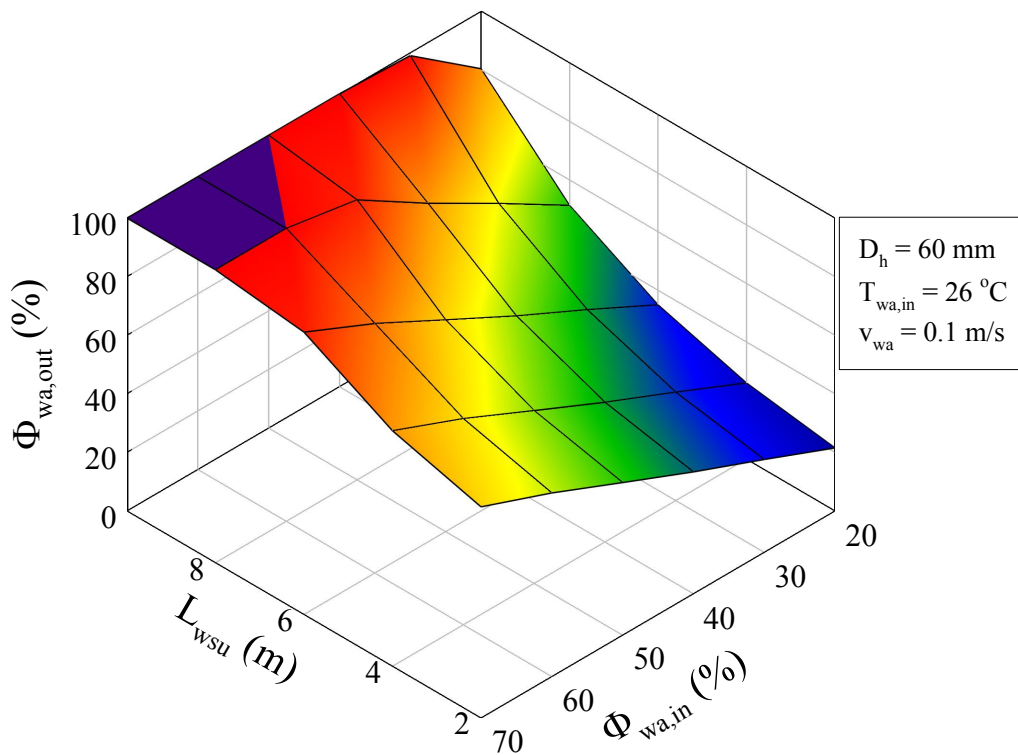
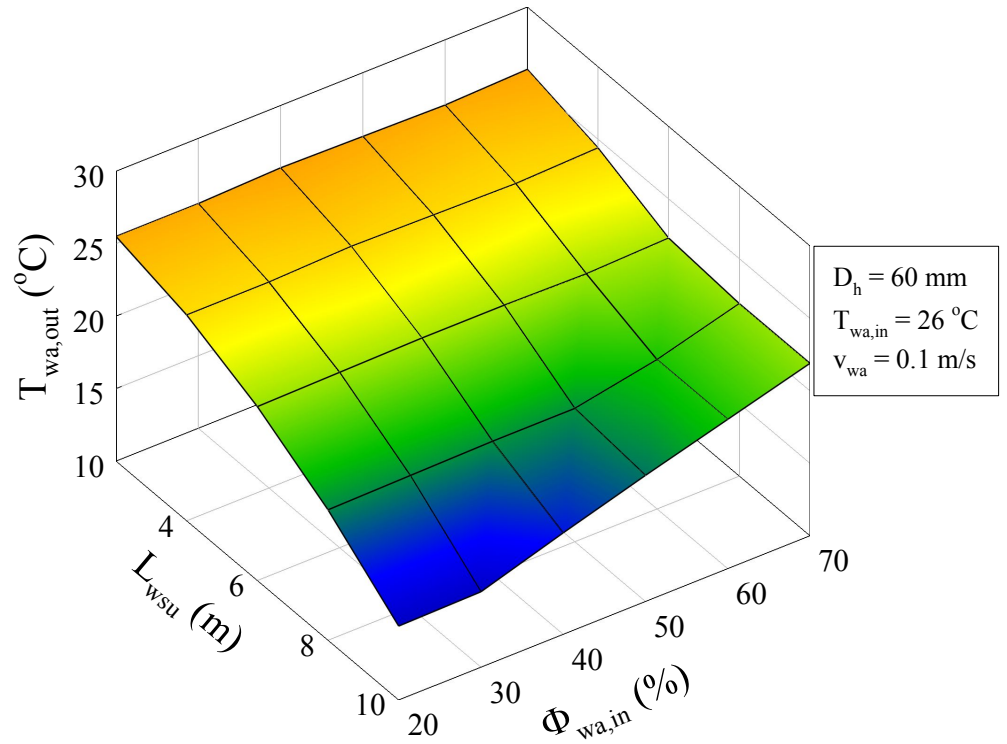


Figure 7.13. Dry-bulb temperature and relative humidity of working air at the outlet of the water spraying unit for $T_{wa,in} = 26$ °C, and as a function of the length of spraying unit.

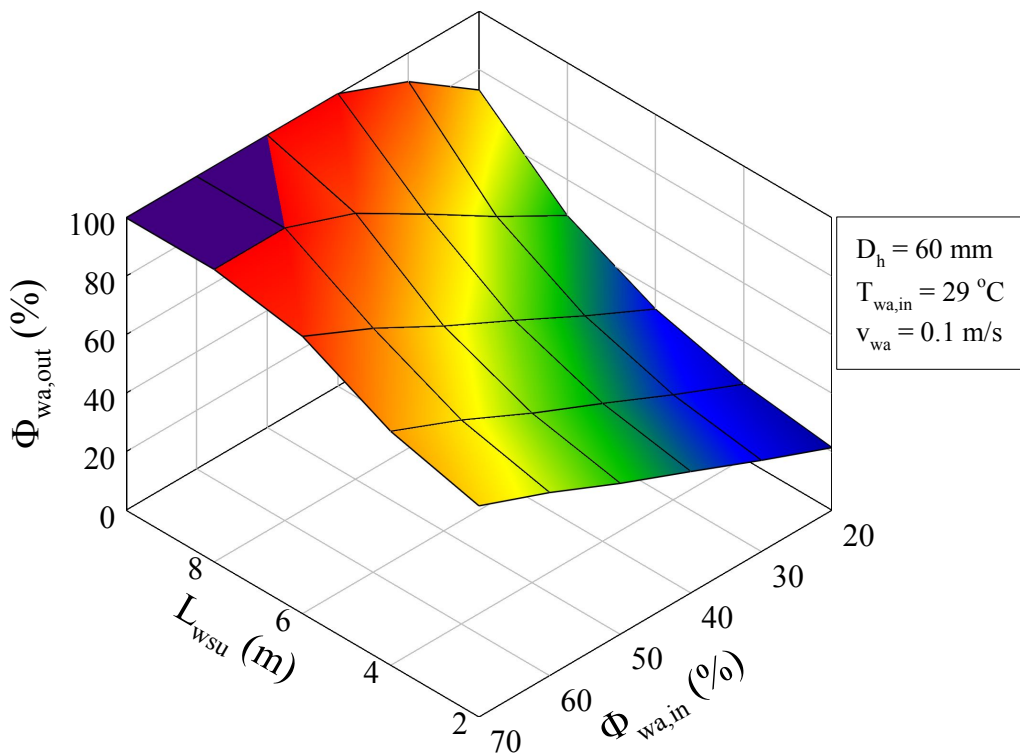
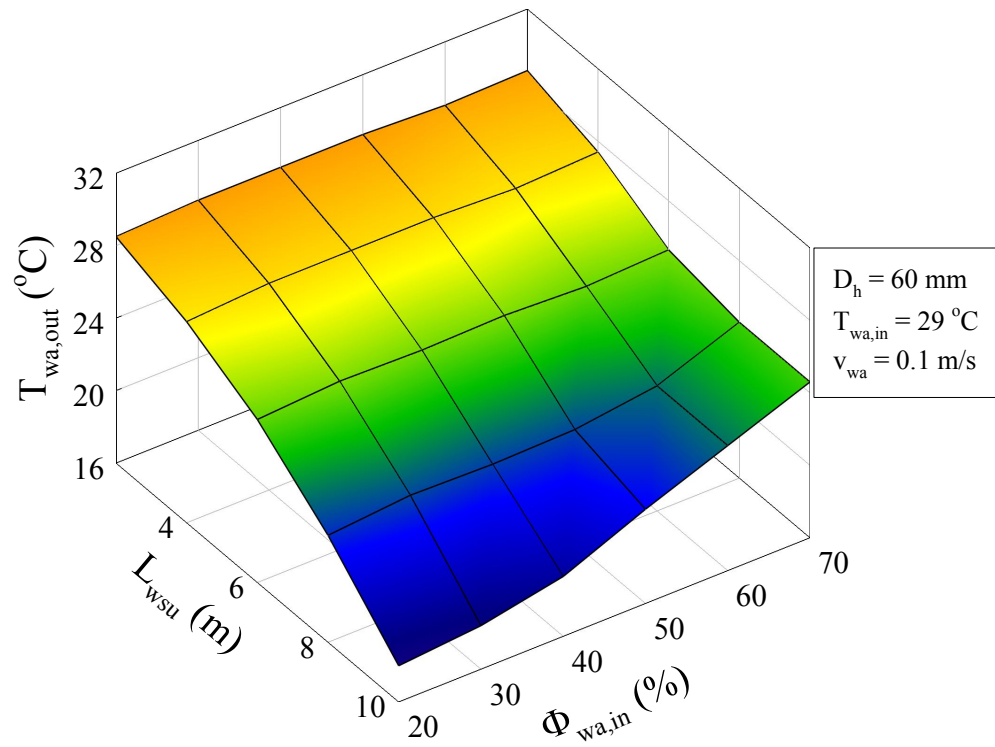


Figure 7.14. Dry-bulb temperature and relative humidity of working air at the outlet of the water spraying unit for $T_{wa,in} = 29$ °C, and as a function of the length of spraying unit.

In the second part of the results, outlet temperature and relative humidity of working air are calculated theoretically for constant spraying unit length and mass flow rate of air ($L_{wsu} = 6m$, $v_{wa} = 0.1 m/s$). The temperature of working air at the inlet is varied from 17 to 29 °C, and the analyses are repeated for different temperatures. Combined effects of hydraulic diameter and relative humidity are assessed as shown in [Figure 7.15](#), [7.16](#), [7.17](#), [7.18](#) and [7.19](#). It is understood from the data that the hydraulic diameter has a considerable influence on outlet temperature of working air. For a hydraulic diameter of 300 mm, $T_{wa,out}$ is expected to drop below 10 °C which is very noticeable. It is also concluded from the results that the relative humidity of working air at the inlet does not exceed 50% for the best case. The working air temperature at the outlet is remarkably affected by the relative humidity of working air at the inlet. For instance, for the inlet working air temperature of 17 °C, the outlet working air temperature can drop only to 13 °C when the inlet relative humidity of working air is taken to be 70%. On the other hand, the working air temperature at the outlet can be reduced below 10 °C if the relative humidity of the working air at the inlet is 20%.

As illustrated in [Figure 7.20](#), [7.21](#), [7.22](#), [7.23](#) and [7.24](#), combined effects of mass flow rate and relative humidity of working air on outlet temperature are also evaluated within the scope of this research. It is obtained from the results that the air velocity needs to be as low as possible for lower working air temperature at the outlet which can be explained with the greater water vapour penetration into the working air with longer time. Another output from the analyses is the fresh air temperature to the indoor environment increases linearly with fresh air temperature from outdoor and working air temperature as depicted in [Figure 7.25](#).

As the final attempt, the influence of temperature of fresh air from outdoor environment on the relative humidity of fresh air to the indoor environment is analysed

as shown in Figure 7.26, 7.27, 7.28 and 7.29. For a case of $\phi_{fa,outdoor} = 40\%$, $\phi_{fa,indoor}$ does not meet the thermal comfort range if outdoor fresh air temperature is greater than $35\text{ }^{\circ}\text{C}$.

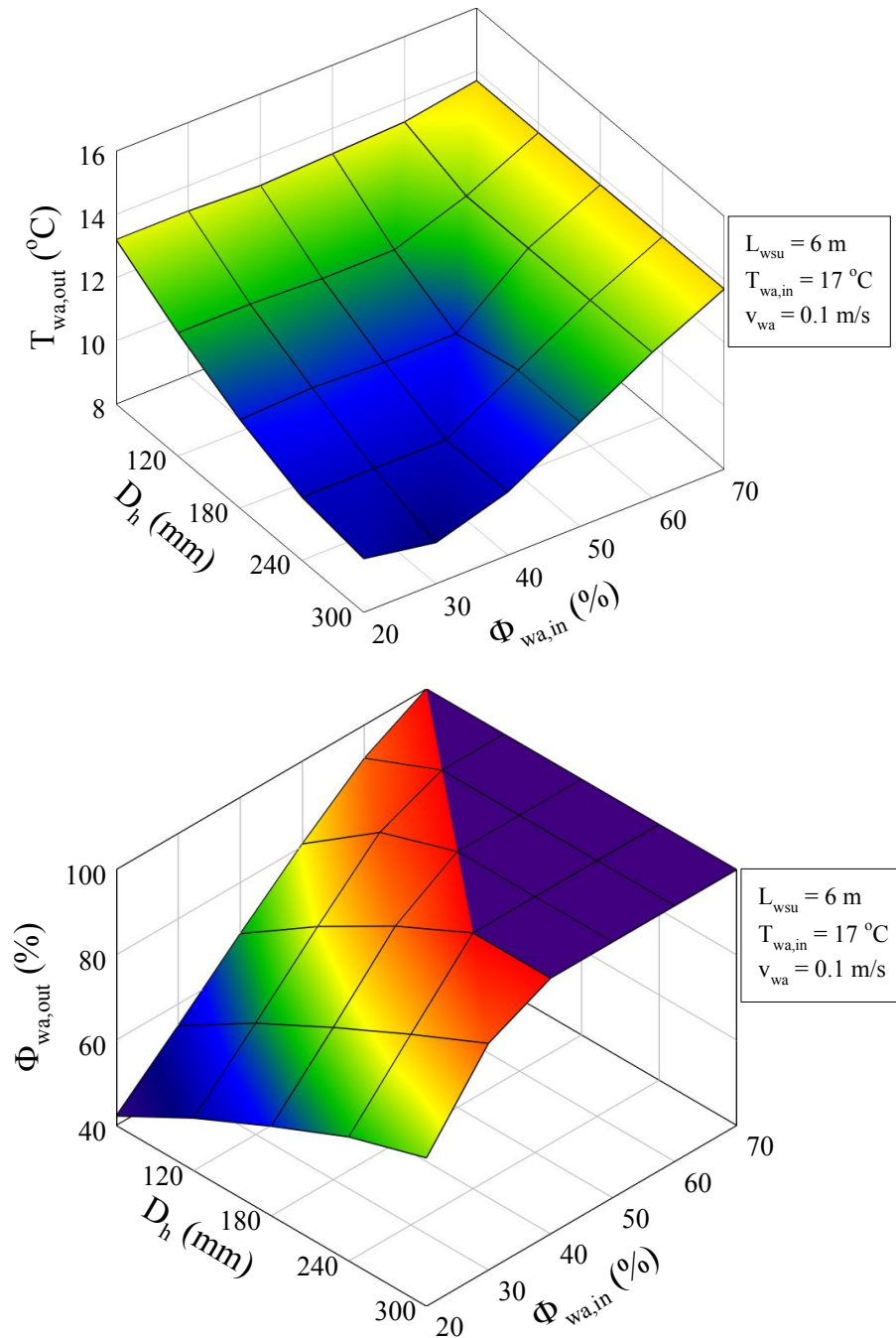


Figure 7.15. Dry-bulb temperature and relative humidity of working air at the outlet of the water spraying unit for $T_{wa,in} = 17\text{ }^{\circ}\text{C}$, and as a function of hydraulic diameter.

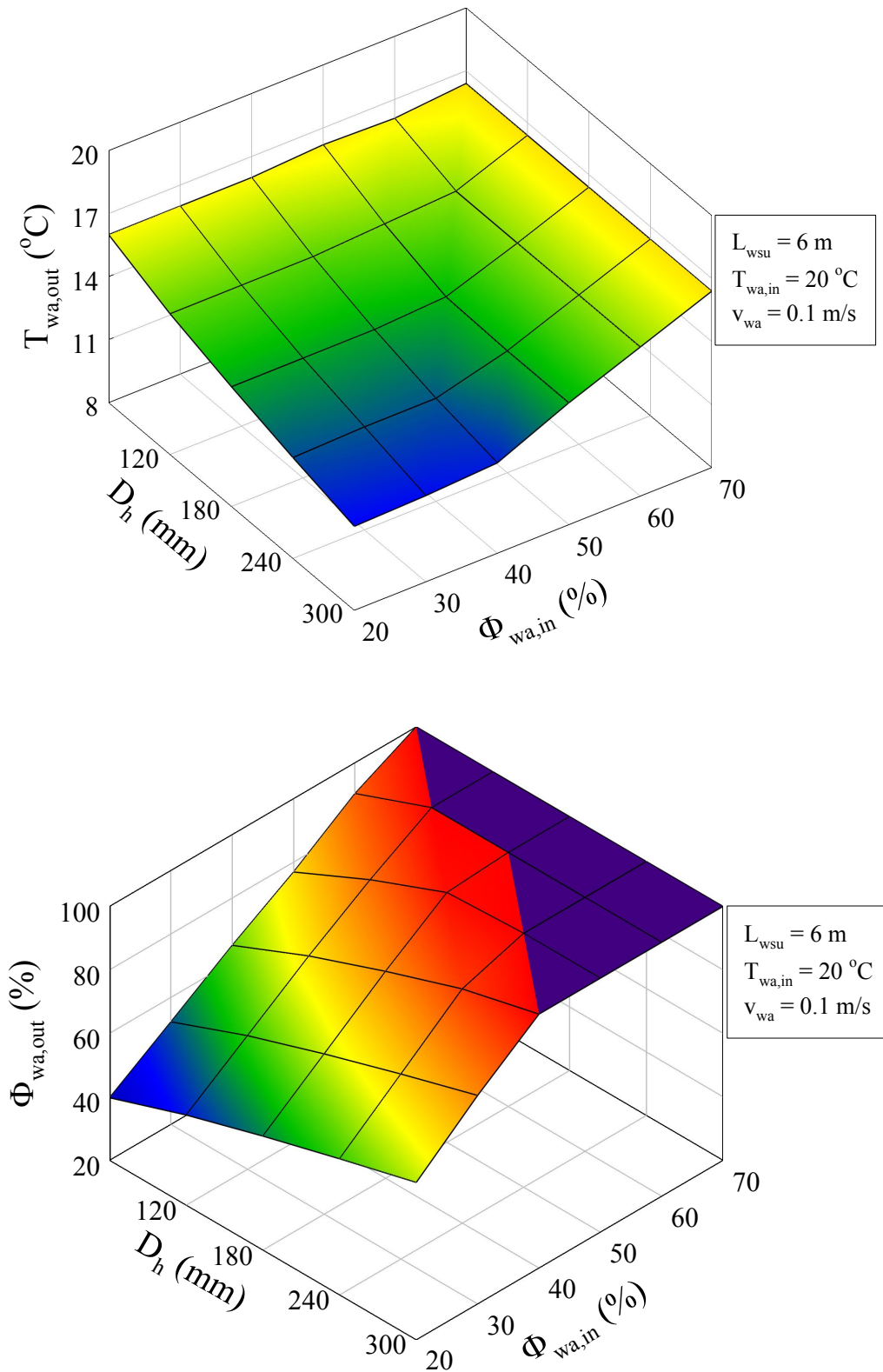


Figure 7.16. Dry-bulb temperature and relative humidity of working air at the outlet of the water spraying unit for $T_{wa,in} = 20$ °C, and as a function of hydraulic diameter.

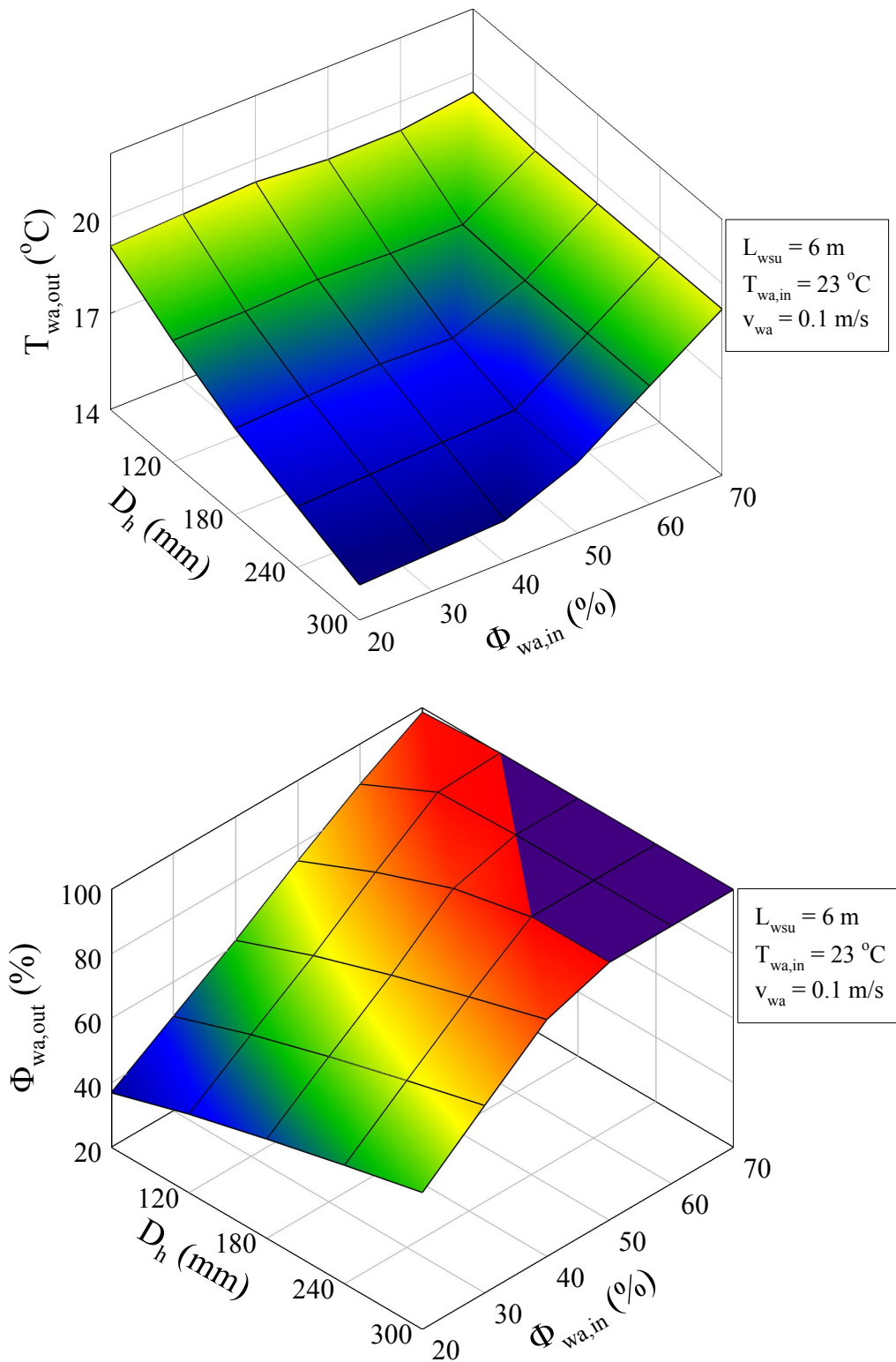


Figure 7.17. Dry-bulb temperature and relative humidity of working air at the outlet of the water spraying unit for $T_{wa,in} = 23$ °C, and as a function of hydraulic diameter.

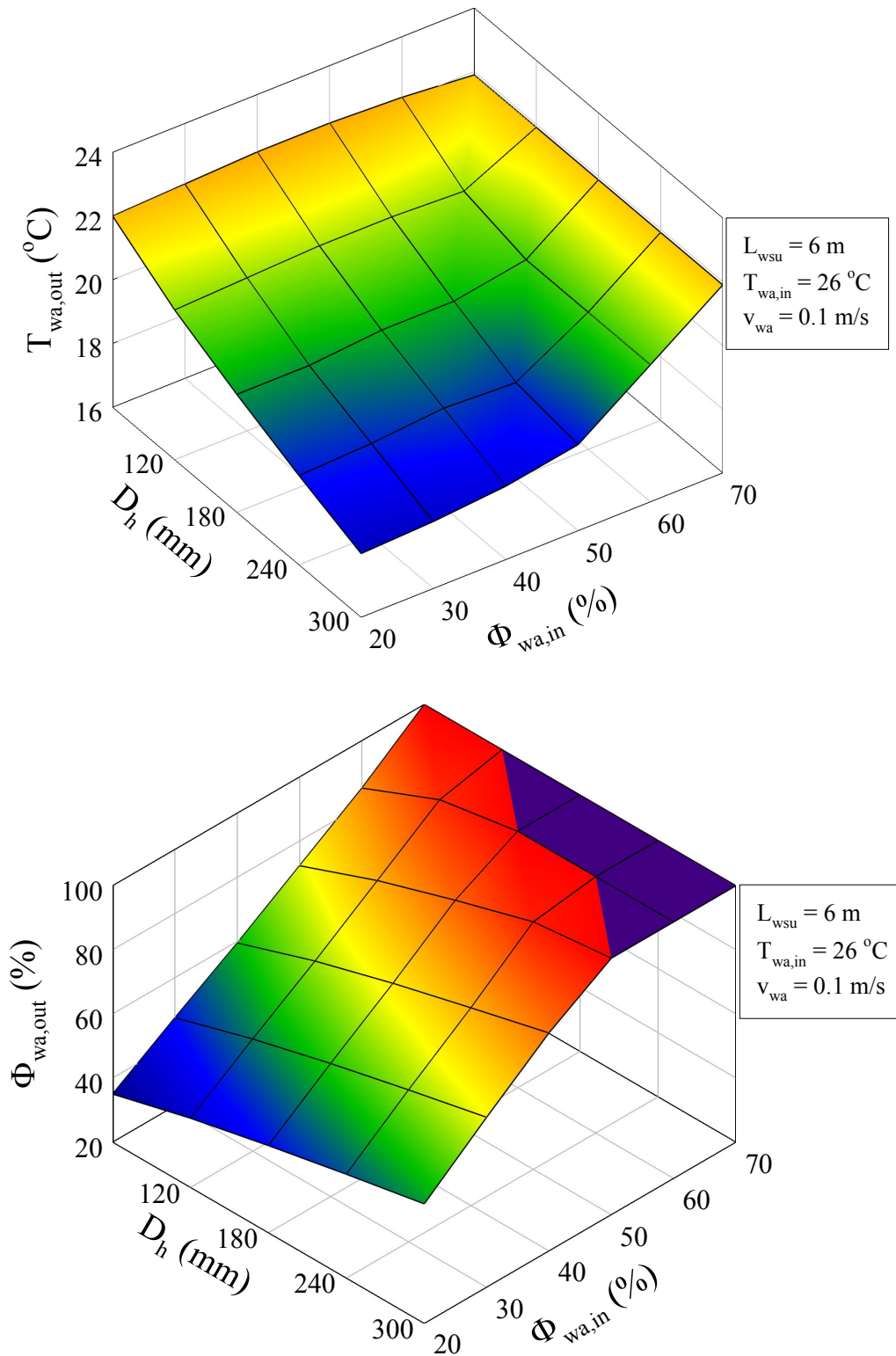


Figure 7.18. Dry-bulb temperature and relative humidity of working air at the outlet of the water spraying unit for $T_{wa,in} = 26$ °C, and as a function of hydraulic diameter.

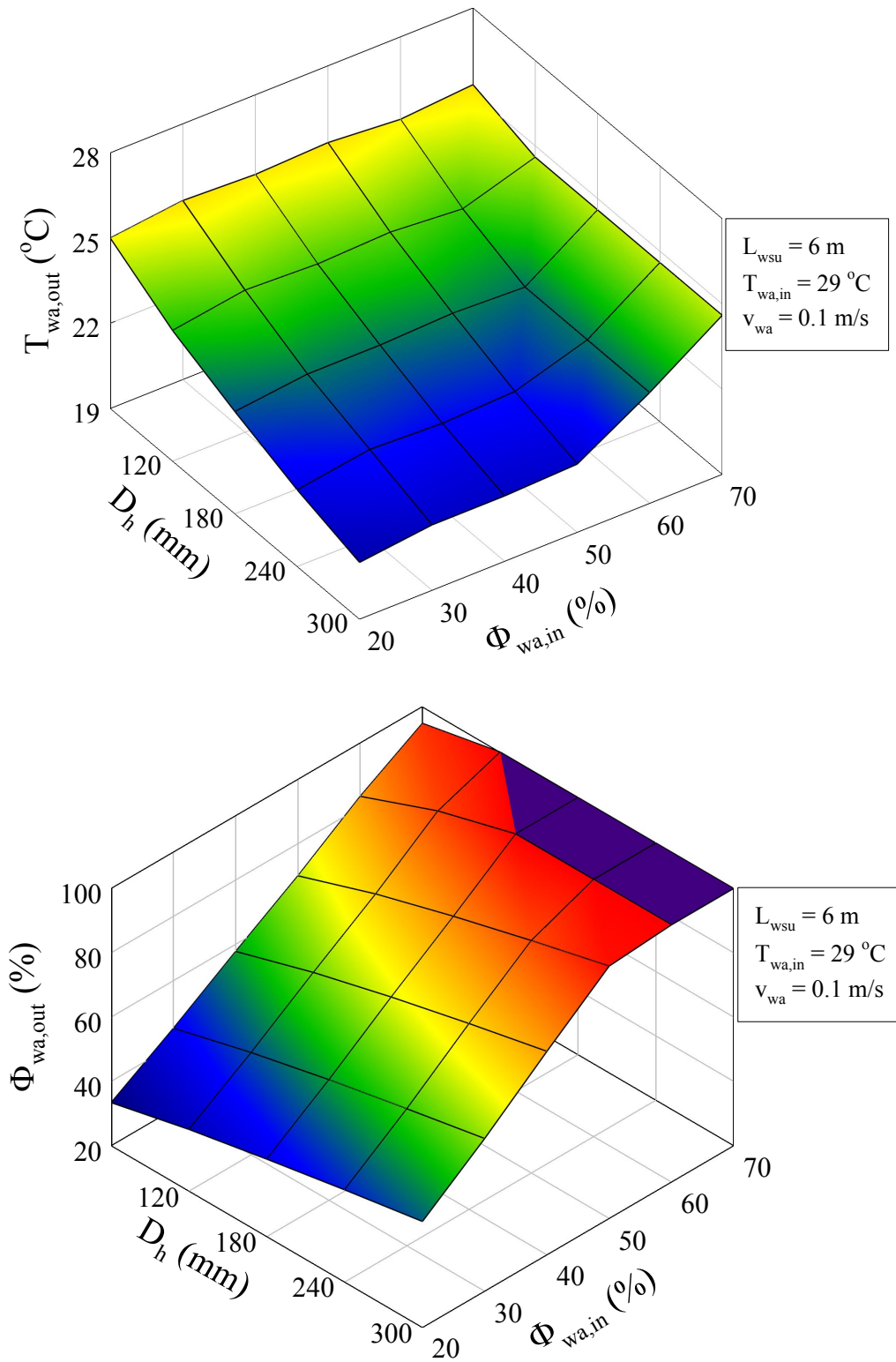


Figure 7.19. Dry-bulb temperature and relative humidity of working air at the outlet of the water spraying unit for $T_{wa,in} = 29$ °C, and as a function of hydraulic diameter.

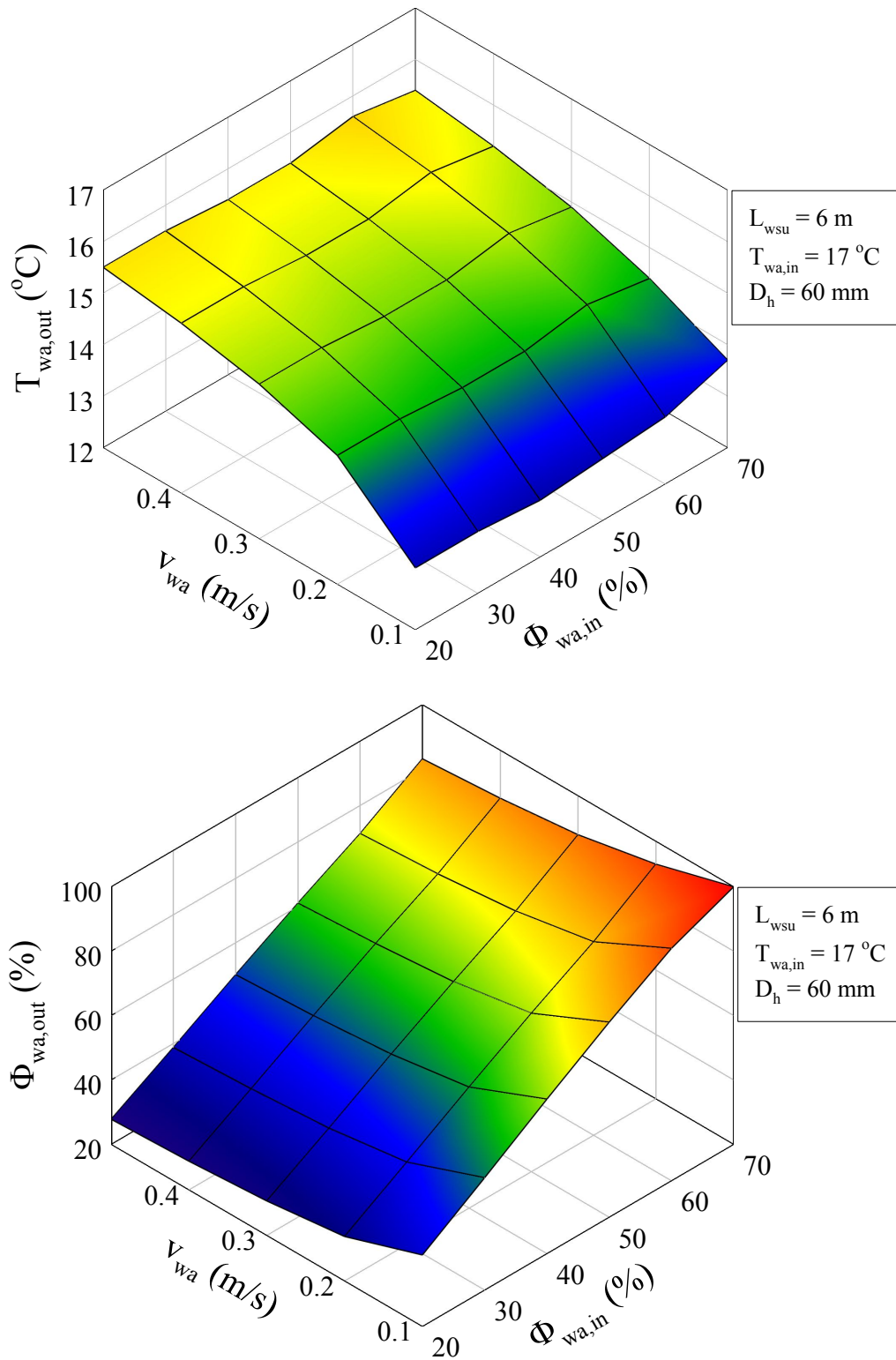


Figure 7.20. Dry-bulb temperature and relative humidity of working air at the outlet of the water spraying unit for $T_{wa,in} = 17$ °C, and as a function of velocity of working air.

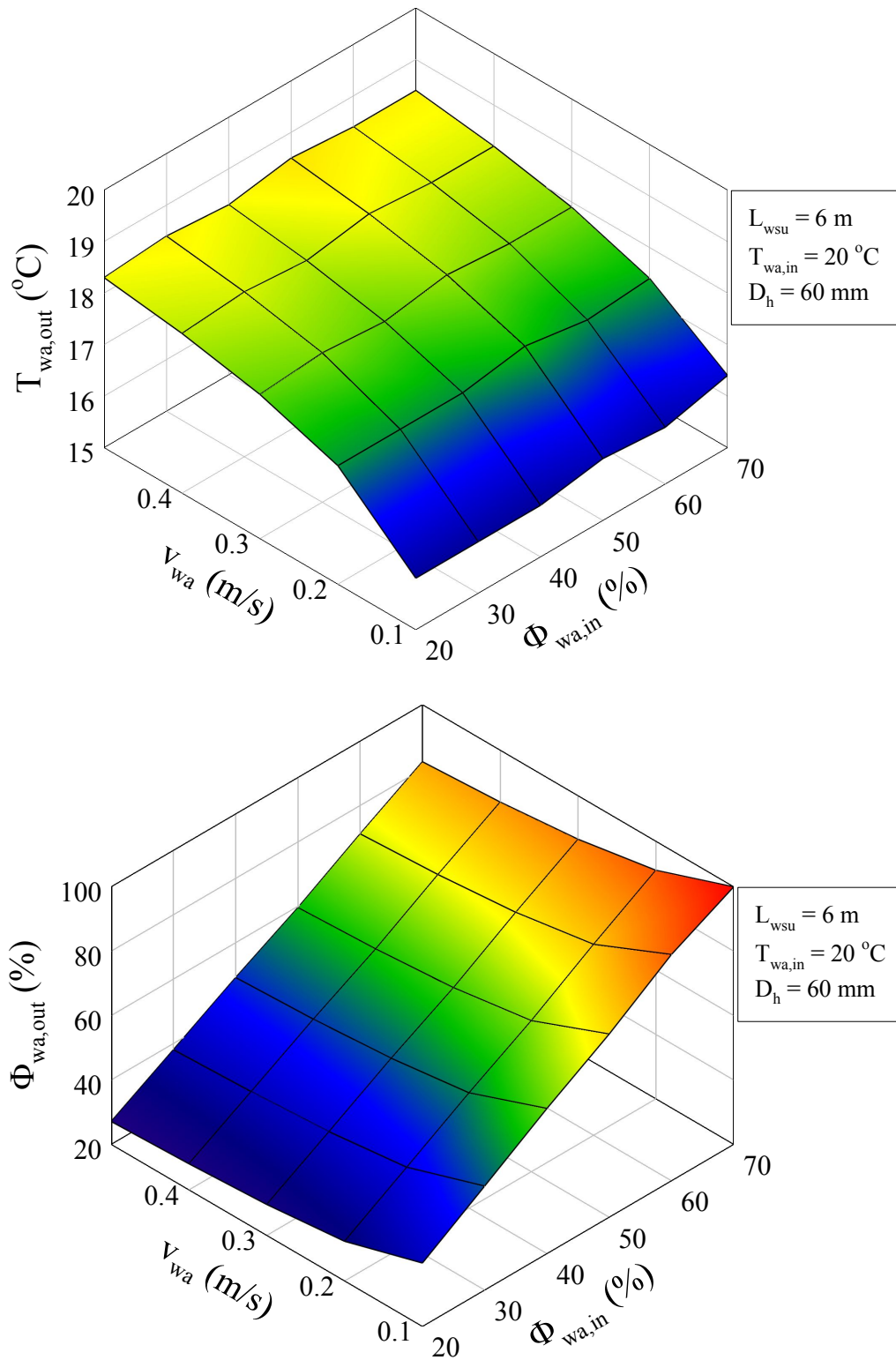


Figure 7.21. Dry-bulb temperature and relative humidity of working air at the outlet of the water spraying unit for $T_{wa,in} = 20$ °C, and as a function of velocity of working air.

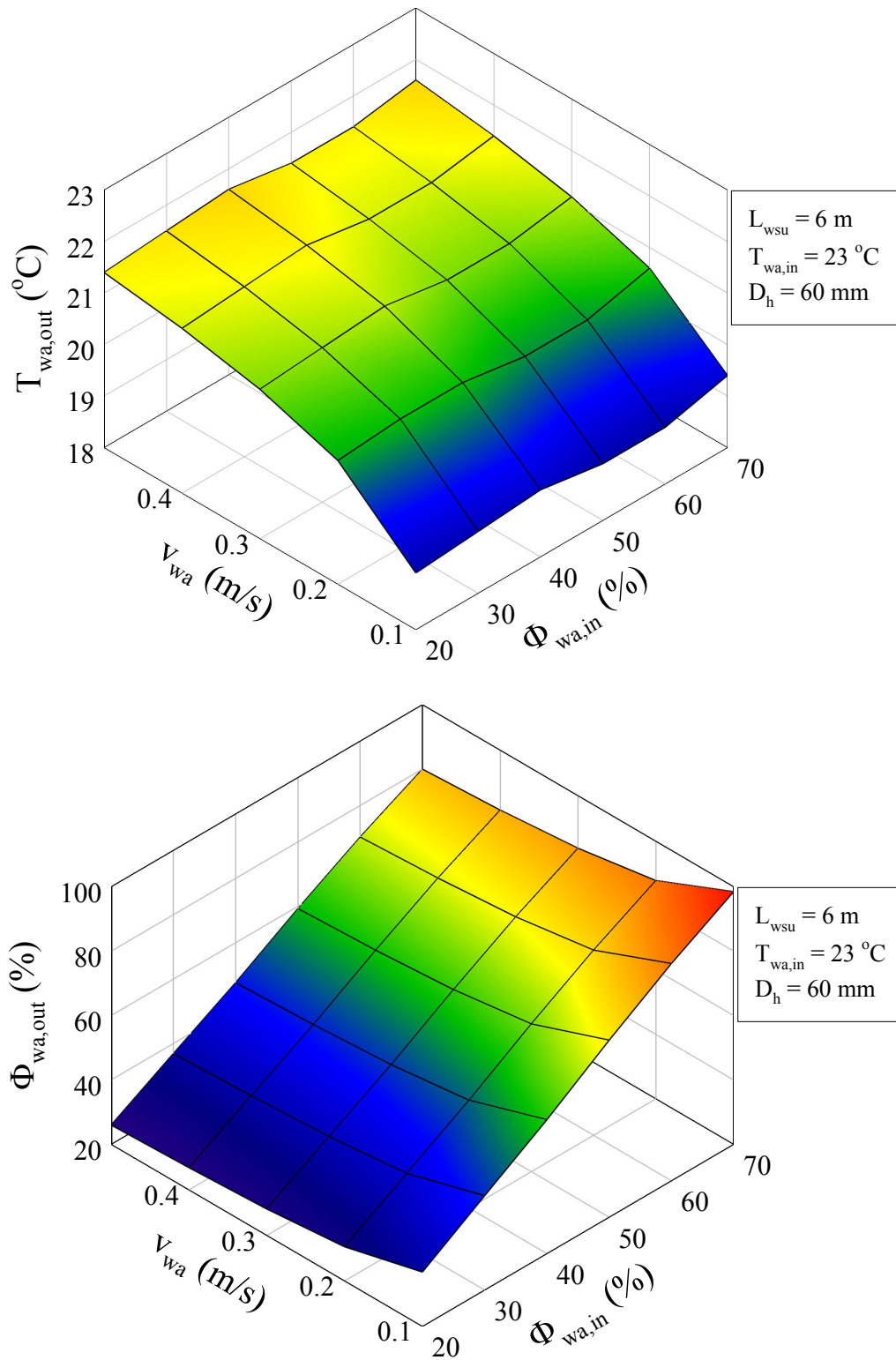


Figure 7.22. Dry-bulb temperature and relative humidity of working air at the outlet of the water spraying unit for $T_{wa,in} = 23$ °C, and as a function of velocity of working air.

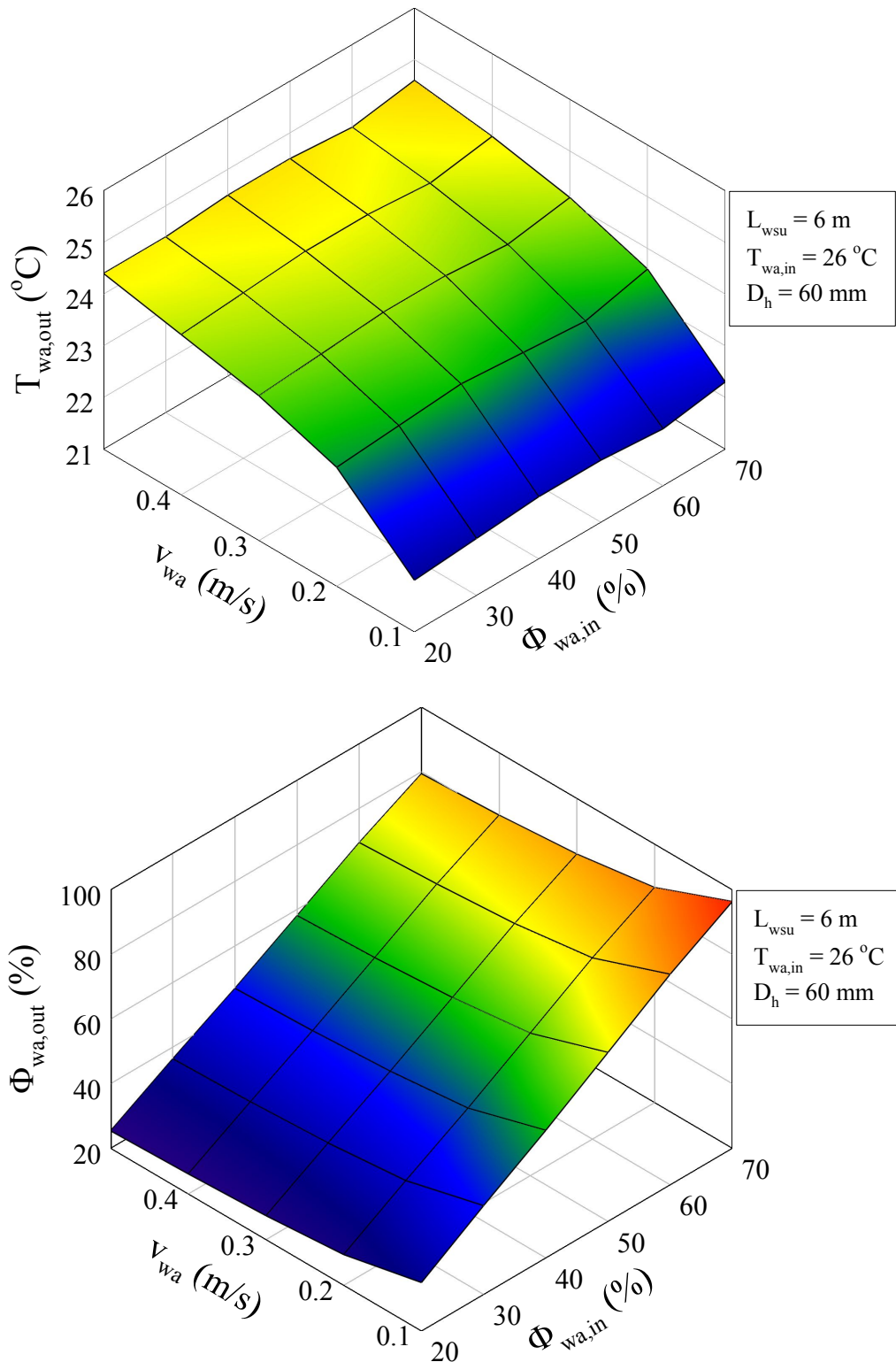


Figure 7.23. Dry-bulb temperature and relative humidity of working air at the outlet of the water spraying unit for $T_{wa,in} = 26$ °C, and as a function of velocity of working air.

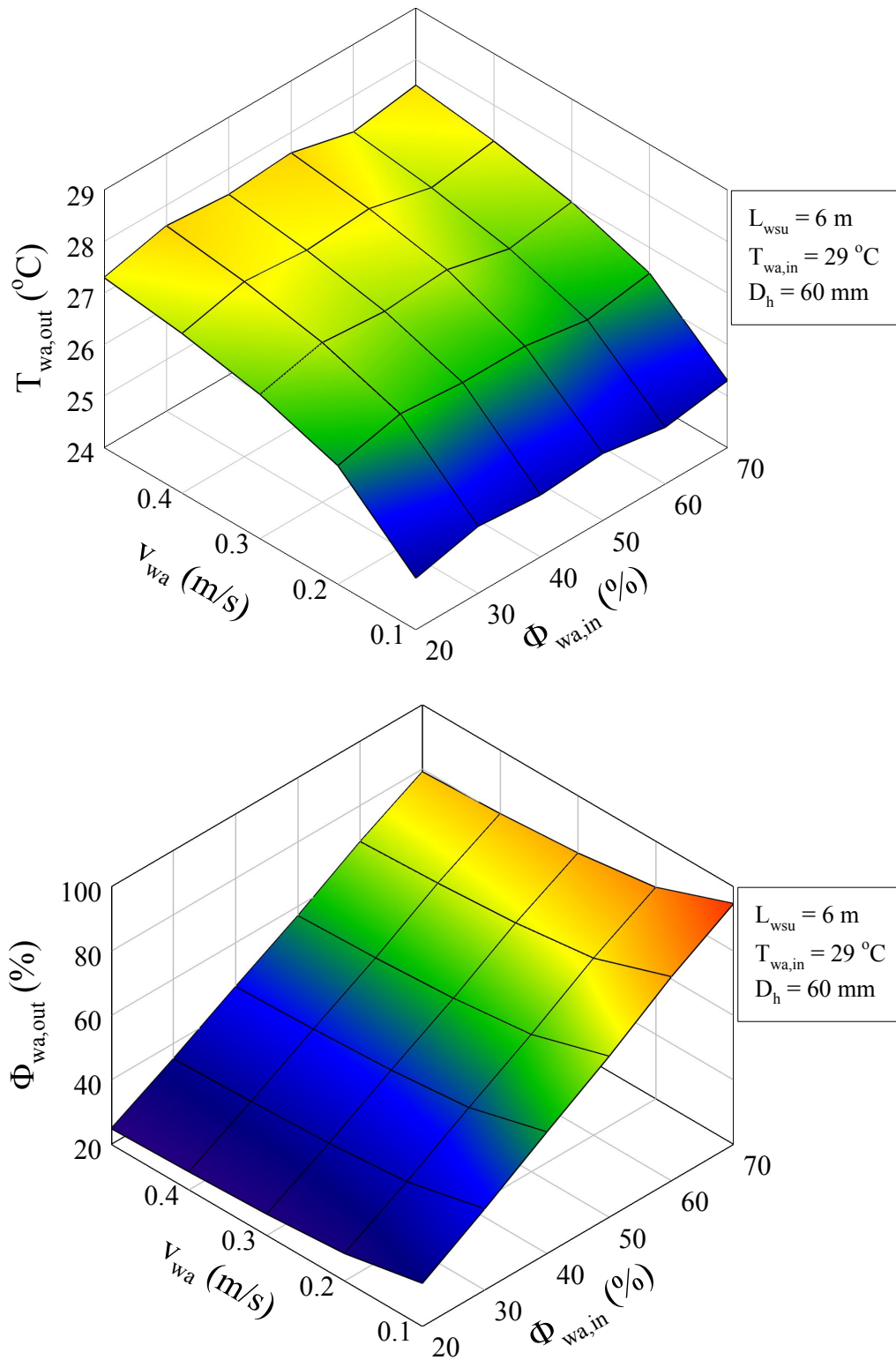


Figure 7.24. Dry-bulb temperature and relative humidity of working air at the outlet of the water spraying unit for $T_{wa,in} = 29$ °C, and as a function of velocity of working air.

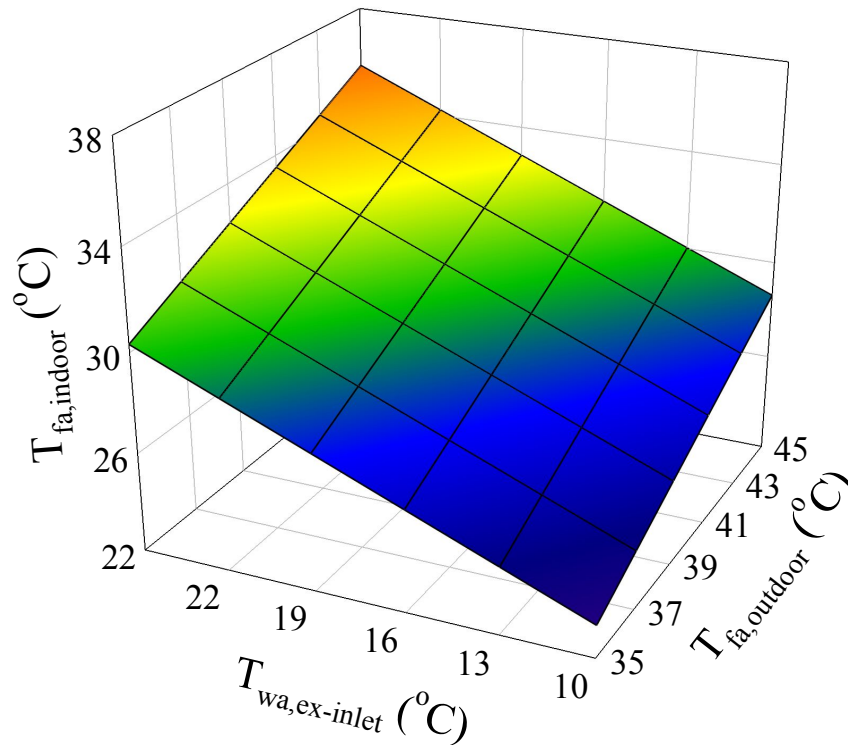


Figure 7.25. Indoor temperature of fresh air by outdoor temperature of fresh air and working air temperature at the inlet of polycarbonate heat exchanger.

7.5. Conclusions

Conclusive remarks can be summarized as follows:

- The amount of evaporated water vapour increases with increasing hydraulic diameter and length of spraying unit as seen in Figure 7.7.
- Water evaporation reduces with increasing velocity of working air as it is seen in Figure 7.8 and 7.9.
- Temperature and relative humidity of working air are important parameters in terms of cooling capacity of the evaporative cooling system. The results indicate that the outlet temperature of working air decreases with increasing values of spraying unit length. On the other hand, relative humidity of working air reaches adiabatic saturation

condition after a specific value of spraying unit length which is the desired condition as it is illustrated in [Figure 7.10](#).

➤ For various temperatures of working air at the inlet, an optimisation procedure is performed, and it is found that the spraying unit length should be at least 8 m to be able to reach the adiabatic saturation condition which corresponds to the best case that can be achieved for the system as seen [Figure 7.11](#).

➤ Similarly, the analysis is carried out for various relative humidity of working air at the inlet. The results show that both temperature and relative humidity of working air at the outlet increases with increasing inlet relative humidity of working air. In this regard, an optimum value should be selected considering indoor thermal comfort conditions as shown in [Figure 7.12–7.14](#).

➤ In the second part of the analyses, outlet temperature and relative humidity of working air are determined for constant spraying unit length and mass flow rate of air ($L_{wsu} = 6m$, $v_{wa} = 0.1 m/s$), and for various temperatures of working air at the inlet. Combined effects of hydraulic diameter and relative humidity are evaluated. It is concluded from the results that the hydraulic diameter has a notable impact on outlet temperature of working air. For a hydraulic diameter of 300 mm, $T_{wa,out}$ falls below 10 °C which is very promising as shown in [Figure 7.15–7.19](#).

➤ For the most desired conditions, relative humidity of working air at the inlet should not be greater than 50%.

➤ Combined effects of mass flow rate and relative humidity of working air on outlet temperature are also investigated in this study. It is understood from the results that the air velocity should be as low as possible for lower working air temperature at the outlet as it is shown in [Figure 7.20–7.24](#).

- Fresh air temperature to the indoor environment increases linearly with working air temperature and fresh air temperature from outdoor as illustrated in Figure 7.25.
- Temperature of fresh air from outdoor environment has a dominant impact on relative humidity of fresh air to the indoor environment. For $\phi_{fa,outdoor} = 40\%$, $\phi_{fa,indoor}$ falls out of the thermal comfort range if outdoor fresh air temperature is greater than $35\text{ }^{\circ}\text{C}$ as it is seen in Figure 7.26–7.29.

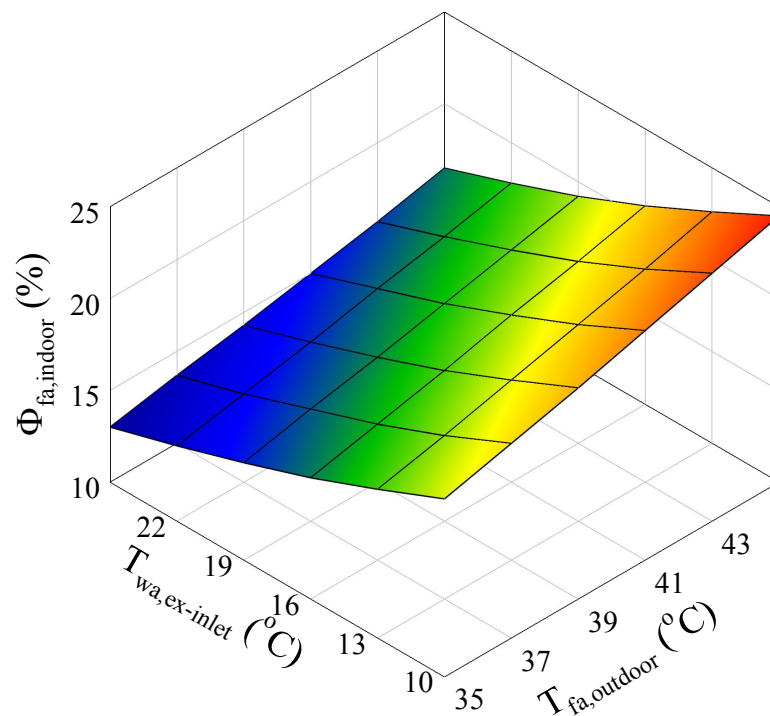


Figure 7.26. Indoor relative humidity of fresh air by outdoor temperature of fresh air and working air temperature at the inlet of polycarbonate heat exchanger for $\phi_{fa,outdoor} = 10\%$.

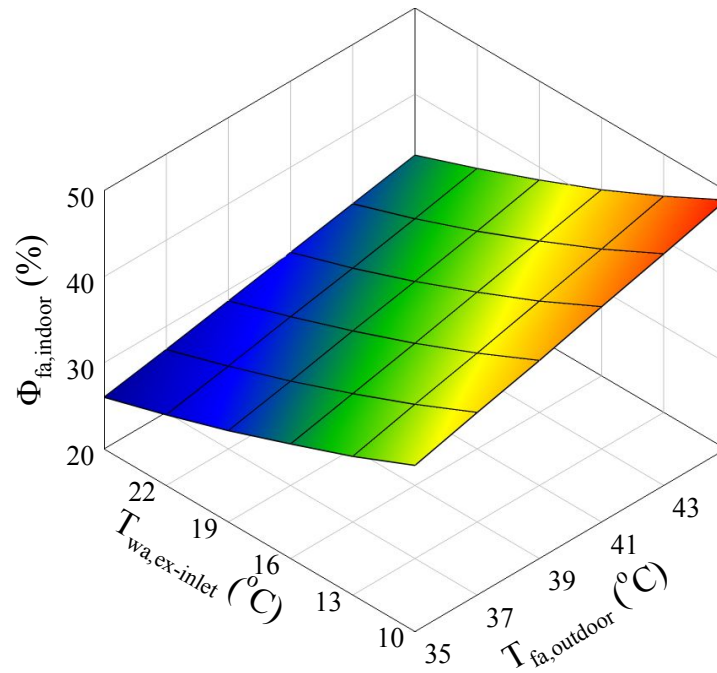


Figure 7.27. Indoor relative humidity of fresh air by outdoor temperature of fresh air and working air temperature at the inlet of polycarbonate heat exchanger for $\phi_{fa,outdoor} = 20\%$.

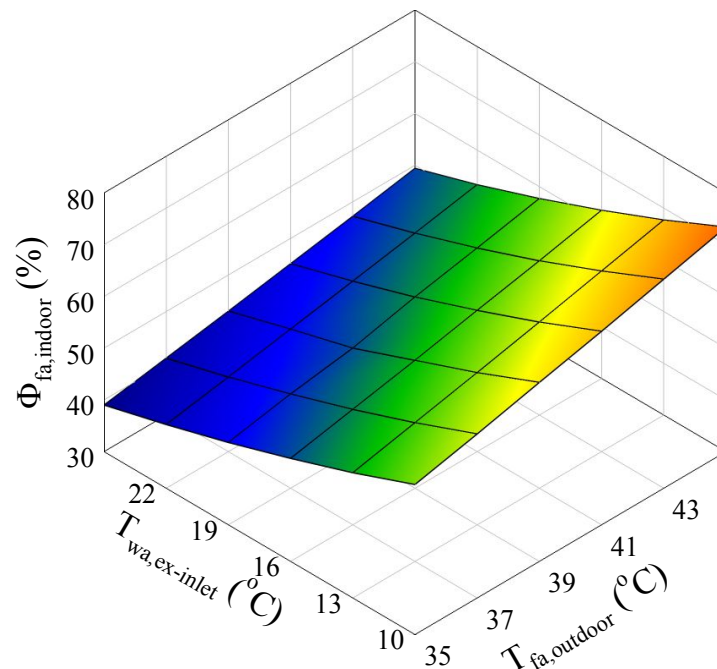


Figure 7.28. Indoor relative humidity of fresh air by outdoor temperature of fresh air and working air temperature at the inlet of polycarbonate heat exchanger for $\phi_{fa,outdoor} = 30\%$.

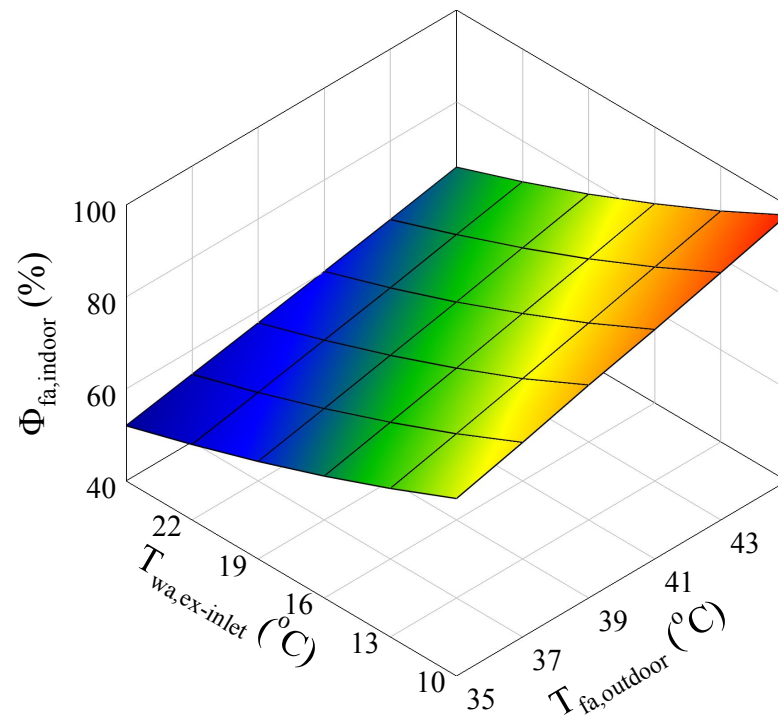


Figure 7.29. Indoor relative humidity of fresh air by outdoor temperature of fresh air and working air temperature at the inlet of polycarbonate heat exchanger for $\phi_{fa,outdoor} = 40\%$.

CHAPTER 8

Comprehensive thermal performance investigation of a novel direct-contact evaporative cooling system

- 8.1. Introduction
- 8.2. Description of a Novel ECS
- 8.3. Experimental Setup and Analysis
- 8.4. Results and Discussion
- 8.5. Conclusions

CHAPTER 8

Comprehensive thermal performance investigation of a novel direct-contact evaporative cooling system

8.1. Introduction

Buildings have a higher energy consumption rate compared to the other relevant sectors [274]. Buildings are responsible for about 40% of total energy consumption in the world. They are also one of the biggest contributors to greenhouse gas emissions as a consequence of the existing energy market dominated by fossil fuel based energy resources. Research to mitigate energy consumed in buildings is therefore of vital importance. Further investigations related to buildings reveal that almost 60% of total energy consumption in building sector is attributed to heating, ventilation and air conditioning. *HVAC* is an indispensable part of a building and causes a significant amount of energy loss. Therefore, *HVAC* is considered as a key solution for remarkable energy savings in buildings. As reported by Hasan [248] in a recent work, the demand for cooling increases day by day as a consequence of the growing demand for better thermal comfort conditions in buildings. It is underlined that the use of air conditioning in building sector is rapidly increasing [275]. On the other hand, increased use of air conditioning creates a serious peak electricity load problem to utilities and increases the cost of electricity [276].

Cooling can be performed in several ways, and one of those is evaporative cooling. Evaporative cooling has a high potential to meet cooling demands at low

energy costs [249]. Riangvilaikul and Kumar [213] note that the evaporative cooling is a good alternative to mechanical vapour compression for air conditioning applications since it requires about four times less electric power than vapour-compression refrigeration [250]. An evaporative cooling system simply works as increasing the moisture contents of the air with use of water. When hot and dry air welcomes water, the water starts to evaporate with help of energy taken from the air. Thus, the air becomes cooler whereas its relative humidity goes up. Current available evaporative cooling systems can be classified as direct-contact and indirect-contact evaporative coolers with respect to interaction between the streams. In a direct evaporative cooling system, working air to be cooled is in a direct contact with a liquid water film. Cooling is accomplished by the adiabatic heat exchange between the working air and the liquid water film [251]. The direct contact evaporative cooling systems are utilised to cool the intake air in hot and dry climatic conditions. It is possible to get adequate cooling by use of this system, but the increasing level of the air humidity might make the occupants uncomfortable. On contrary to direct contact system, an indirect contact evaporative cooling system can deal with undesired living conditions for the occupants owing to its characteristic configuration. As it is mentioned above, direct-contact evaporative cooling systems are appropriate for use only in dry, hot environmental conditions, or in rooms needing both cooling and humidification [252]. On the other hand, in an indirect-contact evaporative cooler, the inlet air is cooled by so-called working (secondary) air which is cooled through evaporation [253]. Thermodynamically, the wet passage absorbs heat from the dry passage by evaporating water, and thus cools the dry passage, while the latent heat of vaporizing water is dissipated into the working air. Within the scope of this research, only the evaporative cooling test and its results are introduced.

Evaporative cooling systems are widely used in building sector nowadays as an alternative to conventional air conditioners. Energy consumed in *HVAC* systems accounts for about 20% of the total world energy consumption [193], and hence novel solution to mitigate this figure is of vital importance due to growing significance of environmental issues [100–105]. Evaporative cooling technology offers a wide range of opportunities for buildings to fulfil this purpose owing to low retrofit costs, high efficiency ranges, insignificant maintenance and attractive payback periods [215].

8.2. Description of a Novel Evaporative Cooling System (ECS)

An evaporative cooling system (*ECS*), which has been recently developed, is a novel system that can be used for both ventilation and air conditioning purposes. A schematic of the system is illustrated in Figure 8.1. The system is capable of meeting cooling demand at hot and arid climatic conditions. The working principle is definitely the same with a standard humidifier. First, outside air at any temperature is welcomed at the humidifying channel via a low power circulating fan with 12 W. Humidification is achieved via adiabatically saturated fibre material (cloth) which are specially designed and filled with water. In the system proposed here, fresh air is exposed to humidification, and its temperature reduces to the thermal comfort level. Drained water is collected at the bottom of the humidification channel and pumped to the water tank, which is fixed at the top of *ECS*. The proposed evaporative cooling system is devised to be used as a roof application. In this respect, its design is compatible with the roof pitch of existing UK building stock. External dimensions of the wooden structure of *ECS* are 1 m width, 1.5 m length and 1.5 m height. Dimension optimisation of *ECS* is expected to yield a slimmer and lighter construction. At this stage, the focal point is to investigate the thermal performance efficiency of *ECS* for different climatic conditions.

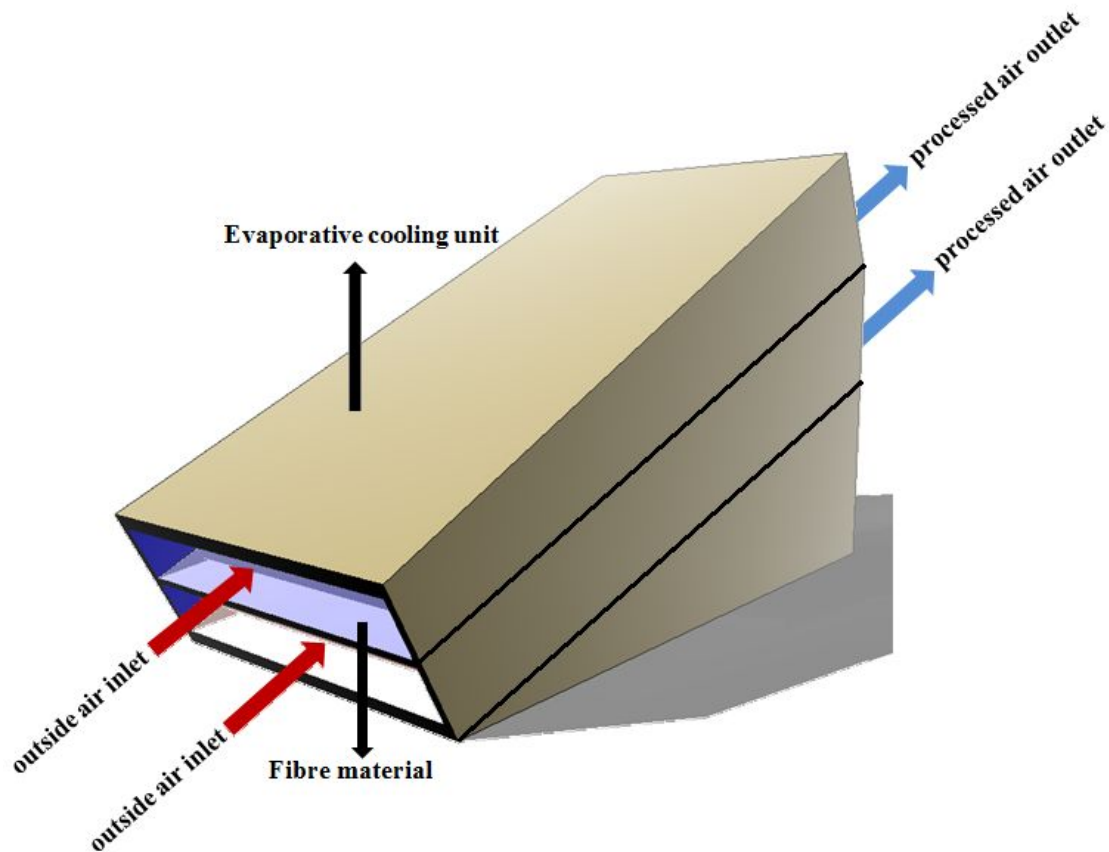


Figure 8.1. Description of the proposed evaporative cooling system.

8.3. Experimental Setup and Analysis

The test rig of a novel evaporative cooling system is built in the Department of Architecture and Built Environment at the University of Nottingham as it is illustrated in Figure 8.2. Real indoor and outdoor thermal conditions are assumed during the experiments. A multi-functional digital environmental chamber is used to adjust the temperature and the relative humidity of incoming fresh air. Two water tanks, a pump and a blower fan are utilised to run the system properly. The system is simulated and designed as to be a roof application of a real house. For a real house case of the proposed system, rain water will be collected to a tank and will be delivered to the system to use it for cooling purposes instead of tap water. Thus, it is achieved to save

large amount of tap water. As it is underlined here, the aforementioned system helps to save both energy and water, and contributes to reduce greenhouse gas emissions.

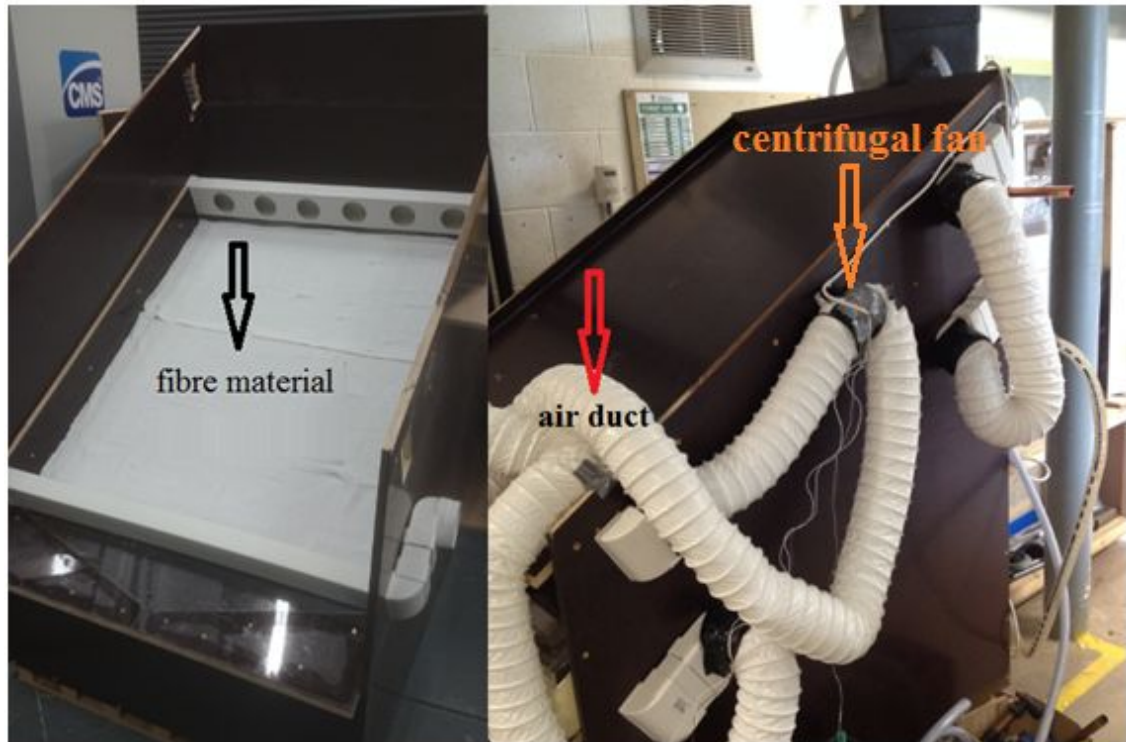


Figure 8.2. Detailed photos of a novel roof type evaporative cooling system.

In this chapter, evaporative cooling performance of a novel *ECS* is experimentally investigated. The mass flow rate for the inlet velocity of 0.3 m/s is calculated to be 0.0042 kg/s whereas it is found to be 0.0070 kg/s for 0.5 m/s . In this respect, for different conditions of fresh air from environmental chamber, time-dependent outlet temperature and outlet relative humidity of air are measured. Following the relevant measurements, humidification effectiveness, wet bulb effectiveness and coefficient of performance of the proposed cooling system are determined for each case. The results are comprehensively analysed for a reliable evaluation and easier understanding.

8.4. Results and Discussion

Evaporative cooling systems require less energy requirement than the other cooling systems such as mechanical vapour compression systems [277]. Therefore, evaporative cooling technologies are extensively preferred for cooling purposes in climatic conditions with medium to low humidity [278]. In this research, a novel design of an evaporative cooling system is experimentally investigated. This study aims to mitigate the energy consumption due to cooling and ventilation. The system developed achieves cooling as well as providing ventilation with a cost-effective and environmentally friendly way. In this section, the laboratory test results of the proposed innovation are given. Through the data obtained, wet bulb effectiveness, humidification effectiveness and coefficient of performance of the system are calculated and the results are discussed. The preliminary testing of evaporative cooling system (*ECS*) is carried out for two different inlet conditions of fresh air supplied by environmental chamber. In the first test, the velocity of the air is determined to be 0.3 m/s . As a natural consequence of evaporative cooling process, air temperature remarkably decreases at the outlet. Steady-state measurements reveal that the average temperature of fresh air at the inlet is $36.9\text{ }^{\circ}\text{C}$, whereas it is $26.7\text{ }^{\circ}\text{C}$ at the outlet. The temperature difference of $10.2\text{ }^{\circ}\text{C}$ achieved by a novel evaporative cooling unit is very promising. The outlet relative humidity of fresh air almost reaches the adiabatic saturation condition. The average humidity values at the inlet and outlet are measured to be 37.2 and 98.4%, respectively. The results of the first test are unequivocally illustrated in [Figure 8.3](#) and [Figure 8.4](#).

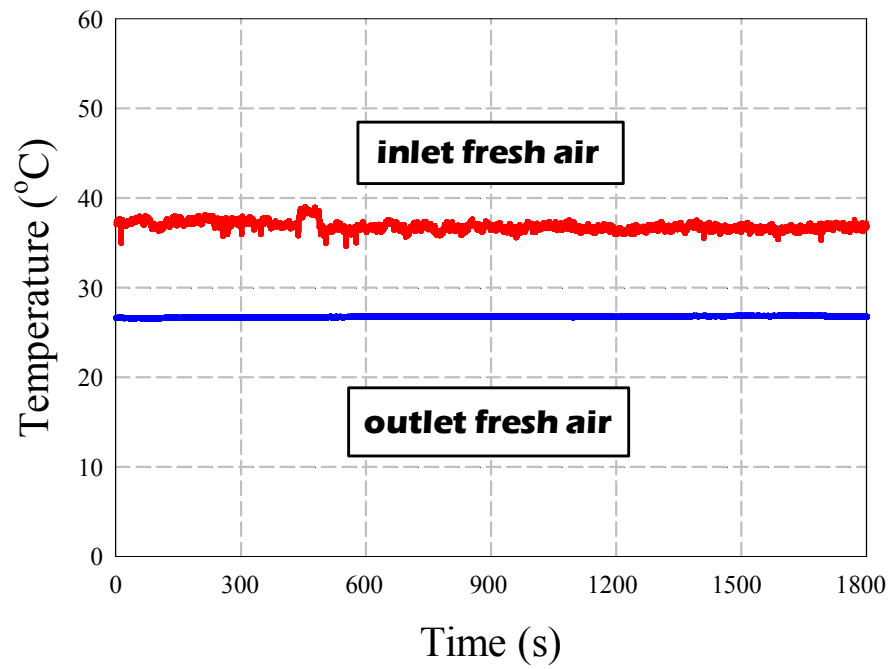


Figure 8.3. Temperature measurement from the first test.

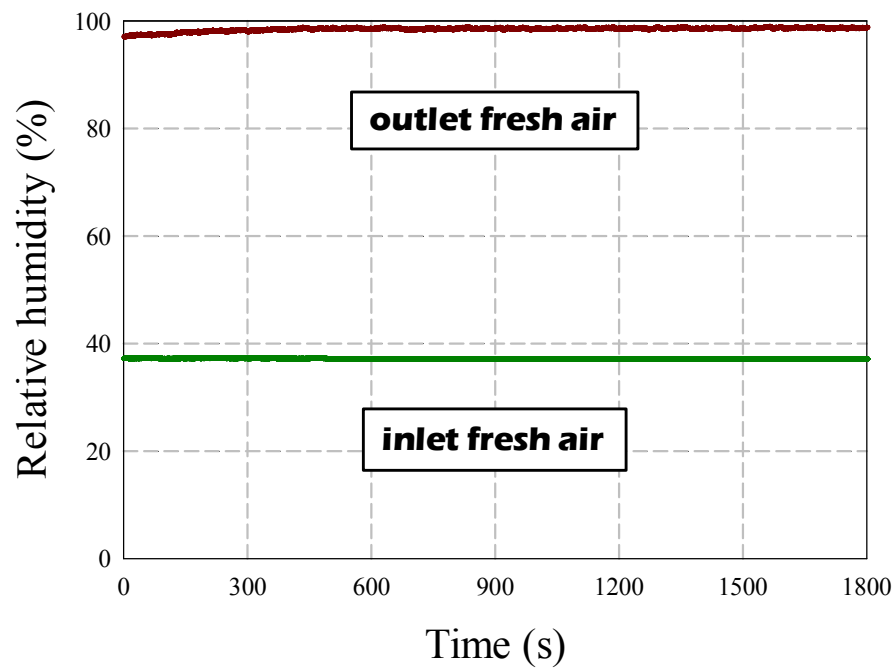


Figure 8.4. Relative humidity measurement from the first test.

The reliability of the system and the accuracy of the measurements are verified by performing a second test as illustrated in Figure 8.5 and Figure 8.6. In the second test, the air velocity is measured to be 0.5 m/s. On the other hand, fresh air enters into the system at different temperature and relative humidity, and arid temperate climatic conditions are considered. Temperature measurements indicate that the temperature difference at the second test is not as high as the first test because of the lower inlet temperature. Average inlet and outlet temperatures of fresh air are determined to be 31.1 and 23.0 °C, respectively. The temperature difference of 8.1 °C is still remarkable since the power consumption of the system is insignificant. The results indicate that the adiabatic saturation condition is almost achieved for the second test as well. Average inlet and outlet relative humidity are measured to be 30.0 and 94.8%, respectively.

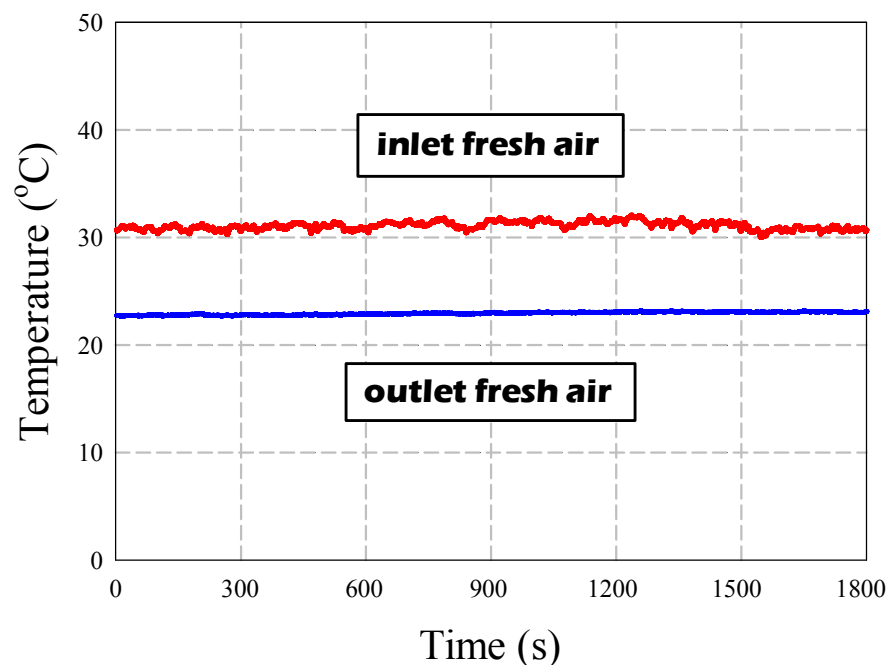


Figure 8.5. Temperature measurement from the second test.

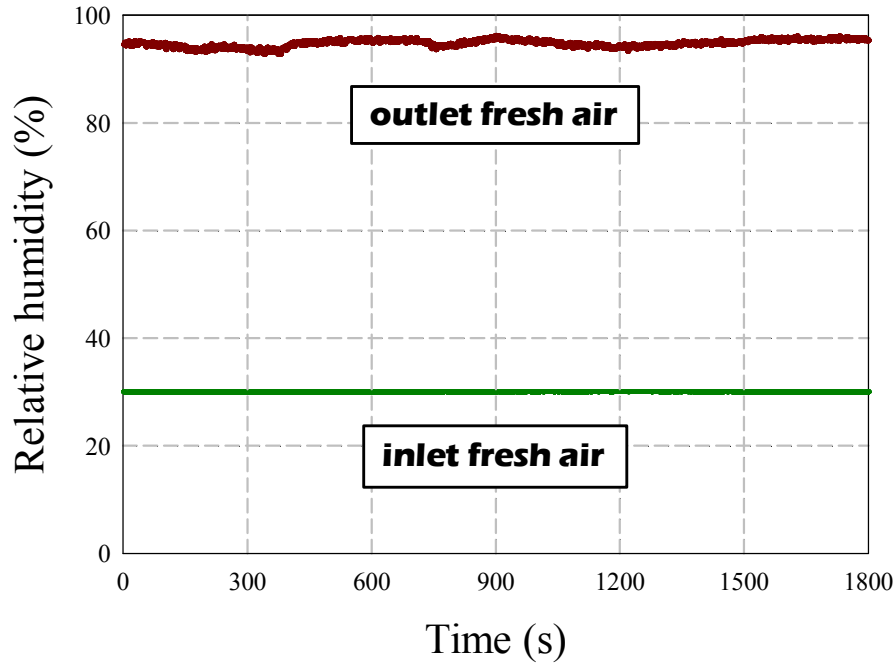


Figure 8.6. Relative humidity measurement from the second test.

The effectiveness of the evaporative cooling unit is also evaluated for two different inlet conditions of air. In this respect, wet bulb and humidification effectiveness of the system are calculated. Mathematical expression of the wet bulb effectiveness is given by using the following equation:

$$\varepsilon_{wb} = \frac{T_{db,in} - T_{db,out}}{T_{db,in} - T_{wb,in}} \quad (8.1)$$

where ε is the effectiveness, $T_{db,in}$ is the dry bulb temperature of the inlet fresh air, $T_{db,out}$ is the dry bulb temperature of the outlet fresh air and $T_{wb,in}$ is the wet bulb temperature of the inlet fresh air.

The humidification effectiveness of the evaporative cooling unit is calculated as follows [279]:

$$\varepsilon_{hum} = \frac{\omega_{out} - \omega_{in}}{\omega_{sat} - \omega_{in}} \quad (8.2)$$

where ω_{in} is the humidity ratio of the inlet fresh air and ω_{out} is the humidity ratio of the outlet fresh air and ω_{sat} is the humidity ratio of saturated air.

The average wet bulb effectiveness of the system is found to be around 86% and 65%, respectively for the first and second tests as shown in [Figure 8.7](#). On the other hand, the average humidification effectiveness is determined to be 80% for the first test whereas it is 53% for the second test.

It can be concluded from the results that the humidification effectiveness is a strong function of the operational parameters. However, general tendency of the humidification effectiveness in [Figure 8.8](#) clearly reveals that there is an insignificant erratic behaviour as a consequence of dynamic characteristics of the laboratory environment. In this respect, it can be easily asserted that the system has almost stagnant humidification effectiveness for any specific operating condition. Much more stable characteristics might be obtained by enhancing thermal insulation feature of the test rig, and maintaining steady-state conditions for the test environment. Following the relevant measurements, the coefficient of performance (*COP*) of *ECS* is calculated for each test as shown in [Figure 8.9](#). For the extreme weather conditions as characterised by the first test, *COP* is expected to be highly attractive, which is verified by the experimental results. The average *COP* of the first test is found to be 8.7. On the other hand, for arid temperate climates given as an example in the second test, somewhat lower values of *COP* is predicted, and this is clearly seen the results of the second test. The average *COP* from the second test is calculated to be 6.7.

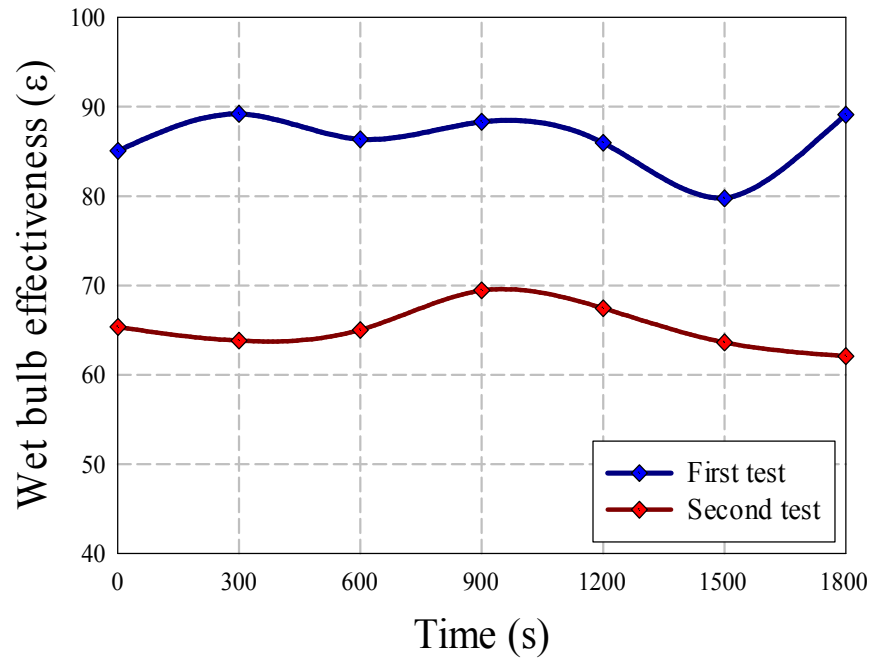


Figure 8.7. Wet bulb effectiveness for the first and second tests.

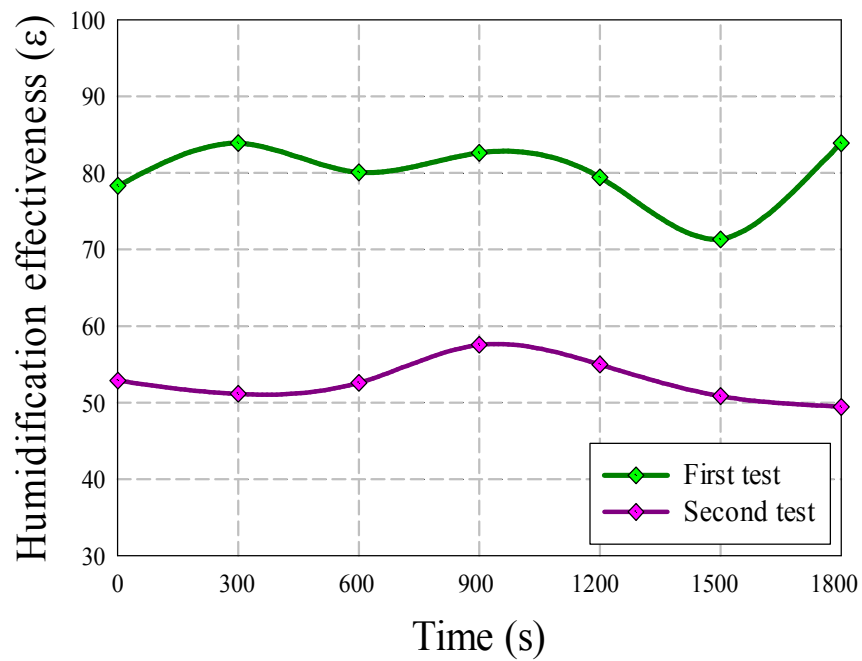


Figure 8.8. Humidification effectiveness for the first and second tests.

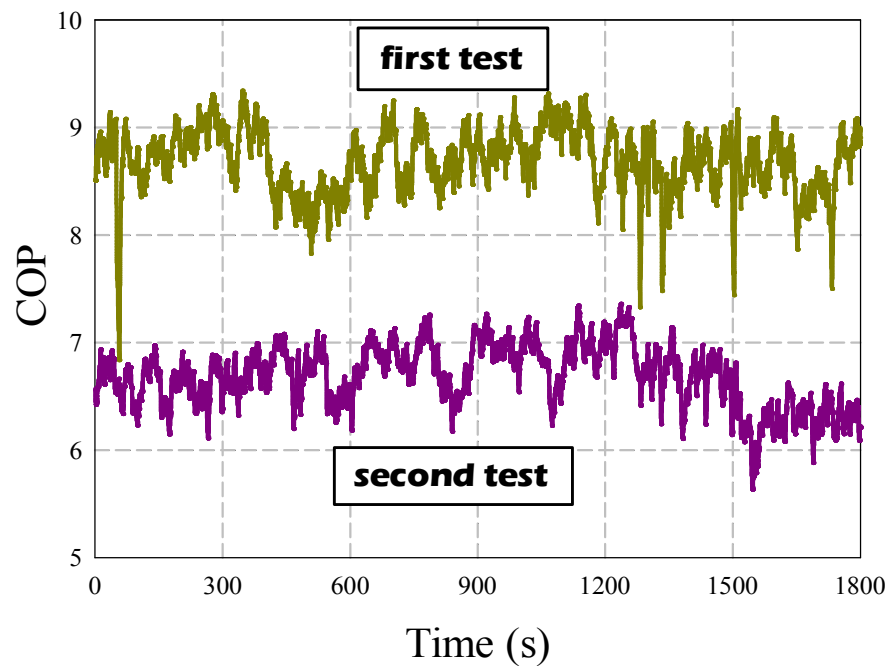


Figure 8.9. Coefficient of performance values for the first and second tests.

8.5. Conclusions

An intelligent building is defined as maximising the efficiency of the service with a minimum cost [246]. Energy consumption of the building sector increases day by day due to good thermal comfort demand of the occupants. That's why, use of energy-efficient technologies in buildings is of prime concern for anyone wishing to save both energy and money [212]. In this comprehensive research, a novel evaporative cooling system (*ECS*) is introduced to mitigate energy consumption in buildings arising from cooling and air conditioning. The results indicate that the *COP* of the said system is greatly affected by the air velocity. The experiments conducted for different velocities clearly show that the *COP* drops from 8.7 to 6.7 when the air velocity increases from 0.3 to 0.5 *m/s*. This can be explained with the limited time of heat and mass transfer inside the unit when the air velocity rises. In this respect, it can be concluded that the determination of optimum air velocity is of vital importance for greater coefficient of

performance of the system. The results indicate that the adiabatic saturation condition is almost achieved for the first and second tests. For the first test, the average humidity values at the inlet and outlet are measured to be 37.2 and 97.7%, respectively whereas they are measured to be 30.0 and 94.8%, respectively for the second test. The preliminary test results for the evaporative cooling system clearly reveal that the system developed is very promising for extreme and temperate climatic conditions. This experimental research basically aims at demonstrating the feasibility of this novel system to reduce the cooling demand of buildings in extreme and temperate environmental conditions. In the next stage, the system will be powered with desiccant filled fibre cloth as well, and the experiments will be repeated for humid conditions of incoming air.

CHAPTER 9

A simplified model for liquid desiccant-based evaporative cooling system

- 9.1. Introduction
- 9.2. Mathematical Model
- 9.3. Results and Discussion
- 9.4. Conclusions

CHAPTER 9

A simplified model for liquid desiccant-based evaporative cooling system

9.1. Introduction

Cooling energy has an important part in buildings' energy consumption levels. As reported by Hasan [248] in a recent work, the demand for cooling increases day by day as a consequence of the growing demand for better thermal comfort conditions in buildings. Evaporative cooling has a high potential to meet cooling demands at low energy costs [249]. Riangvilaikul and Kumar [213] note that the evaporative cooling is a good alternative to mechanical vapour compression for air conditioning applications since it requires about four times less electric power than vapour-compression refrigeration [250]. Current available evaporative cooling systems can be classified as direct-contact and indirect-contact evaporative coolers. In a direct evaporative cooling system, working air to be cooled is in a direct contact with a liquid water film. Cooling is accomplished by the adiabatic heat exchange between the working air and the liquid water film [251]. Direct-contact evaporative cooling systems are appropriate for use only in dry, hot environmental conditions, or in rooms needing both cooling and humidification [252]. On the other hand, in an indirect-contact evaporative cooler, the inlet air is cooled by so-called working (secondary) air which is cooled through evaporation [253]. Thermodynamically, the wet passage absorbs heat from the dry passage by evaporating water, and thus cools the dry passage, while the latent heat of vaporizing water is dissipated into the working air. [Figure 9.1](#) shows the schematic of

an indirect-contact evaporative cooler. The metallic sheet between product and working air is usually an air-to-air heat exchanger, which can be plate type [254,255], tube type [254,256] and heat pipe type [254,257]. Indirect-contact evaporative cooling systems have the advantage of being able to cool the product air without changing its specific humidity [229]. Therefore, these systems are widely utilised in domestic buildings as air-conditioning units since more than a century [253].

The challenging point of evaporative cooling systems is that they are not able to provide the desired conditions in hot and humid areas. Therefore, alternative systems such as desiccant-based cooling are required. Liquid desiccant-based evaporative cooling system is a good alternative to conventional vapour compression cooling systems to be able to control both temperature and relative humidity, especially in hot and humid environmental conditions [280,281]. Chengchao and Ketao [282] also note the advantages of these systems over vapour compression air conditioning systems in terms of its suitability in different climatic conditions. Numerous theoretical and experimental attempts have been made so far on desiccant-based evaporative cooling systems. Oberg and Goswami [283,284] carry out several experimental works at the University of Florida. It is observed that an electrical energy savings around 80% can be achieved by desiccant-based solar cooling system. Ahmed et al. [285] perform a simulation work, and found that the *COP* of the desiccant cooling system is about 50% higher than that of a conventional vapour absorption cooling system. Performance of a desiccant cooling system is related to the amount of water removed from the humid air via desiccant solution. The amount of water condensed in the dehumidifier needs to be evaporated from the desiccant solution in the regenerator.

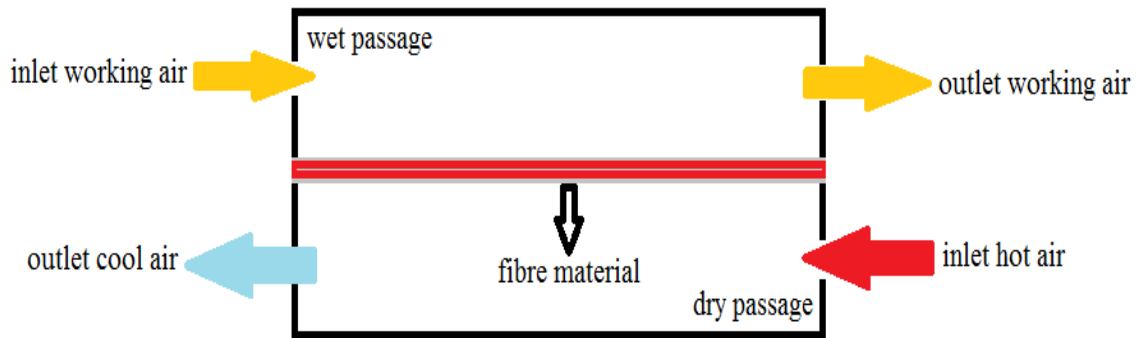


Figure 9.1. Schematic of a typical indirect-contact evaporative cooling system.

Besides the experimental works, several theoretical attempts have been made so far on performance assessment of desiccant-based cooling systems. Liu et al. [286] present a regression analysis to predict the effects of air and desiccant inlet parameters on the regenerator performance. Fumo and Goswami [287,288] evaluate the effectiveness of dehumidifier and regenerator under the effects of various parameters such as air and desiccant flow rate, air and desiccant temperature, air humidity and desiccant concentration. El-Shafei et al. [289] develop a model to estimate the performance of the regenerator of a solar liquid desiccant dehumidification/regeneration via artificial neural network. Abdul-Wahab et al. [290] analyse the effects of various design parameters on the performance of liquid desiccant-based air dehumidifier. Sick et al. [291] investigate the seasonal performance of a hybrid liquid desiccant cooling system. Stevens et al. [292] develop an effectiveness model for liquid desiccant systems. In this chapter, a simple mathematical model is presented for a liquid-desiccant-based evaporative cooling system which is illustrated in Figure 9.2. For several design parameters such as air temperature, desiccant temperature, mass flow rates of incoming air and desiccant, relative humidity and desiccant concentration, humidity ratio and temperature of air at the outlet, cooling level and overall system performance are evaluated.

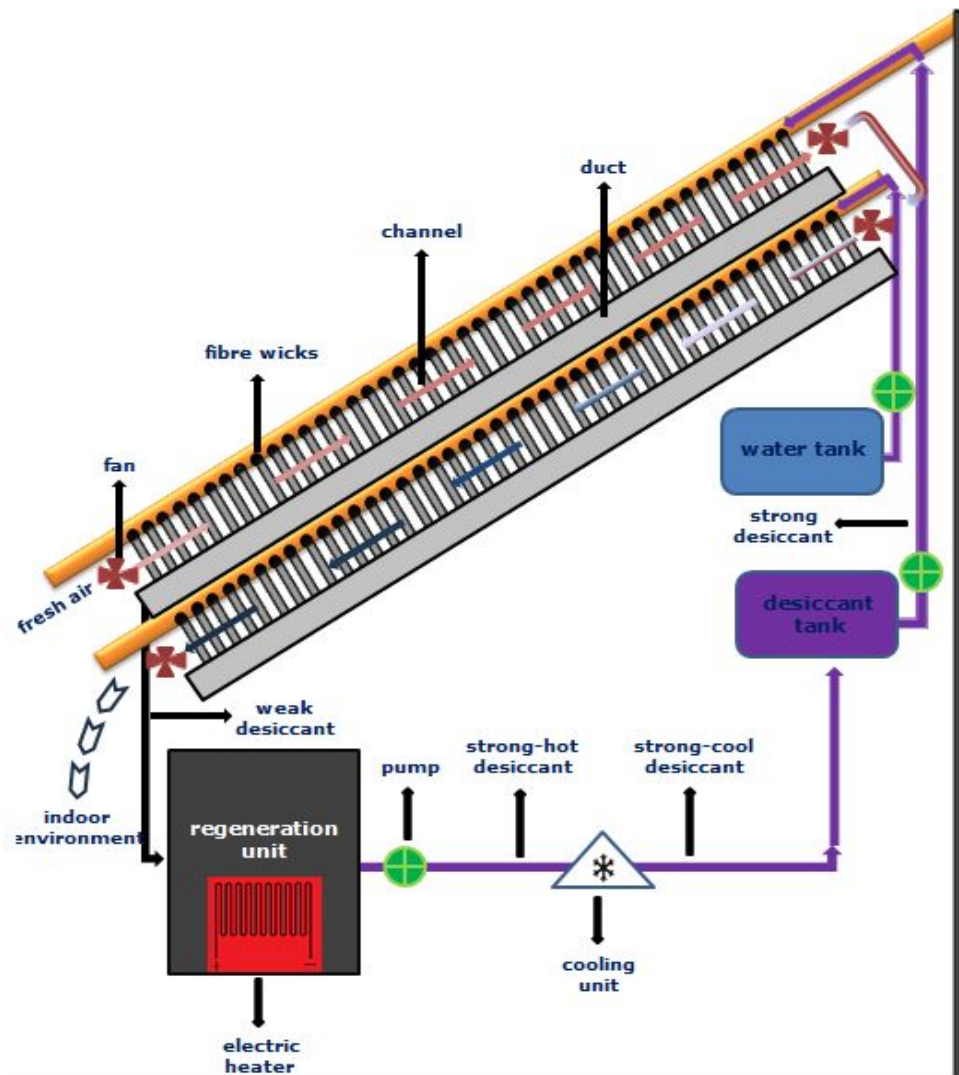


Figure 9.2. Schematic of a novel liquid desiccant-based evaporative cooling system.

9.2. Mathematical Model

The liquid desiccant-based evaporative cooling system which is illustrated in Figure 9.2 can be modelled by splitting the whole system into two main parts as dehumidification process and humidification process. In the first part, moisture content of the incoming fresh air is controlled via liquid desiccant solution whereas its temperature is regulated through evaporative cooling in the second part. It is unequivocal in literature review that the theoretical works on desiccant-based cooling system are very limited since the behaviour of the systems in actual operating

conditions is somewhat instable in most cases, which makes the theoretical evaluation laborious. In a research on dehumidification, the input parameters are often the inlet air temperature ($T_{a,in}$), the inlet solution temperature ($T_{s,in}$), the inlet air humidity ratio ($\omega_{a,in}$) and the inlet solution concentration ($C_{s,in}$). From this point of view, the output parameters are the outlet air temperature ($T_{a,out}$), the outlet solution temperature ($T_{s,out}$), the outlet air humidity ratio ($\omega_{a,out}$) and the outlet solution concentration ($C_{s,out}$). For this part of the modelling work, the statistical approach presented by Mohammad et al. [293] can be utilised for a rapid and accurate evaluation. In this respect, following simplified equations are obtained for the output parameters of the dehumidification process:

$$T_{a,out} = 11.929 + 0.743T_{s,in} + 0.299\omega_{a,in} \quad (9.1)$$

$$T_{s,out} = 5.86 + 0.763T_{s,in} + 0.199\omega_{a,in} \quad (9.2)$$

$$\omega_{a,out} = 7.873 + 0.508T_{s,in} + 0.201\omega_{a,in} \quad (9.3)$$

$$C_{s,out} = 1.309 + 95.7C_{s,in} \quad (9.4)$$

Another important parameter is the condensation water rate (m_{con}) which is given as follows:

$$m_{con} = -0.079 - 0.044\omega_{a,in} + 0.028T_{s,in} - 0.312\dot{m}_a \quad (9.5)$$

where \dot{m}_a is the inlet air mass flow rate. The accuracy of the proposed equations is verified by a previously conducted experimental work of Fumo and Goswami [281]. As it is clearly illustrated in Table 9.1 that there is a very good accordance between the theoretical and the experimental results. The efficacy of the modelling work of the dehumidification part is significant since the evaporative cooling analyses are

completely based on the outputs of dehumidification process. In the second part of the system, dried air after the dehumidification process is welcomed by the evaporative cooling channel for proper humidification, and thus for the desired cooling. In this regard, an accurate mathematical model of the evaporative cooling system is important. A heat transfer analogy for flow in ducts is employed to estimate the evaporation rate. The evaporation rate is a function of the mass transfer coefficient which is characterised by Sherwood number. The Sherwood number represents the ratio of convective to diffusive mass transport, and it is calculated by correlations of Reynolds and Schmidt numbers. To determine the aforementioned dimensionless numbers, thermophysical properties of air at the film temperature are utilised. The film temperature (T_f) is given as follows:

$$T_f = \frac{T_{lwf} + T_{a,out}}{2} \quad (9.6)$$

where T_{lwf} is the liquid water film temperature. The characteristic of the flow is then determined by Reynolds number. Reynolds number is a dimensionless number that gives a measure of the ratio of inertial forces to viscous forces and thus, quantifies the relative importance of these two types of forces for given flow conditions [270]. For flow through noncircular tubes, Reynolds number is based on the hydraulic diameter (D_h) and given as follows:

$$Re = \frac{v\rho D_h}{\mu} \quad (9.7)$$

where

$$D_h = \frac{4A}{p} \quad (9.8)$$

In equation (9.8), A is the cross sectional area of the duct and p is the wetted perimeter. As a second step, Schmidt number is determined by the following equation:

$$Sc = \frac{\nu}{Dm} \quad (9.9)$$

where ν is the kinematic viscosity and Dm is the mass diffusivity. Schmidt number is a dimensionless number which is defined as the ratio of momentum diffusivity and mass diffusivity, and is utilised to characterise fluid flows in which there are simultaneous momentum and mass diffusion convection processes [271]. After determining Re and Sc numbers, Sherwood number (Sh) is calculated as follows:

$$Sh = \frac{KD_h}{Dm} \quad (9.10)$$

where K is the mass transfer coefficient. Sherwood number is a dimensionless number which represents the ratio of convective to diffusive mass transport. The average mass transfer coefficient is computed by the average Sherwood number as follows:

$$\bar{K} = \frac{\bar{Sh}Dm}{D_h} \quad (9.11)$$

To determine the Sherwood number, the following semi-theoretical equation developed by Frossling [272] can be used:

$$Sh = 2 + 0.552Re^{\frac{1}{2}}Sc^{\frac{1}{3}} \quad (9.12)$$

For the mass diffusion coefficient of water vapour, the regression curve fit obtained from the data of Bolz and Tuve [273] can be utilised:

$$Dm = -2.775 \times 10^{-6} + 4.479 \times 10^{-8}T + 1.656 \times 10^{-10}T^2 \quad (9.13)$$

The mass transfer rate is driven by the difference between the concentration of water vapour at the water spraying unit and in the working air. The partial pressure of the water vapour at the water spraying is the saturation pressure of water at T_{lwf} . The concentration of water vapour (C_w) at the water spraying unit is the density of water vapour evaluated at the partial pressure and temperature. The mass fraction of water vapour (mf_w) at the water spraying unit is given by:

$$mf_w = \frac{C_w}{\rho} \quad (9.14)$$

The partial pressure of water in the working air ($P_{w,wa}$) is the product of the relative humidity (ϕ) and the saturation pressure of water vapour ($P_{sat,w}$) at T_{lwf} as given below:

$$P_{w,wa} = \phi P_{sat,w} \quad (9.15)$$

The concentration of water vapour in the working air ($C_{w,wa}$) is the density of water vapour evaluated at the partial pressure and temperature. The mass fraction of water vapour in the working air ($mf_{w,wa}$) is determined by:

$$mf_{w,wa} = \frac{C_{w,wa}}{\rho} \quad (9.16)$$

Blowing factor (BF) is defined as follows to calculate the corrected mass transfer coefficient (\bar{K}_{cor}):

$$BF = \ln \frac{1 + \varpi}{\varpi} \quad (9.17)$$

where

$$\varpi = \frac{mf_w - mf_{w,wa}}{mf_{w,wa} - 1} \quad (9.18)$$

The corrected mass transfer coefficient is given as follows:

$$\bar{K}_{cor} = \bar{K}BF \quad (9.19)$$

Finally, the mass flow rate of water due to evaporation is calculated by the following equation:

$$\dot{m}_w = \bar{K}_{cor}A_{tot,wsu}(C_w - C_{w,wa}) \quad (9.20)$$

where $A_{tot,wsu}$ is the total heat transfer surface area of the water spraying unit. Determining the mass flow rate of water due to evaporation enables to specify the temperature and the relative humidity of the working air at the outlet of the spraying unit.

9.3. Results and Discussion

In the first part of the results, outlet desiccant temperature is theoretically determined as a function of inlet desiccant temperature. It is understood from [Figure 9.3](#) that there is an almost linear relationship between the temperatures of desiccant at inlet and outlet. This output can be attributed to the first law of thermodynamics.

Inlet desiccant temperature plays a significant role in overall dehumidification performance. In this respect, the impact of desiccant temperature at the inlet on other performance related parameters such as humidity ratio needs to be investigated for a thorough assessment. Therefore in [Figure 9.4](#), humidity ratio of fresh air at the outlet of

the dehumidifier is given as a function of inlet desiccant temperature. Humidity ratio of fresh air increases nearly linearly with increasing desiccant temperature at the inlet. Desiccant concentration is of vital importance in desiccant based cooling systems as it notably affects the thermal performance efficiency. For two different cases illustrated in Figure 9.5, outlet fresh air temperature is determined with respect to change in inlet air temperature and desiccant concentration. For each case, desiccant temperature at the inlet and mass flow rate of air are taken to be 24 °C and 0.2 kg/s, respectively. The results indicate that there is a linear relationship between desiccant concentration and outlet fresh air temperature. The lower desiccant concentration and desiccant temperature corresponds to the greater thermal efficiency as concluded from the graphs.

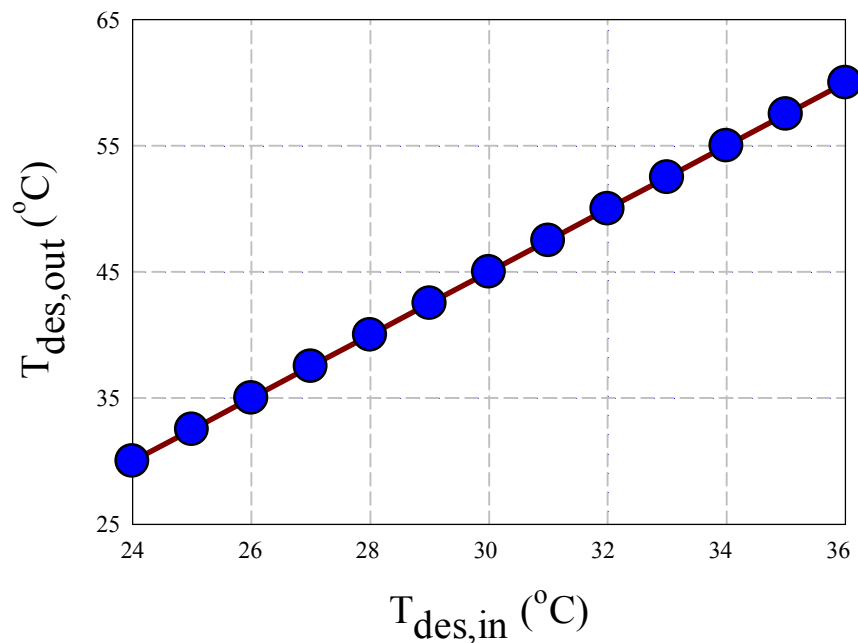


Figure 9.3. Outlet desiccant temperature as a function of inlet desiccant temperature.

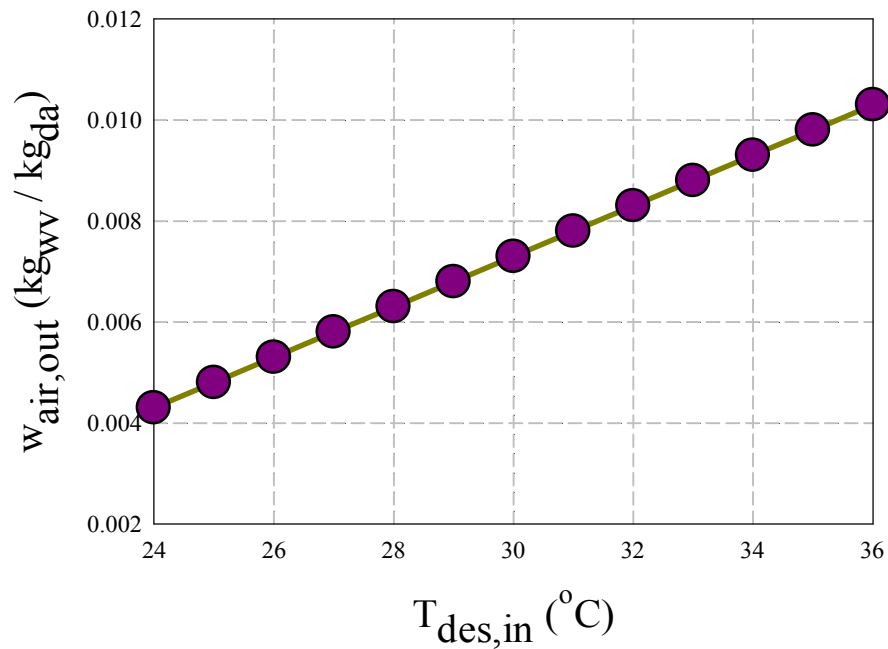


Figure 9.4. Humidity ratio of fresh air at the outlet of the dehumidifier as a function of inlet desiccant temperature.

9.4. Conclusions

In this chapter, a simple mathematical model for the preliminary design of a liquid-desiccant-based evaporative cooling system is presented. The modelling work is split into two sections as dehumidification process and humidification process, and for each section, governing equations of the system are given in detail. For different operating parameters such as air temperature, desiccant temperature, mass flow rates of incoming air and desiccant, humidity ratio and desiccant concentration, humidity ratio and temperature of air at the outlet, cooling level and overall system performance are predicted. The model predictions are compared with a previously published experimental work and an excellent agreement is observed between the results.

The characteristics results of the research can be summarised as follows:

- There is a linear tendency between inlet and outlet desiccant temperatures of the system which is an unequivocal consequence of first law of thermodynamics.

- Desiccant temperature at the inlet needs to be kept as low as possible for desired humidity ratio ranges.
- Desiccant concentration plays a key role in outlet fresh air temperature as well as humidity ratio and thermal comfort parameters for indoor environment.

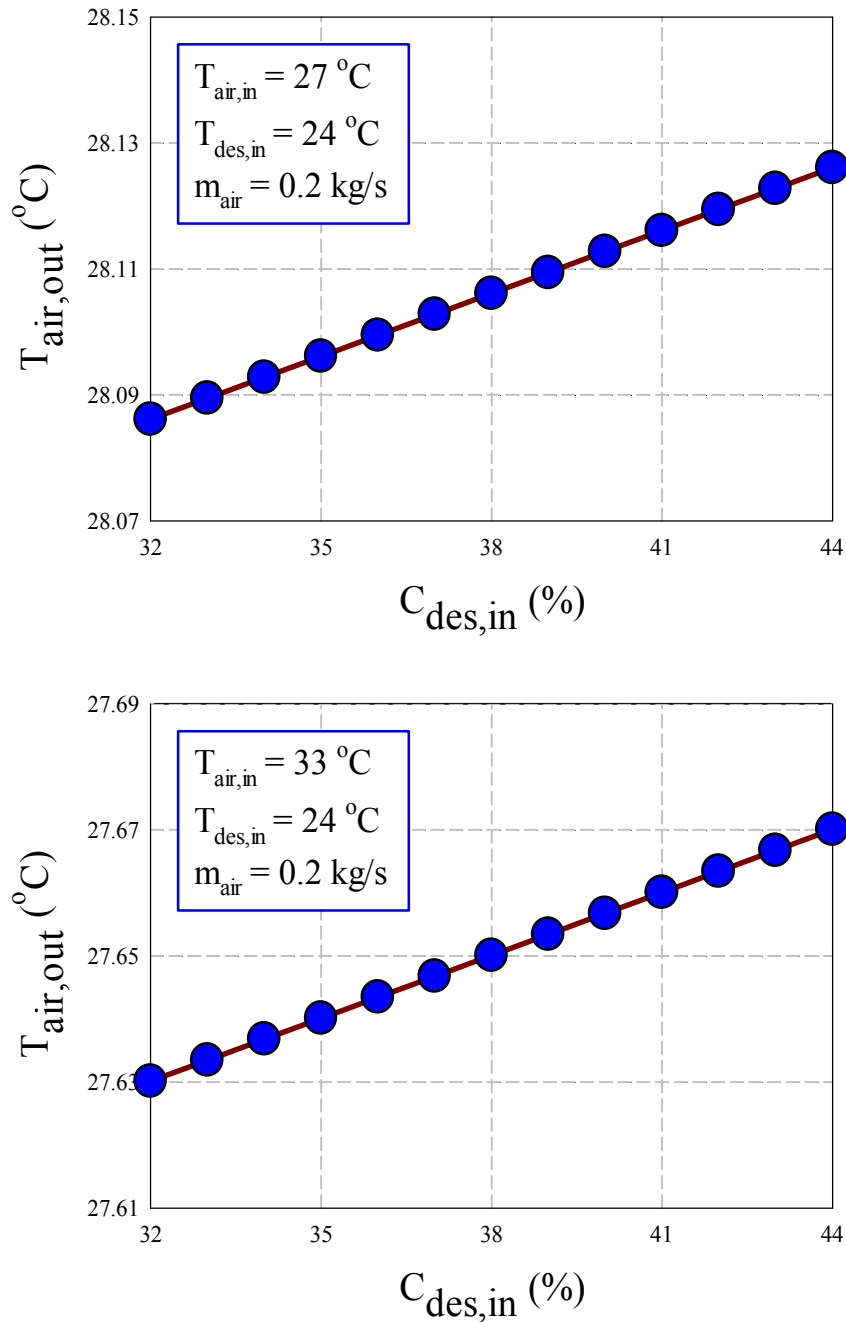


Figure 9.5. Air temperature at the outlet of the dehumidifier as a function of inlet desiccant concentration.

CHAPTER 10

Thermal performance assessment of a novel liquid desiccant-based evaporative cooling system: An experimental investigation

- 10.1. Introduction
- 10.2. Description of DECS
- 10.3. Experimental Setup
- 10.4. Measurements
- 10.5. Results and Discussion
- 10.6. Conclusions

CHAPTER 10

Thermal performance assessment of a novel liquid desiccant-based evaporative cooling system: An experimental investigation

10.1. Introduction

Clean energy generation and its efficient use are significant due to growing significance of environmental issues especially over the last four decades [162]. Sharp increases in energy consumption as a consequence of the population growth and economic development dominate the greenhouse gas concentrations in the atmosphere [294]. Despite intensive efforts to narrow the gap between conventional energy sources and renewables, only about 14% of total world energy demand is supplied by renewable energy technologies at the moment [101]. In this regard, there is a consensus among scientists that research on energy management and efficient minimisation of energy consumption is compulsory. Several decisive measures are taken at global scale for the urgent stabilisation of greenhouse gas concentrations by reducing the energy demand in all sectors. Previous works indicate that building sector accounts for an important part of the world's energy consumption. For instance, buildings are responsible for about 40% of total energy use in the UK. Among the building types, domestic buildings have the largest share with 63% of the total building energy consumption, which is quite remarkable [295]. Baetens et al. [152] also reported that buildings emitted 8.3 Gt CO₂ in 2005 accounting for more than 30% of the greenhouse gas emissions in many

developed countries. Dominant impacts of buildings on both the energy consumption levels and the environment are unequivocal.

HVAC is an indispensable part of a building and causes a significant amount of energy loss. Therefore it is considered as a key solution for remarkable energy savings in buildings. Cooling constitutes an important part of heat loss due to *HVAC*. As emphasised by Hasan [248] in a recent research, the cooling demand increases day by day due to the growing demand for better thermal comfort conditions in buildings. Cooling can be provided in different ways such as evaporative cooling. Evaporative cooling has a remarkable potential to meet cooling demands in a cost-effective way. It is reported that the evaporative cooling is a good alternative to mechanical vapour compression for air conditioning applications since it consumes nearly four times less electricity than vapour-compression refrigeration [213,250]. Current available evaporative cooling systems can be split into two categories as direct-contact and indirect-contact evaporative coolers. In a direct-contact evaporative cooling system, working air to be cooled is in a direct contact with a liquid water film. Cooling is achieved by the adiabatic heat exchange between the working air and the liquid water film [251]. Direct-contact evaporative cooling systems are suitable for using only in dry and hot climatic conditions, or in rooms needing both cooling and humidification [252]. On the other hand, in an indirect-contact evaporative cooler, the inlet air is cooled by working air which is cooled via evaporation [253]. Thermodynamically, the wet passage absorbs heat from the dry passage by evaporating water, and thus cools the dry passage, while the latent heat of vaporising water is dissipated into the working air.

It is well-documented in literature that evaporative cooling provides efficient cooling in a cost-effective way. However, it is expected to be inappropriate for using in humid climates since the air is already close to the state of adiabatic saturation. In this

respect, it is required to dehumidify the outside air before humidification. In order to meet this requirement in a cost-effective way, a novel desiccant-based evaporative cooling system (*DECS*) is devised, constructed and tested. *DECS* is able to be utilised for both cooling and air conditioning purposes with a higher range of coefficient of performance compared to alternative systems. Within the scope of this research, experimental results of desiccant-based evaporative cooling system are introduced.

10.2. Description of Desiccant-Based Evaporative Cooling System (*DECS*)

DECS, which has been recently developed at the University of Nottingham, is a novel system that can be used for both ventilation and air conditioning purposes. A comprehensive description of the system is illustrated in [Figure 10.1](#). The system basically consists of two parts where dehumidification and humidification of incoming fresh air occur, respectively. The system is capable of meeting cooling demand at any particular climatic condition. The working principle is definitely the same with a standard dehumidifier and humidifier. First, outside air at any temperature and relative humidity is welcomed at the dehumidifying channel via a low power circulating fan. Through specially designed desiccant filled fibre cloth, its relative humidity is decreased to a desired level. At the second step, dehumidified fresh air this time is exposed to humidification and its temperature reduces to the thermal comfort level. Similarly, humidification is achieved via adiabatically saturated fibre cloth. Drained water is collected at the bottom of the humidification channel and pumped to the water tank, which is fixed at the top of *DECS*. Drained desiccant is similarly collected at the bottom of dehumidification channel and it is regenerated via a regeneration unit. Then, its temperature is reduced in a water-based heat exchanger and it is pumped to the desiccant tank, which is fixed near the water tank at the top. To be able to dehumidify

the incoming fresh air, potassium formate ($HCOOK$) solution 74% is selected as desiccant. The reason to use this solution is its cost-effectiveness, and it provides environmentally friendly applications compared to the alternatives. It has less corrosive effect and lower density and viscosity than the conventional absorbents such as lithium bromide ($LiBr$) solution [296].

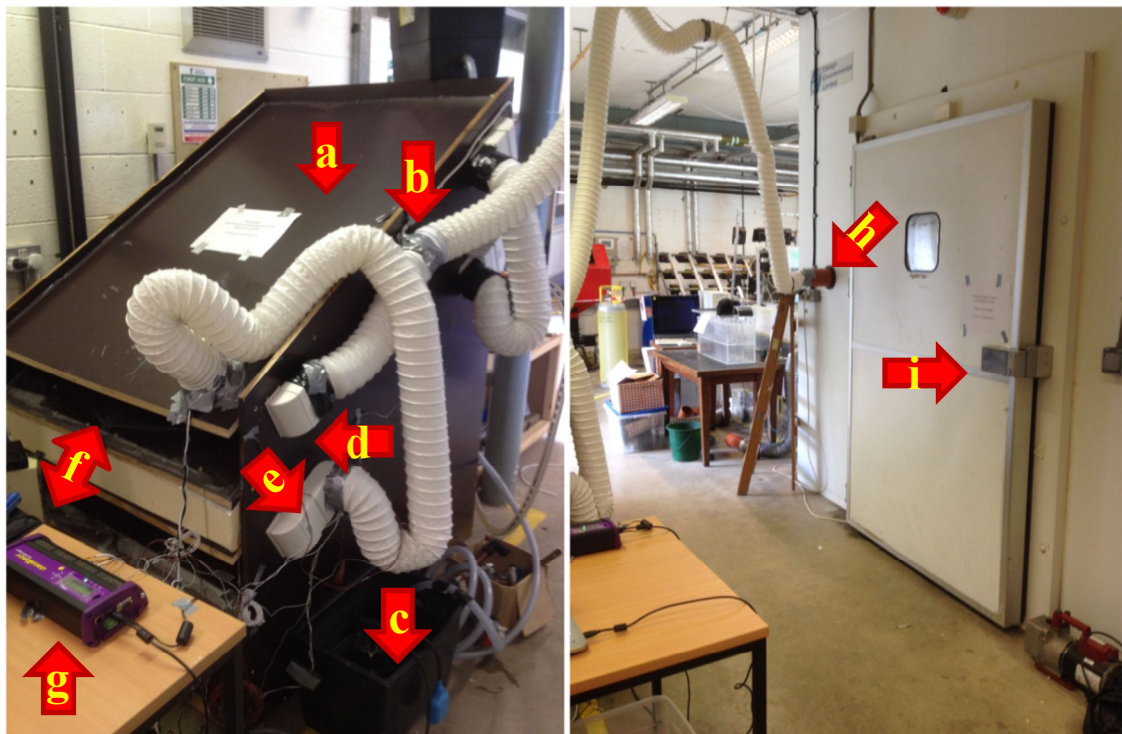


Figure 10.1. Detailed description of *DECS*: a) wooden structure of *DECS*, b) 12 Watt fan for circulating air, c) 15 Watt immersible pump, d) inlet duct to dehumidification, e) outlet duct after humidification, f) collecting ducts for drained water and desiccant, g) data logger, h) inlet fresh air to *DECS* from conditioned environmental chamber and i) digital and multi-functional environmental chamber.

DECS is devised to be used as a roof application. In this respect, its design is compatible with the roof pitch of existing UK building stock. External dimensions of

the wooden structure of *DECS* are 1 m width, 1.5 m length and 1.5 m height. Dimension optimisation of *DECS* is expected to yield a slimmer and lighter construction. At this stage, the focal point is to investigate the thermal performance efficiency of *DECS* for different climatic conditions.

10.3. Experimental Setup

Desiccant-based evaporative cooling system (*DECS*) developed at the University of Nottingham is a novel solution for temperate humid climates which can be used for both ventilation and air conditioning purposes. A thorough description of the system is given in [Figure 10.1](#). The system essentially consists of two parts where incoming supply air is dehumidified and humidified, respectively. As it is well-documented in literature, stand-alone evaporative cooling systems are inconclusive in humid environments due to the excessive moisture content of air. On the contrary, the system presented in this work is capable of meeting the cooling demand at any particular climatic condition. The working principle is definitely the same with a standard dehumidifier and humidifier. First, outside air at any temperature and relative humidity is welcomed at the dehumidifying channel via a low power circulating fan. Through specially designed desiccant filled fibre cloth, its humidity is decreased to an appropriate figure. At the second step, dehumidified supply air this time is exposed to humidification and its temperature is reduced to the thermal comfort level. Similarly, humidification is achieved via adiabatically saturated fibre cloth. Drained water is collected at the bottom of the humidification channel and pumped to the water tank, which is fixed at the top of *DECS*. Drained weak desiccant is similarly collected at the bottom of the dehumidification channel. The collected weak desiccant is regenerated via a solar driven 2 kW immersible electric heater at 70 °C. This process allows desiccant

to be again strong and ready for absorption, however its temperature slightly increases at the end of regeneration process. Therefore, regenerated desiccant is directed to a water based heat exchanger to be able to decrease its temperature. At the end of this process, desiccant is pumped to the second tank at the top for its natural flow into the system. *DECS* is developed to be used as a roof application. In this respect, its design is compatible with the roof pitch of existing UK building stock. External dimensions of the wooden structure of *DECS* are 1 m width, 1.5 m length and 1.5 m height. Dimension optimisation of *DECS* is expected to yield a slimmer and lighter construction. At this stage, the focal point is to investigate the dehumidification effectiveness of *DECS* for different inlet conditions of supply air.

The innovative aspect of this design can be expressed as conditioning fresh air in a cost-effective way irrespective of the change in climatic conditions. Whereas evaporative cooling systems can only be used in hot arid climates, the desiccant-based evaporative cooling system can meet the expectations not only hot arid but also temperate humid environmental conditions. Power input to the system only occurs through a 12 W centrifugal fan. 2 kW immersible electric heater and two 15 W immersible pumps are powered by solar photovoltaics. In this respect, the system is expected to have significantly higher *COP* range. However, it needs to be noted that pumps do not need to work continuously for this system. Once a circulation is achieved, that can provide an air conditioning for a timeframe of 2 hours.

10.4. Measurements

In this part of the research, cooling performance of desiccant based evaporative cooling system is experimentally investigated. The system is run as considering two different values of inlet air velocity. In this respect, for different conditions of fresh air

from environmental chamber, time-dependent inlet temperature and relative humidity values of air let to the dehumidification unit, outlet temperature and relative humidity values of air from dehumidification unit, inlet temperature and relative humidity values of air directed to the humidification unit and outlet temperature and relative humidity values of air from humidification unit are measured, respectively. Following the relevant measurements, dehumidification effectiveness is determined as well as final relative humidity and temperature of supply air. The mass flow rates of two different inlet velocities of 0.3 and 0.5 m/s are calculated to be 0.0042 and 0.0070 kg/s, respectively.

10.5. Results and Discussion

This study aims at decreasing the cooling energy consumption via using liquid desiccant based evaporative cooling system. The system provides cooling as well as ventilation with a cost-effective and environmentally way. In this section, deeper thermal performance analyses of the system are carried out and the results are discussed. Within the concept of this comprehensive research, dehumidification, humidification and wet bulb effectiveness are determined along with the coefficient of performance.

The dehumidification effectiveness of the desiccant part of the whole system is calculated as follows [280]:

$$\varepsilon_{dehum} = \frac{\omega_{in} - \omega_{out}}{\omega_{in} - \omega_{eq}} \quad (10.1)$$

where ε is the effectiveness, ω_{out} is the humidity ratio at the outlet; ω_{in} is the humidity ratio at the inlet and ω_{eq} is the absolute humidity of the air, which is at equilibrium with

the desiccant solution at the inlet concentration and temperature. The absolute humidity of the air is defined as follows [280]:

$$\omega_{eq} = \frac{0.622 P_{vap}}{1.013 \times 10^5 - P_{vap}} \quad (10.2)$$

In the equation above, P_{vap} is the partial vapour pressure on the desiccant solution surface in Pa . The humidification effectiveness of the evaporative cooling part of the whole system is given by [279]:

$$\varepsilon_{hum} = \frac{\omega_{out} - \omega_{in}}{\omega_{sat} - \omega_{in}} \quad (10.3)$$

Finally, wet bulb effectiveness of the evaporative cooling part is also analysed for two different inlet air velocities. Mathematical expressions of the wet bulb and effectiveness are given by using the following equation:

$$\varepsilon_{wb} = \frac{T_{db,in} - T_{db,out}}{T_{db,in} - T_{wb,in}} \quad (10.4)$$

where $T_{db,in}$ is the dry bulb temperature of the inlet air, $T_{db,out}$ is the dry bulb temperature of the outlet air and $T_{wb,in}$ is the wet bulb temperature of the inlet air.

Two separate inlet conditions are considered for the experimental analyses of *DECS*. The reference velocities of supply air are 0.3 and 0.5 m/s . For the case of lower velocity, average relative humidity and temperature values of supply air at the inlet dehumidification are measured to be around 94.7% and 38.6 °C, respectively whereas relative humidity and temperature values of the outlet dehumidification are 34.4% and 39.9 °C, respectively. Relative humidity and temperature values of air for the dehumidification process are shown in [Figure 10.2](#) and [Figure 10.3](#). The

dehumidification effectiveness is also measured to be around 63.7% which is attractive and promising as illustrated in Figure 10.4. On the other hand, average relative humidity and temperature values at the inlet humidification unit show almost the same tendency with the values of outlet dehumidification, as it is expected theoretically, due to the well insulation between two sections. For the average inlet relative humidity of 35.7% and average inlet air temperature of 40.0 °C at the humidification section, the average relative humidity and air temperature values at the outlet humidification unit are determined to be 65.5% and 33.3 °C, respectively as it is illustrated in Figure 10.5 and Figure 10.6. An average of 6.7 °C reduction is achieved in supply air temperature as well as an average of 37.3% humidification effectiveness as it is seen in Figure 10.7.

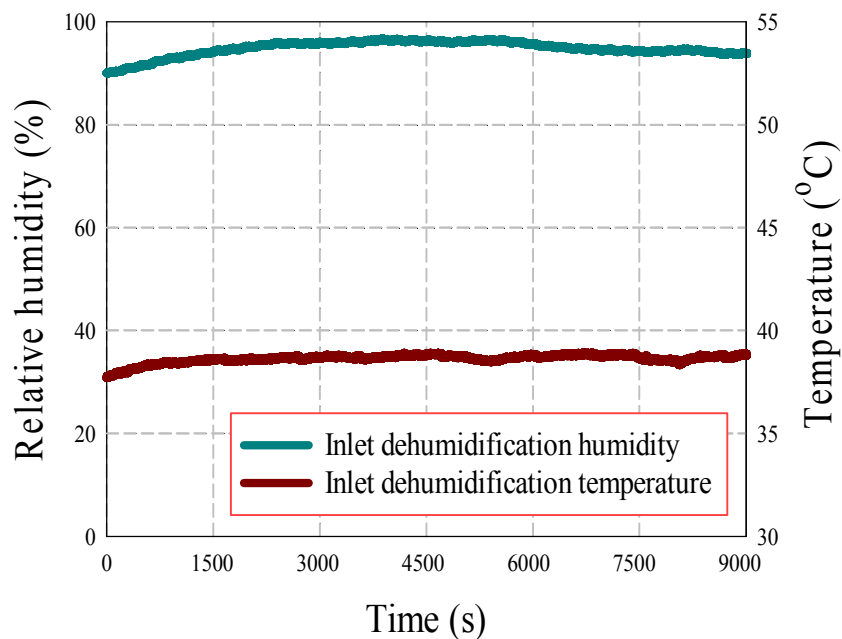


Figure 10.2. Relative humidity and temperature measurement for the air velocity of 0.3 m/s at the inlet of the dehumidification unit.

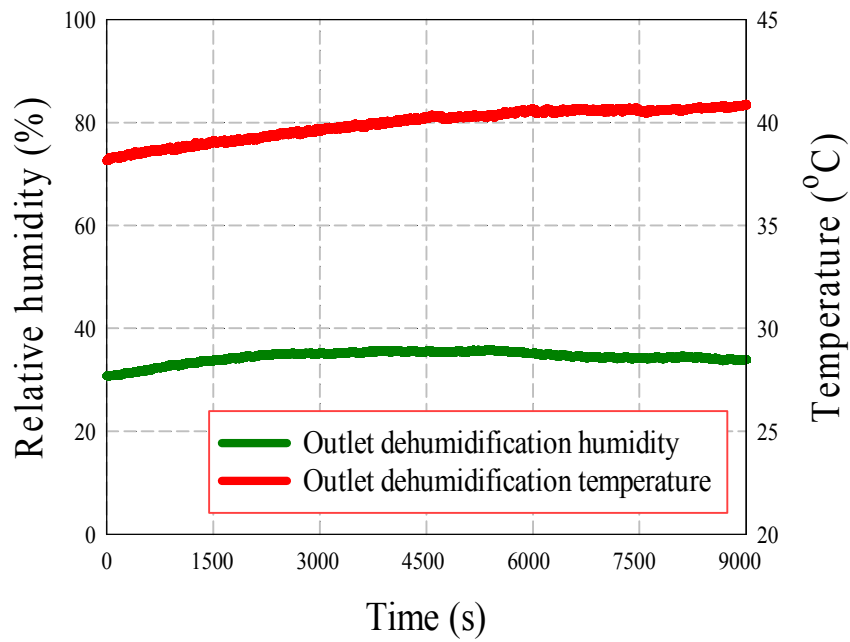


Figure 10.3. Relative humidity and temperature measurement for the air velocity of 0.3 m/s at the outlet of the dehumidification unit.

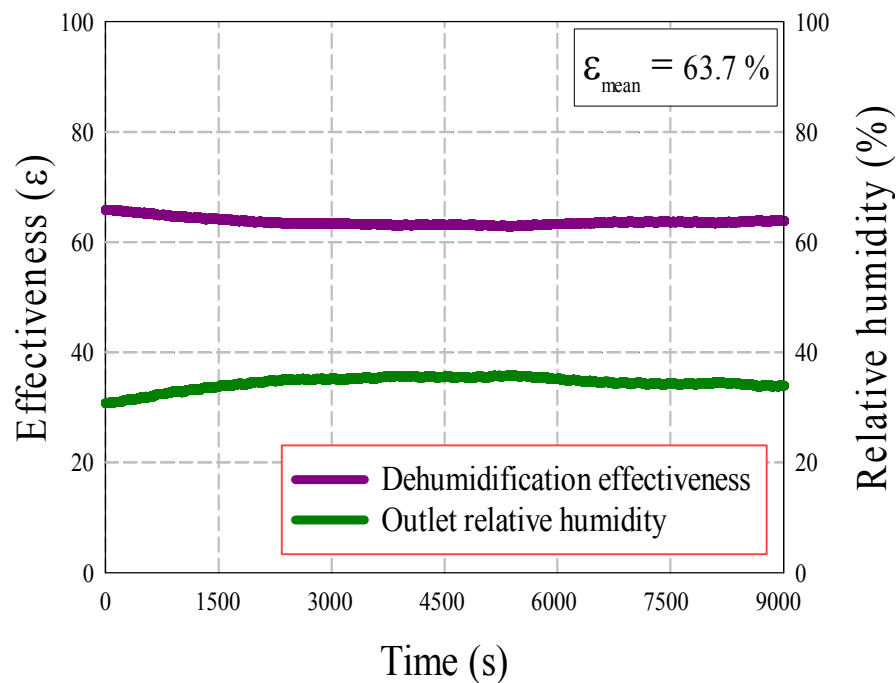


Figure 10.4. Dehumidification effectiveness of the desiccant unit for the air velocity of 0.3 m/s.

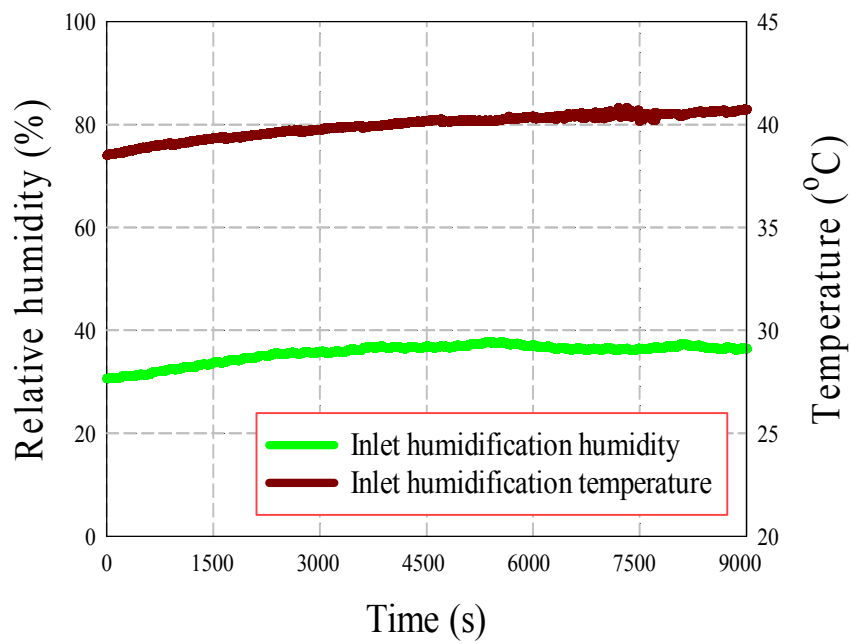


Figure 10.5. Relative humidity and temperature measurement for the air velocity of 0.3 m/s at the inlet of the humidification unit.

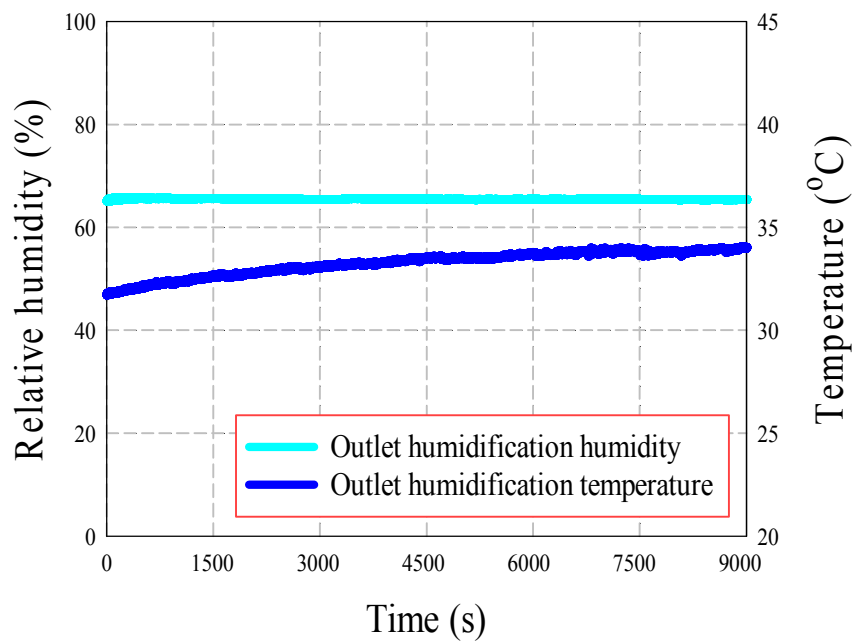


Figure 10.6. Relative humidity and temperature measurement for the air velocity of 0.3 m/s at the outlet of the humidification unit.

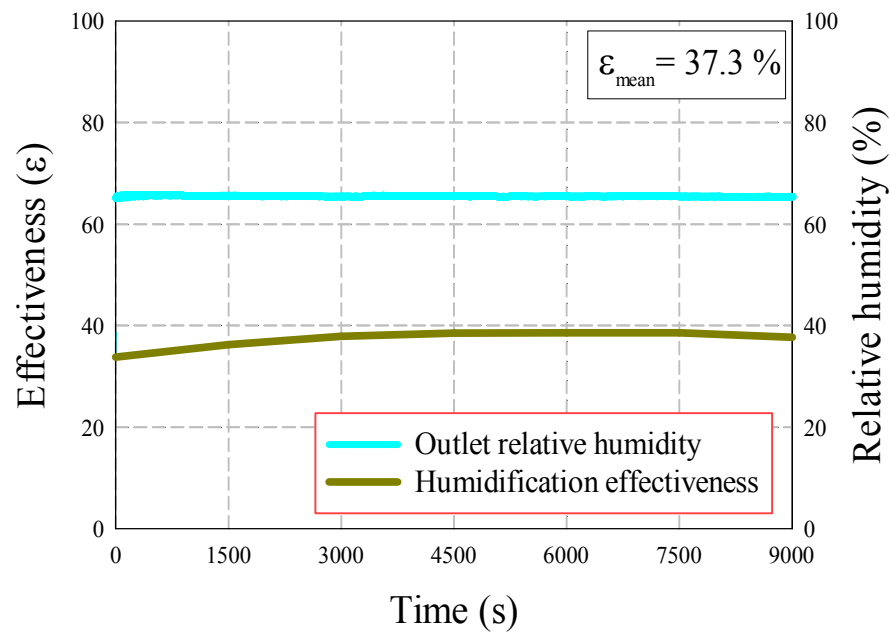


Figure 10.7. Humidification effectiveness of the evaporative cooling unit for the air velocity of 0.3 m/s.

For the case of higher velocity, the average relative humidity before the dehumidification unit is found to be 72.5% and the supply air temperature 38.5 °C as shown in Figure 10.8. In the first section, the outlet relative humidity and temperature values are measured to be 31.9% and 38.9 °C as it is clearly illustrated in Figure 10.9. The dehumidification effectiveness of the system is also calculated and found to be 56.1% as it is given in Figure 10.10. Dehumidification effectiveness is a function of air velocity as it drops from 63.7 to 56.1% when air velocity increases from 0.3 m/s to 0.5 m/s. The inlet humidity and temperature values of the humidification section are found to be similar with the outlet of the dehumidification section as it is depicted in Figure 10.11. The average inlet relative humidity is observed to be 35.6% while the temperature is 40.0 °C at the inlet of humidification unit.

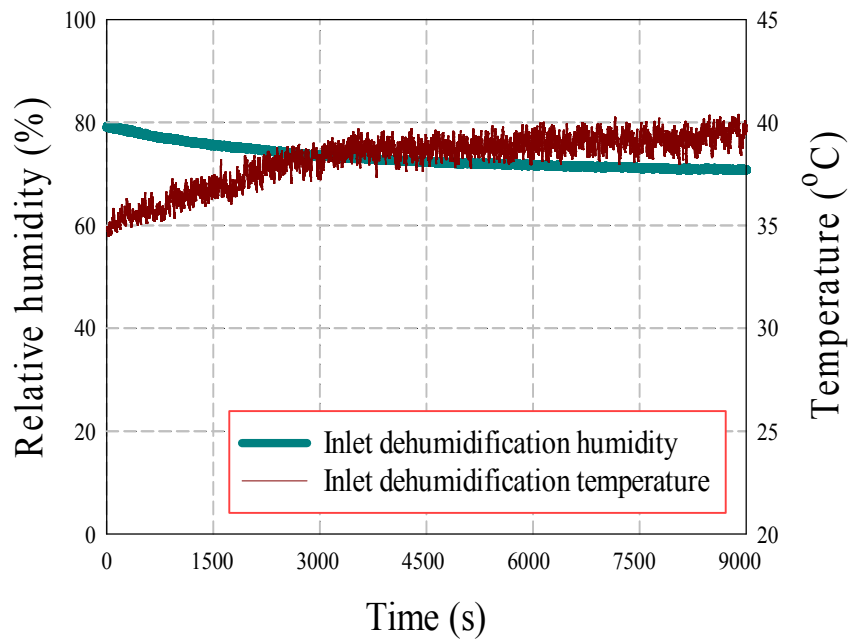


Figure 10.8. Relative humidity and temperature measurement for the air velocity of 0.5 m/s at the inlet of the dehumidification unit.

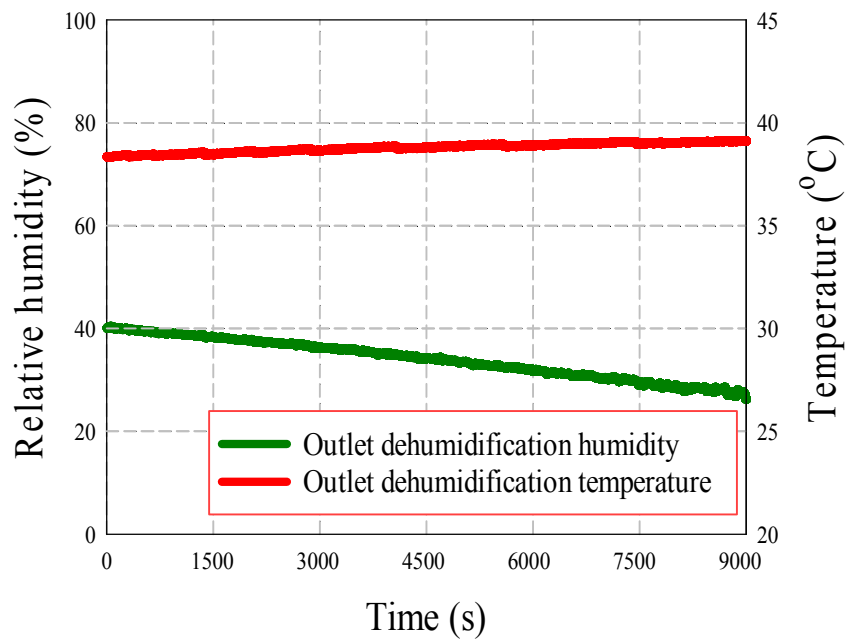


Figure 10.9. Relative humidity and temperature measurement for the air velocity of 0.5 m/s at the outlet of the dehumidification unit.

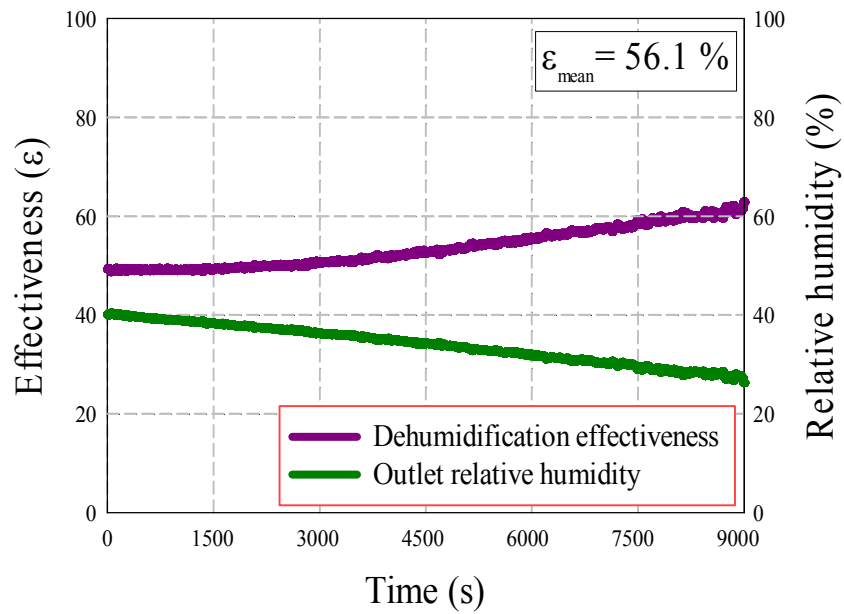


Figure 10.10. Dehumidification effectiveness of the desiccant unit for the air velocity of 0.5 m/s.

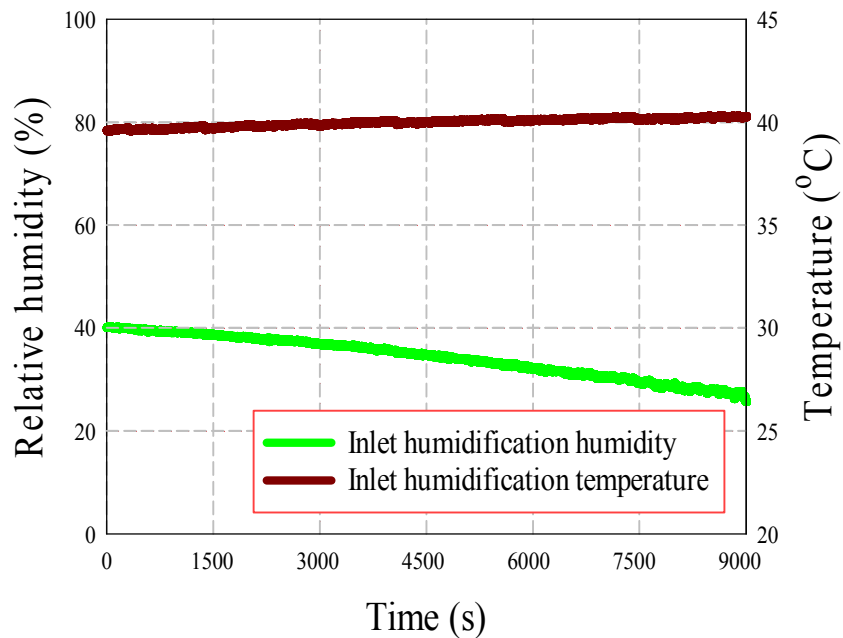


Figure 10.11. Relative humidity and temperature measurement for the air velocity of 0.5 m/s at the inlet of the humidification unit.

After the humidification unit, the average relative humidity and temperature values are determined to be around 63.6% and 34.2 °C, respectively as shown in Figure 10.12. An average temperature reduction of 5.8 °C is achieved as well as a humidification effectiveness of 30.2% as clearly seen in Figure 10.13. It is concluded from the results that the proposed system is a novel, unique and cost-effective innovation to mitigate cooling demand of buildings not only in hot arid but also in temperate humid climates.

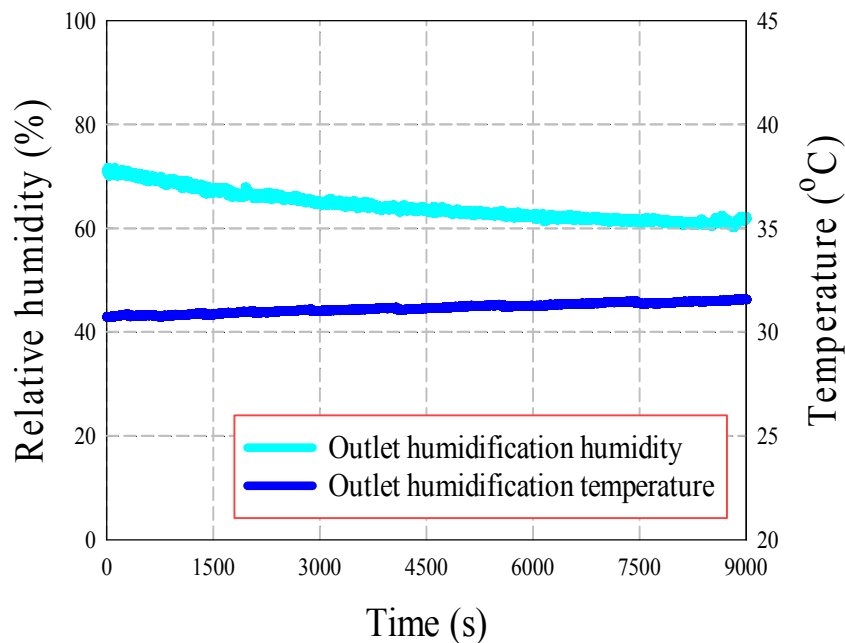


Figure 10.12. Relative humidity and temperature measurement for the air velocity of 0.5 m/s at the outlet of the humidification unit.

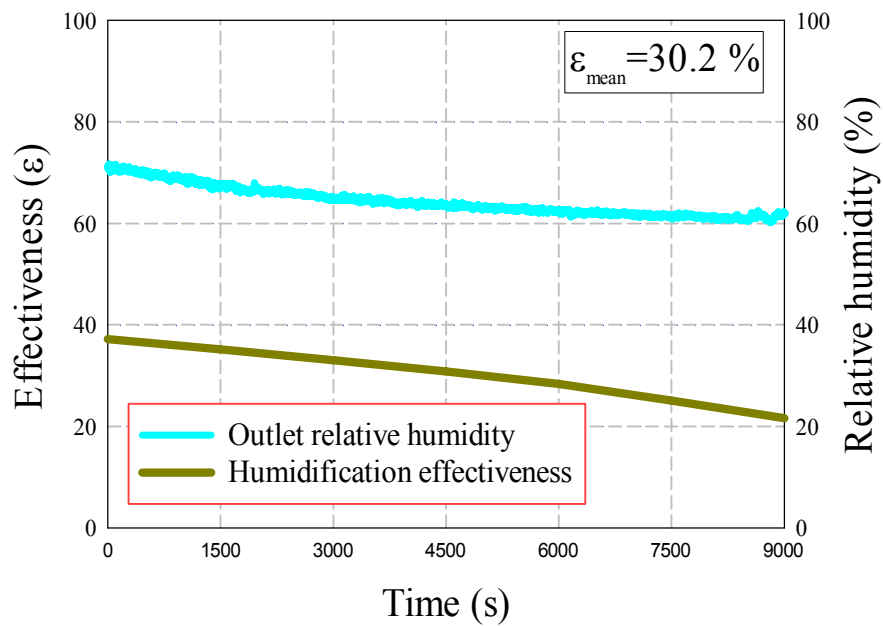


Figure 10.13. Humidification effectiveness of the evaporative cooling unit for the air velocity of 0.5 m/s.

The wet-bulb temperature is the lowest temperature that can be reached under current ambient conditions by the evaporation of water only. On the other hand, the wet bulb temperature equals dry bulb temperature at 100% relative humidity. In this study, wet bulb effectiveness of the evaporative cooling part is also investigated. The wet bulb effectiveness is the ratio of the difference between inlet and outlet air temperature to the difference between inlet air temperature and its wet bulb temperature [213,227] as it is found in equation (10.4). Through the calculation, the average wet bulb effectiveness of the evaporative cooling part is found to be around 50.0% and 42.4% for the first and second cases, respectively as it is clearly illustrated in Figure 10.14. The illustrative results of the experimental study are given in Table 10.1 and Table 10.2.

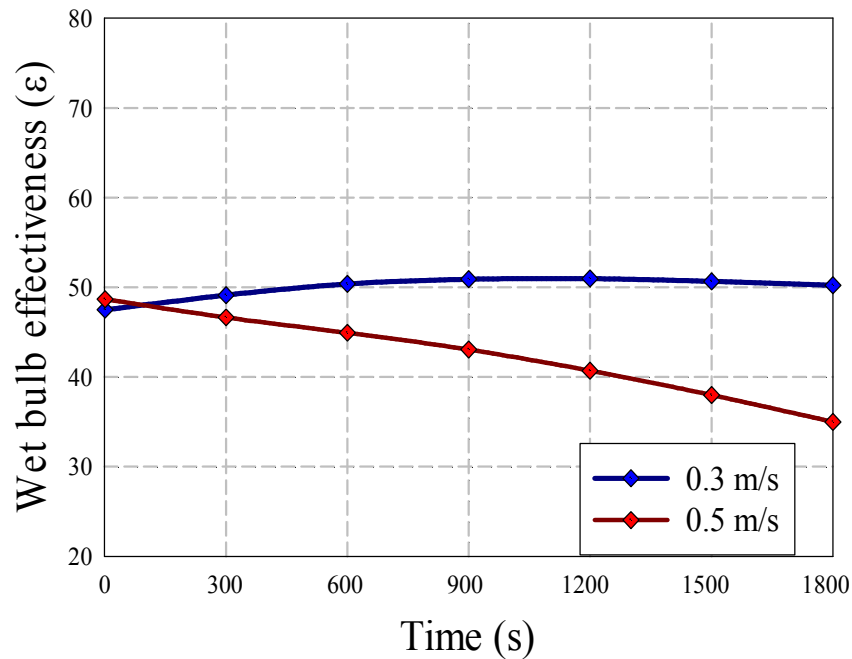


Figure 10.14. Wet bulb effectiveness of the humidification unit for the air velocities of 0.3 and 0.5 m/s.

Table 10.1. Inlet and outlet experimental parameters of the liquid desiccant based evaporative cooling system for the first test

Desiccant Unit			
Inlet parameters	Measurement	Outlet parameters	Measurement
Air velocity (m/s)	0.3	Dry bulb Temperature (°C)	39.9
Mass flow rate (kg/s)	0.0042	Wet bulb temperature (°C)	26.2
Air duct diameter (m)	0.126	Relative humidity (%)	34.4
Dry bulb Temperature (°C)	38.6	Dehumidification effectiveness	0.64
Wet bulb temperature (°C)	37.8	Overall coefficient of performance	5.5
Relative humidity (%)	94.7	Overall temperature decrease (°C)	5.3
Air flow regime	Laminar		
Evaporative Cooling Unit			
Air velocity (m/s)	0.3	Dry bulb Temperature (°C)	33.3
Mass flow rate (kg/s)	0.0042	Wet bulb temperature (°C)	27.7
Air duct diameter (m)	0.126	Relative humidity (%)	65.5
Dry bulb Temperature (°C)	40.0	Humidification effectiveness	0.37
Wet bulb temperature (°C)	26.7	Wet bulb effectiveness	0.50
Relative humidity (%)	35.7	Overall coefficient of performance	5.5
Air flow regime	Laminar	Overall temperature decrease (°C)	5.3
		Temperature decrease by ECS (°C)	6.7

Table 10.2. Inlet and outlet experimental parameters of the liquid desiccant based evaporative cooling system for the second test

Desiccant Unit			
Inlet parameters	Measurement	Outlet parameters	Measurement
Air velocity (m/s)	0.5	Dry bulb Temperature (°C)	38.9
Mass flow rate (kg/s)	0.0070	Wet bulb temperature (°C)	24.8
Air duct diameter (m)	0.126	Relative humidity (%)	31.9
Dry bulb Temperature (°C)	38.5	Dehumidification effectiveness	0.56
Wet bulb temperature (°C)	33.7	Overall coefficient of performance	4.8
Relative humidity (%)	72.5	Overall temperature decrease (°C)	4.3
Air flow regime	Laminar		
Evaporative Cooling Unit			
Air velocity (m/s)	0.5	Dry bulb Temperature (°C)	34.2
Mass flow rate (kg/s)	0.0070	Wet bulb temperature (°C)	28.1
Air duct diameter (m)	0.126	Relative humidity (%)	63.6
Dry bulb Temperature (°C)	39.9	Humidification effectiveness	0.30
Wet bulb temperature (°C)	26.2	Wet bulb effectiveness	0.42
Relative humidity (%)	34.3	Overall coefficient of performance	4.8
Air flow regime	Laminar	Overall temperature decrease (°C)	4.3
		Temperature decrease by ECS (°C)	5.8

10.6. Conclusions

Minimisation of energy consumption levels in all sectors has become significant in the last decades. In the early 21st century, energy consumption levels were specified by sector and the results interestingly indicated that buildings play an important role on global energy consumption. It was reported that the buildings are responsible for more than 30% greenhouse gas emissions in most of the developed countries [17,204,297]. On the other hand, energy consumption levels of buildings increase as a result of economic growth, expansion of building sectors and spread of heating, ventilation and air conditioning (*HVAC*) systems. Buildings have a long life span lasting for 50 years or more and thus, decrease in energy consumption levels of buildings has a notable potential to contribute in mitigating greenhouse gas concentrations for longer periods.

Most of the energy losses in buildings occur in heating, ventilation and air conditioning systems. Therefore, energy-efficient heating, cooling and ventilation technologies may considerably contribute in decreasing energy consumption, and hence carbon abatement. Within the scope of this comprehensive research, a novel energy-efficient cooling system is developed. The proposed system aims to mitigate energy consumption due to cooling as well as providing ventilation via using desiccant-based direct contact evaporative cooling unit. In this research, dehumidification performance of a novel desiccant-based evaporative cooling system is experimentally investigated. For two different values of air velocity, the average temperature and relative humidity of air at the end of the dehumidification process are determined time-dependently. It is concluded from the results that the dehumidification efficiency of the system is highly dependent on the air velocity. For the air velocity of 0.3 m/s , the average outlet relative humidity and air temperature are determined to be 65.5% and $33.3 \text{ }^\circ\text{C}$, respectively where the average inlet relative humidity is 94.7% and the average inlet air temperature is $38.6 \text{ }^\circ\text{C}$. Overall decrease in air temperature is found to be $5.3 \text{ }^\circ\text{C}$ for the whole system. However, the temperature decrease in evaporative cooling part is determined to be $6.7 \text{ }^\circ\text{C}$ which is very remarkable. On the other hand, the dehumidification effectiveness drops from 63.7 to 56.1% when the air velocity increases from 0.3 to 0.5 m/s . The humidification effectiveness of the system is calculated for the two velocity ranges of air. The average values are 37.3 and 30.2 % for the air velocities of 0.3 and 0.5 m/s , respectively. For the air velocities of 0.5 m/s , the overall temperature decrease is $4.3 \text{ }^\circ\text{C}$ whereas it is determined to be $5.8 \text{ }^\circ\text{C}$ for the evaporative cooling unit. In addition to these analyses, the time-dependant *COP* changes of the whole system are also specified with respect to the different air velocities given above. The average *COP* values of the system for the inlet air velocities of 0.3 and 0.5 m/s are determined to be

roughly 5.5 and 4.8, respectively as it is clearly given in Figure 10.15. The results underline that the *COP* of the proposed system is well enough, although the system requires regular regeneration due to the use of liquid desiccant solution. An important reason of achieving high *COP* range is to use renewable based external power input to carry out the regeneration and pumping of the liquids. The system is only tested in laboratory conditions. In this respect, it is expected to have higher *COP* range for the whole scale applications due to the longer time of thermal contact between air and the liquids.

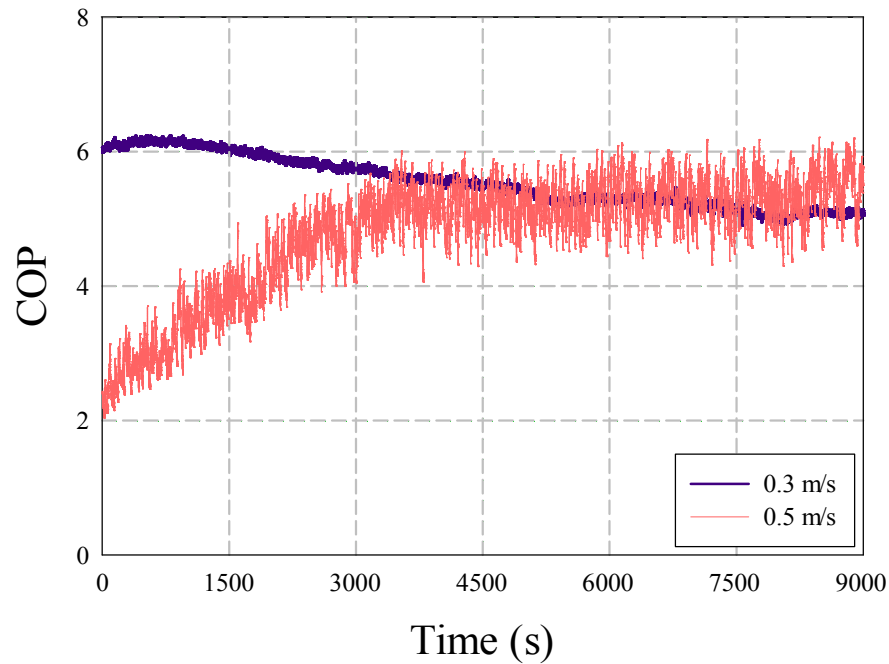


Figure 10.15. Time-dependant coefficient of performance values for the inlet air velocities of 0.3 *m/s* and 0.5 *m/s*.

This experimental study shows that the novel desiccant-based evaporative cooling system might have a notably high dehumidification efficiency range through the optimisation of the operational parameters mainly air velocity. In this system, liquid potassium formate solution (74%) is used owing to its thermophysical properties such

as less corrosive effect, lower density and lower viscosity. It also provides environmentally friendly applications with a cheapest way compared to the alternatives. The proposed innovation is found to be an energy-efficient, cost-effective and environmentally friendly way to mitigate the energy consumption and carbon emissions.

CHAPTER 11

Theoretical investigation of a novel heating system for low-carbon buildings: Moist airflow system

- 11.1. Introduction
- 11.2. Description of MAS
- 11.3. Thermodynamic Model
- 11.4. Heat Transfer Analysis
- 11.5. Duct Diameter Analysis
- 11.6. Results and Discussion
- 11.7. Conclusions

CHAPTER 11

Theoretical investigation of a novel heating system for low-carbon buildings: Moist airflow system

11.1. Introduction

Buildings are the most significant energy consuming sector worldwide [298]. Growing trend on industrialisation and urbanisation in recent years has dramatically increased the energy consumption of the building sector [299]. Predictions of future scenarios underline that the rising energy needs of the population cause a significant amount of contribution to the global energy consumption. The building sector is currently responsible for about 40% of the total energy consumption [297] which constitutes 30% of the annual greenhouse gas emissions [300]. That much of energy consumption of the buildings is directly associated with the building design and construction [16]. The role of buildings in total world energy consumption is somewhat noticeable as a consequence of poor building fabric technologies [294,295,301]. In this respect, airtightness of the buildings is becoming more significant due to its effects on building energy consumption and indoor air quality [302]. Buildings use energy for heating, cooling, lighting and electrical equipment. In Europe, most of the energy consumed in building sector is for space heating requirement [303,304]. Heating demand of buildings still has an increasing trend due to increasing world population, rising comfort levels and technological developments [297]. To be able to fulfil the requirements of low carbon targets, development of the novel energy-efficient heating

systems are of vital importance. In recent years, systems with better features of materials and thermal properties have decreased or stabilised the amount of energy required for space heating [305]. However, current conventional heating systems for buildings are mainly based on heating a working fluid, which is commonly water, cause high first investment and operational cost because of the complex heat distribution elements and remarkable high specific heat capacity of water. Moreover, pumping is not insignificant in such systems as well as notable maintenance cost. Therefore, the proper selection of the working fluid is important and can contribute in reducing the heating demand of buildings in a cost-effective way. Air has remarkably lower specific heat capacity than other working fluids such as water or oil based fluids. Owing to this characteristic feature of air, higher temperature differences are possible to achieve with limited energy input. Within the scope of this research, an air based novel heating system is presented through the aforesaid feature of air.

11.2. Description of Moist Airflow System

The moist airflow system (*MAS*) is basically a cost effective heat distribution system using air as the working fluid. The driving force of the *MAS* is the utilisation of waste heat from different sources such as industrial power plants, and transportation of this energy into the buildings in an efficient way to mitigate the heating demand of buildings. The system can also be operated via renewable energy technologies such as solar thermal collectors, hybrid photovoltaic thermal cogeneration systems and geothermal power. An illustrative schematic of the system is given in [Figure 11.1](#). The novel idea of the *MAS* can be attributed to the utilisation of the air instead of water as the working fluid. In this respect, the energy stored in water by the waste heat sources or renewables is transferred into the air to be utilised in heating a space. In case of the

MAS is powered by renewables, water is collected from the grid and is directed to the solar thermal collector. The water increased in terms of thermal energy content is directed to a hot water tank to store the energy in an insulating medium. The water temperature inside the hot water tank varies from 30 °C to 90 °C, and can be controlled via a temperature control unit depending on solar power available. Following this, as a consequence of the natural evaporation process, hot moist-air is obtained in the upper part of the tank to be used in space heating. Hot moist-air is circulated by a fan through the insulated ducts to dissipate its energy into the cold environment. In the process, moist-air is assumed to be in adiabatic saturation state. Moist-air condensed as passing through the cold environment as a result of losing its thermal energy content. Condensed water from moist-air is collected in a condensation tank and pumped into the storage tank via a small condensation tank as clearly shown in [Figure 11.1](#). The cycle continues to operate as long as the power from renewables is provided. Working principle of the moist airflow system is illustrated in [Figure 11.2](#).

11.3. Thermodynamic Model

In this section, a thermodynamic model of the moist airflow system is introduced. For each separate part of the system, the first law of thermodynamics is performed. Through the principle of the conservation of energy, energy balance is carried out for both air and water in the system. If adiabatic boundary conditions are considered throughout the system, thermal energy stored in water can be given by:

$$\dot{E}_{in} = \dot{E}_{out} \quad (11.1)$$

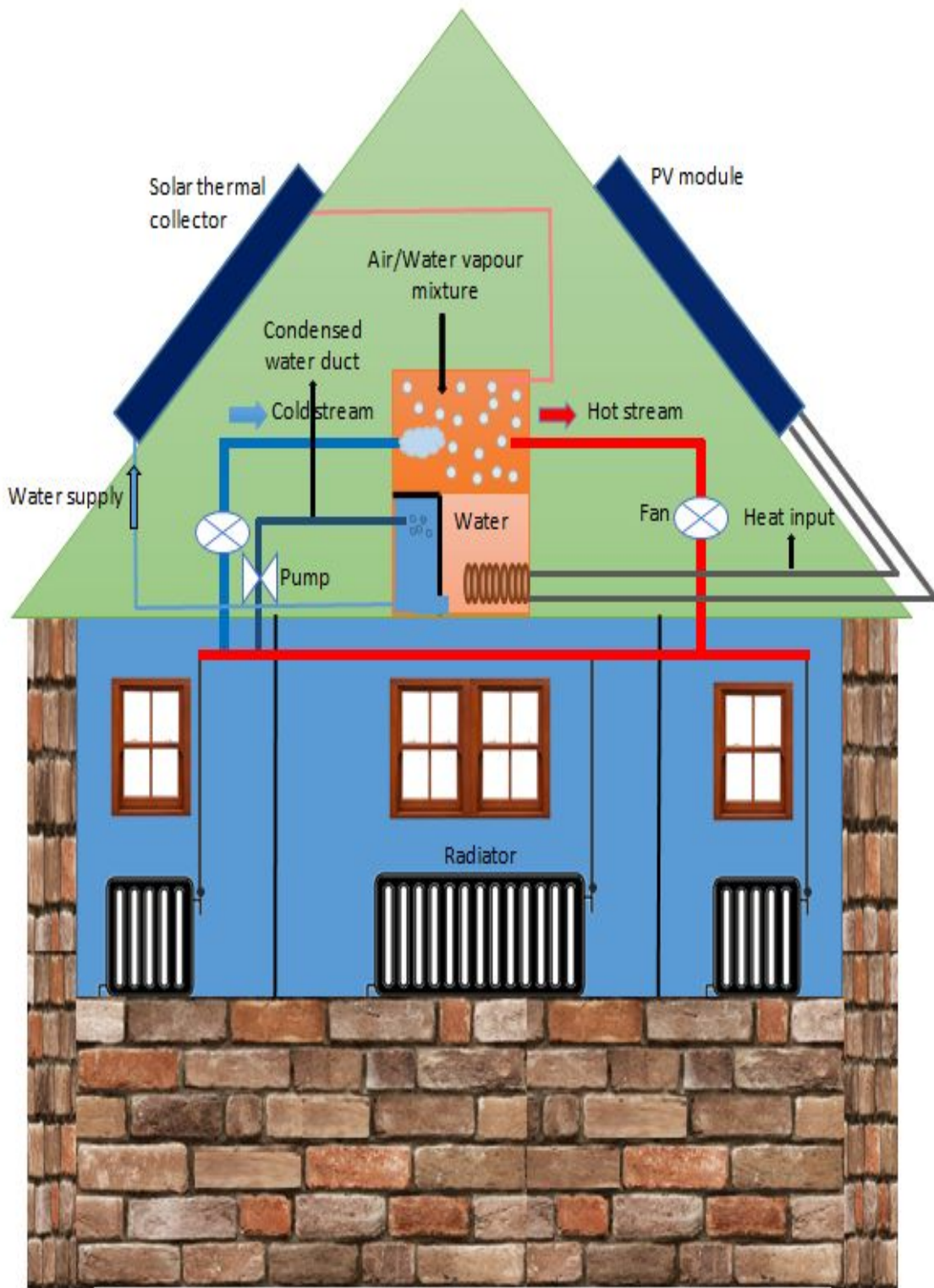


Figure 11.1. Schematic of the proposed moist airflow system.

where \dot{E}_{in} and \dot{E}_{out} correspond to incoming energy from solar thermal collectors and energy stored in water, respectively. Incoming solar energy can be expressed by:

$$\dot{E}_{in} = \alpha GA \quad (11.2)$$

where α is the absorptivity coefficient, G is the solar intensity and A is the surface area of the thermal collectors. Since the thermal energy stored in water yields to temperature increase, sensible thermal energy storage occurs as follows:

$$E_{out} = mc\Delta T \quad (11.3)$$

where m is the mass of water, c is the specific heat capacity of water and ΔT is the temperature difference between initial and final stages. Thermal energy stored in water accelerates the evaporation inside water tank resulting to moist-air in the upper part of the tank as shown in Figure 11.3.

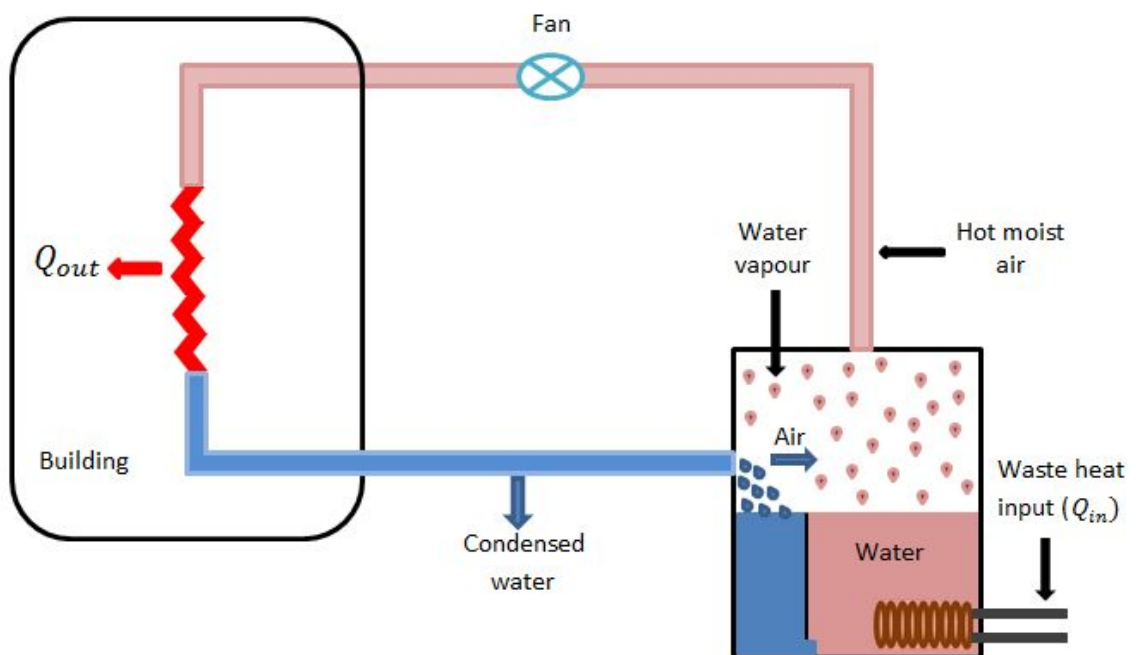


Figure 11.2. Working principle of the moist airflow system.

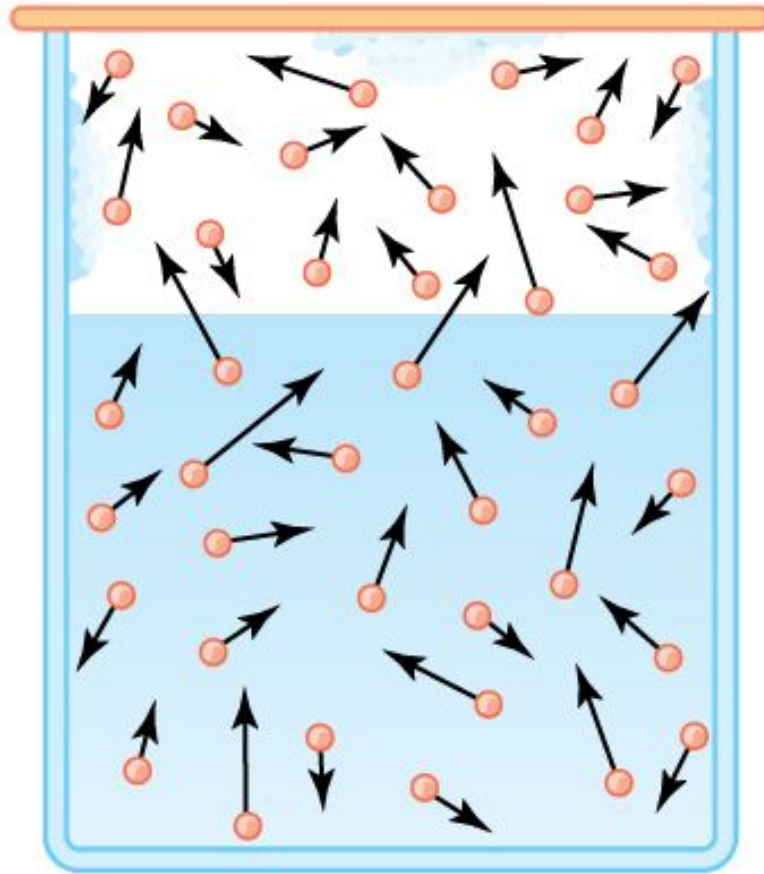


Figure 11.3. Evaporation process and generation of moist-air in water tank.

The evaporation process plays a key role in thermal performance assessment of the moist airflow system. Therefore the enthalpy of evaporation is a significant parameter which needs to be considered in the modelling. The enthalpy of evaporation is basically the quantity of heat which needs to be absorbed if a particular amount of liquid is evaporated at any constant temperature. In thermodynamics, the enthalpy of evaporation is calculated as follows:

$$\Delta H_{evap} = H_{vapour} - H_{liquid} \quad (11.4)$$

where H_{vapour} is the enthalpy of the saturated vapour and H_{liquid} is the enthalpy of the saturated liquid. The enthalpy of evaporation is a function of temperature. For instance, the ΔH_{evap} of water at 90 °C is 2282.5 kJ/kg. Following the evaporation process,

adiabatic saturation condition is achieved which corresponds to a specific point in psychrometric chart where dry and wet bulb temperatures overlap. The saturated air at high temperature is directed to the cold environment so to dissipate its energy content, and this energy exchange is given by the enthalpy exchange of the working air as follows:

$$E_{tec} = H_{air|is} - H_{air|fs} \quad (11.5)$$

where E_{tec} is the thermal energy content of working air, $H_{air|is}$ is the enthalpy of working air at initial state, and $H_{air|fs}$ is the enthalpy of working air at final state. The aforementioned energy exchange can easily be demonstrated as shown in Figure 11.4.

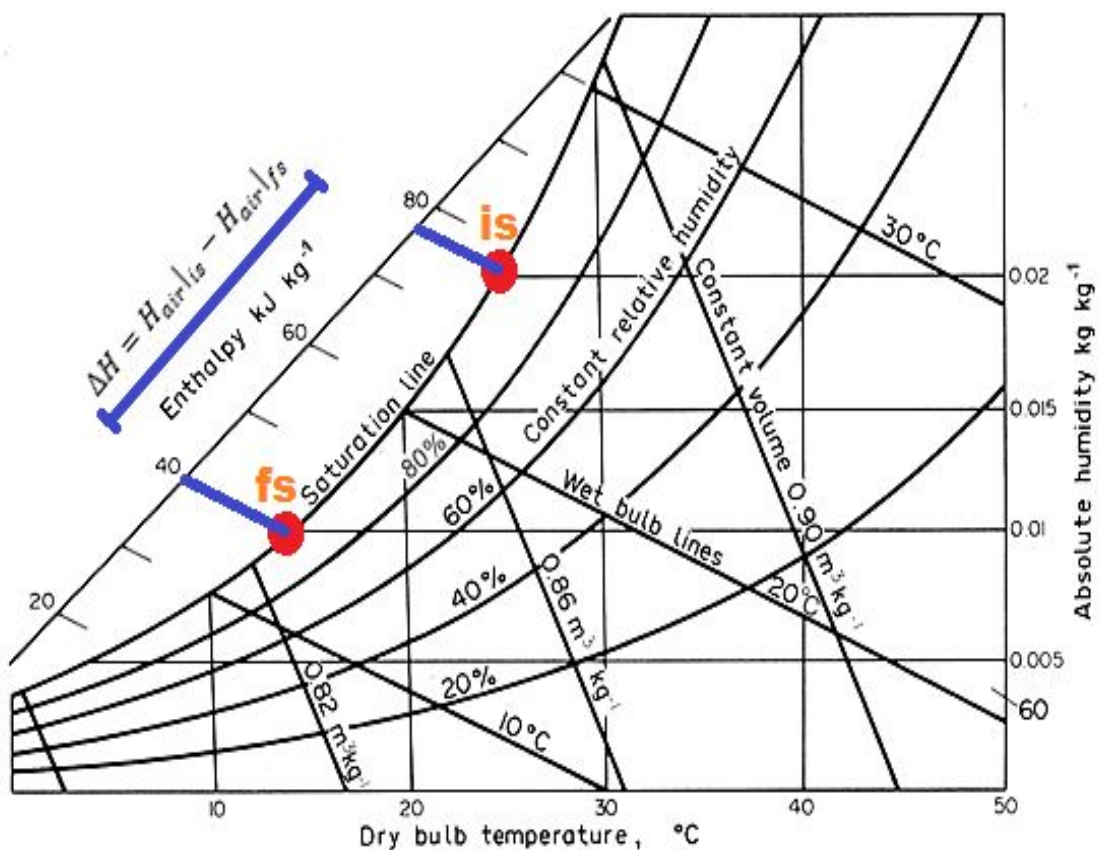


Figure 11.4. Enthalpy exchange of working air in psychrometric chart.

11.4. Heat Transfer Analysis

In this section, heat transfer analysis of *MAS* is introduced. For the aforementioned moist airflow system, a circular tube is used to get the maximum heat transfer with the least pressure drop. The duct diameter of the system is calculated as using the governing equations. The flow arrangement in the duct is assumed to be a turbulent flow due to high Reynolds number which is found to be more than 2500. The Reynolds number can be given by:

$$Re = \frac{vD_h}{\dot{\nu}} \quad (11.6)$$

where Re is the Reynolds number, v is the velocity of air, D_h is hydraulic diameter and $\dot{\nu}$ is the kinematic viscosity of air at a certain temperature. Nusselt number can be expressed by the following equation:

$$Nu = \frac{hD_h}{k} \quad (11.7)$$

where Nu is the Nusselt number, h is the heat convection coefficient and k is the thermal conductivity.

Since most practical applications involve pipes with $L/D \gg 10$, turbulent flows can almost always be considered fully developed [306,307]. Thus, the Nusselt number can be expressed by Dittus-Boelter Correlation as follows:

$$Nu = 0.023Re^{0.8}Pr^n \quad (11.8)$$

where L is the length of the duct, D is the diameter of the duct, Pr is the Prandtl number and n is the constant. Here, n equals 0.4 for heating of the fluid whereas it is 0.3 for cooling of the fluid.

From Newton's law of cooling, the rate of heat transfer to or from a fluid flowing in a circular pipe can be expressed as:

$$Q = hA\Delta T \quad (11.9)$$

where Q is the heat transfer rate, h is the heat convection coefficient, A is the heat transfer surface area and ΔT is the temperature difference of air.

The mean temperature of air is calculated to be average of the inlet and outlet temperatures of air as given in following equation:

$$T_{mean} = \frac{T_{in} + T_{out}}{2} \quad (11.10)$$

where T_{mean} is the average temperature of air and, T_{in} and T_{out} correspond to inlet and outlet temperatures of the air, respectively.

The power output of the *MAS* system at a certain temperature exchange can be found as follows:

$$P_w = \frac{\Delta H}{t} \quad (11.11)$$

where P_w is the power output of the system, ΔH is the enthalpy exchange and t is the heat exchange time of the system. A heat transfer surface area of the *MAS* for a circular tube is shown in [Figure 11.5](#).

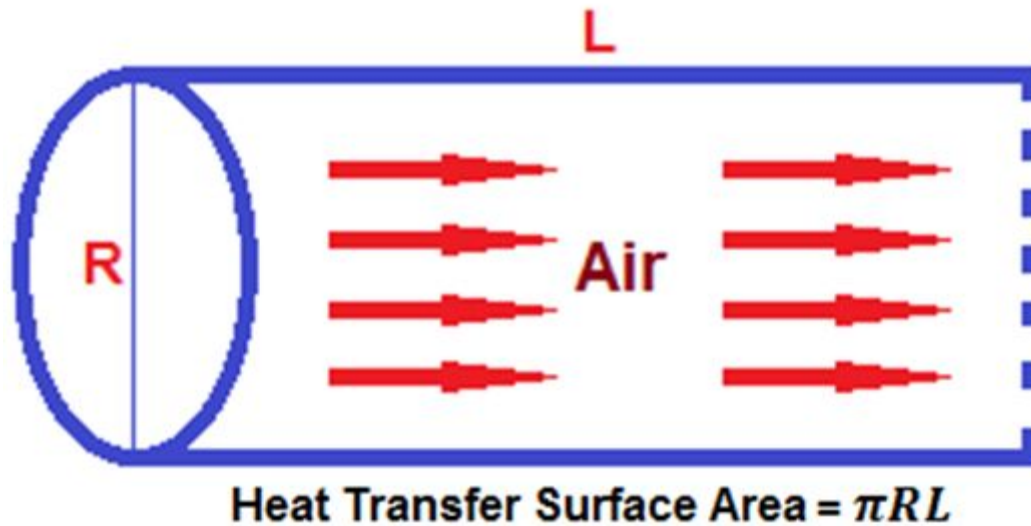


Figure 11.5. Heat transfer surface area in a circular tube.

11.5. Duct Diameter Analysis for Constant Energy Input

In this part of the research, duct diameter analysis of air, moist-air and water based heating system is done for constant energy input and per meter channel length. In this respect, the principle of energy conservation is performed to an internal flow heat transfer problem. The constant heat input to the system is taken to be 1 kW . The figure of 1 kW characterises a particular scale for performance optimisation and the heat input can be scaled depending on the demand. Duct diameter analysis is carried out per meter length of duct to be able to make this parameter independent from the variation of other relevant parameters such as temperature difference. According to the first law of thermodynamics, energy balance for each system can be given by:

$$\dot{E}_{in} = \dot{E}_{out} \quad (11.12)$$

where \dot{E}_{in} and \dot{E}_{out} represent energy input and energy output of the proposed system, respectively. \dot{E}_{in} is assumed to be 1 kW as mentioned before. \dot{E}_{out} is the energy

absorbed by the working fluid, and demonstrates itself as temperature increment of the working fluid. Hence, \dot{E}_{out} can be expressed by:

$$\dot{E}_{out} = \dot{m}_{wf} c_{wf} \Delta T \quad (11.13)$$

where \dot{m}_{wf} is the mass flow rate of working fluid, c_{wf} is the specific heat capacity of working fluid and ΔT is the temperature difference of working fluid at inlet and outlet.

In another word, \dot{E}_{out} corresponds to the enthalpy change of working fluid at initial and final state as given below:

$$\dot{E}_{out} = \dot{m}_{wf} \Delta \dot{h} \quad (11.14)$$

where $\Delta \dot{h}$ is the enthalpy change. \dot{m}_{wf} is a dominant parameter on the energy that working fluid receives and given by:

$$\dot{m}_{wf} = \rho_{wf} v_{wf} A \quad (11.15)$$

where ρ_{wf} is the density of working fluid, v_{wf} is the velocity of working fluid and A is the cross-sectional area of the duct. A can be expressed in terms of duct diameter as follows:

$$A = \pi \frac{D^2}{4} \quad (11.16)$$

where D is the duct diameter. Specific heat capacity and density of the working fluid are characteristic properties and dependent on the temperature. For an accurate and reliable analysis, their values need to be taken at mean temperature which is given as follows:

$$T_{mean} = \frac{T_{wf,in} + T_{wf,out}}{2} \quad (11.17)$$

where T_{mean} is the mean temperature where fluid properties are taken, $T_{wf,in}$ is the working fluid temperature at initial state and $T_{wf,out}$ is the working fluid temperature at the outlet. Through the aforesaid parameters and equations, \dot{E}_{out} can be given by:

$$\dot{E}_{out} = \rho_{wf} v_{wf} c_{wf} \Delta T \pi \frac{D^2}{4} \quad (11.18)$$

For three different working fluid options, which are mainly air, moist-air and water, the duct diameter is determined for unit duct length and the results are compared for different temperature difference of working fluid at inlet and outlet.

In the duct diameter of moist-air, specific heat capacity needs to be determined as taking the humidity ratio inside air into consideration. In this respect, following equation can be utilised for determination of specific heat capacity of moist-air at any mean temperature:

$$c_{ma} = 1.005 + 1.82\omega \quad (11.19)$$

where c_{ma} is the specific heat capacity of moist-air and ω is the humidity ratio of moist-air at a certain mean temperature. In the analyses, the velocity of each working fluid is assumed to be 0.5 m/s for a reliable assessment.

11.6. Results and Discussion

In this part of the research, keys results are given regarding the thermodynamic optimisation, heat transfer analysis and duct diameter analysis of moist airflow system, respectively. The details are interpreted in separate headings as it is shown below.

11.6.1. Results from thermodynamic optimisation

The theoretical investigation of the moist airflow system is performed under some assumptions for both water and air utilised in the system. Firstly, thermal energy input to the water is considered for unit mass of water. In this respect, initial state for the water temperature is assumed to be 15 °C, which is the average water temperature from the grid. The final state for the water temperature is considered to be an independent parameter and varied from 30 to 90 °C as it is shown in [Table 11.1](#) depending on the solar power available. For the unit mass of water, the amount of energy required to increase the water temperature to the different levels illustrated is shown in [Figure 11.6](#). To be able to obtain a totally saturated moist-air, the amount of energy required is determined by adding the enthalpy of evaporation of water to the waste heat required given in [Table 11.1](#). Final energy required for the working air in the moist airflow system can be given as illustrated in [Figure 11.7](#).

[Table 11.1](#). Initial and final water temperatures considered for the MAS

INITIAL WATER TEEMPERATURE (°C)	FINAL WATER TEEMPERATURE (°C)	MASS OF WATER (kg)	WASTE HEAT REQUIRED (kJ)
15	30	1.00	62.7
15	35	1.00	83.6
15	40	1.00	104.5
15	45	1.00	125.4
15	50	1.00	146.3
15	55	1.00	167.2
15	60	1.00	188.1
15	65	1.00	209.0
15	70	1.00	229.9
15	75	1.00	250.8
15	80	1.00	271.7
15	85	1.00	292.6
15	90	1.00	313.5

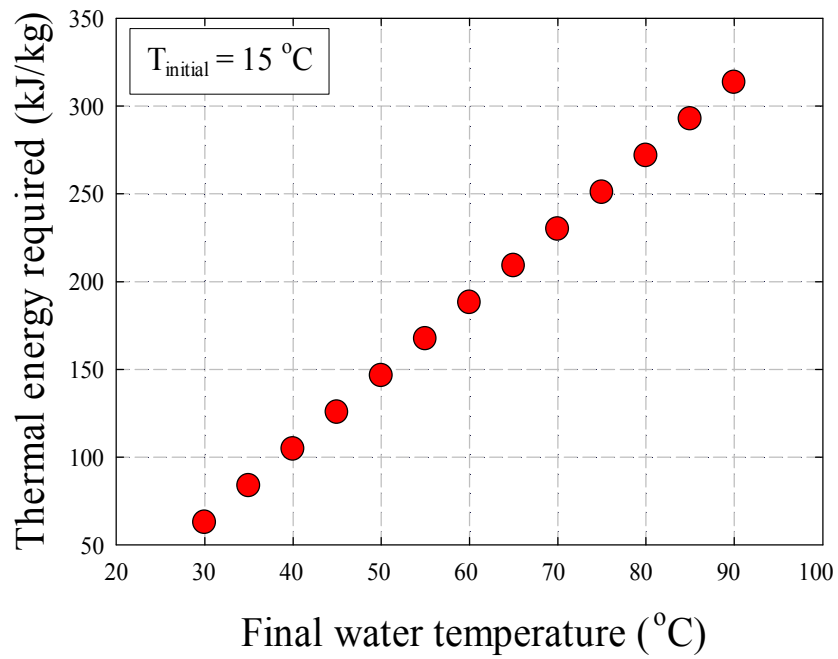


Figure 11.6. Thermal energy required for the water in the tank.

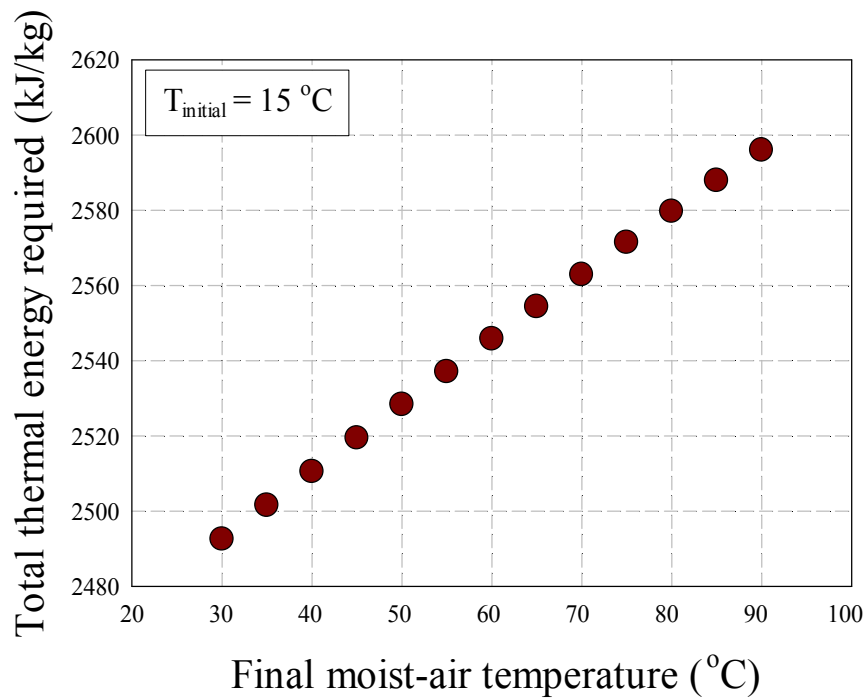


Figure 11.7. Final thermal energy required for the moist-air.

As adiabatically saturated moist-air passes through the cold environment, its thermal energy content decreases as a consequence of heat transfer between the hot stream and the cold medium. The amount of energy transfer can be given by the enthalpy exchange of working air for the temperatures of initial and final state. The enthalpy exchange can easily be determined through psychrometric chart. For different temperature values of the hot moist-air at initial state, the values of enthalpy exchange are shown in [Table 11.2](#).

Thermal performance assessment of the moist airflow system is also carried out for the different values of fan power and operation time. In this respect, fan power is varied from 25 to 100 W, whereas the operation time is changed from 3 to 9 hours per day. To be able to cover a wide range of climatic conditions, the aforesaid operational parameters are considered in the study. In addition to those independent variables, final water temperature is also investigated as an effective parameter on the coefficient of performance of the MAS.

Table 11.2. Enthalpy exchange of air for different initial conditions

DRY-BULB TEEMPERATURE (⁰C)	RELATIVE HUMIDITY (%)	INTIAL ENTHALPY (kJ/kg)	FINAL ENTHALPY (kJ/kg)	ENTHALPY CHANGE (kJ/kg)
30	100	99.7	76.30	23.4
35	100	129.0	76.30	52.7
40	100	166.0	76.30	89.7
45	100	213.2	76.30	136.9
50	100	274.0	76.30	197.7
55	100	353.2	76.30	276.9
60	100	458.1	76.30	381.8
65	100	599.9	76.30	523.6
70	100	797.4	76.30	721.1
75	100	1084.2	76.30	1007.9
80	100	1527.4	76.30	1451.1
85	100	2283.7	76.30	2207.4
90	100	3823.4	76.30	3747.1

The analyses are repeated for both cases of with and without renewable energy generation. In the case of renewable energy generation, the moist airflow system is assumed to be integrated with a solar thermal collector and PV panel. On the other hand, the system is considered as receiving the energy required from the grid completely for the case of without renewable energy generation. The results obtained for each case are illustrated in Figure 11.8-11.15. If the system is integrated with a renewable based energy source, the COP varies from 0.007 to 13.878, depending on the fan power, working hour and final water temperature. On the other hand, the COP is determined to be between 0.004 and 1.307. It is concluded from the results that the COP of the MAS is highly dependent on the operational parameters which are mainly under the influence of climatic conditions. The temperate climates, which correspond to minimum fan power and minimum working time, result with higher values of the COP for each case as expected. However, the system is found to be impractical is there is no renewable energy generation or waste heat recovery.

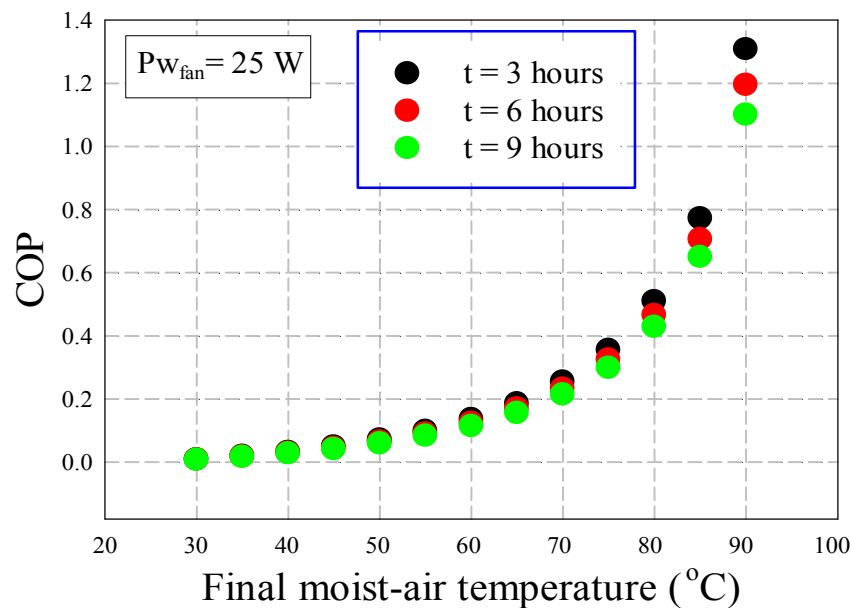


Figure 11.8. Coefficient of performance values for different working hours of MAS with a fan power of 25 W .

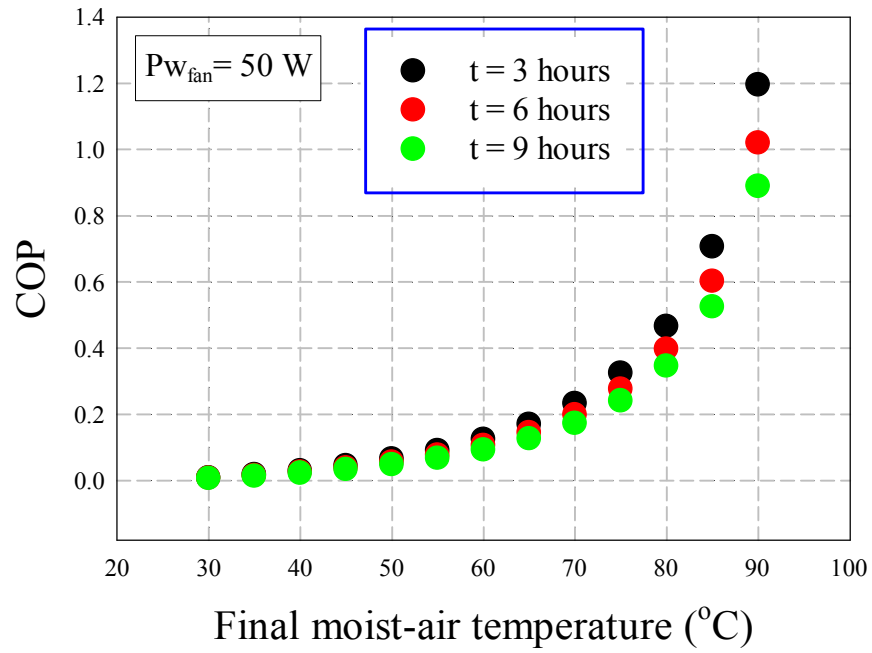


Figure 11.9. Coefficient of performance values for different working hours of MAS with a fan power of 50 W.

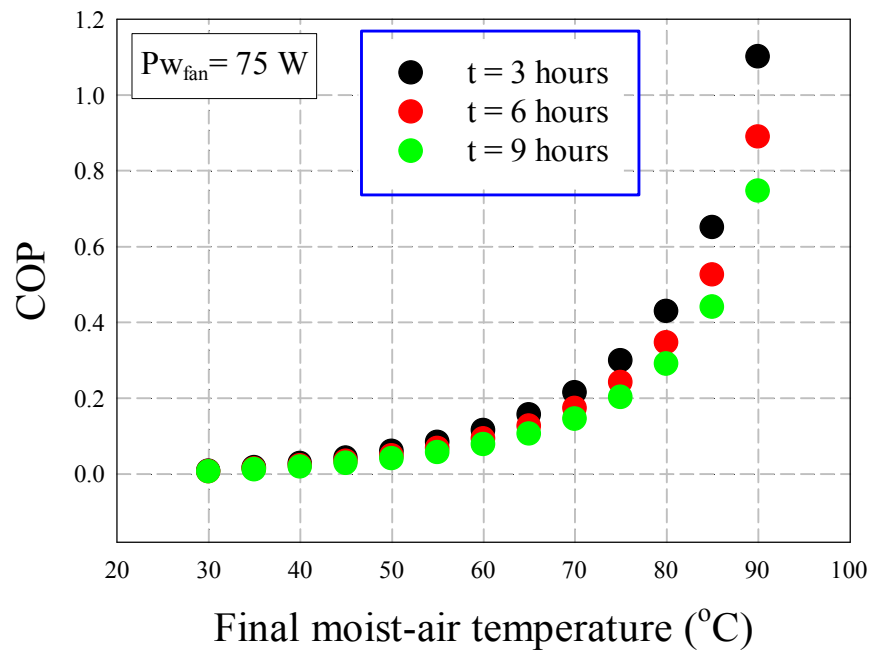


Figure 11.10. Coefficient of performance values for different working hours of MAS with a fan power of 75 W.

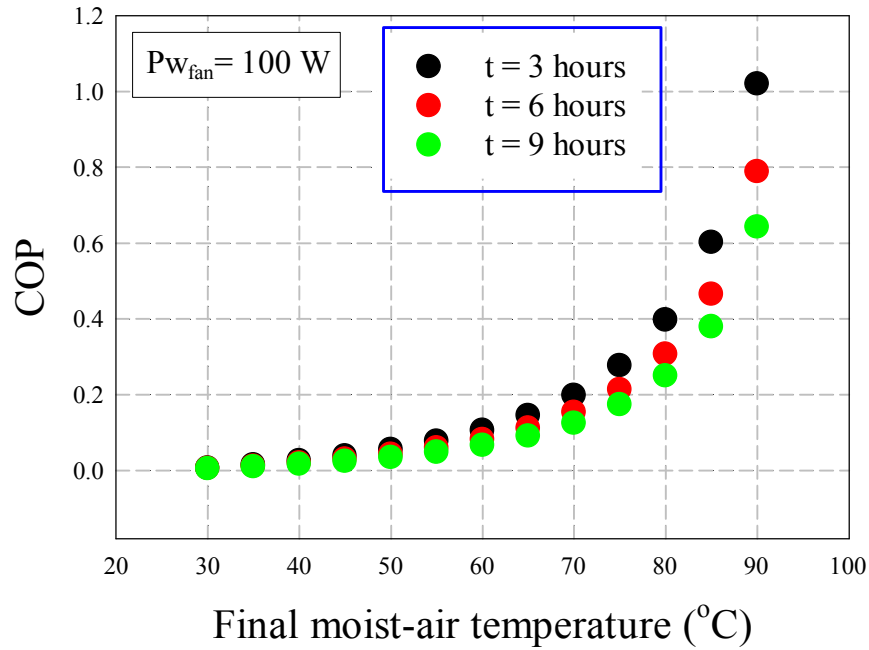


Figure 11.11. Coefficient of performance values for different working hours of MAS with a fan power of 100 W.

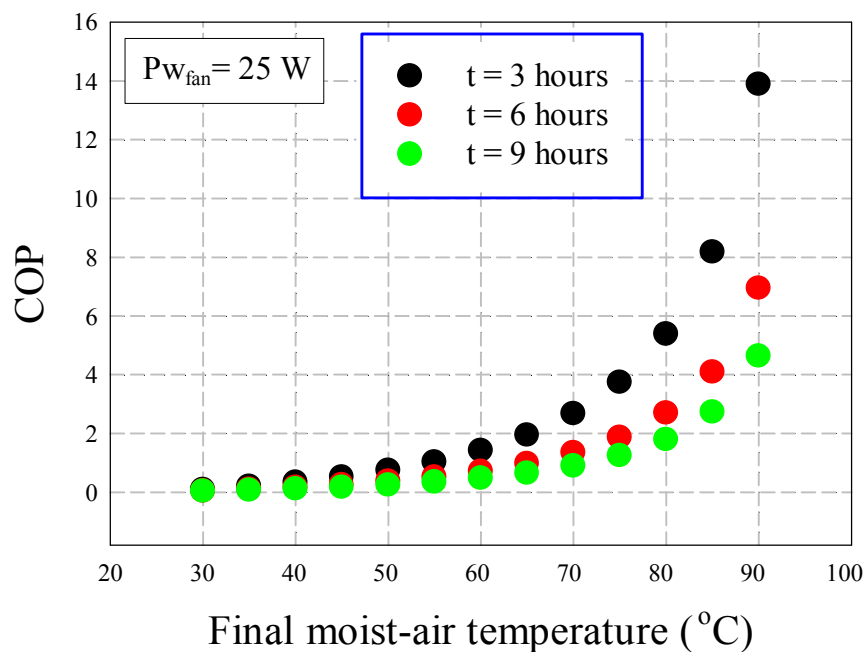


Figure 11.12. Coefficient of performance values for different working hours of MAS integrated with solar power with a fan power of 25 W.

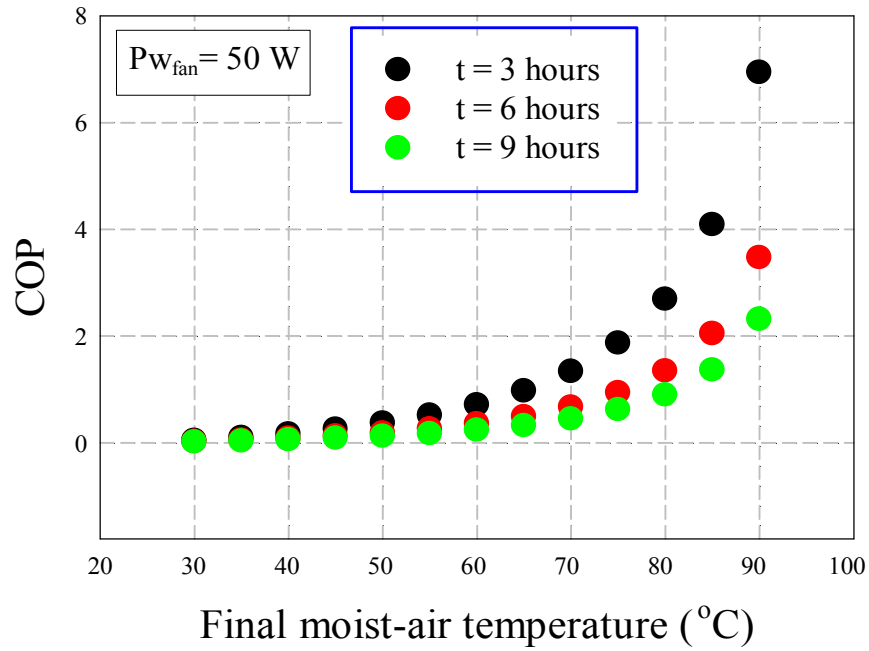


Figure 11.13. Coefficient of performance values for different working hours of MAS integrated with solar power with a fan power of 50 W.

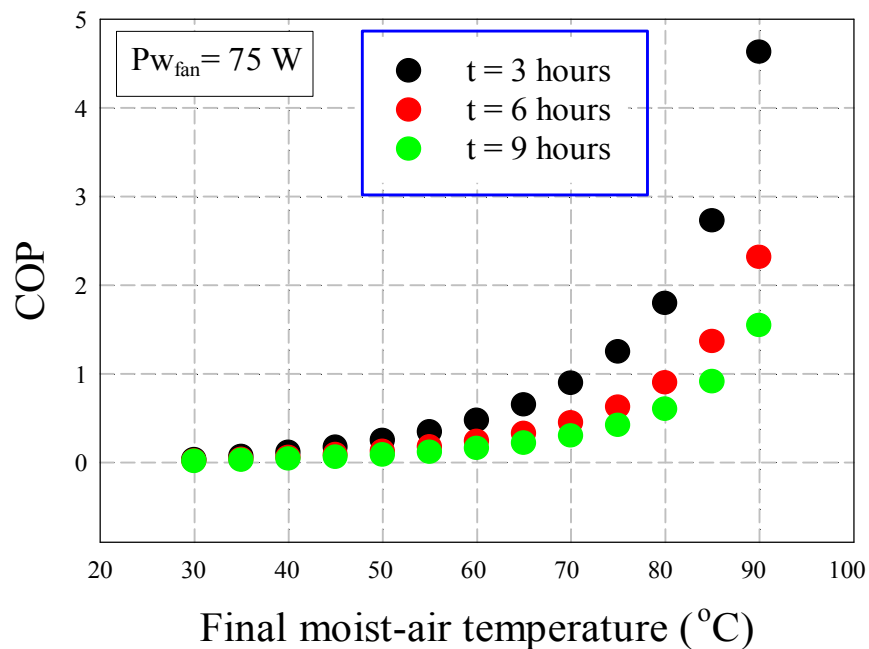


Figure 11.14. Coefficient of performance values for different working hours of MAS integrated with solar power with a fan power of 75 W.

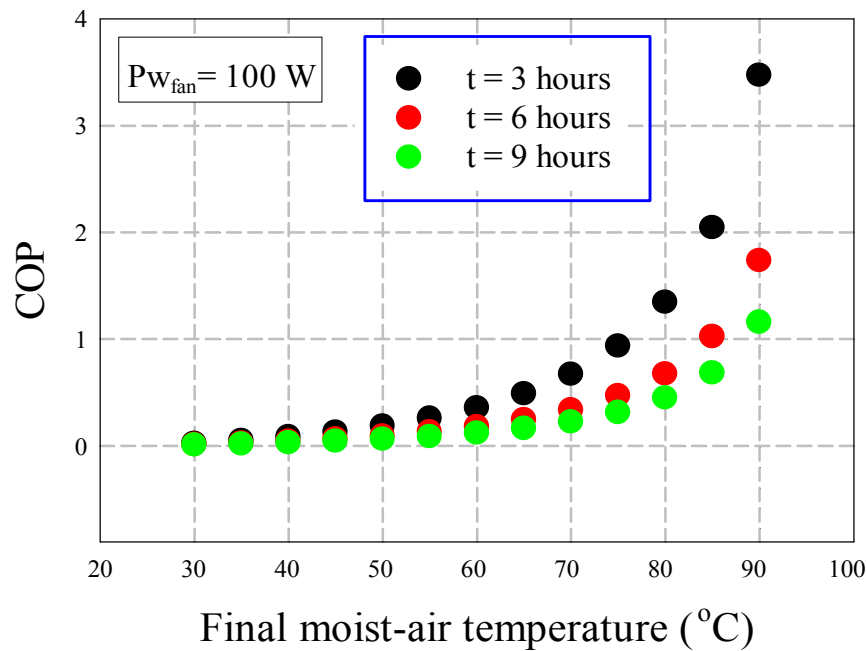


Figure 11.15. Coefficient of performance values for different working hours of MAS integrated with solar power with a fan power of 100 W.

11.6.2. Results from heat transfer analysis

In the second part of the research, a comprehensive heat transfer analysis is carried out to determine the duct diameter for different values of duct length and operation time. In this respect, the duct length is varied from 40 to 70 m and the operation time 1, 1.5 and 2 hours as independent parameters in the analysis. The value of duct diameter is calculated for each case and the results are interpreted for an easier understanding. Duct diameter is found to be a strong function of both final moist-air temperature and duct length as it is seen in Figure 11.16-11.19. An exponential increase of duct diameter with increasing final moist-air temperature is observed for each case. Longer operation times result to smaller duct diameters which is expected from heat transfer phenomenon.

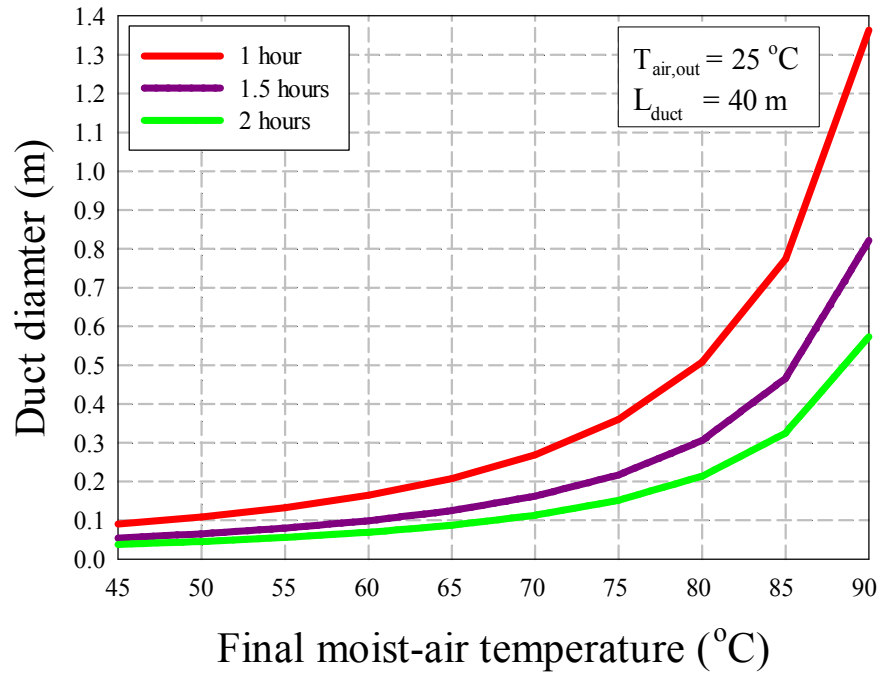


Figure 11.16. Variation of duct diameter with the operation time for the duct length of 40 metres.

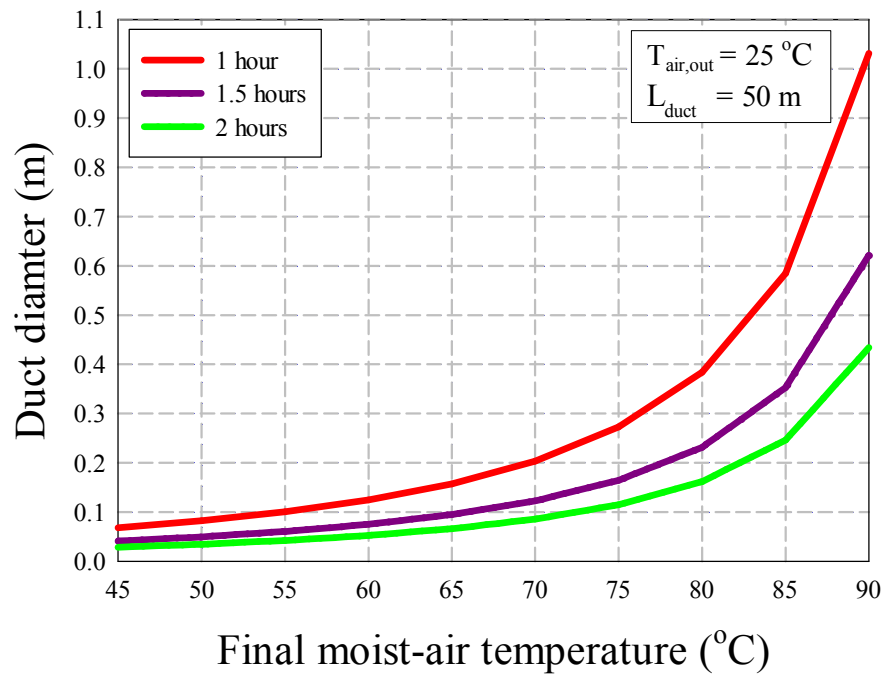


Figure 11.17. Variation of duct diameter with the operation time for the duct length of 50 metres.

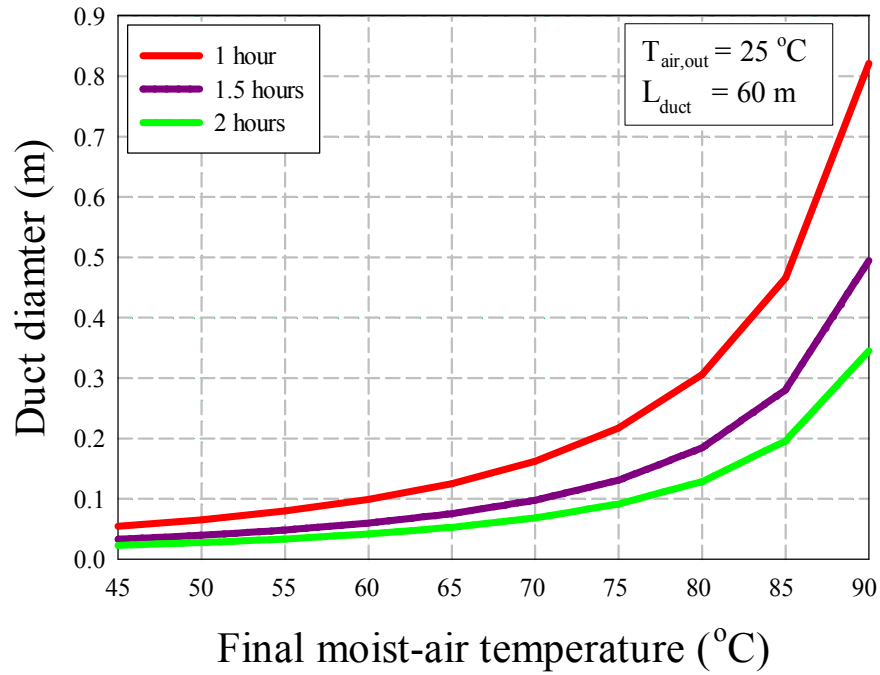


Figure 11.18. Variation of duct diameter with the operation time for the duct length of 60 metres.

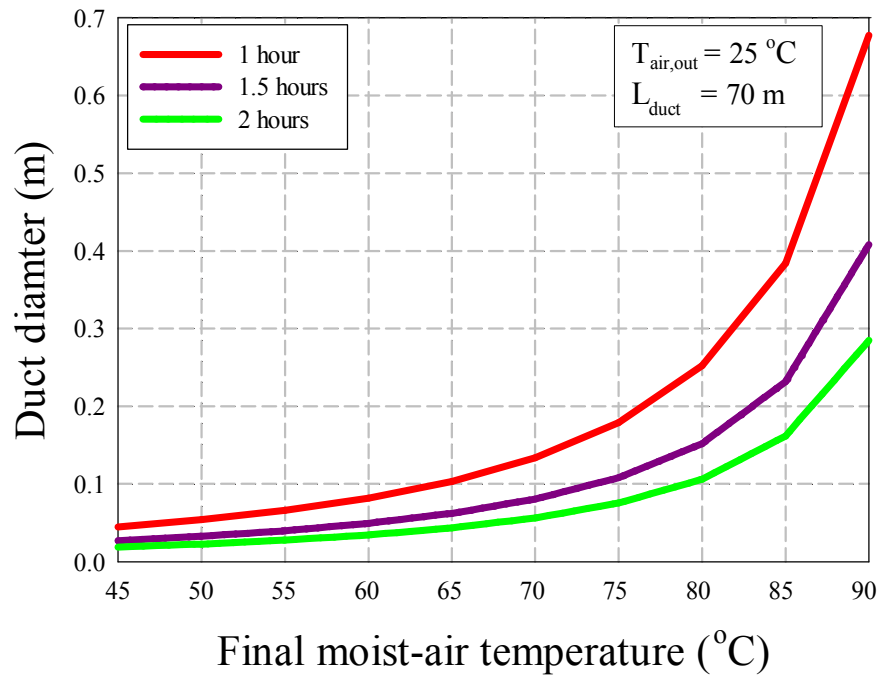


Figure 11.19. Variation of duct diameter with the operation time for the duct length of 70 metres.

The influence of duct length on the duct diameter is also demonstrated for different values of heat output as shown in Figure 11.20-11.22. A linear relationship between duct diameter and heat output is obtained for each case considered. The duct diameter has an increasing tendency with increasing heat output for different values of operation time. As it is clearly seen in the figures that the duct diameter slightly decreases when the time of operation increases. It can be easily concluded from the results that the final moist-air temperature, duct length, operation time and heat output of the system are dominant parameters for the determination of duct diameter at a particular case. These independent variables are required to be optimised for a proper and reliable estimation of the duct diameter.

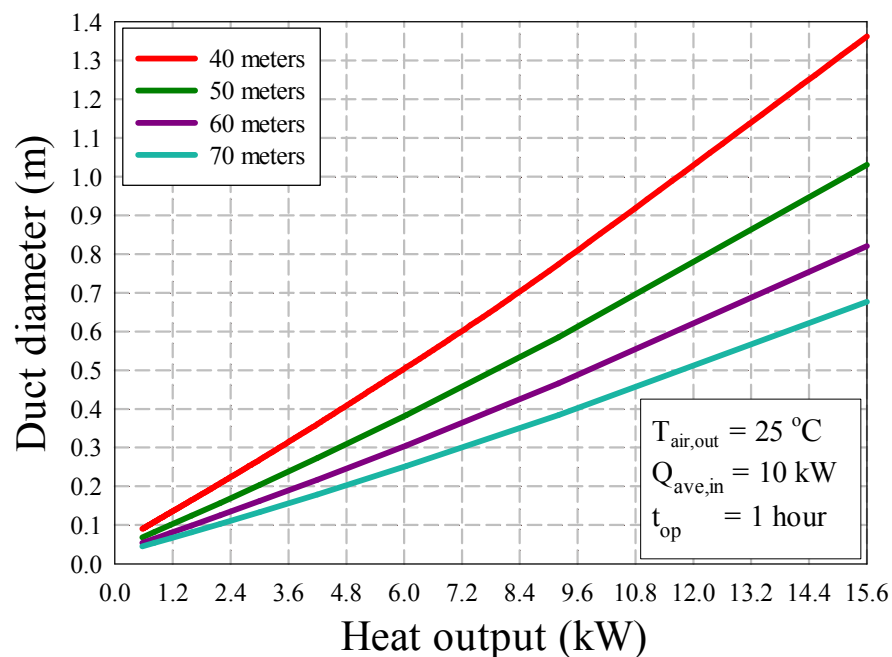


Figure 11.20. Variation of duct diameter with heat output and duct length of 40 to 70 metres for an operation time of 1 hour.

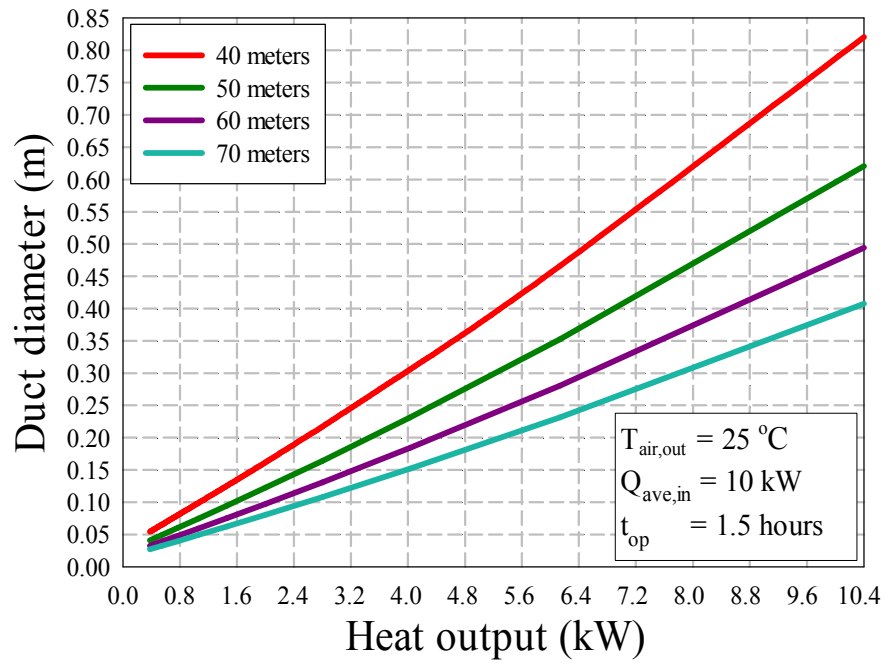


Figure 11.21. Variation of duct diameter with heat output and duct length of 40 to 70 metres for an operation time of 1.5 hours.

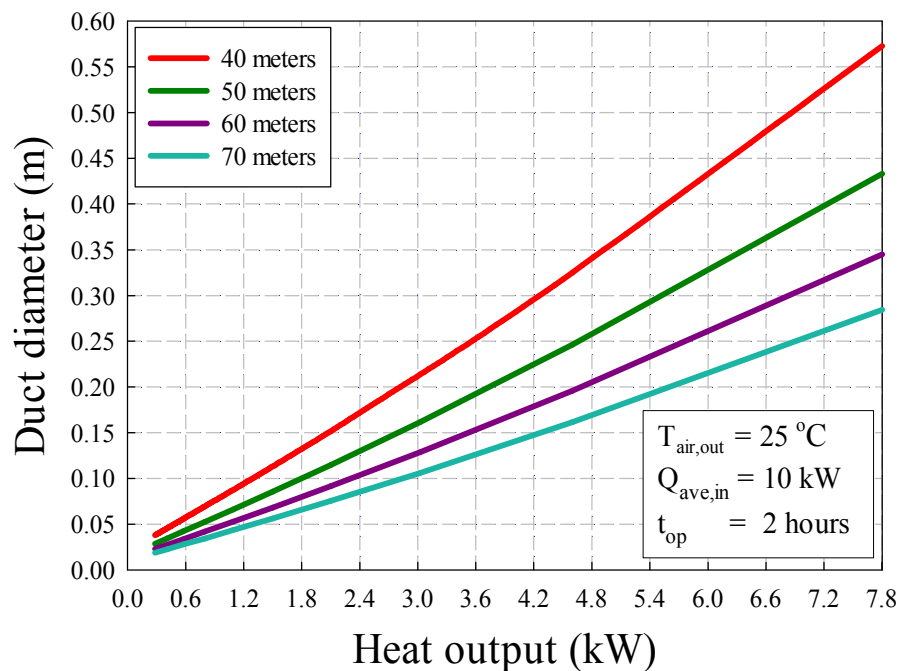


Figure 11.22. Variation of duct diameter with heat output and duct length of 40 to 70 metres for an operation time of 2 hours.

11.6.3. Results from duct diameter analysis

In Figure 11.23, duct diameter ratio of water and air based heating system is given in terms of temperature difference of working fluid. The temperature difference is investigated in the range of 50-75 °C. It is understood from the results that duct diameter ratio has an increasing trend with temperature difference of the working fluid. This can be attributed to the greater change in the duct diameter of water based system with temperature difference than that of air based system. It is also clear that duct diameter of water based system is found to be remarkably lower than that of air based system as a consequence of the difference in the density values.

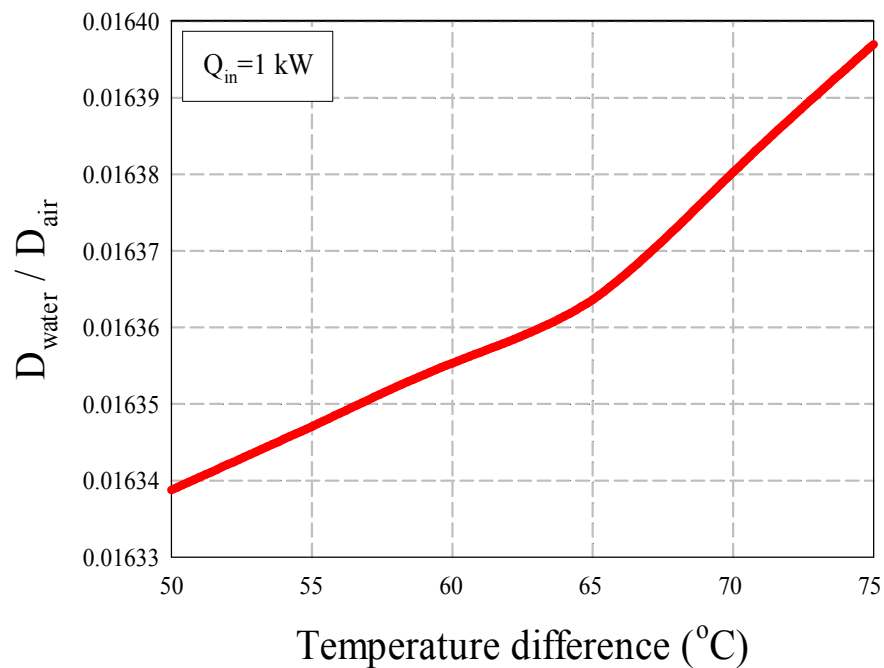


Figure 11.23. Duct diameter ratio of water and air based heating system.

In Figure 11.24, duct diameter ratio of water and moist-air based heating system is shown as a function of temperature difference. As it is seen from the results that a similar tendency is observed. However, the duct diameter values reveal that moist-air based heating system has lower duct diameter at the same temperature compared to the system utilising dry-air. For an easier tracking of the results, the variation of duct diameter with the temperature difference of working fluid is illustrated in Figure 11.25. It is concluded from the data obtained that the greatest duct diameter is achieved by air based heating system whereas the lowest one by the system using water as working fluid. This is an expected output which can be explained by the variations of density and specific heat capacity.

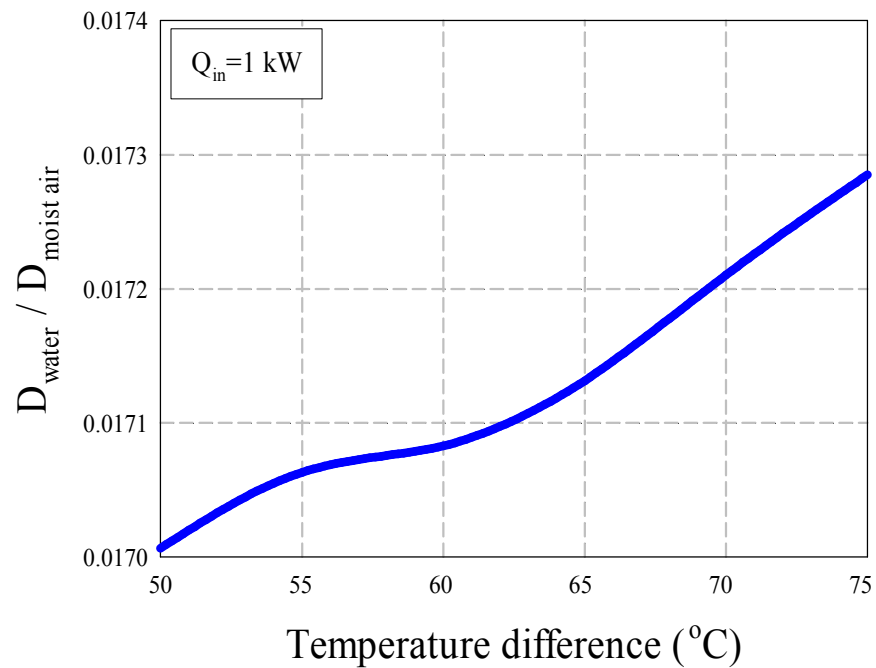


Figure 11.24. Duct diameter ratio of water and moist-air based heating system.

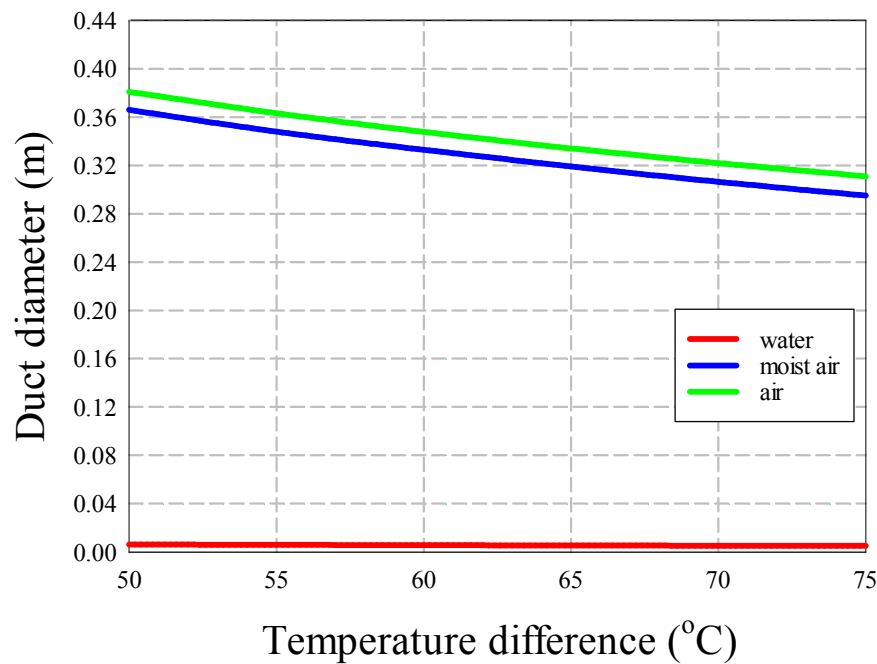


Figure 11.25. Duct diameter comparison for water, moist-air and air.

11.7. Conclusions

Buildings are responsible for a significant part of the total world energy consumption, and cost-effective solutions to mitigate their role in energy use are therefore important. Due to poor thermal insulation characteristics of the existing conventional building elements, heating demand of current building stock worldwide is remarkable. Intensive efforts are made to reduce heating demand of buildings through low-cost and environmentally friendly applications. However, there is a consensus among scientists that further improvements are required to meet the latest low carbon targets released by the developed countries.

In this research, a unique heating system called moist airflow system (*MAS*) is introduced and its thermal performance investigation is done for different operational parameters. Through a thermodynamic based modelling approach and a thorough heat transfer analysis, following conclusive results can be achieved from the study:

- Thermal performance of the moist airflow system is highly affected by the moist-air temperature, fan power and the working time.
- The *COP* values are very promising with the case of solar thermal collector and PV panel which range from 0.007 to 13.878, depending on the moist-air temperature, fan power and the working time.
- The highest *COP* which can be achieved from the case of without renewable energy generation or waste heat recovery is about 1.307.
- For any constant value of duct length, the duct diameter slightly decreases with increasing operation time.
- Duct diameter slightly decreases with increasing duct length.
- Duct diameter exponentially increases with increasing final moist-air temperature.
- Duct diameter varies linearly with a rising trend depending on the heat output of the system.
- For a particular case covering moist-air output temperature of 25 °C, 10 kW heat input, operation time of 2 hours and 6 kW heat output; duct diameter is found to be 22, 26, 32 and 43 cm for the duct length of 70, 60, 50 and 40 m, respectively.
- The moist airflow system is found to be very attractive to mitigate the heating demand of buildings if the system can be supported via renewable energy source, and if the climatic conditions are not severe.

Within the scope of this research, the duct diameter analysis of a novel heating system is also presented for three different working fluids, which are mainly air, moist-air and water. The calculations are based on a constant power input (1 kW) to the reference system and conducted for a temperature difference in the range of 50-75 °C.

- It is concluded from the results that the duct diameter of water based system is considerably lower than that of air based system depending on the difference in the

density values. A similar tendency is observed for the duct diameter ratio of water and moist-air based heating system.

➤ For the same temperature difference, the greatest duct diameter is required by air based heating system whereas the lowest one by the water based system as a consequence of the variations in density and specific heat capacity.

The cost effectiveness of the *MAS* is incomparable with conventional heating systems as the system is powered by a fan only, and uses the moist-air as the working fluid. The proposed system can substantially contribute in reducing greenhouse gas emissions due to buildings.

CHAPTER 12

Conclusions and future works

12.1. Conclusions

12.2. Future Works

CHAPTER 12

Conclusions and future works

12.1. Conclusions

Increasing trend on energy prices, concerns about climate change and sustainability make the issues of building sector energy efficiency, renewable energy and potential waste energy recovery technologies [308]. The building sector is considered as the greatest single contributor to total world energy consumption and greenhouse gas emissions. In this respect, a good understanding of the nature and structure of energy consumption in buildings is of vital importance for establishing the sufficient future energy and climate change policies [309]. Latest research by International Energy Agency (*IEA*) reveals that 47% of total world energy consumption belongs to buildings, and future predictions show that the trend will continue to rise [208–210]. Depending on the everlasting technological developments and increasing thermal comfort levels of occupants, building sector is considered to be key option to meet the latest targets released for the buildings of 2050s [301]. In addition, the role of buildings in total greenhouse gas emissions is significant as a consequence of remarkable energy consumption levels of buildings worldwide. Further investigations on energy consumed in building sector demonstrate that heating, cooling and ventilation systems are responsible for the greatest energy consumed in any typical building [310]. In this respect, analysing the optimum operation conditions of *HVAC* systems for minimum energy consumption and greenhouse gas emissions is of great importance as underlined by Zeng et al. [311]. Optimising *HVAC* control systems can also play an important role in mitigating energy consumption of buildings as shown by

Wang et al. [312] for a case study of school building. Besides constructional and operational optimisation of conventional *HVAC* systems utilised in buildings, integrated *HVAC* systems with heat/energy recovery are preferred for extreme climates to reduce energy consumption as emphasised by Nasr et al. [313]. Attempts on developing novel energy efficient and environmentally friendly *HVAC* systems are also in progress for drastic mitigation of energy consumption and greenhouse gas emissions related to *HVAC* [314,315]. Within the scope of this thesis, several energy efficient *HVAC* systems are introduced, and performance parameters of the said technologies are investigated both theoretically and experimentally. Techno-economic assessment of the technologies developed is evaluated as well as discussing the optimised constructional and operational conditions. Relevant comparisons are also made to be able to demonstrate the practicality, reliability and efficiency of each technology presented. Following bullet points can be concluded from the research conducted:

- Recent research by International Energy Agency on total world energy consumption reveals that the building sector is responsible for 47% of total energy use. Future predictions also indicate that this dramatic scenario will continue if decisive and efficient measures are not taken.
- Further investigations on the role of building type in global energy consumption notify that the domestic buildings account for 20-40% of total primary energy consumption in the world. In addition to this, most of this energy is essentially utilised for heating and cooling purposes in domestic buildings.
- Heating, cooling and air conditioning systems constitute of the greatest energy consumption in a typical domestic building. For an instance, they account for 62% of current residential energy consumption in the UK because of poor performance

parameters of existing *HVAC* technologies and insufficient thermal insulation ability of existing building envelopes.

➤ Current *HVAC* systems utilised in domestic buildings are not cost-effective. In this respect, either developing novel energy efficient and environmentally friendly *HVAC* solutions or enhancing the existing efficiency range of the conventional systems via optimisation of constructional and operational parameters are considerably required.

➤ Energy efficient utilisation of heat recovery techniques in conventional *HVAC* has a remarkable potential to mitigate the energy demand of buildings, and thus the greenhouse gas emissions in the atmosphere. The enhancement becomes much more remarkable especially for ventilation systems where the thermal energy contents of fresh and stale air are exchanged. Recent research in the scope indicates that 60-95% of waste heat can be recovered in such systems resulting in higher overall efficiency of *HVAC* systems.

➤ Waste heat recovery in ventilation systems can be performed through direct or indirect systems. In a direct contact heat recovery unit, heat is directly transferred between hot and cold fluids. On the other hand, in an indirect contact heat recovery unit, there is a separating wall between hot and cold fluids throughout the duct. Therefore, there is no direct contact between two fluids with different initial temperatures. Compared to indirect contact recuperators and regenerators, direct contact heat recovery systems have notably greater heat transfer rates.

➤ Development of low-cost and highly thermally conductive heat recovery materials and systems is required to mitigate energy consumption for ventilation purposes. Latest works clearly show that poly-carbonate based heat recovery units are very promising, and become widespread day after day owing to their low-cost, high conductance and being easy to fabricate.

- Among the existing waste heat recovery systems, plate-type heat recovery systems have some characteristic advantages such as high efficiency, and low fabrication and operation cost. Plate-type heat recover units are constructed from thin plates which form flow channels. The channels produced are used for transferring the heat for any combination of gas, liquid and two-phase streams, and they are mainly made of metal plates for better heat transfer rates. The overall system efficiency of plate-type heat recovery systems is in the range of 50-80%.
- In recent years, intensive efforts are made to improve the overall efficiency range of waste heat recovery systems as well as reducing their cost to be able to make them much more attractive, practical and reliable. In this respect, there is a strong stimulation of developing and using renewable energy powered waste heat recovery systems aiming at remarkably rising the coefficient of performance (*COP*) of the said technologies.
- Recent theoretical and experimental attempts reveal that solar powered heat recovery systems not only enhances the thermal energy content of fresh air from outdoor to indoor environment but also improves the electricity generation as a consequence of lower cell temperatures due to heat recovery.
- The practicality of solar powered waste heat recovery system is also verified by recent attempts through energy and exergy analyses. The results indicate that maximum exergy efficiency of the system is found to be around 60% which is very promising compared to conventional ventilation systems. Moreover, it is noted that this efficiency value can be enhanced via optimisation of the system parameters such as duct geometry, mass flow rates of the fluids and packing factor for the solar powered unit.
- Experimental performance of waste heat recovery systems for ventilation purposes is essentially based on some constructional and operational parameters such as hydraulic diameter, duct length and fan speed. Fans are the only energy consuming devices

utilised in such systems. In this respect, optimised conditions have a strong potential to result in high heat recovery efficiency and overall coefficient of performance. Recent experimental research on a plate-type waste heat recovery system clearly shows that around 89% of heat recovery efficiency can be achieved for an air velocity of 0.4 m/s and the hydraulic diameter of 90 mm. In addition, the average coefficient of performance of the system is calculated to be around 4.5 which is incomparable with conventional ventilation systems.

➤ Since the real time behaviour of building systems is not easy to predict, real time monitoring performance of waste heat recovery technologies is significant as well as preliminary theoretical and experimental investigation. In this respect, the aforesaid plate-type waste heat recovery unit is retrofitted to a residential building to determine the system performance in real operating conditions through a monitoring analysis. Within the concept of monitoring case, the fresh air and stale air temperatures at the inlet and outlet, the relative humidity and CO_2 concentration for both pre and post-retrofit cases are measured time dependently. In terms of numerical assessment, the relative humidity is in a range of 61 to 72% before retrofitting, whereas it is 53 to 62% after retrofitting. Maximum temperature rise in fresh air temperature is noted to be about 7 °C. Similarly, a considerable change is observed in the temperature of stale air at inlet and outlet. An average 4 °C temperature decrease of stale air is achieved within the test period.

➤ The results indicate that the internal CO_2 concentration is not at desirable range due to lack of ventilation in the test house at the pre-retrofit case. However, following the integration of the novel ventilation system into the test house, CO_2 concentration is found to be varying notably from 350 to 400 ppm which is very appropriate in term of

indoor air quality. In addition, average relative humidity is found to be 57%, which is in the desired range whereas it is considerably high before retrofitting.

- The role of *HVAC* in total energy consumed in residential buildings is investigated by several researchers worldwide, and the results show a similar tendency for different climatic regions. For instance, the air conditioning and heating systems in China are responsible for 65% of the total building energy consumption [316] whereas it is 39% for the US. Ventilation systems account for a remarkable energy consumption in *HVAC*. According to Khan et al. [317], energy consumption in buildings due to ventilation and infiltration is approximately 30-50% of total energy consumption. The figures can be more dramatic (>50%) for modern buildings as noted by Mardiana and Riffat [318].
- Evaporative cooling is a very promising method to reduce energy consumption of buildings related to ventilation and cooling demand especially in hot and arid climates. As a general statement, evaporative cooling systems are low-cost and energy efficient as a consequence of their remarkable high *COP* range. A recent study shows that 12.05% saving in annual power consumption of a building is achieved with use of a simple evaporative cooling system [242].
- System performance of an evaporative cooling system is affected by several parameters such as duct length, hydraulic diameter, air velocity, working air inlet temperature, fresh air inlet temperature, relative humidity of fresh air, relative humidity of working air, film temperature and thermal insulation performance of the system.
- The amount of evaporated water vapour increases with increasing hydraulic diameter and length of spraying unit. Water evaporation reduces with increasing velocity of working air. The outlet temperature of working air decreases with increasing values of spraying unit length. On the other hand, relative humidity of working air reaches adiabatic saturation condition after a specific value of spraying unit length which is the

desired condition. The spraying unit length should be at least 8 m to be able to reach the adiabatic saturation condition which corresponds to the best case that can be achieved for the system. Both temperature and relative humidity of working air at the outlet increases with increasing inlet relative humidity of working air. The hydraulic diameter has a notable impact on outlet temperature of working air. For a hydraulic diameter of 300 mm, $T_{wa,out}$ falls below 10 °C which is very promising. For the most desired conditions, relative humidity of working air at the inlet should not be greater than 50%. Fresh air temperature to the indoor environment increases linearly with working air temperature and fresh air temperature from outdoor. Temperature of fresh air from outdoor environment has a dominant impact on relative humidity of fresh air to the indoor environment. For $\phi_{fa,outdoor} = 40\%$, $\phi_{fa,indoor}$ falls out of the thermal comfort range if outdoor fresh air temperature is greater than 35 °C.

➤ The theoretical results presented above are supported by an experimental research conducted in test house in the UK. As a natural consequence of evaporative cooling process, air temperature remarkably decreases at the outlet. Steady-state measurements reveal that the average temperature of fresh air at the inlet is 36.9 °C, whereas it is 26.7 °C at the outlet. The temperature difference of 10.2 °C achieved by evaporative cooling system is very promising. The outlet relative humidity of fresh air almost reaches the adiabatic saturation condition as clearly shown. The average humidity values at the inlet and outlet are measured to be 37.2 and 98.4%, respectively.

➤ The reliability of the system and the accuracy of the measurements are verified by performing a second test. Temperature measurements indicate that the temperature difference at the second test is not as high as the first test because of the lower inlet temperature. Average inlet and outlet temperatures of fresh air are determined to be 31.1 and 23.0 °C, respectively. The temperature difference of 8.1 °C is still remarkable

since the power consumption of the system is insignificant. The adiabatic saturation condition is almost achieved for the second test as well. Average inlet and outlet relative humidity are measured to be 30.0 and 94.8%, respectively.

➤ For the extreme weather conditions as characterised by the first test, *COP* is expected to be highly attractive, which is verified by the experimental results. The average *COP* of the first test is found to be 8.7. On the other hand, for arid temperate climates given as an example in the second test, somewhat lower values of *COP* is predicted, and this is clearly seen the results of the second test. The average *COP* from the second test is calculated to be 6.7.

➤ Evaporative cooling has a high potential to meet cooling demands at low energy costs [249]. Riangvilaikul and Kumar [213] note that the evaporative cooling is a good alternative to mechanical vapour compression for air conditioning applications since it consumes about four times less electricity than vapour-compression refrigeration [250]. However, the challenging point of evaporative cooling systems is that they are not able to provide the desired conditions in hot and humid areas. Therefore, alternative systems such as desiccant-based cooling are required. For instance, liquid desiccant-based evaporative cooling system is a good alternative to conventional cooling systems to be able to control both temperature and relative humidity, especially in hot and humid environmental conditions [247].

➤ Desiccant concentration is of vital importance in desiccant-based cooling systems as it notably affects the thermal performance efficiency. The lower desiccant concentration and desiccant temperature corresponds to the greater thermal efficiency.

➤ There is a linear tendency between inlet and outlet desiccant temperatures of the system which is an unequivocal consequence of first law of thermodynamics. Desiccant temperature at the inlet needs to be kept as low as possible for desired relative humidity

ranges. Desiccant concentration plays a key role in outlet fresh air temperature as well as humidity ratio and thermal comfort parameters for indoor environment.

➤ Experimental performance of desiccant-based evaporative cooling systems is also investigated within the scope of this research. The experiments are carried out for two different velocity values of 0.3 and 0.5 m/s .

➤ For a case of average inlet relative humidity of 94.7% and average inlet air temperature of 38.6 °C, the average outlet relative humidity and air temperature are determined to be 65.5% and 33.3 °C, respectively. An average of 5.3 °C reduction is achieved in supply air temperature as well as an average of 63.7% dehumidification effectiveness which is attractive and promising.

➤ For the case of higher velocity, the average relative humidity before the dehumidification unit is found to be 72.5% and the supply air temperature 38.5 °C. After the humidification unit, the average relative humidity is determined to be 63.6% and the average air temperature 34.2 °C. An average temperature reduction of 4.3 °C is achieved as well as a dehumidification effectiveness of 56.1%.

➤ Dehumidification effectiveness is a function of air velocity as it drops from 63.7 to 56.1% when air velocity increases from 0.3 to 0.5 m/s . It is concluded from the results that desiccant-based evaporative cooling system is a novel, unique and cost-effective design to mitigate cooling demand of buildings not only in hot arid but also in temperate humid climates.

➤ The average *COP* values of the desiccant based evaporative cooling system for the inlet air velocities of 0.3 and 0.5 m/s are determined to be roughly 5.5 and 4.8, respectively.

➤ The moist airflow system (*MAS*) is basically a cost effective heat distribution system using air as the working fluid. The driving force of the *MAS* is the utilisation of waste

heat from different sources such as industrial power plants, and transportation of this energy into the buildings in an efficient way to mitigate the heating demand of buildings. The system can also be operated via renewable energy technologies such as solar thermal collectors, hybrid photovoltaic thermal cogeneration systems and geothermal power.

- The novel idea of the *MAS* can be attributed to the utilisation of the air instead of water as the working fluid. In this respect, the energy stored in water by the waste heat sources or renewables is transferred into the air to be utilised in heating a space.
- Duct diameter ratio has an increasing trend with temperature difference of the working fluid. This can be attributed to the greater change in the duct diameter of water based system with temperature difference than that of air based system. The duct diameter values reveal that moist-air based heating system has lower duct diameter at the same temperature compared to the system utilising dry-air.
- The greatest duct diameter is achieved by air based heating system whereas the lowest one by the system using water as working fluid. This is an expected output which can be explained by the variations of density and specific heat capacity.
- For a particular case covering moist-air output temperature of 25 °C, 10 kW heat input, operation time of 2 hours and 6 kW heat output; duct diameter is found to be 22, 26, 32 and 43 cm for the duct length of 70, 60, 50 and 40 m, respectively.
- The duct diameter of water based system is considerably lower than that of air based system depending on the difference in the density values. A similar tendency is observed for the duct diameter ratio of water and moist-air based heating system.
- The cost effectiveness of the *MAS* is incomparable with conventional heating systems as the system is powered by a fan only, and uses the moist-air as the working fluid.

➤ The proposed system can substantially contribute in reducing greenhouse gas emissions due to buildings.

12.2. Future Works

In light of this research, theoretical and experimental investigations of novel heating, cooling and ventilation systems have been presented. For each technology considered, overall system efficiency has been determined for different constructional and operational conditions. In addition to these, in-situ performance assessment of the said technologies has been done through research conducted in different test houses. The works carried out so far have mainly been based on residential buildings, thus further works are expected to focus on different types of buildings such as commercial, industrial and public buildings. In this respect, more complicated monitoring analyses are planned to conduct at whole building scale.

In order to improve the waste heat recovery efficiency in ventilation systems, novel cost-effective and highly thermally conductive materials will be developed and utilised. The units fabricated by these materials will be both theoretically and experimentally investigated prior to retrofit to target buildings. The accuracy of the results will be verified by *CFD* simulations performed via reliable commercial software such as *ANSYS FLUENT*. Further experimental attempts will be made for an accurate performance assessment of solar powered waste heat recovery systems. Different configurations of evaporative cooling systems such as direct-contact, indirect-contact or combination of both will be evaluated in terms of different techno-economic aspects. Different fibre materials such as membrane fibres and polymer fibres will be considered to use in desiccant-based evaporative cooling systems for better liquid absorption and

greater mass transfer rates. Different desiccant solutions as well as potassium formate will be used for better dehumidification performance.

BIBLIOGRAPHY

References

REFERENCES

- [1] Cox PM, Betts RA, Jones CD, Spall SA, Totterdell IJ. Acceleration of global warming due to carbon-cycle feedbacks in a coupled climate model. *Nature* 2000; 408: 184–187.
- [2] Sahin AD, Dincer I, Rosen MA. Thermodynamic analysis of solar photovoltaic cell systems. *Solar Energy Materials and Solar Cells* 2007; 91: 153–159.
- [3] Perez-Lombard L, Ortiz J, Pout C. A review on buildings energy consumption information. *Energy and Buildings* 2008; 40: 394–398.
- [4] Saidur R. Energy consumption, energy savings, and emission analysis in Malaysian office buildings. *Energy Policy* 2009; 37: 4104–4113.
- [5] Hasan MA, Sumathy K. Photovoltaic thermal module concepts and their performance analysis: a review. *Renewable and Sustainable Energy Reviews* 2010; 14: 1845–1859.
- [6] Panwar NL, Kaushik SC, Kothari S. Role of renewable energy sources in environmental protection: a review. *Renewable and Sustainable Energy Reviews* 2011; 15: 1513–1524.
- [7] Wang R, Liu W, Xiao L, Liu J, Kao W. Path towards achieving of China's 2020 carbon emission reduction target—A discussion of low-carbon energy policies at province level. *Energy Policy* 2011; 39(5): 2740–2747.
- [8] Solangi KH, Islam MR, Saidur R, Rahim NA, Fayaz H. A review on global solar energy policy. *Renewable and Sustainable Energy Reviews* 2011; 15(4): 2149–2163.
- [9] International Energy Agency. Technology roadmap – Energy efficient building envelopes, December 2013.

- [10] Liu D, Zhao FY, Tang GF. Active low-grade energy recovery potential for building energy conservation. *Renewable and Sustainable Energy Reviews* 2010; 14: 2736–2747.
- [11] Kolokotsa D, Rovas D, Kosmatopoulos E, Kalaitzakis K. A roadmap towards intelligent net zero-and positive-energy buildings. *Solar Energy* 2011; 85: 3067–3084.
- [12] Zhao H, Magoules F. A review on the prediction of building energy consumption. *Renewable and Sustainable Energy Reviews* 2012; 16: 3586–3592.
- [13] Sadineni SB, Madala S, Boehm RF. Passive building energy savings: A review of building envelope components. *Renewable and Sustainable Energy Reviews* 2011; 15: 3617–3631.
- [14] Janda KB, Busch JF. Worldwide status of energy standards for buildings. *Energy* 1994; 19(1): 27–44.
- [15] Cuce PM, Cuce E, Riffat SB. Theoretical investigation of solar powered heat recovery panels in buildings. 12th International Conference on Sustainable Energy Technologies. 26–29 August 2013, Hong Kong, China.
- [16] Perez-Lombard L, Ortiz J, Coronel JF, Maestre IR. A review of HVAC systems requirements in building energy regulations. *Energy and Buildings* 2011; 43: 255–268.
- [17] Cuce PM, Riffat S. A comprehensive review of heat recovery systems for building applications. *Renewable and Sustainable Energy Reviews* 2015; 47: 665–682.

- [18] Fong KF, Hanby VI, Chow TT. HVAC system optimization for energy management by evolutionary programming. *Energy and Buildings* 2006; 38(3): 220–231.
- [19] Vakiloroaya V, Samali B, Fakhar A, Pishghadam K. A review of different strategies for HVAC energy saving. *Energy Conversion and Management* 2014; 77: 738–754.
- [20] Yu T, Heiselberg P, Lei B, Pomianowski M, Zhang C. A novel system solution for cooling and ventilation in office buildings: A review of applied technologies and a case study. *Energy and Buildings* 2015; 90: 142–155.
- [21] Zhang LZ. Total heat recovery: Heat and moisture recovery from ventilation air. Nova Science Publishers, Inc. 2008, New York, USA.
- [22] Vitousek PM. Beyond global warming: Ecology and global change. *Ecology* 1994; 75(7): 1861–1876.
- [23] Whitesides GM, Simanek EE, Mathias JP, Seto CT, Chin DN, Mammen M, Gordon DM. Nancovalent synthesis: Using physical-organic chemistry to make aggregates. *Account of Chemical Research* 1995; 28: 37–44.
- [24] America's Climate Choices. The National Academies Press, 2011, Washington, USA.
- [25] Bell LE. Cooling, heating, generating power and recovering waste heat with thermoelectric systems. *Science* 2008; 321: 1457–1461.
- [26] Wan KKW, Li DHW, Liu D, Lam JC. Future trends of building heating and cooling loads and energy consumption in different climates. *Building and Environment* 2011; 46: 223–234.

- [27] IPCC, Climate Change 2007: The physical science basis. Solomon S, Qin D, Manning M, Marquis M, Averyt K, Tignor MMB, Miller HL, Chen Z. Contribution of the working group I to the fourth assessment report of the Intergovernmental Panel on Climate Change. Cambridge University Press 2007, Cambridge, UK.
- [28] IPCC, Climate Change 2007: Mitigation of climate change. Metz B, Davidson OR, Bosch PR, Dave R, Meyer LA. The Physical Science Basis. Contribution of the working group III to the fourth assessment report of the Intergovernmental Panel on Climate Change. Cambridge University Press 2007, Cambridge, UK.
- [29] Heating, ventilation and air conditioning. <http://eex.gov.au/technologies/heating-ventilation-and-air-conditioning/>. (Last access is on 09.09.2015).
- [30] Omer AM. Low energy building materials: An overview. In: Proceedings of the Environment 2010: Situation and Perspectives for the European Union, pp. 16–21. 6–10 May 2003, Porto, Portugal.
- [31] Sugarman SC. HVAC fundamentals. The Fairmont Press, Inc. 2005, Lilburn, USA.
- [32] Fehrm M, Reiners W, Ungemach M. Exhaust air heat recovery in buildings. *International Journal of Refrigeration* 2002; 25: 439–449.
- [33] Brumbaugh JE. HVAC fundamentals. Wiley Publishing 2004, USA.
- [34] Gupton GW. HVAC controls: Operation and maintenance. The Fairmont Press 2002, Lilburn, USA.
- [35] Mardiana-Idayu A, Riffat SB. Review on heat recovery technologies for building applications. *Renewable and Sustainable Energy Reviews* 2012; 16: 1241–1255.

- [36] Heat Recovery Ventilation System. http://www.soloheatinginstallations.co.uk/heat_recovery.htm. (Last access is on 02.04.2013).
- [37] Shah RK, Sekulic DP. Fundamentals of heat exchanger design. John Wiley & Sons, Inc. 2003, New Jersey, USA.
- [38] Montgomery R, McDowall R. Fundamentals of HVAC control systems. Elsevier 2008, USA.
- [39] Heuckeroth OH, Middlebrooks SE. An investigation of combat vehicle ventilation requirements. Army Research Laboratory, 2011, USA.
- [40] Yilmaz M, Sara ON, Karsli S. Performance evaluation criteria for heat exchangers based on second law analysis. *Exergy, An International Journal* 2001; 1(4): 278–294.
- [41] Guo JF, Xu MT, Cheng L. Principle of equipartition of entransy dissipation for heat exchanger design. *Science China Technological Sciences* 2010; 53(5): 1309–1314.
- [42] Cakmak G, Yucel HL, Argunhan Z, Yildiz C. Experimental investigation of thermal performance in a concentric-tube heat exchanger with wavy inner pipe. *International Journal of Thermophysics* 2012; 33(6): 1055–1067.
- [43] Xia L, Abreu-Garcia JAD, Hartley TT. Modelling and simulation of a heat exchanger. IEEE International Conference on Systems Engineering 1-3 August 1991.
- [44] Kreith F, Boehm RF. Direct-contact heat transfer. Hemisphere Publishing Corporation 1986, Washington, USA.
- [45] Kreith F, Manglik RM, Bohn MS. Principles of heat transfer. Seventh Edition, Cengage Learning, Inc. 2011, USA.
- [46] Kuppan T. Heat exchanger design handbook. Marcel Dekker, Inc. 2000, USA.

- [47] Kakac S, Liu H. Heat exchangers: Selection, rating and thermal design. Second Edition, CRC Press. 2002, Florida, USA.
- [48] Larowski A, Taylor MA. Systematic procedure for selection of heat exchangers. Proceedings of the Institution of Mechanical Engineers, Part A: *Journal of Power and Energy* 1983; 197: 51–69.
- [49] Double Pipe Heat Exchanger. <http://www.made-in-china.com/showroom/cnjyybkj/product-detailDMZxkwNVwIhq/China-Double-Pipe-Heat-Exchanger.html>. (Last access is on 03.04.2013).
- [50] D. Chisholm, Developments in Heat Exchanger Technology, Applied Science Publishers 1980, London, UK.
- [51] El-Harbawi M, Acellam D, Yin CY. Development of educational software for designing shell-and-tube heat exchangers. *International Journal of Mechanical Engineering Education* 2011; 39(4): 291–296.
- [52] Heat Exchangers. <http://www.maxx-engineering.th.com/products.php?prodId=4>. (Last access is on 10.04.2013).
- [53] Shell and Tube Heat Exchangers. <http://www.evaporatorplants.com/heat-exchanger.html#shell-and-tube-heat-exchangers>. (Last access is on 10.04.2013).
- [54] Titanium Tube Cooler Coil Heat Exchanger. <http://sell.lulusoso.com/selling-leads/1011232/titanium-tube-cooler-coil-heat-exchanger.html>. (Last access is on 11.04.2013).
- [55] Copper Heat Exchanger. <http://www.coolersindia.co/copper-heat-exchanger.html>. (Last access is on 11.04.2013).
- [56] Gasketed Plate Heat Exchangers. <http://www.techaidgroup.com/products/gasketed-plate-heat-exchangers/>. (Last access is on 12.04.2013).

- [57] Gasketed Plate Heat Exchanger. <http://www.directindustry.com/prod/ciat/product-8605-413522.html>. (Last access is on 12.04.2013).
- [58] Spiral Plate Heat Exchanger. http://www.diytrade.com/china/pd/10875175/spiral_plate_heat_exchanger.html. (Last access is on 24.04.2013).
- [59] Lamellar Heat Exchanger. <http://www.gidroterm.all.biz/en/lamellar-heat-exchanger-gg1004229>. (Last access is on 24.04.2013).
- [60] Schlunder EU, Bell KJ, Chisholm D, Hewitt GF, Schmidt FW, Spalding DB, Taborek J, Zukauskas A, Gnielinski V. Heat exchanger design handbook. Hemisphere Publishing Corporation 1983, USA.
- [61] Gaugler, RS. Heat transfer device. U.S. Patent, 2350348, 1944.
- [62] Yau YH, Ahmadzadehtalatapeh M. A review on the application of horizontal heat pipe heat exchangers in air conditioning systems in the tropics. *Applied Thermal Engineering* 2010; 30: 77–84.
- [63] Shao L, Riffat SB. Flow loss caused by heat pipes in natural ventilation stacks. *Applied Thermal Engineering* 1997; 17(4): 393–399.
- [64] Heat Exchangers. <http://www.power-technology.com/contractors/cooling/faco/faco3.html>. (Last access is on 06.05.2013).
- [65] Plate Finned Type Heat Exchanger. <http://www.jcequipments.com/plate-finned-type-heat-exchanger.html>. (Last access is on 06.05.2013)
- [66] Heat Pipe Technology. <http://www.forsteel.cz/heat-pipes.html>. (Last access is on 08.05.2013)
- [67] Tauscher R, Dinglreiter U, Durst B, Mayinger F. Transport processes in narrow channels with application to rotary exchangers. *Heat and Mass Transfer* 1999; 35: 123–131.

- [68] Swanepoel DC, Kroger DG. Rotary regenerator design theory and optimisation. *R&D Journal* 1996; 12(13): 90–97.
- [69] Mardiana-Idayu A, Riffat SB. An experimental study on the performance of enthalpy recovery system for building applications. *Energy and Buildings* 2011; 43: 2533–2538.
- [70] Abd El-Baky MA, Mohamed MM. Heat pipe heat exchanger for heat recovery in air conditioning. *Applied Thermal Engineering* 2007; 27: 795–801.
- [71] Fernandez-Seara J, Diz R, Uhia FJ, Dopazo A, Ferro JM. Experimental analysis of an air-to-air heat recovery unit for balanced ventilation systems in residential buildings. *Energy Conversion and Management* 2011; 52: 635–640.
- [72] Lu Y, Wang Y, Zhu L, Wang Q. Enhanced performance of heat recovery ventilator by airflow-induced film vibration (HRV performance enhanced by FIV). *International Journal of Thermal Sciences* 2010; 49: 2037–2041.
- [73] Juodis E. Extracted ventilation air heat recovery efficiency as a function of a building's thermal properties. *Energy and Buildings* 2006; 38: 568–573.
- [74] Hviid CA, Svendsen S. Analytical and experimental of a low-pressure heat exchanger suitable for passive ventilation. *Energy and Buildings* 2011; 43: 275–284.
- [75] Persily A. Evaluation of an air-to-air heat exchanger. *Environment International* 1982; 8: 453–459.
- [76] Riffat SB, Gan G. Determination of effectiveness of heat-pipe heat recovery for naturally-ventilated buildings. *Applied Thermal Engineering* 1998; 18: 121–130.
- [77] Manz H, Huber H, Helfenfinger D. Impact of air leakages and short circuits in ventilation units with heat recovery on ventilation efficiency and energy requirements for heating. *Energy and Buildings* 2001; 33: 133–139.

- [78] Roulet CA, Heidt FD, Foradini F, Pibiri MC. Real heat recovery with air handling units. *Energy and Buildings* 2001; 33: 495–502.
- [79] Hemzal K. Rotary heat exchanger efficiency influenced by air tightness. 17th Air-Conditioning and Ventilation Conference, Prague, May 17-19, 2006.
- [80] Abe OO, Simonson CJ, Besant RW, Shang W. Effectiveness of energy wheels from transient measurements. Part I: Prediction of effectiveness and uncertainty. *International Journal of Heat and Mass Transfer* 2006; 49: 52–62.
- [81] Abe OO, Simonson CJ, Besant RW, Shang W. Effectiveness of energy wheels from transient measurements: Part II: Results and verification. *International Journal of Heat and Mass Transfer* 2006; 49: 63–77.
- [82] Zhong K, Kang Y. Applicability of air-to-air heat recovery ventilators in China. *Applied Thermal Engineering* 2009; 29: 830–840.
- [83] Nguyen A, Kim Y, Shin Y. Experimental study of sensible heat recovery of heat pump during heating and ventilation. *International Journal of Refrigeration* 2005; 28: 242–252.
- [84] Martinez FJR, Plasencia MAAG, Gomez EV, Diez FV, Martin RH. Design and experimental study of a mixed energy recovery system, heat pipes and indirect evaporative equipment for air conditioning. *Energy and Buildings* 2003; 35: 1021–1030.
- [85] Yau YH. Application of a heat pipe heat exchanger to dehumidification enhancement in a HVAC system for tropical climates—a baseline performance characteristics study. *International Journal of Thermal Sciences* 2007; 46: 164–171.

- [86] Nasif M, Al-Waked R, Morrison G, Behnia M. Membrane heat exchanger in HVAC energy recovery systems, systems energy analysis. *Energy and Buildings* 2010; 42: 1833–1840.
- [87] Liang CH, Zhang LZ, Pei LX. Independent air dehumidification with membrane-based total heat recovery: Modelling and experimental validation. *International Journal of Refrigeration* 2010; 33: 398–408.
- [88] Zhang LZ. Energy performance of independent air dehumidification systems with energy recovery measures. *Energy* 2006; 31: 1228–1242.
- [89] Mahmud K, Mahmood GI, Simonson CJ, Besant RW. Performance testing of a counter-cross-flow run-around membrane energy exchanger (RAMEE) system for HVAC applications. *Energy and Buildings* 2010; 42: 1139–1147.
- [90] Noie-Baghban SH, Majideian GR. Waste heat recovery using heat pipe heat exchanger (HPHE) for surgery room in hospitals. *Applied Thermal Engineering* 2000; 20: 1271–1282.
- [91] Riffat SB, Warren AP, Webb RA. Rotary heat pump driven by natural gas. *Heat Recovery Systems and CHP* 1995; 15(6): 545–554.
- [92] Riffat SB, Gillott MC. Performance of a novel mechanical ventilation heat recovery heat pump system. *Applied Thermal Engineering* 2002; 22: 839–845.
- [93] Kragh J, Rose J, Nielsen TR, Svendsen S. New counter flow heat exchanger designed for ventilation systems in cold climates. *Energy and Buildings* 2007; 39: 1151–1158.
- [94] Manz H, Huber H, Schalin A, Weber A, Ferrazzini M, Studer M. Performance of single room ventilation units with recuperative or regenerative heat recovery. *Energy and Buildings* 2000; 31: 37–47.

- [95] Manz H, Huber H. Experimental and numerical study of a duct/heat exchanger unit for building ventilation. *Energy and Buildings* 2000; 32: 189–196
- [96] Nazaroff WW, Boegel ML, Hollowell CD, Roseme GD. The use of mechanical ventilation with heat recovery for controlling radon and radon-daughter concentrations in houses. *Atmospheric Environment* 1981; 15: 263–270.
- [97] Gong G, Zeng W, Wang L, Wu C. A new heat recovery technique for air-conditioning/heat pump system. *Applied Thermal Engineering* 2008; 28: 2360–2370.
- [98] Gu Z, Liu H, Li Y. Thermal energy recovery of air conditioning system–heat recovery system calculation and phase change materials development. *Applied Thermal Engineering* 2004; 24: 2511–2526.
- [99] Riffat SB, Cuce E. A review on hybrid photovoltaic/thermal collectors and systems. *International Journal of Low-Carbon Technologies* 2011; 6(3): 212–241.
- [100] Cuce PM, Cuce E. A novel model of photovoltaic modules for parameter estimation and thermodynamic assessment. *International Journal of Low-Carbon Technologies* 2012; 7(2): 159–165.
- [101] Cuce E, Cuce PM. A comprehensive review on solar cookers. *Applied Energy* 2012; 102: 1399–1421.
- [102] Cuce PM, Cuce E. Homotopy perturbation method for temperature distribution, fin efficiency and fin effectiveness of convective straight fins. *International Journal of Low-Carbon Technologies* 2014; 9(1): 80–84.

- [103] Cuce E, Cuce PM. Homotopy perturbation method for temperature distribution, fin efficiency and fin effectiveness of convective straight fins with temperature-dependent thermal conductivity. Proceedings of the Institution of Mechanical Engineers, Part C, *Journal of Mechanical Engineering Science* 2013; 227(8): 1754–1760.
- [104] Cuce PM, Cuce E. Optimization of configurations to enhance heat transfer from a longitudinal fin exposed to natural convection and radiation. *International Journal of Low-Carbon Technologies* 2014; 9(4): 305–310.
- [105] Cuce E, Cuce PM. Energetic and exergetic performance assessment of solar cookers with different geometrical designs. *International Journal of Ambient Energy* 2015; 36(2): 62–69.
- [106] Riffat SB, Cuce E. Aerogel with its outstanding features and building applications. 11th International Conference on Sustainable Energy Technologies. 2-5 September 2012, Vancouver, Canada.
- [107] Riffat SB, Cuce E. A review on performance analysis of photovoltaic/thermal collectors. 10th International Conference on Sustainable Energy Technologies. 4-7 September 2011, Istanbul, Turkey.
- [108] Cuce PM, Cuce E. Effects of concavity level on heat loss, effectiveness and efficiency of a longitudinal fin exposed to natural convection and radiation. 10th International Conference on Sustainable Energy Technologies. 4-7 September 2011, Istanbul, Turkey.
- [109] Sukamongkol Y, Chungpaibulpatana S, Limmeechokchai B, Sripadungtham P. Condenser heat recovery with a PV/T air heating collector to regenerate desiccant for reducing energy use of air conditioning room. *Energy and Buildings* 2010; 42: 315–325.

- [110] Liu S. A novel heat recovery/desiccant cooling system. PhD Thesis, 2008, University of Nottingham, Nottingham, UK.
- [111] Cuce PM, Cuce E, Riffat SB. Second law analysis of solar powered heat recovery panels in buildings. 12th International Conference on Sustainable Energy Technologies. 26–29 August 2013, Hong Kong, China.
- [112] Golubovic MN, Hettiarachchi HDM, Worek WM. Evaluation of rotary dehumidifier performance with and without heated purge. *International Communications of Heat and Mass Transfer* 2007; 34: 785–795.
- [113] Dallaire J, Gosselin L, Da Silva AK. Conceptual optimization of a rotary heat exchanger with a porous core. *International Journal of Thermal Sciences* 2010; 49: 454–462.
- [114] Zhang LZ, Niu JL. Performance comparisons of desiccant wheels for air dehumidification and enthalpy recovery. *Applied Thermal Engineering* 2002; 22: 1347–1367.
- [115] Ghodsipour N, Sadrameli M. Experimental and sensitivity analysis of a rotary air preheater for the flue gas heat recovery. *Applied Thermal Engineering* 2003; 23: 571–580.
- [116] Simonson CJ, Besant RW. Energy wheel effectiveness: Part I—development of dimensionless groups. *International Journal of Heat and Mass Transfer* 1999; 42: 2161–2170.
- [117] Nobrega CEL, Brum NCL. Modeling and simulation of heat and enthalpy recovery wheels. *Energy* 2009; 34: 2063–2068.
- [118] Liu X, Jiang Y, Xia J, Chang X. Analytical solutions of coupled heat and mass transfer processes in liquid desiccant air dehumidifier/regenerator. *Energy Conversion and Management* 2007; 48: 2221–2232.

- [119] Zhang LZ, Zhu DS, Deng XH, Hua B. Thermodynamic modeling of a novel air dehumidification system. *Energy and Buildings* 2005; 37: 279–286.
- [120] Niu JL, Zhang LZ. Membrane-based enthalpy exchanger: Material considerations and clarification of moisture resistance. *Journal of Membrane Science* 2001; 189: 179–191.
- [121] Liang CH, Zhang LZ, Pei LX. Performance analysis of a direct expansion air dehumidification system combined with membrane-based total heat recovery. *Energy* 2010; 35: 3891–3901.
- [122] Min J, Su M. Performance analysis of a membrane-based energy recovery ventilator: Effects of membrane spacing and thickness on the ventilator performance. *Applied Thermal Engineering* 2010; 30: 991–997.
- [123] Zhang LZ, Jiang Y. Heat and mass transfer in a membrane-based energy recovery ventilator. *Journal of Membrane Science* 1999; 163: 29–38.
- [124] Bazilian MD, Prasad D. Modelling of a photovoltaic heat recovery system and its role in a design decision support tool for building professionals. *Renewable Energy* 2002; 27: 57–68.
- [125] Maffezzoni P, Codecasa L, D'Amore D. Modeling and simulation of a hybrid photovoltaic module equipped with a heat-recovery system. *IEEE Transactions on Industrial Electronics* 2009; 56(11): 4311–4318.
- [126] Crawford RH, Treloar GJ, Fuller RJ, Bazilian M. Life-cycle energy analysis of building integrated photovoltaic systems (BiPVs) with heat recovery unit. *Renewable and Sustainable Energy Reviews* 2006; 10: 559–575.

- [127] Sayed-Ahmadi M, Erb B, Simonson CJ, Besant RW. Transient behavior of run-around heat and moisture exchanger system. Part I: Model formulation and verification. *International Journal of Heat and Mass Transfer* 2009; 52: 6000–6011.
- [128] Vali A, Simonson CJ, Besant RW, Mahmood G. Numerical model and effectiveness correlations for a run-around heat recovery system with combined counter and cross flow exchangers. *International Journal of Heat and Mass Transfer* 2009; 52: 5827–5840.
- [129] Lin S, Broadbent J, McGlen R. Numerical study of heat pipe application in heat recovery systems. *Applied Thermal Engineering* 2005; 25: 127–133.
- [130] Gan G, Riffat SB. Naturally ventilated buildings with heat recovery: CFD simulation of thermal environment. *Applied Thermal Engineering* 2005; 25: 127–133.
- [131] Yau YH. Theoretical determination of effectiveness for heat pipe heat exchangers operating in naturally ventilated tropical buildings. Proceedings of the Institution of Mechanical Engineers, Part A: *Journal of Power and Energy* 2001; 215: 389–397.
- [132] Shao L, Riffat SB, Gan G. Heat recovery with low pressure loss for natural ventilation. *Energy and Buildings* 1998; 28: 179–184.
- [133] Rasouli M, Simonson CJ, Besant RW. Applicability and optimum control strategy of energy recovery ventilators in different climatic conditions. *Energy and Buildings* 2010; 42: 1376–1385.
- [134] Zhou YP, Wu JY, Wang RZ. Performance of energy recovery ventilator with various weathers and temperature set-points. *Energy and Buildings* 2007; 39: 1202–1210.

- [135] Arias J, Lundqvist P. Heat recovery and floating condensing in supermarkets. *Energy and Buildings* 2006; 38: 73–81.
- [136] Simonson CJ, Besant RW. Energy wheel effectiveness: Part II—correlations. *International Journal of Heat and Mass Transfer* 1999; 42: 2171–2185.
- [137] Sayed-Ahmadi M, Erb B, Simonson CJ, Besant RW. Transient behavior of run-around heat and moisture exchanger system. Part II: Sensitivity studies for a range of initial conditions. *International Journal of Heat and Mass Transfer* 2009; 52: 6012–6020.
- [138] Jokisalo J, Kurnitski J, Vuolle M, Torkki A. Performance of balanced ventilation with heat recovery in residential buildings in a cold climate. *International Journal of Ventilation* 2003; 2(3): 223–236.
- [139] Soylemez MS. On the thermoeconomical optimization of heat pipe heat exchanger HPHE for waste heat recovery. *Energy Conversion and Management* 2003; 44: 2509–2517.
- [140] Butcher CJ, Reddy BV. Second law analysis of a waste heat recovery based power generation system. *International Journal of Heat and Mass Transfer* 2007; 50: 2355–2363.
- [141] Reddy BV, Ramkiran G, Kumar KA, Nag PK. Second law analysis of a waste heat recovery steam generator. *International Journal of Heat and Mass Transfer* 2002; 45: 1807–1814.
- [142] Esen H, Inalli M, Esen M, Pihtili K. Energy and exergy analysis of a ground-coupled heat pump system with two horizontal ground heat exchangers. *Building and Environment* 2007; 42: 3606–3615.

- [143] Sarkar J, Bhattacharyya S, Gopal MR. Transcritical CO₂ heat pump systems: Exergy analysis including heat transfer and fluid flow effects. *Energy Conversion and Management* 2005; 46: 2053–2067.
- [144] Kotcioglu I, Caliskan S, Cansiz A, Baskaya S. Second law analysis and heat transfer in a cross-flow heat exchanger with a new winglet-type vortex generator. *Energy* 2010; 35: 3686–3695.
- [145] Wu SY, Yuan XF, Li YR, Xiao L. Exergy transfer effectiveness on heat exchanger for finite pressure drop. *Energy* 2007; 32: 2110–2120.
- [146] Hepbasli A, Akdemir O. Energy and exergy analysis of a ground source (geothermal) heat pump system. *Energy Conversion and Management* 2004; 45: 737–753.
- [147] Pulat E, Etemoglu AB, Can M. Waste-heat recovery potential in Turkish textile industry: Case study for city of Bursa. *Renewable and Sustainable Energy Reviews* 2009; 13: 663–672.
- [148] Teke I, Agra O, Atayilmaz SO, Demir H. Determining the best type of heat exchangers for heat recovery. *Applied Thermal Engineering* 2010; 30: 577–583.
- [149] Niu JL, Zhang LZ, Zuo HG. Energy savings potential of chilled-ceiling combined with desiccant cooling in hot and humid climates. *Energy and Buildings* 2002; 34:487–495.
- [150] Axelsson H, Harvey S, Asblad A, Berntsson T. Potential for greenhouse gas reduction in industry through increased heat recovery and/or integration of combined heat and power. *Applied Thermal Engineering* 2003; 23: 65–87.
- [151] Herzog T. World greenhouse gas emissions in 2005. WRI Working Paper, World Resources Institute, Washington, DC 2009; 1–5.

- [152] Baetens R, Jelle BP, Gustavsen A. Aerogel insulation for building applications: A state-of-the-art review. *Energy and Buildings* 2011; 43: 761–769.
- [153] Dimoudi A, Tompa C. Energy and environmental indicators related to construction of office buildings. Resources, Conservation and Recycling 2008; 53: 86–95.
- [154] Yan H, Shen Q, Fan LCH, Wang Y, Zhang L. Greenhouse gas emissions in building construction: A case study of One Peking in Hong Kong. *Building and Environment* 2010; 45: 949–955.
- [155] McKinsey & Company, Pathways to a Low-Carbon Economy – Version 2 of the Global Greenhouse Gas Abatement Cost Curve, 2009.
- [156] Enkvist PA, Naucler T, Rosander J. A cost curve for greenhouse gas reduction. *McKinsey Quarterly* 2007;1: 35–45.
- [157] Mills E, Wilson D, Johansson TB. No-regrets strategies for reducing greenhouse gas emissions. *Energy Policy* 1991; 19(6): 526–542.
- [158] Vandeweghe JR, Kennedy C. A spatial analysis of residential greenhouse gas emissions in the Toronto Census Metropolitan Area. *Journal of Industrial Ecology* 2007; 11(2): 133–144.
- [159] Cutting Greenhouse Gas Emissions. <http://www.scotch-whisky.org.uk/media/16319/csgasemissions.pdf>. (Last access is on 14.05.2013).
- [160] Reducing Greenhouse Gas Emissions. <http://www.alfalaval.com/campaigns/waste-heat-recovery/profitting-on-waste-heat/reducing-greenhouse-gas-emissions/Pages/reducing-greenhouse-gas-emissions.aspx>. (Last access is on 14.05.2013).
- [161] Low-energy Buildings. <http://www.ashden.org/low-energy-buildings>. (Last access is on 17.05.2013).

- [162] Cuce E, Cuce PM, Bali T. An experimental analysis of illumination intensity and temperature dependency of photovoltaic cell parameters. *Applied Energy* 2013; 111: 374–382.
- [163] Cuce E, Cuce PM. Improving thermodynamic performance parameters of silicon photovoltaic cells via air cooling. *International Journal of Ambient Energy* 2014; 35(4): 193–199.
- [164] Cuce E, Cuce PM. Theoretical investigation of hot box solar cookers having conventional and finned absorber plates. *International Journal of Low-Carbon Technologies* 2013; doi:10.1093/ijlct/ctt052.
- [165] Pacca S, Horvath A. Greenhouse gas emissions from building and operating electric power plants in the Upper Colorado River Basin. *Environmental Science and Technology* 2002; 36(14): 3194–3200.
- [166] Lazzarin RM, Gasparella A. Technical and economical analysis of heat recovery in building ventilation systems. *Applied Thermal Engineering* 1998; 18: 47–67.
- [167] Feist W, Schieders J, Dorer V, Haas A. Re-inventing air heating: convenient and comfortable within the frame of passive house concept. *Energy and Buildings* 2005; 37: 1186–1203.
- [168] Davidsson H, Bernardo R, Hellstrom B. Hybrid ventilation with innovative heat recovery – A system analysis. *Buildings* 2013; 3: 245–257.
- [169] McGuire T. McGuire Air Compressors, Inc. <http://searchwarp.com/swa323676.htm>. (Last access is on 22.05.2013).
- [170] Davidsson H, Bernardo R, Hellstrom B. Theoretical and explanation investigation of a heat exchanger suitable for a hybrid ventilation system. *Buildings* 2013; 3: 18–38.

- [171] Comakli K, Yuksel B. Environmental impact of thermal insulation thickness in buildings. *Applied Thermal Engineering* 2004; 24(5–6): 933–940.
- [172] America's Climate Choices: Panel on Advancing the Science of Climate Change; National Research Council, 2010.
- [173] Ozel M. Cost analysis for optimum thicknesses and environmental impacts of different insulation materials. *Energy and Buildings* 2012; 49: 552–559.
- [174] Woodwell GM. The carbon dioxide question. *Scientific American* 1978; 238: 34–43.
- [175] Houghton JT, Jenkins GJ, Ephraums JJ. *Climate Change: The IPCC Scientific Assessment*. Cambridge University Press, 1990, Cambridge, UK.
- [176] Cuce E, Cuce PM, Riffat S. Novel glazing technologies to mitigate energy consumption in low-carbon buildings: a comparative experimental investigation. *International Journal of Energy Research* 2015; doi:10.1002/er.3478.
- [177] Cuce E, Cuce PM. Vacuum glazing for highly insulating windows: Recent developments and future prospects. *Renewable and Sustainable Energy Reviews* 2016; 54: 1345–1357.
- [178] Hegazy AA. Comparative study of the performances of four photovoltaic/thermal solar air collectors. *Energy Conversion and Management* 2000; 41: 861–881.
- [179] Sopian K, Liu HT, Kakac S, Veziroglu TN. Performance of a double pass photovoltaic thermal solar collector suitable for solar drying systems. *Energy Conversion and Management* 2000; 41: 353–365.
- [180] Kalogirou SA. Use of TRNSYS for modelling and simulation of a hybrid PV thermal solar system for Cyprus. *Renewable Energy* 2001; 23: 247–260.

- [181] Chow TT, Hand JW, Strachan PA. Building-integrated photovoltaic and thermal applications in a subtropical hotel building. *Applied Thermal Engineering* 2003; 23: 2035–2049.
- [182] Jones AD, Underwood CP. A thermal model for photovoltaic systems. *Solar Energy* 2001; 70(4): 349–359.
- [183] Chow TT. Performance analysis of photovoltaic–thermal collector by explicit dynamic model. *Solar Energy* 2003; 75: 143–152.
- [184] Tiwari A, Sodha MS, Chandra A, Joshi JC. Performance evaluation of photovoltaic thermal solar air collector for composite climate of India. *Solar Energy Materials and Solar Cells* 2006; 90(2): 175–189.
- [185] Dubey S, Tiwari GN. Thermal modelling of a combined system of photovoltaic thermal (PV/T) solar water heater. *Solar Energy* 2008; 82: 602–612.
- [186] Tiwari A, Sodha MS. Parametric study of various configurations of hybrid PV/thermal air collector: experimental validation of theoretical model. *Solar Energy Materials and Solar Cells* 2007; 91: 17–28.
- [187] Tiwari A, Sodha MS. Performance evaluation of solar PV/T system: An experimental validation. *Solar Energy* 2006; 80(7): 751–759.
- [188] Dubey S, Sandhu GS, Tiwari GN. Analytical expression for electrical efficiency of PV/T hybrid air collector. *Applied Energy* 2009; 86: 697–705.
- [189] Cuce PM, Cuce E. Comments on “Analytical expression for electrical efficiency of PV/T hybrid air collector” by S. Dubey, G.S. Sandhu, and G.N. Tiwari. *International Journal of Ambient Energy* 2015; 36(4): 206–208.
- [190] Evans DL. Simplified method for predicting PV array output. *Solar Energy* 1981; 27: 555–560.

- [191] Skoplaki E, Palyvos JA. On the temperature dependence of photovoltaic module electrical performance: A review of efficiency/power correlations. *Solar Energy* 2009; 83: 614–624.
- [192] Desideri U, Proietti S, Sdringola P. Solar-powered cooling systems: Technical and economic analysis on industrial refrigeration and air-conditioning applications. *Applied Energy* 2009; 86: 1376–1386.
- [193] Chengqin R, Nianping L, Guangfa T. Principles of exergy analysis in HVAC and evaluation of evaporative cooling schemes. *Building and Environment* 2002; 37: 1045–1055.
- [194] Zmeureanu R, Wu XY. Energy and exergy performance of residential heating systems with separate mechanical ventilation. *Energy* 2007; 32: 187–195.
- [195] Sakulpipatsin P, Itard LCM, van der Kooi HJ, Boelman EC, Luscuere PG. An exergy application for analysis of buildings and HVAC systems. *Energy and Buildings* 2010; 42: 90–99.
- [196] McGovern J, Smyth BP. Rational efficiency of a heat exchanger. Articles, 2011, Paper 27. <http://arrow.dit.ie/engschmecart/27>. (Last access is on 14.07.2013).
- [197] Gan G, Riffat SB. A numerical study of solar chimney for natural ventilation of buildings with heat recovery. *Applied Thermal Engineering* 1998; 18: 1171–1187.
- [198] Dadoo A, Gustavsson L, Sathre R. Primary energy implications of ventilation heat recovery in residential buildings. *Energy and Buildings* 2011; 43: 1566–1572.
- [199] Chwieduk D. Towards sustainable-energy buildings. *Applied Energy* 2003; 76: 211–217.

- [200] Thiers S, Peuportier B. Thermal and environmental assessment of a passive building equipped with an earth-to-air heat exchanger in France. *Solar Energy* 2008; 82: 820–831.
- [201] Tommerup H, Svendsen S. Energy savings in Danish residential building stock. *Energy and Buildings* 2006; 38: 618–626.
- [202] Omer AM. Renewable building energy systems and passive human comfort solutions. *Renewable and Sustainable Energy Reviews* 2008; 12: 1562–1587.
- [203] T’Joen C, Park Y, Wang Q, Sommers A, Han X, Jacobi A. A review on polymer heat exchangers for HVAC&R applications. *International Journal of Refrigeration* 2009; 32: 763–779.
- [204] Cuce PM, Cuce E, Riffat SB. A novel roof type heat recovery panel for low-carbon buildings: An experimental investigation. *Energy and Buildings* 2016; 113: 133–138.
- [205] Pfafferott J. Evaluation of earth-to-air heat exchangers with a standardised method to calculate energy efficiency. *Energy and Buildings* 2003; 35: 971–983.
- [206] Kwong QJ, Adam NM, Sahari BB. Thermal comfort assessment and potential for energy efficiency enhancement in modern tropical buildings: A review. *Energy and Buildings* 2014; 68: 547–557.
- [207] Agrawal S, Simon T, North M, Cui T. An experimental study on the effects of agitation on convective heat transfer. *International Journal of Heat and Mass Transfer* 2015; 90: 302–313.
- [208] International Energy Agency. Key world energy statistics, 2006.
- [209] International Energy Agency. Key world energy statistics, 2013.
- [210] International Energy Agency. Key world energy statistics, 2012.

- [211] Balaras CA, Droutsas K, Dascalaki E, Kontoyiannidis S. Heating energy consumption and resulting environmental impact of European apartment buildings. *Energy and Buildings* 2005; 37: 429–442.
- [212] Li X, Bowers CP, Schnier T. Classification of energy consumption in buildings with outlier detection. *IEEE Transactions on Industrial Electronics* 2010; 57(11): 3639–3644.
- [213] Riangvilaikul B, Kumar S. An experimental study of a novel dew point evaporative cooling system. *Energy and Buildings* 2010; 42: 637–644.
- [214] Chandrakant W, Satyashree G, Chaitanya S. A review on potential of Maisotsenko cycle in energy saving applications using evaporative cooling. *International Journal of Advance Research in Science, Engineering and Technology* 2012; 1: 15–20.
- [215] Delfani S, Esmaeliani J, Pasharshahi H, Karami M. Energy saving potential of an indirect evaporative cooler as a pre-cooling unit for mechanical cooling systems in Iran. *Energy and Buildings* 2010; 42: 2169–2176.
- [216] Belarbi R, Ghiaus C, Allard F. Modeling of water spray evaporation: Application to passive cooling of buildings. *Solar Energy* 2006; 80: 1540–1552.
- [217] Ghosal MK, Tiwari GN, Srivastava NSL. Modeling and experimental validation of a greenhouse with evaporative cooling by moving water film over external shade cloth. *Energy and Buildings* 2003; 35: 843–850.
- [218] Wanphen S, Nagano K. Experimental study of the performance of porous materials to moderate the roof surface temperature by its evaporative cooling effect. *Building and Environment* 2009; 44: 338–351.
- [219] Cheikh HB, Bouchair A. Passive cooling by evapo-reflective roof for hot dry climates. *Renewable Energy* 2004; 29: 1877–1886.

- [220] He J, Hoyano A. Experimental study of cooling effects of a passive evaporative cooling wall constructed of porous ceramics with high water soaking-up ability. *Building and Environment* 2010; 45: 461–472.
- [221] Bowman N, Lomas K, Cook M, Eppel H, Ford B, Hewitt M, Cucinella M, Francis E, Rodriguez E, Gonzalez R, Alvarez S, Galata A, Lanarde P, Belarbi R. Application of passive draught evaporative cooling (PDEC) to non-domestic buildings. *Renewable Energy* 1997; 10(2/3): 191–196.
- [222] Costelloe B, Finn D. Indirect evaporative cooling potential in air-water systems in temperate climates. *Energy and Buildings* 2003; 35: 573–591.
- [223] Heidarinejad G, Bozorgmehr M, Delfani S, Esmaeelian J. Experimental investigation of two-stage indirect/direct evaporative cooling system in various climatic conditions. *Building and Environment* 2009; 44: 2073–2079.
- [224] Ibrahim E, Shao L, Riffat SB. Performance of porous ceramic evaporators for building cooling application. *Energy and Buildings* 2003; 35: 941–949.
- [225] Hajidavalloo E. Application of evaporative cooling on the condenser of window-air-conditioner. *Applied Thermal Engineering* 2007; 27: 1937–1943.
- [226] Maheshwari GP, Al-Ragom F, Suri RK. Energy-saving potential of an indirect evaporative cooler. *Applied Energy* 2001; 69: 69–76.
- [227] Riangvilaikul B, Kumar S. Numerical study of a novel dew point evaporative cooling system. *Energy and Buildings* 2010; 42: 2241–2250.
- [228] Bruno F. On-site experimental testing of a novel dew point evaporative cooler. *Energy and Buildings* 2011; 43: 3475–3483.
- [229] Zhao X, Liu S, Riffat SB. Comparative study of heat and mass exchanging materials for indirect evaporative cooling systems. *Building and Environment* 2008; 43: 1902–1911.

- [230] El-Dessouky HT, Ettouney HM, Bouhamra W. A novel air conditioning system: Membrane air drying and evaporative cooling. *Transactions of the Institution of Chemical Engineering* 2000; 78(A): 999–1009.
- [231] Velasco Gomez E, Rey Martinez FJ, Varela Diez F, Molina Leyva MJ, Herrero Martin R. Description and experimental results of a semi-indirect ceramic evaporative cooler. *International Journal of Refrigeration* 2005; 28: 654–662.
- [232] Chen P, Qin H, Huang YJ, Wu H, Blumstein C. The energy saving potential of precooling incoming outdoor air by indirect evaporative cooling. *ASHRAE Transactions* 1993; 99(1): 322–331.
- [233] El-Dessouky H, Ettouney H, Al-Zeefari A. Performance analysis of two-stage evaporative coolers. *Chemical Engineering Journal* 2004; 102: 255–266.
- [234] Zhang H, You SJ, Yang HX, Niu JL. Enhanced performance of air-cooled chillers using evaporative cooling. *Building Services Engineering Research Technology* 2000; 21(4): 213–217.
- [235] Kruger E, Cruz EG, Givoni B. Effectiveness of indirect evaporative cooling and thermal mass in a hot arid climate. *Building and Environment* 2010; 45: 1422–1433.
- [236] Kanoglu M, Carpinlioglu MO, Yildirim M. Energy and exergy analyses of an experimental open-cycle desiccant cooling system. *Applied Thermal Engineering* 2004; 24: 919–932.
- [237] Caliskan H, Hepbasli A, Dincer I, Maisotsenko V. Thermodynamic performance assessment of a novel air cooling cycle: Maisotsenko cycle. *International Journal of Refrigeration* 2011; 34: 980–990.

- [238] Cuce PM, Riffat SB, Bayraktar KG. An experimental study on a novel heat recovery system. 13th International Conference on Sustainable Energy Technologies. 25–28 August 2014, Geneva, Switzerland.
- [239] Taufiq BN, Masjuki HH, Mahlia TMI, Amalina MA, Faizul MS, Saidur R. Exergy analysis of evaporative cooling for reducing energy use in a Malaysian building. *Desalination* 2007; 209: 238–243.
- [240] Energy Conservation Building code 2007 (ECBC), Bureau of Energy Efficiency, Ministry of Power, Government of India, 2007.
- [241] Yik FWH, Burnett J, Prescott I. Predicting air-conditioning energy consumption of a group of buildings using different heat rejection methods. *Energy and Buildings* 2001; 33: 151–166.
- [242] Khandelwal A, Talukdar P, Jain S. Energy savings in a building using regenerative evaporative cooling. *Energy and Buildings* 2011; 43: 581–591.
- [243] Ford B, Patel N, Zaveri P, Hewitt M. Cooling without air conditioning: The Torrent Research Centre, Ahmedabad, India. *Renewable Energy* 1998; 15: 177–182.
- [244] Zhan C, Zhao X, Smith S, Riffat SB. Numerical study of a M-cycle cross-flow heat exchanger for indirect evaporative cooling. *Building and Environment* 2011; 46(3): 657–668.
- [245] Goldsworthy M, White S. Optimisation of a desiccant cooling system design with indirect evaporative cooler. *International Journal of Refrigeration* 2011; 34: 148–158.
- [246] Gonzalez PA, Zamarreno JM. Prediction of hourly energy consumption in buildings based on a feedback artificial neural network. *Energy and Buildings* 2005; 37: 595–601.

- [247] CIBSE Guide F. Energy Efficiency in Buildings. Second edition, 2004, Chartered Institution of Building Services Engineers London, UK.
- [248] Hasan A. Indirect evaporative cooling of air to a sub-wet bulb temperature. *Applied Thermal Engineering* 2010; 30: 2460–2468.
- [249] San Jose Alonso JF, Rey Martinez FJ, Velasco Gomez E, Alvarez-Guerra Plasencia MA. Simulation model of an indirect evaporative cooler. *Energy and Buildings* 1998; 29: 23–27.
- [250] Cerci Y. A new ideal evaporative freezing cycle. *International Journal of Heat and Mass Transfer* 2003; 46: 2967–2974.
- [251] Guo XC, Zhao TS. A parametric study of an indirect evaporative air cooler. *International Communications in Heat and Mass Transfer* 1998; 25(2): 217–226.
- [252] Zhao X, Li JM, Riffat SB. Numerical study of a novel counter-flow heat and mass exchanger for dew point evaporative cooling. *Applied Thermal Engineering* 2008; 28: 1942–1951.
- [253] Jiang Y, Xie X. Theoretical and testing performance of an innovative indirect evaporative chiller. *Solar Energy* 2010; 84: 2041–2055.
- [254] Watt JR. Nationwide evaporative cooling is here. *ASHRAE Transactions* 1987; 93(1): 1237–1251.
- [255] Wu H, Yellott JI. Investigation of a plate-type indirect evaporative cooling system for residences in hot and arid climates. *ASHRAE Transactions* 1987; 93(1): 1252–1260.
- [256] Tulsidasani TR, Sawhney RL, Singh SP, Sodha MS. Recent research on an indirect evaporative cooler (IEC) part I: Optimization of the COP. *International Journal of Energy Research* 1997; 21(12): 1099–1108.

- [257] Scofield CM. The heat pipe used for dry evaporative cooling. *ASHRAE Transactions* 1986; 92(1B): 371–381.
- [258] Maclaine-Cross IL, Banks PJ. A general theory of wet surface heat exchangers and its application to regenerative evaporative cooling. *Journal of Heat Transfer* 1981; 103(3): 579–585.
- [259] Kettleborough CF, Hsieh CS. The thermal performance of the wet surface plastic plate heat exchanger used as an indirect evaporative cooler. *Journal of Heat Transfer* 1983; 105(2): 366–373.
- [260] Kettleborough CF, Waugaman DG, Johnson M. The thermal performance of the cross-flow three-dimensional flat plate indirect evaporative cooler. *Journal of Energy Resources Technology* 1992; 114(3): 181–186.
- [261] Wassel AT, Mills AF. Design methodology for a counter-current falling film evaporative condenser. *Journal of Heat Transfer* 1987; 109(3): 784–787.
- [262] Hsu ST, Lavan Z, Worek WM. Optimization of wet surface heat exchanger. *Energy* 1989; 14: 757–770.
- [263] Erens PJ, Dreyer AA. Modelling of indirect evaporative air coolers. *International Journal of Heat and Mass Transfer* 1993; 36(1): 17–26.
- [264] Tsay YL. Analysis of heat and mass transfer in a countercurrent-flow wet surface heat exchanger. *International Journal of Heat and Fluid Flow* 1994; 15(2): 149–156.
- [265] Halasz B. A general mathematical model of evaporative cooling devices. *Revue Générale de Thermique* 1998; 37(4): 245–255.
- [266] Riffat SB, Zhu J. Mathematical model of indirect evaporative cooler using porous ceramic and heat pipe. *Applied Thermal Engineering* 2004; 24: 457–470.

- [267] Zhan C, Zhao X, Duan Z, Riffat SB. Numerical study on indirect evaporative cooling performance comparison between counterflow and crossflow heat exchangers. *International Journal of Low-Carbon Technologies* 2011; 6(2): 100–106.
- [268] Crafton EF, Black WZ. Heat transfer and evaporation rates of small liquid droplets on heat horizontal surfaces. *International Journal of Heat and Mass Transfer* 2004; 47: 1187–1200.
- [269] Kaiser AS, Lucas M, Viedma M, Zamora B. Numerical model of evaporative cooling processes in a new type of cooling tower. *International Journal of Heat and Mass Transfer* 2005; 48: 986–999.
- [270] Falkovich G. *Fluid Mechanics*. Cambridge University Press, 2011, UK.
- [271] Cengel YA, Ghajar AJ. *Heat and Mass Transfer: Fundamentals & Applications*. The McGraw-Hill Companies, 2011, Inc. Fourth Edition, New York, USA.
- [272] Frossling N. Uber die Verdunstung fallender Tropfen. *Gerlands Beitr. Geophysik* 1938; 52: 170–216.
- [273] Bolz RE, Tuve GL. *Handbook of Tables for Applied Engineering Science*. CRC Press, 1976, Second Edition, New York, USA.
- [274] Santamouris M, Kolokotsa D. Passive cooling dissipation techniques for buildings and other structures: The state of the art. *Energy and Buildings* 2013; 57: 74–94.
- [275] Santamouris M. *Advances in passive cooling*. Earthscan Publishers, 2007, London, UK.

- [276] Santamouris M, Pavlou K, Synnefa A, Niachou K, Kolokotsa D. Recent progress on passive cooling techniques. Advanced technological developments to improve survivability levels in low-income households. *Energy and Buildings* 2007; 39: 859–866.
- [277] Heidarinejad G, Moshari S. Novel modelling of an indirect evaporative cooling system with cross-flow configuration. *Energy and Buildings* 2015; 92: 351–362.
- [278] Giabaklou Z, Ballinger JA. A passive evaporative cooling system by natural ventilation. *Building and Environment* 1996; 31(6): 503–507.
- [279] Zhang LZ, Huang SM. Coupled heat and mass transfer in a counter flow hollow fiber membrane module for air humidification. *International Journal of Heat and Mass Transfer* 2011; 54: 1055–1063.
- [280] Bassuoni MM. A simple analytical method to estimate all exit parameters of a cross-flow air dehumidifier using liquid desiccant. *Journal of Advanced Research* 2014; 5: 175–182.
- [281] Fumo N, Goswami DY. Study of an aqueous lithium chloride desiccant system: air dehumidification and desiccant regeneration. *Solar Energy* 2002; 72(4): 351–361.
- [282] Chengchao F, Ketao S. Analysis and modeling of solar liquid desiccant air conditioning system. *Acta Energiae Sinica* 1997; 18(2): 128–133.
- [283] Oberg V, Goswami DY. Experimental study of the heat and mass transfer in a packed bed liquid desiccant air dehumidifier. *Journal of Solar Energy Engineering* 1998; 120: 289–297.
- [284] Oberg V, Goswami DY. A review of liquid desiccant cooling. *Advances in Solar Energy* 1998; 12: 431–470.

- [285] Ahmed KS, Gandhidasan P, Al-Farayedhi AA. Simulation of a hybrid liquid desiccant based air-conditioning system. *Applied Thermal Engineering* 1997; 17(2): 125–134.
- [286] Liu XH, Jiang Y, Qu KY. Heat and mass transfer model of cross flow liquid desiccant air dehumidifier/regenerator. *Energy Conversion and Management* 2005; 48: 546–554.
- [287] Fumo N, Goswami Y. Study of the aqueous lithium chloride desiccant system, Part I: air dehumidification. Proceedings of Millennium Solar Forum 2000. Asociacion Nacional de Energia Solar 2000; 307–312.
- [288] Fumo N, Goswami Y. Study of the aqueous lithium chloride desiccant system, Part II: desiccant regeneration. Proceedings of Millennium Solar Forum 2000. Asociacion Nacional de Energia Solar 2000; 313–318.
- [289] El-Shafei BZ, Ayman AA, Ahmed MH. Investigation on the effect of operating parameters of solar desiccant cooling system using artificial neural networks. *International Journal of Thermal and Environmental Engineering* 2010; 1: 91–98.
- [290] Abdul-Wahab SA, Zurigat YH, Abu-Arabi MK. Predictions of moisture removal rate and dehumidification effectiveness for structured liquid desiccant air dehumidifier. *Energy* 2004; 29: 19–34.
- [291] Sick F, Buschulte TK, Klein S, Northey P, Duffie JA. Analysis of the seasonal performance of hybrid liquid desiccant cooling systems. *Solar Energy* 1988; 40: 211–217.
- [292] Stevens DI, Braun JE, Klein SA. An effectiveness model of liquid desiccant system heat/mass exchangers. *Solar Energy* 1989; 42: 449–455.

- [293] Mohammad AT, Mat SB, Sulaiman MY, Sopian K, Al-Abidi AA. A statistical analysis of a liquid desiccant dehumidifier/regenerator in an air conditioning system. *International Journal of Thermal and Environmental Engineering* 2013; 5(1): 41–50.
- [294] Cuce E, Cuce PM, Wood CJ, Riffat SB. Optimizing insulation thickness and analysing environmental impacts of aerogel-based thermal superinsulation in buildings. *Energy and Buildings* 2014; 77: 28–39.
- [295] Cuce E, Cuce PM, Wood CJ, Riffat SB. Toward aerogel based thermal superinsulation in buildings: A comprehensive review. *Renewable and Sustainable Energy Reviews* 2014; 34: 273–299.
- [296] Riffat SB, James SE, Wong CW. Experimental analysis of the absorption and desorption rates of HCOOK/H₂O and LiBr/H₂O. *International Journal of Energy Research* 1998; 22: 1099–1103.
- [297] Cuce PM, Riffat S. A state of the art review of evaporative cooling systems for building applications. *Renewable and Sustainable Energy Reviews* 2016; 54: 1240–1249.
- [298] Santamouris M. Energy and climate in the urban built environment. James & James Science Publishers, 1999, London, UK.
- [299] Santamouris M, Papanikolaou N, Livada I, Koronakis I, Georgakis C, Argiriou A, Assimakopoulos DN. On the impact of urban climate on the energy consumption of buildings. *Solar Energy* 2001; 70(3): 201–216.
- [300] Babaei T, Abdi H, Lim CP, Nahavandi S. A study and a directory of energy consumption data sets of buildings. *Energy and Buildings* 2015; 94: 91–99.

- [301] Cuce E. Development of innovative window and fabric technologies for low-carbon buildings. PhD Thesis, 2014, University of Nottingham, Nottingham, UK.
- [302] Sfakianaki A, Pavlou K, Santamouris M, Livada I, Assimakopoulos MN, Mantas P, Christakopoulos A. Air tightness measurements of residential houses in Athens, Greece. *Building and Environment* 2008; 43: 398–405.
- [303] Santamouris M. Energy in the urban environment—the role of natural ventilation. In: Allard F, Ghiaus C, editors. *Natural ventilation in the urban environment*. James & James Science Publishers, 2005, London, UK.
- [304] Marszal AJ, Heiselberg P, Bourrelle JS, Musall E, Voss K, Sartori I, Napolitano A. Zero energy building – A review of definitions and calculation methodologies. *Energy and Buildings* 2011; 43: 971–979.
- [305] Santin OG. Behavioural patterns and user profiles related to energy consumption for heating . *Energy and Buildings* 2011; 43: 2662–2672.
- [306] Saini SK, Saini RP. Development of correlations for Nusselt number and friction factor for solar air heater with roughened duct having arc-shaped wire as artificial roughness. *Solar Energy* 2008; 82: 1118–1130.
- [307] Han JC, Park JS, Lei CK. Heat transfer enhancement in channels with turbulence promoters. *Journal of Engineering for Gas Turbines and Power* 2008; 107; 629–635.
- [308] Howard B, Parshall L, Thompson J, Hammer S, Dickinson J, Modi V. Spatial distribution of urban building energy consumption by end use. *Energy and Buildings* 2012; 45: 141–151.

- [309] Allouhi A, El Fouih Y, Kousksou T, Jamil A, Zeraouli Y, Mourad Y. Energy consumption and efficiency in buildings: Current status and future trends. *Journal of Cleaner Production* 2015; 109: 118–130.
- [310] Si P, Li A, Rong X, Feng Y, Yang Z, Gao Q. New optimized model for water temperature calculation of river-water source heat pump and its application in simulation of energy consumption. *Renewable Energy* 2015; 84: 65–73.
- [311] Zeng Y, Zhang Z, Kusiak A. Predictive modelling and optimisation of a multi-zone HVAC system with data mining and firefly algorithms. *Energy* 2015; 86: 393–402.
- [312] Wang Y, Kuckelkorn J, Zhao FY, Liu D, Kirschbaum A, Zhang JL. Evaluation on classroom thermal comfort and energy performance of passive school building by optimising HVAC control systems. *Building and Environment* 2015; 89: 86–106.
- [313] Nasr MR, Kassai M, Ge G, Simonson CJ. Evaluation of defrosting methods for air-to-air heat/energy exchangers on energy consumption of ventilation. *Applied Energy* 2015; 151: 32–40.
- [314] Cuce PM, Bayraktar KG, Riffat S, Omer S. Preliminary performance investigation of a novel direct contact evaporative cooling system. 14th International Conference on Sustainable Energy Technologies. 25–27 August 2015, Nottingham, United Kingdom.
- [315] Cuce PM, Bayraktar KG, Riffat S, Omer S. Building applications of heat recovery systems: A review. 14th International Conference on Sustainable Energy Technologies. 25–27 August 2015, Nottingham, United Kingdom.
- [316] International Energy Agency. Energy policies of IEA countries, 2012, UK.

- [317] Khan N, Su Y, Riffat SB. A review on wind driven ventilation techniques. *Energy and Buildings* 2008; 40: 1586–1604.
- [318] Mardiana A, Riffat SB. Building energy consumption and carbon dioxide emissions: Thread to climate change. *Journal of Earth Science and Climate Change* 2015; doi:10.4172/ 2157-7617.S3-001.

APPENDICES

Publications

Papers in Science Citation Index Journals

1. **Cuce PM**. Thermal performance monitoring of a novel heat recovery unit integrated to a residential house. [Indoor and Built Environment](#) 2016; under review.
2. Cuce E, **Cuce PM**, Riffat SB. A smart building material for low/zero carbon applications: Heat insulation solar glass – Characteristic results from laboratory and in-situ tests. [International Journal of Low-Carbon Technologies](#) 2016; under review.
3. **Cuce PM**, Cuce E, Riffat SB. A novel roof type heat recovery panel for low-carbon buildings: An experimental investigation. [Energy and Buildings](#), 2016; 113: 133–138.
4. Cuce E, **Cuce PM**. The impact of internal aerogel retrofitting on the thermal bridges of residential buildings: An experimental and statistical research. [Energy and Buildings](#) 2016; 116: 449–454.
5. Cuce E, **Cuce PM**, Young CH. Energy saving potential of heat insulation solar glass: Key results from laboratory and in-situ testing. [Energy](#) 2016, 97: 369–380.
6. Cuce E, **Cuce PM**, Riffat SB. Novel glazing technologies to mitigate energy consumption in low-carbon buildings: a comparative experimental investigation. [International Journal of Energy Research](#) 2016; doi:10.1002/er.3478.
7. Cuce E, **Cuce PM**. Vacuum glazing for highly insulating windows: Recent developments and future prospects. [Renewable and Sustainable Energy Reviews](#) 2016; 54: 1345–1357.

8. **Cuce PM**, Riffat SB. A state of the art review of evaporative cooling systems for building applications. *Renewable and Sustainable Energy Reviews* 2016; 54: 1240–1249.
9. **Cuce PM**, Riffat SB. A comprehensive review of heat recovery systems for building applications. *Renewable and Sustainable Energy Reviews* 2015; 47: 665–682.
10. Cuce E, **Cuce PM**. A successful application of homotopy perturbation method for efficiency and effectiveness assessment of longitudinal porous fins. *Energy Conversion and Management* 2015; 93: 92–99.
11. Cuce E, **Cuce PM**. Theoretical investigation of hot box solar cookers having conventional and finned absorber plates. *International Journal of Low-Carbon Technologies* 2015; 10(3): 238–245.
12. **Cuce PM**, Cuce E, Aygun C. Homotopy perturbation method for temperature distribution, fin efficiency and fin effectiveness of convective straight fins. *International Journal of Low-Carbon Technologies* 2014; 9(1): 80–84.
13. Cuce E, **Cuce PM**, Wood CJ, Riffat SB. Toward aerogel based thermal superinsulation in buildings: A comprehensive review. *Renewable and Sustainable Energy Reviews* 2014; 34: 273–299.
14. Cuce E, **Cuce PM**, Wood CJ, Riffat SB. Optimizing insulation thickness and analysing environmental impacts of aerogel-based thermal superinsulation in buildings. *Energy and Buildings* 2014; 77: 28–39.

15. **Cuce PM**, Cuce E. Optimization of configurations to enhance heat transfer from a longitudinal fin exposed to natural convection and radiation. *International Journal of Low-Carbon Technologies* 2014; 9(4): 305–310.
16. Cuce E, **Cuce PM**. Tilt angle optimization and passive cooling of building-integrated photovoltaics (BIPVs) for better electrical performance. *Arabian Journal for Science and Engineering* 2014; 39(11): 8199–8207.
17. Cuce E, **Cuce PM**, Bali T. An experimental analysis of illumination intensity and temperature dependency of photovoltaic cell parameters. *Applied Energy* 2013; 111: 374–382.
18. Cuce E, **Cuce PM**. Homotopy perturbation method for temperature distribution, fin efficiency and fin effectiveness of convective straight fins with temperature-dependent thermal conductivity. Proceedings of the Institution of Mechanical Engineers, Part C: *Journal of Mechanical Engineering Science* 2013; 227(8): 1754–1760.
19. Cuce E, **Cuce PM**. A comprehensive review on solar cookers. *Applied Energy* 2013; 102: 1399–1421.
20. Cuce E, **Cuce PM**. Effects of concavity level on heat loss, effectiveness and efficiency of a longitudinal fin exposed to natural convection and radiation. *International Journal of Numerical Methods for Heat and Fluid Flow* 2013; 23(7): 1169–1178.
21. **Cuce PM**, Cuce E. A novel model of photovoltaic modules for parameter estimation and thermodynamic assessment. *International Journal of Low-Carbon Technologies* 2011; 7(2): 159–165.

Papers in Other International Journals

1. **Cuce PM**, Cuce E. Comments on “Analytical expression for electrical efficiency of PV/T hybrid air collector” by S. Dubey, G.S. Sandhu, and G.N. Tiwari. *International Journal of Ambient Energy* 2015; 36(4): 206–208.
2. Cuce E, **Cuce PM**. Energetic and exergetic performance assessment of solar cookers with different geometrical designs. *International Journal of Ambient Energy* 2015; 36(2): 62–69.
3. Cuce E, **Cuce PM**. Improving thermodynamic performance parameters of silicon photovoltaic cells via air cooling. *International Journal of Ambient Energy* 2014; 35(4): 193–199.
4. Cuce E, **Cuce PM**. He’s homotopy perturbation method for prey and predator problem considering real life situations. *Far East Journal of Applied Mathematics* 2013; 76(1): 13–24.

Papers in International Conference Proceedings

1. **Cuce PM**, Bayraktar KG, Riffat SB, Omer S. Preliminary performance investigation of a novel direct contact evaporative cooling system. Fourteenth International Conference on Sustainable Energy Technologies. 25–27 August 2015, Nottingham, United Kingdom.

2. **Cuce PM**, Bayraktar KG, Riffat SB, Omer S. Building applications of heat recovery systems: A review. Fourteenth International Conference on Sustainable Energy Technologies. 25–27 August 2015, Nottingham, United Kingdom.
3. **Cuce PM**. ETRI Solar Energy Workshop. Invited delegate for the conference at the University of Nottingham. 18 February 2015, Nottingham, United Kingdom.
4. Cuce E, **Cuce PM**. Thermal performance assessment of porous fins via homotopy perturbation method. Fourteenth International Conference on Sustainable Energy Technologies. 25–27 August 2015, Nottingham, United Kingdom.
5. **Cuce PM**, Riffat SB, Bayraktar KG. An experimental study on a novel heat recovery system. Thirteenth International Conference on Sustainable Energy Technologies. 25–28 August 2014, Geneva, Switzerland.
6. **Cuce PM**. Novel energy and biotechnology developments in the sustainable built environment. Invited researcher for the workshop at Istanbul Technical University. 24–27 March 2014, Istanbul, Turkey.
7. Cuce E, **Cuce PM**. Tilt angle optimization of building-integrated photovoltaics (BIPVs) for cooler operating temperatures. MEGS IV Annual Conference. 12–13 September 2013, Loughborough, United Kingdom.
8. **Cuce PM**, Cuce E. Passive cooling of building-integrated photovoltaics (BIPVs) for better electrical performance. MEGS IV Annual Conference. 12–13 September 2013, Loughborough, United Kingdom.

9. Cuce E, **Cuce PM**, Wood CJ, Riffat SB. Optimum insulation thickness of aerogel in buildings. Twelfth International Conference on Sustainable Energy Technologies. 26–29 August 2013, Hong Kong, China.
10. **Cuce PM**, Cuce E, Riffat SB. Theoretical investigation of solar powered heat recovery panels in buildings. Twelfth International Conference on Sustainable Energy Technologies. 26–29 August 2013, Hong Kong, China.
11. **Cuce PM**, Cuce E, Riffat SB. Second law analysis of solar powered heat recovery panels in buildings. Twelfth International Conference on Sustainable Energy Technologies. 26–29 August 2013, Hong Kong, China.
12. **Cuce PM**, Cuce E. Effects of concavity level on heat loss, effectiveness and efficiency of a longitudinal fin exposed to natural convection and radiation. Tenth International Conference on Sustainable Energy Technologies. 4–7 September 2011, Istanbul, Turkey.